Universidade do Minho
I3Bs - Instituto de Investigação em Biomateriais, Biodegradáveis e Biomiméticos

Ana Catarina Freitas Salazar de Oliveira

Fucoidan-based strategies envisioning antitumor therapies

dezembro de 2019

UMinho | 2019 Ana Catarina Freitas Salazar de Oliveira **Fucoidan-based strategies envisioning antitumor therapies**

Universidade do Minho
I3Bs - Instituto de Investigação em Biomateriais, Biodegradáveis e Biomiméticos

Ana Catarina Freitas Salazar de Oliveira

Fucoidan-based strategies envisioning antitumor therapies

Tese de Doutoramento
Doutoramento em Engenharia de Tecidos, Medicina Regenerativa e Células Estaminais

Trabalho efetuado sob a orientação de
Doutor Albino Manuel Pereira Martins
Doutor Tiago José Quinteiros Lopes Henriques da Silva

dezembro de 2019

ACKNOWLEDGMENTS

This thesis is the last chapter of my PhD journey and now is the time to acknowledge all the people, which in one way or another, guided, supported and helped me during all this time.

First, I would like to acknowledge my supervisors, Dr. Albino Martins and Dr. Tiago H. Silva, for all the help, knowledge, support, patience and availability. Their enthusiasm about my work and all the ideas and suggestions were a great incitement during all the steps of this PhD. They always believed in me and gave me challenges that made me grow both as a researcher and as a person.

To Professor Rui L. Reis for the opportunity to develop my PhD in an institute of excellence and the opportunity to attend relevant scientific conferences. Thank you also for the support regarding this project.

To all my co-authors for the help in the development of the different works and valuable insights in research areas that I was less familiar. Thank you for all the tips and suggestions.

Finally, I would like to acknowledge all the funding that allowed me to perform all this work referred specifically in each chapter and Norte 2020, for financing my PhD scholarship "Norte-08-5369-000037".

To all my colleagues from 3B's that helped and supported me whenever I needed. To all the friends I made at 3B's, thank you for all the moments we have spent together. I am sure we will have many more adventures to come. A special thanks to Gabriela, who was always there for me in every step of the way. It is really nice to see that the time we have spent together turned into an incredible friendship.

To my friends from Biomedical Engineering that supported me during all this time and are part of my life since my first days at University of Minho. You know how important you are to me. Tina, thank you for your unconditional friendship. You were always by my side, in the saddest and happiest moments. I know that no matter of what happens, you will always be my person.

To André, for his love, patience, support and understanding. Thank you for everything!

To all my family, thank you for all your support and enthusiasm about my PhD, for believing and helping me in every situation.

To my brother and to my parents. Thank you so much for your love, for believing in me unconditionally, for all the support in every step I make, for encouraging me in pursuing my dreams. For always encouraging me and for giving me all the opportunities. For your wise advices and patience. I could have not done this without you. You are my model and my inspiration. I would never be able to thank you enough.

STATEMENT OF INTEGRITY

I hereby declare having conducted this academic work with integrity. I confirm that I have not used plagiarism or any form of undue use of information or falsification of results along the process leading to its elaboration.

I further declare that I have fully acknowledged the Code of Ethical Conduct of the University of Minho.

ABSTRACT

Current cancer treatments present some drawbacks, namely unwanted side effects of chemotherapeutics, due to their toxicity over healthy tissues. Trying to overcome this impactful limitation, the use of natural compounds that may present diminished effects over non-cancer cells is of great interest. Among them, fucoidan, a sulfated polysaccharide extracted from brown algae, has been highlighted over the last years due to its interesting biological features.

Since different fucoidans may present distinct antitumor behaviors, one of the main goals of this PhD work was to optimize fucoidan usage by developing more effective antitumor therapies. Accordingly, in Chapter III, different fucoidan extracts from *Fucus vesiculosus* were tested over human breast cancer and normal cells. Three types of biological outcomes were observed: i) toxicity to cancer and normal cells; ii) toxicity to cancer cells at lower concentrations than normal cells (an effective antitumor behavior) and iii) toxicity to normal cells at lower dosages than cancer cells (for high concentrations). These discrepant activities were attributed to differences in the sulfates position and branching of fucoidan. The anti-angiogenic potential of the effective fucoidan extract (type ii) was also validated by an endothelial cell tube formation assay (*in vitro*) and a Chick Chorioallantoic Membrane assay (*in vivo*) (Chapter IV). The cytotoxic effect of the same fucoidan extract was also demonstrated to human melanoma cells (Chapter V). In a complementary approach, a skin patch to treat melanoma was developed by the immobilization of fucoidan at the surface of an electrospun nanofibrous mesh.

Empowering the use of this marine-origin polymer, the fucoidan extract type iii was chosen to develop a drug delivery system for breast cancer. Gemcitabine, a chemotherapeutic drug, was successfully encapsulated into fucoidan/chitosan nanoparticles showing higher toxicity to cancer cells than to normal endothelial cells (Chapter VI). Aiming to reduce gemcitabine side-effects and to develop more precise therapies, an ErbB-2 antibody was immobilized at the surface of the previously described nanoparticles (Chapter VII). The targeting to cancer cells was confirmed in a co-culture system (increased toxicity to cancer cells) and *in vivo*, observing the impaired tumor growth and reduced lungs metastasis.

These studies proposed fucoidan-based strategies (either extracts or systems) that should be further explored in the development of more effective antitumor therapies based in natural compounds.

Keywords: Antitumor, Breast Cancer, Drug Delivery System, Fucoidan, Nanofibrous Mesh, Nanoparticles, Melanoma, Targeting System

RESUMO

Os tratamentos atualmente utilizados para o cancro apresentam algumas limitações. A utilização de compostos naturais, que poderão apresentar efeitos reduzidos sobre células não cancerígenas, constitui uma potencial alternativa. De entre os vários compostos, a fucoidana, um polissacarídeo sulfatado extraído de algas castanhas, apresenta propriedades biológicas interessantes. Uma vez que diferentes fucoidanas podem apresentar diferentes comportamentos antitumorais, um dos principais objetivos deste trabalho de doutoramento foi otimizar a utilização da fucoidana para o desenvolvimento de abordagens terapêuticas. Neste sentido, no Capítulo III, diferentes fucoidanas extraídas de *Fucus vesiculosus* foram testadas sobre células tumorais de mama e células normais. Três comportamentos biológicos distintos foram observados: i) toxicidade para células tumorais e normais; ii) toxicidade para células tumorais a concentrações mais baixas do que para células normais (i.e. comportamento antitumoral efetivo) e iii) toxicidade para células normais a concentrações mais baixas que células tumorais (para concentrações elevadas). A discrepância entre estes comportamentos foi atribuída a diferenças na posição dos grupos sulfato e às ramificações na cadeia polimérica. O potencial anti-angiogénico do extrato antitumoral efetivo foi validado através de um ensaio de formação de vasos (*in vitro*) e implantação na membrana corioalantóide (*in vivo*) (Capítulo IV). Os efeitos citotóxicos deste extrato foram também demonstrados sobre uma linha celular de melanoma. Numa abordagem complementar, uma membrana para o tratamento do melanoma foi desenvolvida mediante imobilização da fucoidana na superfície de malhas de nanofibras produzidas por electrofiação (Capítulo V). Para potenciar o uso deste polímero de origem marinha, a fucoidana tipo iii foi utilizada no desenvolvimento de um sistema de libertação de fármaco para o tratamento do cancro da mama. Gemcitabina, um fármaco quimioterapêutico, foi eficazmente encapsulada em nanopartículas (NPs) de fucoidana/quitosano, demonstrando maior toxicidade sobre células tumorais do que sobre células endoteliais (Capítulo VI). Tendo por objetivo reduzir os efeitos secundários do fármaco e para desenvolver terapias mais precisas, um anticorpo (ErbB-2) foi imobilizado à superfície das NPs (Capítulo VII). A capacidade das NPs serem direcionadas para as células tumorais foi confirmada através de um sistema de co-cultura (maior toxicidade para as células tumorais). Ensaios *in vivo*, demonstraram comprometimento do crescimento dos tumores e metastização nos pulmões. Estes estudos apresentam estratégias à base de fucoidana (quer na forma de extratos quer de sistemas) tendo em vista o desenvolvimento de terapias antitumorais mais eficientes. **Palavras-chave:** Antitumoral, cancro da mama, fucoidana, malhas de nanofibras, melanoma, sistemas de libertação de fármacos, sistemas direcionados

TABLE OF CONTENTS

LIST OF ABBREVIATIONS

A

Abs – Absorbance
ABTS - 2,2′-azino-bis (3-ethylbenzthiazoline-6-sulfonic acid
AFM – Atomic force microscopy
ANOVA – Analysis of variance
ATCC - American Type Culture Collection

B

bFGF – Basic fibroblast growth factor
BSA – Bovine serum albumin

C

Calcein-AM – Calcein-Acetoxymethyl
CAM – Chick chorioallantoic membrane
CF – Crude Fucoidan
CH – Chitosan
CH_3OH - Methanol
$CHCl_3$ – Chloroform
Cl^- – Chloride ion
cm – centimeter
CO_2 – Carbon dioxide
CTR – control

D

°C – Degree Celsius
d – Days
Da – Dalton
DA – Degree of acetylation
DAB - 3,3'-diaminobenzidine
DAPI – 4',6-diamidino-2-phenylindole
DDS – Drug delivery system
DGAV – Direcção Geral de Alimentação e Veterinária
DLS – Dynamic light scattering
DMEM – Dulbecco's modified Eagle's medium
DMF - N,N-dimethylformamide
DMSO – Dimethylsulfoxide
DNA - Deoxyribonucleic acid
DOX - Doxorubicin
DTAF - 5-([4,6-Dichlorotriazin-2-yl] amino)fluorescein hydrochloride
2D – 2-Dimensional
3D – 3-Dimensional

E

EC – Endothelial cells
ECGS – Endothelial cell growth supplement
ECM – Extracellular matrix
EDC - 1-[3-(Dimethylamino) propyl]-3-ethylcarbodiimide hydrochloride
e.g. – For example, from Latin *exempli gratia*
ELISA – Enzyme-linked immunosorbent Assay

EMEM – Eagle's Minimum Essential Medium
Erb-2 or HER-2 – human epidermal growth factor
et al. – And others
EtOH - ethanol
eV – electron Volt
Ex/Em – Excitation/Emission

F
FBS – Fetal bovine serum
FDA – Food and drug administration
FE - Fucoidan extract
FELASA – Federation for Laboratory Animal Science Associations
FGF-2 – Fibroblast growth factor
FITC – Fluorescein isothiocyanate
Fu – Fucoidan

G
g – grams
GC – Gas cromatography
GC-qMS – Gas cromatograhy – quadrupole mass spectrometry
Gem – Gemcitabine (2'-Deoxy-2',2'-difluorocytidine)
GFs – Growth factors
GPC – Gel permeation chromatography

H
h – Hours
HCl – Hydrochloric acid
HCO_3^{2-} – Bicarbonate ion
hDFs – human dermal fibroblasts
H&E – Hematoxylin–eosin
HG – High glucose
HIF-1 – Hypoxia-inducible factor-1
hKCs – Human keratinocytes
HMW – High molecular weight
H_2O_2 – Hydrogen peroxide
HRP – Horseradish peroxidase
Hz – Hertz

I
i.e. – "In other words", from latin *id est*

K
K^+ – Potassium ion
K_2SO_4 – Potassium sulfate
kDa – kiloDalton
kV - kiloVolt

L
LCGS - Low Serum Growth Supplement
LG – Low glucose
LMW – Low molecular weight

M

M – Molar
M106 – Medium 106
M199 - Medium 199
MEM – Minimum Essential Medium
MEX – Methotretaxe
mg – milligram
Mg^{2+} – Magnesium ion
Min – minute
mL – Milliliter
mm – Millimeter
mM – Millimolar
Mol – Mole
MTS – Tetrazolium
Mw– Molecular weight
µL - microliter
µm – micrometer
µg mL^{-1} – microgram per milliliter
mg mL^{-1} - milligram per milliliter

N

n – Number of samples
N.a. – Not applicable, Not available
Na^{+} – Sodium ion
$NaBD_4$ – Sodium borodeuteride
$NaBH_4$ – Sodium borohydride
NaF – Sodium Fluoride
$NaHCO_3$ – Sodium Bicarbonate
NaH_2PO_4 – Monosodium Phosphate
NaCl – Sodium chloride
NaOH – Sodium hydroxide
N.d. – Not defined
NFM – Nanofibrous mesh
NFM_Fu – Nanofibrous mesh with immobilized fucoidan
NH_2 - amine group
NHS - *N*-hydroxysuccinimide
nm – Nanometer
NPs – Nanoparticles
NPs+Gem – Nanoparticles with gemcitabine
NPs+Gem+Ab – Nanoparticles with gemcitabine and immobilized ErbB-2
NTA - Nanoparticle tracking analysis

O

OW – osmotized water

P

% – Percentage
PAX – Paclitaxel
PBS – Phosphate buffer saline
PCL – Polycaprolactone
PDGF - Platelet-derived growth factor
Pdi – Polydispersive index
Pen/strep – Penicillin-Streptomycin

PFA – Paraformaldehyde
pH - Hydrogenionic potential
Phalloidin - Phalloidin–Tetramethylrhodamine B isothiocyanate
PI – Propidium iodide
p – Statistical level of significance
þg – picogram

R

Rpm – Rotations per minute
RT – Room temperature
Ru – Rutin

S

SD – Standard deviation
SAR - Structure activity relationship
SDF-1 – Stromal derived factor-1
SEM – Scanning electron microscopy
SO_4^{2-} - Sulfate
STEM – Scanning transmission electron microscopy

T

TBO – Toluidine blue
TCPs – Tissue culture polystyrene
TFA – Tube formation assay
TME – Tumor microenvironment

U

U – Units
UP W – Ultra-pure wáter
USA – United States of America
UV – Ultraviolet
UV-O – Ultraviolet-Ozone

V

V – Volume
(v/v) – Percentage of volume/volume
VEGF – Vascular endothelial growth factor

X

XPS - X-ray photoelectron spectroscopy

W

(w/v) – Percentage of weight/volume
%wt. – Percentage of weight

λ – Wavelength

Z

ZP – Zeta potential

LIST OF EQUATIONS

LIST OF FIGURES

LIST OF TABLES

SHORT *CURRICULUM VITAE*

Ana Catarina Freitas Salazar de Oliveira was born on the 15th of April 1990, in Guimarães, Portugal. She is currently a PhD student at 3B's Research Group, I3Bs Research Institute on Biomaterials, Biodegradables and Biomimetics, at University of Minho, Headquarters of the European Institute of Excellence on Tissue Engineering and Regenerative Medicine at Avepark, Caldas das Taipas, Guimarães, Portugal.

She graduated in Biomedical Engineering at University of Minho, Braga, Portugal with a final grade of 15/20, in 2013. During the master thesis, she had the opportunity to go abroad during 6 months, to the Developmental BioEngineering Group at University of Twente, The Netherlands, under the scope of the ERASMUS program. During this period, she worked with hydrogel-based systems for islet of Langerhans encapsulation to treat diabetes, which resulted in a publication. Afterwards, she concluded her master thesis at 3B's Research Group with a final grade of 19/20. The work developed under this thesis resulted in a publication and an international patent application about the functionalization of electrospun nanofiber meshes with different antibodies for the specific binding of different growth factors, depending on the final intended application.

In 2014, she started a research grant at the 3B's Research Group, University of Minho, Portugal, where she started working with marine-based polymers. In 2016 she started her PhD, under the supervision of Dr. Albino Martins and Dr. Tiago H. Silva in the field of antitumor behavior of marine-based materials

Scientifically, Catarina has contributed with 6 peer-reviewed papers in international journals (plus 5 submitted), 3 book chapters and 1 international patent. Furthermore, she participated in international conferences with 2 oral communications and 9 poster communications.

LIST OF PUBLICATIONS

The work performed during the PhD period resulted in the publications listed below:

INTERNATIONAL PUBLICATIONS IN SCIENTIFIC PEER-REVIEWED JOURNALS

Oliveira C., Ferreira, A. S., Novoa-Carballal R., Nunes C., Pashkuleva I., Neves N. M., Coimbra M. A., Reis R. L., Martins A., Silva T. H. *The Key Role of Sulfation and Branching on Fucoidan Antitumor Activity*. Macromolecular Bioscience, 17(5), doi:10.1002/mabi.201600340, 2017

Oliveira C., Neves N. M., Reis R. L., Martins A., Silva T. H. *Gemcitabine delivered by fucoidan/chitosan nanoparticles presents increased toxicity over human breast cancer cells*. Nanomedicine, 13 (16), doi:10.2217/nnm-2018-0004, 2018

Oliveira C., Granja S., Neves N. M., Reis R. L., Baltazar F., Silva T. H., Martins A. *Fucoidan from Fucus Vesiculosus inhibits new blood vessel formation and breast tumor growth in vivo.* Carbohydrate Polymers, 223 (115034), doi.org/10.1016/j.carbpol.2019.115034, 2019

Oliveira C., Gonçalves C., Neves N. M., Reis R. L., Costa B., Silva T. H., Martins A. *Functionalized marine-polymeric nanoparticles targeting ErbB-2 impair breast cancer cells growth and metastasis*. (Submitted)

Oliveira C., Soares A, I., Neves N. M., Reis R. L., Marques A. P., Silva T. H., Martins A. *Effective fucoidan-based therapeutic strategies to treat melanoma.* (Submitted)

Oliveira C., Neves N. M., Reis R. L., Martins A., Silva T. H. *Fucoidan: from a biological active compound to a component for anti-cancer strategies.* (Submitted)

Sousa R. O., Alves A., Carvalho D., Martins E., **Oliveira C.,** Silva T. H., Reis R. L. *Acid and enzymatic extraction of collagen from Atlantic cod (Gadus morhua) swim bladders envisaging health-related applications.* Journal of Biomaterials Science, doi.org/10.1080/09205063.2019.1669313, 2019

Sousa R. O., Martins E., Carvalho D., Alves A., **Oliveira C.**, Duarte A. R. C., Silva T. H., Reis R. L. *Collagen from Atlantic cod (Gadus morhua) skins extracted using CO_2 acidified water with potential application in healthcare.* (Submitted)

Casanova M. R., **Oliveira C.**, Fernandes E. M., Reis R. L., Silva T. H., Martins A., Neves N. M. *Spatial immobilization of autologous growth factors to control vascularization in bone tissue engineering*. (Submitted)

BOOK CHAPTERS

Reys L. L., **Oliveira C.**, Oliveira J. M., López-Cebral R., Silva S. S., Silva T. H., and Reis R. L., *Polissacarídeos de origem marinha para aplicação em estratégias de engenharia de tecidos.* Valorização dos Recursos Marinhos: Biomateriais em Regeneração de Tecidos e Libertação de Fármacos, Eds. Sotelo, C. G., Pilar S. P., Marato, J., José V. A., Pérez-Martín R.I., Silva, T. H., and Reis R. L., IIM-CSIC, Vigo, Espanha, pp. 107-145, 2015.

Reys L. L., Silva S. S., **Oliveira C.**, López-Cebral R., Neves N. M., Martins A., Oliveira J. M., Silva T. H., Reis R. L. *Marine origin polysaccharides for tissue engineering and regenerative medicine: chitosan and fucoidan as illustrative examples*. (Under Editor revision)

Oliveira C., Carvalho A. C., Neves N. M., Reis R. L., Martins A., Silva T. H. *Marine derived biomaterials for cancer treatment.* (Biomaterials for 3D tumor Modeling, Elsevier. Under editor revision)

CONFERENCE ORAL PRESENTATIONS

Silva T. H., **Oliveira C**., Reys L. L., Soares da Costa D., Novoa-Carballal R., Oliveira N. M., Ferreira A. S., Nunes C., Silva S. S., Martins A., Coimbra M. A., Mano J. F., Neves N. M., and Reis R. L. Biomedical potential of fucoidan, a seaweed sulfated polysaccharide: from an anticancer agent to a building block of cell encapsulating systems for regenerative medicine. Front. Bioeng. Biotechnol, pp. 221, doi:10.3389/conf.FBIOE.2016.01.00221, 10th World Biomaterials Congress, Montréal, Canada, 2016.

Oliveira C., Neves N. M., Reis R. L., Martins A., Silva T. H. *Synergistic toxic effect of marine-origin polymeric nanoparticle loaded with gemcitabine over human breast cancer cells*. European Society for Biomaterials, Maastrich, The Netherlands, 2018

Oliveira C., Granja S., Neves N. M., Reis R. L., Baltazar F., Silva T. H., Martins, A. *Fucoidan impairs the formation of tubular-like structures in vitro and inhibits tumor growth in vivo.* TERMIS-EU, Rhodes, Greece, 2019

CONFERENCE POSTERS

Oliveira C., Ferreira A. S., Novoa-Carballal R.; Nunes C., Pashkuleva I., Neves N.M., Coimbra M.A., Reis R.L.; Martins A., Silva T.H. *Structure-activity relationship on fucoidan extracts towards anti-tumor therapy*. TERM-STEM, Guimarães, Portugal, 2016

Oliveira C., Neves N. M., Reis R. L., Martins A., Silva T. H. *Fucoidan-based nanoparticles for the delivery of antitumor agents.* Chem2nature, Porto, Portugal, 2017

Oliveira C., Neves N. M., Reis R. L., Martins A., Silva T. H. *Gemcitabine delivered by fucoidan-based nanoparticles presents increased toxicity over human breast cancer cells.* TERM-STEM, Porto, Portugal, 2017

Oliveira C., Granja S., Neves N. M., Reis R. L., Baltazar F., Silva T. H., Martins A. *Fucoidan impairs angiogenesis and tumor growth in vivo.* Chem2Nature, Porto, Portugal, 2018

Oliveira C., Granja S., Neves N. M., Reis R. L., Baltazar F., Silva T. H., Martins A. *Fucoidan inhibits new blood vessels formation in a tumor microenvironment*. TERMIS-WC, Kyoto, Japan, 2018

Oliveira C., Neves N. M., Reis R. L., Silva T. H., Martins A. *Fibrous meshes coated with fucoidan induces skin cancer cells death without affecting normal fibroblasts*. Gene2Skin, Guimarães, Portugal, 2018

Oliveira C., Neves N. M., Reis R. L., Silva T. H, Martins A. *Fucoidan-coated Fibrous Mesh as a Skin Patch to Treat Melanoma*. SFB, Seatle, USA, 2019

Oliveira C., Neves N. M., Reis R. L., Silva T. H., Martins A. *ErbB-2 antibody immobilized at the surface of marine-polymeric nanoparticles targeting breast cancer cells*. Forecast, Porto, Portugal, 2019

Sousa R. O., Alves, A., Carvalho, D., Martins, E., **Oliveira, C.,** Silva, T. H., Reis, R. L. *Collagen extraction from codfish (Gadus morhua) skins using CO2 acidified water.* Chem2Nature, Porto, Portugal, 2018

OTHER PUBLICATIONS (work not directly related with the PhD):

Oliveira C., Costa-Pinto A. R., Reis R. L., Martins A. and Neves N. M. *Biofunctional nanofibrous substrate comprising immobilized antibodies and selective binding of autologous growth factors*. Biomacromolecules, 15(6) 2196-2205, doi.org/10.1021/bm500346s. 2014

Marchioli G., Zellner L., **Oliveira C.**, Engelse M., Koning E., Mano J., Karperien M., Apeldoorn, A, and Moroni, L. *Layered PEGDA hydrogel for islet of Langerhans encapsulation and improvement of vascularization*. Journal of materials science. Materials in medicine. 6004-6, doi.org/10.1007/s10856-017-. 2017

Patent: Martins A., **Oliveira C.**, Reis R. L., Neves N. M., "*Polymeric substrates with immobilized antibodies and method of production thereof*". Application Number: EP 15724363.5/ Application Number US: 15/307,698

AWARDED GRANTS

Horizonte Norte2020 PhD scholarship (Norte-08-5369-FSE-000037)

INTRODUCTION TO THE THESIS FORMAT

To make a clear organization of the work performed under the scope of this PhD, this thesis is divided into four main sections (1 to 4), comprising eight chapters (**I** to **VIII**).

In Section I, a general introduction can be found that includes **Chapter I.** This section is followed by a complete Materials and Methods description, corresponding to Section 2, that includes **Chapter II**. Experimental studies and results, as well as their discussion are present in Section 3, comprising **Chapters III** to **VII**. This corresponds to the main body of the thesis and is based on a series of publications published or submitted for publication in international journals. These chapters are presented in a research paper format, *i.e.* abstract, introduction, experimental section, results, discussion, conclusion and acknowledgments. At the end of each chapter a list of relevant references is also stated. Final Conclusions and Future Perspectives can be found in the last section of this thesis, Section 4 (**Chapter VIII**).

Section 1 – General introduction

Chapter I – Introduction: This chapter provides a state of the art to the fucoidan antitumor activity. The latest advances and its mechanism of action are stated, as well as the most recent fucoidan-based systems, namely for drug delivery.

Section 2 – Detailed description of experimental materials and methodologies

Chapter II – Materials and Methods: A description of the materials used along the different chapters of this thesis, as well as the methods/techniques applied to obtain the results described in Section 3 is provided.

Section 3 – Experimental work regarding the different fucoidan-based approaches for the development of anti-cancer strategies

Chapter III – The key role of sulfation and branching in fucoidan antitumor activity: This chapter describes the biological and chemical characterization of different fucoidan extracts that present distinct antitumor responses, trying to understand which chemical features that play a decisive biological role.

Chapter IV – Fucoidan from *Fucus vesiculosus* inhibits new blood vessel formation and breast tumor growth *in vivo*: An effective fucoidan extract (the one that presented toxicity to cancer cells without affecting normal cells at a defined concentration) was used to assess its anti-angiogenic potential. Two standard angiogenesis models, i.e. the endothelial cell tube formation (*in vitro*) and the CAM (*in vivo*) assays were conducted.

Chapter V – Effective fucoidan-based therapeutic strategies to treat melanoma: The cytotoxic effects of the effective fucoidan extract was assessed over human melanoma and normal skin cells (i.e. fibroblasts and keratinocytes). Fucoidan was also immobilized at the surface of an electrospun nanofibrous mesh aiming to develop a skin patch.

Chapter VI – Gemcitabine delivered by fucoidan/chitosan nanoparticles presents increased toxicity over human breast cancer cells: A fucoidan that did not present antitumor activity was combined with another marine-origin polymer (i.e. chitosan) to produce nanoparticles for the delivery of gemcitabine, a chemotherapeutic drug. The nanoparticles system was optimized and its cytotoxic effects were evaluated over human normal and breast cancer cells.

Chapter VII – Marine-polymeric nanoparticles targeting ErbB-2 impair breast cancer cells growth and metastasis: An antibody that specifically targets a group of breast cancer cells was immobilized at the surface of the previously described nanoparticles, aiming to reduce the side effects of gemcitabine. This targeting system was validated *in vitro* in a co-culture system and in a mice model.

Section 4 – Concluding remarks

Chapter IX – General Conclusions and Future Perspectives: The general conclusions of the developed work, namely current limitations and potential benefits to be pursued are described in this last section of the thesis.

"*The important thing is to not stop questioning. Curiosity has its own reason for existing.*"

Albert Einstein

SECTION 1

GENERAL INTRODUCTION

Chapter I

Introduction

Chapter I*

Introduction

ABSTRACT

Due to the severe side-effects and the toxicity to healthy tissues, cancer treatments based in chemotherapy do not fully achieve the desire outcomes so far. The use of natural substances with similarities to native tissues may be of great value to develop better tolerated therapies. Fucoidan is a marine sulfated polysaccharide extracted from brown algae that, besides other biological activities (namely anti-viral, anti-inflammatory and angiogenic), has been reported to present interesting anticancer potential. This review briefly describes fucoidan structure, chemical properties and the above-mentioned biological features, focusing on its anticancer capability. Fucoidan usage as soluble agent or in combination with different chemotherapeutic drugs presents promising results herein described for different types of cancer (lung, colorectal, breast and melanoma). Since different mechanisms of action have been reported, the underlines behind fucoidan antitumor behavior are also addressed. Trying to enhance and optimize fucoidan usage in the cancer field, different systems, namely drug delivery, have been recently developed to target different types of cancers, that will be presented in detail. The production and features of these drug delivery systems are described, highlighting the role of fucoidan on their reported or envisaged performance.

* This chapter is based on the following publications:

Oliveira C., Neves N. M., Reis R. L., Martins A., Silva T. H. *Fucoidan: from a biological active compound to a component for anti-cancer strategies.* (Review paper, submitted)

Oliveira C., Carvalho A. C., Neves N. M., Reis R. L., Martins A., Silva T. H. *Marine derived biomaterials for cancer treatment.* (*Biomaterials for 3D tumor Modeling, Elsevier*. Under editor revision)

I-1. INTRODUCTION

Cancer is one of the leading causes of death worldwide, with an increasing tendency over the last years. Among the different types of cancer, breast, lung and colon cancer are the most common, being lung cancer the deadliest for both man and woman [1]. The heterogeneity of cancer cells, as well as the different development stages compromise the advances and availability of more effective anti-cancer therapies. Current treatment approaches of cancer can be surgery, radiation therapy, chemotherapy, targeted and immunotherapies, which may be used alone or in combination, depending on the properties of each cancer [2]. Radiation therapy uses high doses of radiation to kill cancer cells and shrink tumors, whereas chemotherapy uses anticancer drugs to kill cancer cells. Both treatments may present severe side effects since they affect not only cancer cells but also healthy ones [3, 4]. Immunotherapy is a type of biological treatment that helps the immune system to fight cancer, while targeted therapies aim to develop more effective treatments that specifically affect cancer cells, aiming to reduce the side effects over non-cancerous cells and tissues [5]. To develop effective anticancer therapies, the tumor microenvironment needs to be considered since it comprises not only the cancer cells but also surrounding healthy tissues [6]. In this sense, the use of natural-based approaches with low-toxicities over healthy tissues are interesting possibilities to develop more effective strategies with less side-effects [4].

The oceans represent the largest habitat of the earth, covering more than 70% of its surface. The different oceanic zones and environments offers a wide variety of marine organisms with unique chemical and biological properties that terrestrial natural products may not present. Each year the seafood processing industries produce about 75% of by-products from marine-origin organisms that despite being currently considered as waste or directed to lower added value fields, as animal feed, may be further explored and processed to produce compounds and materials [7-9]. The compounds may present different physicochemical features that result in interesting biological properties to the biomedical field, namely low toxicity and low-cost production [10, 11]. Different biopolymers may be isolated from marine organisms, which can be divided into three different groups: proteins, polysaccharides and nucleic acids [7]. Among them, sulfated polysaccharides have received particular attention given the wide range of biological activities being reported. In particular, fucoidan, mainly produced from brown algae, will be described in this introduction, namely in relation to its anti-cancer capabilities. Its physicochemical similarities to compounds present in native human tissues and the low toxicity are features of interest. However, it presents some limitations like batch-to-batch variability, since the season and local of harvesting may influence the polysaccharide properties, as well as the use of different extractions

methods that may influence the final biological outcomes. In this sense, sustainable and standardize methods are required to obtain controlled and reproducible compounds, as currently the biological activity of a fucoidan extract cannot be taken for granted, being always required to confirm it previously to application (and not rarely such biological activity is not confirmed) [12, 13].

I-2. FUCOIDAN STRUCTURE AND CHEMICAL FEATURES

Fucoidans are a class of sulfated polysaccharides mainly composed by fucose that can be extracted from different species of brown algae [14]. Fucoidans are already available in food and dietary supplements and in cosmetics; however, are not yet approved in biomedical applications neither by direct administration nor by its incorporation within biomaterials [15]. Therefore, intensive research is being performed in drug delivery, biomaterials and as a topical and orally delivered bioactive agent, showing promising outcomes [16]. Despite these achievements, variable and contradictory results compromise fucoidan usage in clinic [17]. The huge variety of algae fucoidan sources, allied to various extraction and purification methods, may influence fucoidan's intrinsic properties and bioactivity [14, 16]. Molecular weight and sulfation degree have been the most studied factors, although carbohydrates composition and sulfates position also play a role (**Figure I-1**).

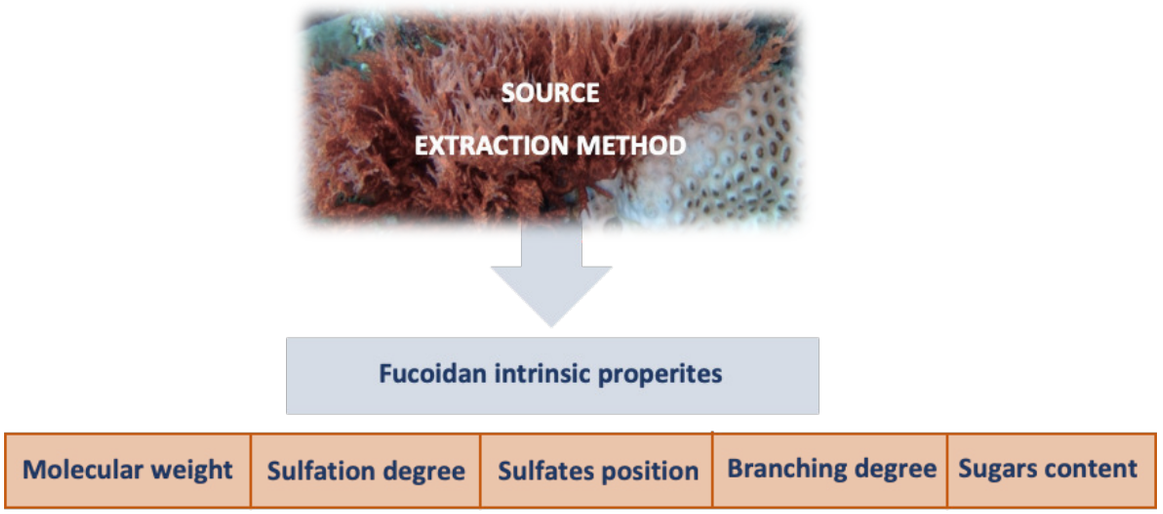

Figure I-1 The source and extraction method may influence fucoidan intrinsic properties, influencing biological outcomes.

I-3. FUCOIDAN COMPOSITION AND CHEMICAL STRUCTURE

Fucoidan may be extracted from different seaweed species presenting different chemical compositions. In general, fucoidans from brown algae present a backbone of α(1→3) L-fucopyranose residues or of alternating α(1→3) and α(1→4)-linked L-fucopyranosyls, that can be replaced by sulfate or acetate and/or have side branches containing fucopyranoses or other glycosyl units, e.g. glucuronic acid. Fucoidan structures may also be composed of other monosaccharides as glucose, xylose, galactose and mannose [18, 19].

Fucus vesiculosus (belongs to the order of Fucales) is the most common fucoidan's species source, being mainly composed of 1,2-α-fucose often sulfated. Most of sulfate groups are located at position C-4 of the fucose units. Despite the relatively simpler composition of fucoidan from *Fucus vesiculosus*, most fucoidans present much more complex structures. In the case of fucoidan extracted from *Ascophyllum nodosum* (Fucales), an α(1→3)-linked fucose backbone and a high proportion of α(1→4) linkages mainly sulfated at O-2, to a lesser extent at O-3, and only slightly at O-4, and fucose 2, 3-O-disulfate residues were observed. In the same order of Fucales, *Fucus evanescens* and *Fucus serratus*, give rise to fucoidans presenting similar structures, with a large proportion of both α(1→3)- and α(1→4)-linked L-fucopyranose residues, which may be substituted with sulfate (SO_3^-) on C-2 and C-4. Fucoidan in the order of Laminariales present a chemical structure that is mainly composed of a backbone of α(1→3)-linked L-fucopyranose residues with sulfates at the C-2 position. Fucoidans isolated from *L. saccharina* consist of α(1→3)-linked L-fucopyranose units, however they can present sulfates at C-4 alone or at both C-2 and C-4. *Chorda filum* (Laminariales) present a similar structure, consisting of a backbone structure of poly-α(1→3)-linked L-fucopyranoses sulfated mainly at C-4. However, it can also be sulfated at the C-2 position, and with some of the α(1→3)-linked fucose residues being 2-*O*-acetylated [18-20]. This information on chemical structures of different fucoidan sources is collected in **Figure I-2**.

Despite the backbone structure is mainly the same, (1→3)-linked α-L-fucopyranose, there might be different sulfates substitutions, molecular weights, branching and sugar residues, which may lead to different biological outcomes. Thus, although all receive the same designation as fucoidan each extract is an individual entity.

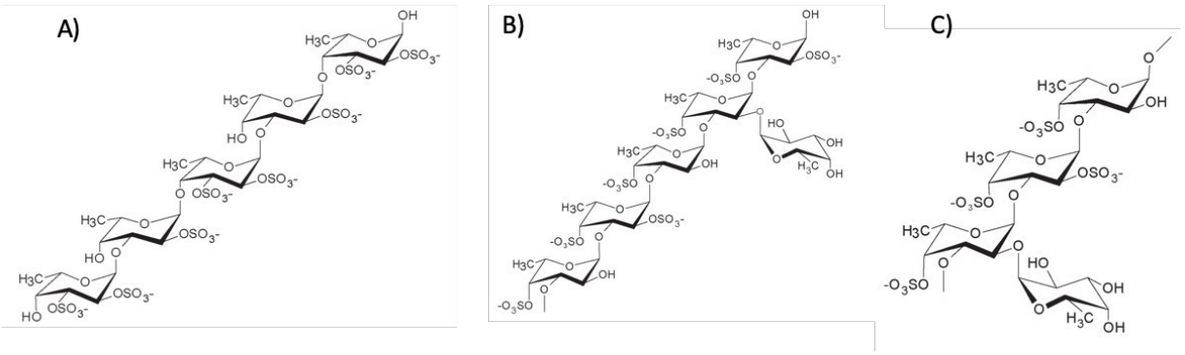

Figure I-2 Fucoidan chemical structure obtained from: A) *Fucus vesiculosus* and *Ascophyllum nodosum*, B) *Laminaria saccharina* and C) *Chorda filum*.

I-4. FUCOIDAN INTRINSIC PROPERTIES

As previously stated, the extraction conditions, algae species and life cycle state, among other, have a huge influence over fucoidan composition and chemical structure, providing extracts with different molecular weights and sulfate patterns [21]. The molecular weight is one of the factors that influence the biological activity of fucoidan, although it is difficult to establish a direct correlation based only in one property [22]. Specifically, low molecular weight fucoidan extracts have gained most attention due to their bioavailability, being explored in several biological conditions. For example, the synergistic effect of low-molecular-weight fucoidan (0.8 kDa) and fucoxanthin was studied in a diabetic mouse model, and this combination was able to maintain the homeostasis of glucose levels, having improved outcomes than when they were separately administered [23]. In a clinical trial, low-molecular-weight fucoidan (0.8 kDa) in combination with chemotherapeutic agents was shown to increase the disease control rate by 24% in patients with metastatic colorectal cancer [24]. In another attempt, fucoidan was hydrolyzed in fractions with different molecular weights, being observed cytotoxic effects over cancer cells were higher when using lower molecular weight fractions (<30 kDa). It was suggested that low molecular weight fractions have greater mobility and diffusivity than high molecular weight fucoidan, improving the interaction with cancer cell components [25]. The bioactivity of low molecular weight fucoidan fractions (10 - 37 kDa) obtained by gamma irradiation also demonstrated increased antioxidant effects [26]. Controversially, high molecular weight fucoidan was also reported to present anticancer and anti-inflammatory effects, which might indicate the relevance of other factors on the determination of biological activity [27, 28].

Besides the molecular weight, the sulfate content has been deeply studied regarding fucoidan biological responses. From previously reported works higher sulfation degree has been related with

enhanced bioactivity responses, namely anti-angiogenic and anticancer activities, which have motivated the production of oversulfated fucoidans [29, 30]. Over-sulfation leads to molecules with higher negative charge, which enables the formation of fucoidan-protein complexes that may hinder cells proliferation and thus, indirectly exerting the referred biological activities [31]. Besides the sulfate content, the position of the sulfate groups along fucoidan backbone and branching degree may also be related with fucoidan biological activities. In a previous paper, a fucoidan with effective anti-tumor activity presented higher percentage of fully branched chains (together in 3-O and 4-O-Fuc) than other fucoidan extracts that did not presented this biological activity [32].

The carbohydrate composition is another aspect that should be analyzed. As previously stated, fucoidans are mainly composed of fucose residues, often sulfated, but they also present other carbohydrates in its composition, as neutral sugars: xylose, galactose, mannose and glucose [33, 34]. They may also present uronic acids, which may be associated with the biological response of fucoidan [35]. The absence of fucoidan carbohydrate composition determination and its relation to the biological activities may be the cause of some contradictory results, being structure-activity relationship studies of utmost importance to reach more elucidative and consistent findings.

I-5. FUCOIDAN BIOLOGICAL ACTIVITIES

Fucoidans have been reported to present different biological activities, namely antiviral, both pro and anti-angiogenic, anti-inflammatory or anti-tumor. These activities will be discussed in this section, followed by a more detailed exploitation of the anti-tumor activity as this is the main focus of this thesis.

I-5.1. Anti-viral

Treatments against antiviral infections have been extremely challenging due to viruses' unique structures and their complex life cycle. Despite developments in vaccination and treatments against some viral infection, there are still several infections that affect people all around the word with no available and effective treatments. Better understanding of viral proliferation cycle and continuous research on the topic have helped in the discovery of new antiviral drugs. However, the control and treatment of viral infections has not yet reached the desired outcomes [36].

The anti-viral activity of fucoidan has been studied both *in vitro* and *in vivo.* Its low cytotoxicity, when compared with other anti-viral drugs currently in clinical use, seems promising regarding the development of more effective therapies [35]. It was reported that the key antiviral agents contained in brown algae are the sulfated polysaccharides, which mainly act by inhibiting the entry of enveloped viruses into host cells [37, 38].

The anti-viral effect of fucoidan has been studied mainly over Herpes Simplex Virus type I and type 2 (HSV-1 and HSV-2), Human Immunodeficiency Virus (HIV) and Hepatitis B Virus (HBV). Fucoidan from *Undaria pinnatifida* and *Cystoseira indica* have been studied over HSV-1 and HSV-2, presenting a more efficient antiviral activity when added at the time of the viral infection than when added after viral infection[38]. In another study, a crude extract had effective antiviral activity against HSV-1 and HSV-2, without presenting cytotoxicity for Vero cell cultures [39]. The potential effect of fucoidan extracted from three different species was evaluated to treat HIV [40]. When the extracts were pre-incubated with the virus, they block the early steps of HIV entry into the targeted cells. In this particular case, highly sulfated fucoidan did not demonstrate increased anti-viral activity and the authors suggested that maybe molecular weight or other structural were influencing. The anti-viral potential of fucoidan from *Fucus vesiculosus* has also been explored to treat HBV, showing promising results since fucoidan decreased serum HBV DNA, HBsAg and HBeAg levels, and hepatic HBcAg expression in HBV-infected mice [41]. The authors concluded that the activation of the extracellular signal-regulated kinase (ERK) pathway was related with fucoidan's inhibitory activity. Taken together, these results demonstrate the use of fucoidan as a potential anti-viral bioactive agent.

I-5.2. Anti-inflammatory

Inflammation may have two phases: acute and chronic, being distinguishable by their duration. Acute inflammation may occur during short periods of time and it is associated with accumulation of fluids, increased blood flow and number of leucocytes and other mediators, whereas chronic inflammation occurs during longer periods and it is associated with progression of specific cellular immune responses [42]. The advances in the field of inflammatory diseases lead to a better understanding of the different pathologies, although current treatment approaches still lack more effective anti-inflammatory drugs [43]. Marine algae may present an interesting source of unexplored anti-inflammatory compounds like polyphenols, sulfated polysaccharides and proteins. These marine-derived active agents may provide

interesting alternatives to currently available synthetic drugs, having potential protective effects over the pathogenesis of inflammatory diseases [44].

Fucoidan from *Fucus vesiculosus* has been described to reduce the severity of acute pancreatis in mice by decreasing neutrophil infiltration and systemic inflammation [45]. Fucoidan from the same species has demonstrated capability of reducing the inflammation of bowel disease when oral administered [46]. Fucoidan was reported to decrease neutrophil and macrophage accumulation, as well as the expression of inflammatory cytokines inhibiting radiation-induced pneumonitis and lung fibrosis [47]. Furthermore, fucoidan from *Undaria pinnatifida* had a similar effect as a glucocorticoid on an animal model of atopic dermatitis [48]. By its side, low molecular weight fucoidan, in a mice model of astheroclerosis, inhibited the production and expression of inflammatory cytokines, reducing the innflammatory response, validating fucoidan usage as an anti-inflammatory polyssacharide [49].

I-5.3. Angiogenic

Angiogenesis comprises the formation of new blood vessels. Usually, this process occurs under normal conditions, during tissue growth and repair. However, this process is also observed in some pathological conditions like diabetes and inflammatory diseases, being an unregulated process in tumor progression [50, 51]. Angiogenesis is mediated by different growth factors, like vascular endothelial growth factor (VEGF), fibroblast growth factors (FGF) and platelet-derived growth factor (PDGF), which activate cell migration, tube formation and maturation [52, 53]. The potential of fucoidan to regulate angiogenesis is still controversial since both pro- and anti-angiogenic potential responses have been reported.

The pro-angiogenic potential of fucoidans with several molecular weights has been evaluated, showing new blood vessel formation *in vivo* regarding bone repair [54] and an increased pro-angiogenic potential on HUVECs for low molecular weight fucoidan when compared with medium molecular weight [55]. In a different study, fucoidan did not present toxicity over melanoma cells lines, showing protective and pro-angiogenic potential instead [56].

Regarding the anti-angiogenic response, that is of significant importance as anti-cancer therapy as the lack of blood vessels hinders the tumor growth, intraperitoneal injections of fucoidan from *Laminaria saccharina*, inhibited tumor-related angiogenesis and breast tumor growth *in vivo* [57]. The authors associated differences in fucoidan fractions activities with the presence of high levels of O-sulfated fucose

units. In another study, fucoidan also inhibited angiogenesis and bladder cancer growth, which was associated with the down-regulation of HIF-1/VEGF signaling pathway [58]. The addition of fucoidan to endothelial cells seeded on top of matrigel, destroyed their typical tubular-like structures, diminishing both VEGF and PDGF expression [59]. Furthermore, low doses of fucoidan impaired angiogenesis and expression of VEGF and SDF-1 (stromal derived factor-1) in co-cultures models for bone repair and for vascularization processes in osteosarcoma [60]. Due to these contradictory results, a deep chemical and biological characterization of the different fucoidan extracts needs to be performed, but the apparent uniqueness of each fucoidan extract can already be highlighted.

I-5.4. Anti-cancer activity

Cancer is characterized by an uncontrolled cell growth and can start at any tissue of the body. Cancer cells can spread to tissues other than where they started, causing metastasis [61]. Although more people than ever have survived different types of cancer after treatment, cancer is still one of the main causes of death worldwide (**Figure I-3**) [1]. The type of cancer, size, location and development will influence the treatment modalities that may comprise chemotherapy, surgery and radiotherapy [62]. Surgery is the mostly common treatment modality used to remove the tumor, whereas chemotherapy uses cytotoxic drugs in a systemic way, which may affect healthy tissues leading to severe side effects [63]. Radiation therapy uses high energy beams to destroy cancer cells and may be used before surgery [3]. Target therapies rely on targeting specific markers leading to less side effects [64]. These treatments may be applied in a single or combined way.

Depending on the drugs and treatment duration, severe side effects may be observed, the reason why more effective anti-cancer drugs are needed. Fucoidan anti-cancer capability has gained tremendous interest in the last years and has been studied over different types of cancer like breast, lung, colorectal and melanoma that will be further discussed.

Estimated New Cases

Males			Females		
Prostate	174,650	20%	Breast	268,600	30%
Lung & bronchus	116,440	13%	Lung & bronchus	111,710	13%
Colon & rectum	78,500	9%	Colon & rectum	67,100	8%
Urinary bladder	61,700	7%	Uterine corpus	61,880	7%
Melanoma of the skin	57,220	7%	Melanoma of the skin	39,260	4%
Kidney & renal pelvis	44,120	5%	Thyroid	37,810	4%
Non-Hodgkin lymphoma	41,090	5%	Non-Hodgkin lymphoma	33,110	4%
Oral cavity & pharynx	38,140	4%	Kidney & renal pelvis	29,700	3%
Leukemia	35,920	4%	Pancreas	26,830	3%
Pancreas	29,940	3%	Leukemia	25,860	3%
All Sites	**870,970**	**100%**	**All Sites**	**891,480**	**100%**

Estimated Deaths

Males			Females		
Lung & bronchus	76,650	24%	Lung & bronchus	66,020	23%
Prostate	31,620	10%	Breast	41,760	15%
Colon & rectum	27,640	9%	Colon & rectum	23,380	8%
Pancreas	23,800	7%	Pancreas	21,950	8%
Liver & intrahepatic bile duct	21,600	7%	Ovary	13,980	5%
Leukemia	13,150	4%	Uterine corpus	12,160	4%
Esophagus	13,020	4%	Liver & intrahepatic bile duct	10,180	4%
Urinary bladder	12,870	4%	Leukemia	9,690	3%
Non-Hodgkin lymphoma	11,510	4%	Non-Hodgkin lymphoma	8,460	3%
Brain & other nervous system	9,910	3%	Brain & other nervous system	7,850	3%
All Sites	**321,670**	**100%**	**All Sites**	**285,210**	**100%**

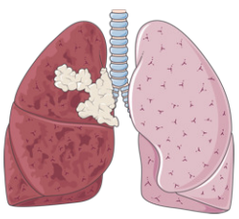
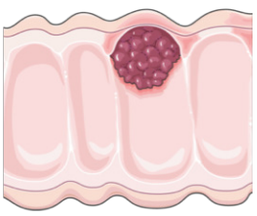
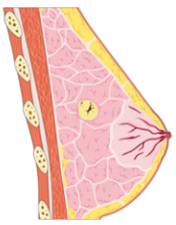
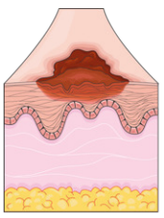

LUNG	COLON	BREAST	MELANOMA
Chance to develop:	Chance to develop:	Most common in women	Most aggressive skin cancer
1 in 15 men	1 in 22 men	2nd deadliest in women	Most diagnosed cancer in young adults
1 in 17 women	1 in 24 women	1 in 37 women are expected die	96,480 new cases
13% of new cancers	2nd most common (both sex)		7,230 estimated deaths
	2nd deadliest (both sex)		

Figure I-3 Ten Leading Cancer Types for the Estimated New Cancer Cases and Deaths by Sex, United States, 2019 [1]. Statistics of lung, colon, breast and melanoma.

I-5.4.1. Lung cancer

Lung cancer is the second most common cancer (both in man and woman) and the deadliest. About 13% of all new cancers are lung cancers [1, 2]. There are different types of lung cancer: carcinoid tumors, small cell and non-small cell, with the latest being the most common, accounting for 85% of all lung cancers. Like in most cancers, the possible treatments include surgery, radiation therapy, chemotherapy and targeted therapies, which may be used as single or combined treatments [65-67]. Native fucoidan from *Turbinaria conoides* presented an increased inhibition of lung cancer cells proliferation when compared with native fucoidan from *Undaria pinnatifida* [68]. In a different approach, fucoidan exhibited anti-metastatic effects over A549 cells via the down-regulation of different signaling pathways, resulting in decreased cell migration and invasion [69]. Furthermore, typical apoptotic characteristics, such as chromatin condensation and an increase in the population of sub-G1 hypodiploid cells, were observed by the addition of fucoidan, with an effective antiproliferative activity [70]. The effects of molecular weight was also analyzed with A549 cells showing that hydrolysis in boiling water with HCl significantly increased anticancer activity when compared with microwave hydrolysis of native fucoidan [71]. The simultaneous administration of fucoidan and cisplatin presented a synergistic effect by inhibiting cancer cells viability, inducing apoptosis trough upregulation of cleaved caspase-3 and poly (ADP ribose) polymerase expression [72]. This dual drug application allowed a decrease in cisplatin concentration, leading to diminished side effects. In another study, fucoidan activated the TLR4/ROS/ER signaling pathway, resulting in apoptotic cell death, both *in vitro* and *in vivo,* resulting in tumor shrinkage [73].

I-5.4.2. Colorectal cancer

Colon cancer is the second most common cause of cancer deaths, considering both man and woman (Figure I-3) [1]. Surgery is the most common treatment, where the tumor and adjacent lymph nodes are removed. Chemotherapy is often used in colon cancer treatments, which may also help to shrink the tumor before surgeries. Fucoidan from *Sargassum feldmannii* and *S. duplicatum* at different concentrations were tested over different types of colon cancer cell lines (DLD-1, HT-29 and HCT-116) and did not show any cytotoxicity [74]. However, in a similar study native and deacetylated fucoidan at 200 μg mL^{-1} inhibited colony formation of colon cancer cells [74]. Fucoidan inhibited HT-29 cell growth, migration and sphere formation by suppressing the PI3K/Akt/mTOR pathway [75]. A study that comprises *in vitro* and *in vivo* assays showed that fucoidan inhibited the growth and angiogenesis of colon

cancer cells [76]. Specifically, the intraperitoneal injection of fucoidan reduced tumor volume which was associated with induction of apoptosis and decreased angiogenesis mediated by Akt signaling. In another *in vivo* study over colon-26 cancer cell line, the oral administration of fucoidan suppressed tumor growth and prolonged survival times of tumor-bearing mice [77]. The molecular weight was defined as determinant of fucoidan anti-tumor effects, being an increased size of the population of natural killer cells the possible mechanism of action. In another attempt, the activation of caspases (via both the death receptor-mediated and mitochondria-mediated apoptotic pathways) was associated to fucoidan growth inhibition and induction of apoptosis in human colon cancer cells [78]. Complementary, fucoidan administration led to sub-G1 phase cell cycle arrest and inhibited cell growth and increased apoptotic cell death [79]. Since the human intestine does not have enzymes able to hydrolyze fucoidan, the administration of fucoidan may result in an increased concentration of luminal fucoidan within the large intestine [75, 80]. Having this in consideration, fucoidan seems to be an interesting alternative for the prevention of colon cancer. Besides this preventive effect, these studies showed that fucoidan has a potent anti-cancer effect over colon cancer both *in vitro* and *in vivo*.

I-5.4.3. Breast cancer

Breast cancer is the most common cancer in women and the second cause of death. The chance of woman dying of breast cancer is 1 in 37 [1, 81]. This type of cancer is characterized by a lump or thickening of the breast. Surgery, radiation and chemotherapies are the common possible treatments. Chemotherapeutics such as doxorubicin, paclitaxel and gemcitabine have been used in breast cancer chemotherapy [82, 83]. However, these chemotherapeutic agents often present severe side effects, namely toxicity to healthy tissues. Fucoidan decreased the viability of MCF-7 human breast cancer cells in a dose-dependent manner and arrested cell cycle in G1 phase which was associated with a decrease in the expression of specific markers [84]. Using a different breast cancer cell type, low molecular weight fucoidan inhibited MDA-MB-231 human breast cancer cells proliferation and promoted apoptosis, which was associated with caspases activation and mitochondrial malfunction [85]. The critical effect of molecular weight was analyzed by comparing the effects of low and high molecular weight fucoidan, over two breast cancer cell lines - MCF-7 and MDA-MB-231[86]. Low molecular weight fucoidan significantly increased cytotoxicity for both cell types. Fucoidan presented a time-dependent action over MCF-7, whereas induction of caspase-dependent apoptosis was observed in the MDA-MB-231 cells. Fucoidan at 400 mg/kg body weight per day inhibited the proliferation of MCF-7 cells implanted in rats, inducing

cancer cells apoptosis and suppressing cell migration by modulating *E*-cadherin and MMP-9 expression [87]. Proliferation of MDA-MB-231 and 4T1 (mouse breast cancer cells) was inhibited *in vitro,* and tumorigenesis and metastasis of the 4T1 cells was inhibited in mice, showing a decreased tumor volume and metastatic nodules in the lungs [88]. Fucoidan from *Fucus vesiculosus* presented toxicity over 4T1 cells, inducing apoptosis and down-regulation of VEGF. The tumor size and weight, as well as lung metastasis were reduced when fucoidan was injected in mice breast cancer cell models [89]. These in vivo results corroborate the *in vitro* studies, since this response was associated with decreased in angiogenesis and enhanced apoptosis. The combination of fucoidan with chemotherapeutic drugs (i.e.cisplatin, tamoxifen and paclitaxel) was also evaluated over breast cancer cell lines. This combination increased the therapeutic efficacy of the treatments, enhancing apoptosis in cancer cells, showing an increased level of ROS, suggesting that induction of oxidative stress is important for induction of cancer cell death [90].

I-5.4.4. Melanoma

Melanoma is not the most common skin cancer, but it is the most aggressive since it tends to spread and metastasize. It's one of the most diagnosed cancer in young adults (age group 25 to 30) [1]. Melanoma is mostly found in the skin, although it can also be found in other parts of the body such as eyes, mouth, genitals, and anal area. This cancer appears when melanocytes mutate and become cancerous. In the particular case of melanoma, surgery is the most common treatment, since unlike many internal cancers, it is easier to access and remove. Less common treatments for skin cancer may include chemotherapy and biological therapy [91, 92].

Fucoidan from *Undaria pinnatifida* was evaluated over different melanoma cells lines. It has been demonstrated that melanoma occurs by the activation of ERBB signaling, specifically through the ERBB3/ERBB2 cascade [93]. The authors demonstrated that the addition of fucoidan to a currently clinical approved inhibitor (lapatinib) of ERBB2/EGFR, inhibited melanoma cells' viability in 85%. Besides tumor growth inhibition, fucoidan also reduced the morbidity associated with prolonged use of lapatinib. In another attempt, fucoidan from two different sources presented toxicity over B16 cells (murine melanoma cells) in a dose-dependent manner [94]. Complementary results showed that the addition of fucoidan led to morphological changes in melanoma cells, indicating apoptosis. Furthermore, in a mice model used to validate the fucoidan efficiency *in vivo* it was observed that natural killers' activity was enhanced with fucoidan presence, acting as the key mediators of tumor cell death. In a similar study,

fucoidan from *Sargassum henslowianum* C. Agardh (FSAR) and *Fucus vesiculosus* (FVES) were evaluated over B16 cells, indicating a decreased cell proliferation [95]. FSAR presented more effective anti-cancer effects at lower doses than FVES, whereas the latter presented higher toxicities at higher doses than FSAR. Annexin V studies showed that both polymers induced apoptosis which was also achieved by the activation of caspase-3. In a recent study, fucoidan from *Fucus vesiculosus* showed increased cytotoxicity over melanoma cells in dose-dependent fashion, demonstrating cells morphological changes and apoptosis [96]. Despite the use of fucoidan is less studied for melanoma, it has shown interesting and effective results that should be further explored to develop more effective therapies to treat this aggressive type of skin cancer.

I-5.5. Drug delivery systems for anti-cancer therapies

Despite chemotherapy positive results in the treatment of different cancers, there are some associated problems and adverse side effects. Due to drugs poor bioavailability there is the need to administer them in increased dosages that can compromise the surrounding healthy tissues, having low therapeutic outcomes and the development of drug resistance [62, 97]. In this sense, the development of drug delivery systems, particularly featuring targeting functionality may overcome some of these current limitations since the carriers will not only protect the encapsulated drugs from the host immune system, but was also be able to transport them specifically to the cancerous tissues, releasing the drug at specific sites, thus reducing side effects as well as the needed dose to exert a therapeutic effect [98]. An increasing knowledge on tumor biology and the use of new materials have led to the development of more efficient systems with improved therapeutic efficacy. Additionally, nanotechnology, by the development of different types of nanoparticles (NPs, being metallic, polymeric, liposomes, micelles or hybrid), have showed interesting and effective results. They can be used to deliver a variety of therapeutic molecules and tend to accumulate in tumors site due to a leaky vascularization site and active cellular uptake [99, 100]. These systems also increase macromolecules circulation, protecting drugs from enzymatic circulation and control the drug release, reducing cytotoxicity and increasing therapeutic index. Nevertheless, these types of system may also present some drawbacks, since nanoparticles may be unstable during circulation and may be associated with uncertain toxicity (also related with accumulation in specific organs), especially for long-term administration [101-103]. The use of natural polymers to develop effective drug delivery systems have been explored by different groups, investigating several strategies

[103]. In this section, drug delivery systems that have been developed specifically based on fucoidan, will be described.

I-5.5.1. Fucoidan-based systems for anti-cancer therapies

Most of the studies that explore the potential use of fucoidan to treat different types of cancer, use it in the soluble form, as previously described. However, in recent years, fucoidan-based systems have been developed aiming more effective anti-cancer strategies. Most of them are nanosystems that comprise the use of nanoparticles, micelles or liposomes, playing an important role in biological systems [104]. Indeed, fucoidan have been included in nanosystems for diagnostic, drug delivery and regenerative medicine. The fucoidan-based systems developed for cancer applications have been summarized in **Table I-1**.

The majority of the systems have been developed for breast cancer. Fucoidan has been electrostatically assembled with positively charged polyethylenimine, and doxorubicin (DOX) has been loaded during the production of the nanoparticles system [105]. The produced NPs presented a size range between 41 to 160 nm (increase in fucoidan ratio lead to bigger NPs), a polydispersive index (Pdi) of 0.153 and were negatively charged. The release of DOX was evaluated at different pH and around 30% was released in the first 24h. Nanoparticles arrested the cell cycle progression in G1-S phase, followed by apoptosis. The system presented increased cytotoxicity when compared to the free drug, both *in vitro* and *in vivo*, where tumor shrinkage was observed. DOX has also been encapsulated into protamine/fucoidan nanoparticles [106]. These two compounds were able to produce stable nanoparticles only when weight ratios were lower than 1.0, indicating that the surface of NPs was covered with fucoidan. Therefore, negatively charged NPs were produced with a size around 180 nm. Around 70% of DOX was released in the first 24h at pH 7.4, whereas at lower pH 4.5 the release was much faster with 80% of dox being released in 12h. This result was attributed to deionized chemical groups and consequent weakness of electrostatic interactions between the NPs and the drug. The developed NPs presented increased cytotoxicity over MDA-MB-231 breast cancer cells when compared to the same concentration of free DOX, attributed to different cellular trafficking pathways. Gold nanoparticles coated with fucoidan and loaded with DOX were also developed, demonstrating to be stable up to 6 months [107]. This system showed to release the drug faster at the physiological pH, which may reduce the toxicity of the system over normal tissues. The IC50 of the nanoparticles was 5 $\mu g\ mL^{-1}$, whereas for the drug was 30 $\mu g\ mL^{-1}$, corroborating the efficacy of the system over MDA-MB-231 breast cancer cells. In

a similar approach, fucoidan coated gold nanoparticles incorporating DOX, were applied to remove eye tumors [108]. Nanoparticles were stable at physiological conditions and the system did not present toxicity to normal cells, although presenting increased cytotoxicity over cancer cells. The combination of the system with laser irradiation was even more effective, inducing around 90% of cell death (laser alone did not present significant toxicity). The combination therapy was also the most effective strategy *in vivo* when compared with loaded NPs or laser alone. In a different attempt, calcium carbonate microparticles produced by layer-by-layer technique (fucoidan and poly-L-ornithine), and incubated with doxorubicin, showed an efficient release of the drug and presented toxicity to cancer cells in a dose-dependent manner [109]. Gemcitabine (Gem) was loaded into fucoidan/chitosan nanoparticles with 115-140 nm, a Pdi<0.2, a positive zeta potential of 29 mV and a maximum entrapment efficiency of 42% [110]. These nanoparticles presented increased toxicity over cancer cells (around 25%) without increasing toxicity over normal cells when compared to the free drug. Two other studies also tested the developed systems for breast cancer. Methotretaxe (MEX) is a commonly used drug to treat osteosarcoma and breast cancer, although due to its short blood retention time, high doses are required. Trying to circumvent this problem, self-assembled nanoparticles comprising fucoidan and MEX were produced [111]. Nanoparticles' size increased from 130 nm to 163 nm with the incorporation of MEX and around 60% of the drug was released within 24h. The developed system presented increased cytotoxicity effects over MCF-7 and HeLa cells when compared with free MEX. In another attempt, fucoidan nanoparticles with affinity to P-selectin were developed [112]. The P-selectin was chosen because it presents increased expression on tumor cells and tumor vasculature than in normal tissues. These nanoparticles also encapsulate different drugs (i.e. paclitaxel, doxorubicin and MEK) aiming to develop more efficient systems to treat melanoma and breast cancer. The targeting systems presented increased toxicity when compared with untargeted drugs and nanoparticles.

Fucoidan-coated manganese dioxide nanoparticles in combination with radiation therapy resulted in significant pancreatic tumor shrinkage (by 46%) when compared with the control group without treatment, and by 22.5% compared to radiation therapy alone [113]. Two different fucoidan-based systems were developed aiming to treat cervical cancer: a novel complex of rutin-fucoidan presented higher toxicity over cancer cells than to normal cells, whereas silver nanoparticles coated with chitosan/fucoidan presented toxicity to cancer cells at 50 $\mu g\ mL^{-1}$ [114, 115]. Fucoidan-coated sulfide nanoparticles induced apoptosis in cancer cells in combination with near-infrared induced hyperthermic effect. This combination was applied to different tumors (Cervical, Lung and Leukemia), eliminating several tumors *in vivo* [116]. In another attempt, SPIONs were coated with fucoidan, which conferred a longer blood circulating half-time,

presented a 2x fold increase in glioma tumors uptake [117]. Regarding colon cancer therapies, the internalization of doxorubicin by the cells were much higher for acetylated fucoidan nanoparticles loaded with doxorubicin when compared with fucoidan-doxorubicin mixture or the free drug [118]. Fucoidan-coated gold nanoparticles presented cytotoxicity to colon cancer cells with no toxicity to normal fibroblasts [119]. Liposomes encapsulating fucoidan were also developed, inducing apoptosis of osteosarcoma cells and reducing tumor volume and weight *in vivo* comparing to native fucoidan [120]. In a different approach, fucoidan was added at the surface of an hydrogel (fluorenylmethoxycarbonyl) [121]. This self-assembly process was able to maintain fucoidan bioactivity, so that the scaffold provides a non-toxic environment for fibroblasts, although presenting toxicity to cancer cells.

These proposed systems presented interesting results regarding their effectiveness in different types of cancer. The use of fucoidan either for the development of drug delivery system or as a coating increased the toxicity over different cancer cells when compared to free drugs. However, due to the cytotoxic effects over non-cancer cells, it is also important to develop more effective therapies with fewer side effects, which is an aspect that is still missing in some studies.

Table I-1 Fucoidan-based systems for anti-cancer therapies.

CANCER TYPE	SPECIES	SYSTEM	DRUG	PREPARATION METHOD	REF
Breast	*F. vesiculosus*	Fucoidan/ polyethylenimine NPS	DOX	Electrostatic interactions	[105]
	F. vesiculosus	Fucoidan/chitosan NPs	Gem	Polyelectrolyte complexation	[110]
	F. vesiculosus	Fucoidan capped gold nanoparticles	DOX	The addition of fucoidan to $HAuCl4{\cdot}3H_2O$, under magnetic heater stirrer, resulted in the formation of AuNPs coated with fucoidan.	[107]
	F. vesiculosus	Fucoidan-drug based NPs	PAX (FiPAX); DOX (FiDOX)	FiPAX and FiMEK co-encapsulation and a near-infrared fluorophore. FiDOX: layer-by-layer assembly.	[112]

			MEK (FiMEK)		
	L. japonica	Fucoidan/ protamine NPs	DOX	Different protamine-to-fucoidan weight ratios	[106]
	n.d	Poly-allylamine hydrochloride (PAH) and fucoidan NPs	MEX	Self-assembly of two polyelectrolytes	[111]
	n.d	Calcium carbonate microparticles ($CaCO_3$MPs) coated with fucoidan and poly-L-ornithine (PLO)	DOX	CaCO3 MPs were prepared by co-precipitation. (PLO) and fucoidan where added by layer by layer.	[109]
Cervical	*F. vesiculosus*	Rutin-fucoidan complex	Rutin	Fucoidan was added dropwise to a completely dissolved solution of rutin	[114]
	F. vesiculosus	Silver nanoparticles with chitosan/fucoidan coating	-	Silver nitrate was added to fucoidan solution, followed by the addition of fucoidan.	[115]
	F. vesiculosus	Fucoidan-coated copper sulfide nanoparticles (F-CuS)	-	Synthesis of sodium citrate-stabilized copper sulfide nanoparticles (CuS) and coating using the layer-by-layer (LbL) technique (PAH and Fu)	[116]
	n.d	Poly-allylamine hydrochloride (PAH) and fucoidan NPs	MEX	Self-assembly of two polyelectrolytes	[111]
Colon	*F. vesiculosus*	Acetylated fucoidan (AcFu) nanoparticles	DOX	Fucoidan was dissolved in formamide solution, followed by addition of	[118]

				pyridine acetic anhydride. AcFu NPs were added into Dox solution.	
	n.d	Fucoidan coated gold nanoparticles (FMG–Au–NPs)	-	Synthesis of Fucoidan-mimetic(FM)-glycopolymers via a free-radical chain transfer polymerization reaction. Coating gold nanoparticles with FM-glycopolymers.	[122]
Eye	*F. vesiculosus*	Gold NPs coated with fucoidan	DOX	Fucoidan was poured into a solution to obtain Fu-coated Au-NPs.	[108]
Glioma	*F. vesiculosus*	dextran-coated superparamagnetic iron oxide nanoparticles (SPIONs) with fucoidan	-	Coating of SPIONs with fucoidan	[117]
Leukemia	*F. vesiculosus*	Fucoidan-coated copper sulfide nanoparticles (F-CuS)	-	Synthesis of sodium citrate-stabilized copper sulfide nanoparticles (CuS) and coating using the layer-by-layer (LbL) technique (PAH and Fu)	[116]
Lung	*F. vesiculosus*	Fucoidan-coated copper sulfide nanoparticles (F-CuS)	-	Synthesis of sodium citrate-stabilized copper sulfide nanoparticles (CuS) and coating using the layer-by-layer (LbL) technique (PAH and Fu)	[116]
Melanoma	*F. vesiculosus*	Fucoidan-drug based NPs	PAX	FiPAX and FiMEK co-encapsulation and a near-	[112]

			(FiPAX); DOX (FiDOX) MEK (FiMEK)	infrared fluorophore. FiDOX: layer-by-layer assembly.	
Osteosarcoma	*C. okamuranus*	Liposome Encapsulating Fucoidan	-	Liposome fraction was prepared by the mechanochemical method	[120]
Pancreatic	*F. vesiculosus*	Fucoidan-coated manganese dioxide nanoparticles (Fuco-MnO_2-NPs)	-	Manganese nanoparticles were produced, followed by a coating with fucoidan.	[113]
Tongue carcinoma	*n.d*	3D ECM-like scaffold	-	Fucoidan was added on the surface of co-assembled hydrogel formation	[121]

I-6. Conclusion and Future Perspectives

In this review, a briefly description of fucoidan chemical properties and the different biological activities that make fucoidan a promising and versatile polysaccharide to be applied in different biomedical fields are explained. Despite these enthusiastic results and the fact that fucoidan products have been commercialized as dietary or nutritional supplements for different diseases, including cancer, the use of fucoidan in the clinic has not been approved so far. Some contradictory results regarding its biological outcomes may be one of the possible reasons. To try to overcome this issue, and achieve more consistent and reproducible results, some aspects need to be considered. It is known that different extraction methods can lead to fucoidans with different chemical features that will have an impact in the final biological outcomes. This aspect was confirmed from the different reported works, regarding fucoidan anti-cancer activity. Optimization and standardization of extraction methods, that retaining the structural features of interest, should be addressed considering the most common and promising fucoidan species sources, namely *Fucus vesiculosus*. Another relevant aspect is to perform structure-activity relationship studies to elucidate the final chemical structure. As previously stated, different molecular weight, sulfates position and degree, as well as the polymer branching had a huge influence over the final biological

activity of fucoidan. Regarding the main focus of this review, fucoidan anticancer behavior, the mechanisms behind its action were discussed. However, as it was possible to conclude, different mechanisms may be involved, making it difficult to understand and get to a consensual pathway, which should be elucidate. An important aspect that is missing in some studies is the effects of fucoidan over non-cancer cells. There are innumerous reports regarding fucoidan usage as soluble bioactive anti-cancer agent. However, despite some clear evidences that fucoidan inhibits different cancer cell proliferation and tumor growth, its effects over normal cells is not always stated. It is known that current anti-cancer treatments can present severe side effects and, in this sense, it is important that the tumor microenvironment (that comprises other normal cells besides the cancer cells) is taken into consideration when trying to develop more effective anti-cancer therapies. Having this in consideration, the mechanism by which some fucoidan extracts present a selective behavior (concentration where fucoidan presents toxicity to cancer cells without affecting normal cells), should be investigated. To try to overcome the cytotoxic effects of current chemotherapeutic drugs, drug delivery systems have proposed. Chitosan, as marine polymers, has been one of the most reported materials to develop drug delivery systems, which showed interesting results. The use of fucoidan to develop more complex systems, namely DDS, have been recently reported. catIn this case, most of the developed fucoidan-based nanoparticles systems increased the cytotoxic effects over cancer cells when compared with the free form of the drug, as previously described. A convincing chemical characterization, knowing the mechanism of action and the recent development of fucoidan-based systems that reduce the cytotoxic effects of chemotherapeutic drugs, aligned with fucoidan natural origin, offers promising and reasonable hope on developing more effective fucoidan-based treatments and therapies to fight cancer.

I-7. ACKNOWLEDGMENTS

This work was developed under the scope of the Structured projects for R&D&I NORTE-01-0145-FEDER-000021 and NORTE-01-0145-FEDER-000023 supported by the Northern Portugal Regional Operational Programme (NORTE 2020), and the Mobilizing Project ValorMar, POCI-01-0247-FEDER-024517, supported by the Operational Programme for Competitiveness and Internationalization (COMPETE 2020), under the Portugal 2020 Partnership Agreement, co-funded by European Regional Development Fund (ERDF). The authors would like also to thank Norte 2020, for financing the PhD scholarship of C.O. “Norte-08-5369-000037” and FCT for the Investigator grant of A.M. (IF/00376/2014).

I-8. REFERENCES

[1] R.L. Siegel, K.D. Miller, A. Jemal, Cancer statistics, 2019, CA Cancer J Clin 69(1) (2019) 7-34.

[2] K.D. Miller, R.L. Siegel, C.C. Lin, A.B. Mariotto, J.L. Kramer, J.H. Rowland, K.D. Stein, R. Alteri, A. Jemal, Cancer treatment and survivorship statistics, 2016, CA Cancer J Clin 66(4) (2016) 271-89.

[3] R. Baskar, K.A. Lee, R. Yeo, K.-W. Yeoh, Cancer and radiation therapy: current advances and future directions, International journal of medical sciences 9(3) (2012) 193-199.

[4] K. Nurgali, R.T. Jagoe, R. Abalo, Editorial: Adverse Effects of Cancer Chemotherapy: Anything New to Improve Tolerance and Reduce Sequelae?, Frontiers in Pharmacology 9 (2018) 245.

[5] J.S. McCune, Rapid Advances in Immunotherapy to Treat Cancer, Clinical Pharmacology & Therapeutics 103(4) (2018) 540-544.

[6] F.R. Balkwill, M. Capasso, T. Hagemann, The tumor microenvironment at a glance, Journal of cell science 125(Pt 23) (2012) 5591-6.

[7] T.H. Silva, A. Alves, E.G. Popa, L.L. Reys, M.E. Gomes, R.A. Sousa, S.S. Silva, J.F. Mano, R.L. Reis, Marine algae sulfated polysaccharides for tissue engineering and drug delivery approaches, Biomatter 2(4) (2012) 278-289.

[8] P.N.S. T. Gomathi, Jayachandran Venkatesan,, a.S. Ani, Marine Biopolymers for Anticancer Drugs, in: P.N. Sudha (Ed.), Industrial Applications of Marine Biopolymers, CRC Press2017.

[9] T.H. Silva, A. Alves, B.M. Ferreira, J.M. Oliveira, L.L. Reys, R.J.F. Ferreira, R.A. Sousa, S.S. Silva, J.F. Mano, R.L. Reis, Materials of marine origin: a review on polymers and ceramics of biomedical interest, International Materials Reviews 57(5) (2012) 276-306.

[10] S.C. Shit, P.M. Shah, Edible Polymers: Challenges and Opportunities, Journal of Polymers 2014 (2014) 13.

[11] I. Hamed, F. Özogul, J.M. Regenstein, Industrial applications of crustacean by-products (chitin, chitosan, and chitooligosaccharides): A review, Trends in Food Science & Technology 48 (2016) 40-50.

[12] U. Lindequist, Marine-Derived Pharmaceuticals - Challenges and Opportunities, Biomol Ther (Seoul) 24(6) (2016) 561-571.

[13] H. Malve, Exploring the ocean for new drug developments: Marine pharmacology, J Pharm Bioallied Sci 8(2) (2016) 83-91.

[14] L. Cunha, A. Grenha, Sulfated Seaweed Polysaccharides as Multifunctional Materials in Drug Delivery Applications, Marine drugs 14(3) (2016) 42.

[15] M.L. Wells, P. Potin, J.S. Craigie, J.A. Raven, S.S. Merchant, K.E. Helliwell, A.G. Smith, M.E. Camire, S.H. Brawley, Algae as nutritional and functional food sources: revisiting our understanding, Journal of applied phycology 29(2) (2017) 949-982.

[16] J.H. Fitton, D.N. Stringer, S.S. Karpiniec, Therapies from Fucoidan: An Update, Marine Drugs 13(9) (2015) 5920-5946.

[17] F. Atashrazm, R.M. Lowenthal, G.M. Woods, A.F. Holloway, J.L. Dickinson, Fucoidan and Cancer: A Multifunctional Molecule with Anti-Tumor Potential, Marine Drugs 13(4) (2015) 2327-2346.

[18] M.T. Ale, A.S. Meyer, Fucoidans from brown seaweeds: an update on structures, extraction techniques and use of enzymes as tools for structural elucidation, RSC Advances 3(22) (2013) 8131-8141.

[19] M.T. Ale, J.D. Mikkelsen, A.S. Meyer, Important determinants for fucoidan bioactivity: a critical review of structure-function relations and extraction methods for fucose-containing sulfated polysaccharides from brown seaweeds, Mar Drugs 9(10) (2011) 2106-30.

[20] B. Mulloy, O. Berteau, Sulfated fucans, fresh perspectives: structures, functions, and biological properties of sulfated fucans and an overview of enzymes active toward this class of polysaccharide, Glycobiology 13(6) (2003) 29R-40R.

[21] W. Mak, N. Hamid, T. Liu, J. Lu, W.L. White, Fucoidan from New Zealand Undaria pinnatifida: Monthly variations and determination of antioxidant activities, Carbohydrate Polymers 95(1) (2013) 606-614.

[22] M. Álvarez-Viñas, N. Flórez-Fernández, M.J. González-Muñoz, H. Domínguez, Influence of molecular weight on the properties of Sargassum muticum fucoidan, Algal Research 38 (2019) 101393.

[23] V.H.-T. Lin, Y.-C. Tsou, Y.-T. Chen, W.-J. Lu, P.-A. Hwang, Effects of Low-Molecular-Weight Fucoidan and High Stability Fucoxanthin on Glucose Homeostasis, Lipid Metabolism, and Liver Function in a Mouse Model of Type II Diabetes, Marine Drugs 15(4) (2017) 113.

[24] H.-L. Tsai, C.-J. Tai, C.-W. Huang, F.-R. Chang, J.-Y. Wang, Efficacy of Low-Molecular-Weight Fucoidan as a Supplemental Therapy in Metastatic Colorectal Cancer Patients: A Double-Blind Randomized Controlled Trial, Marine drugs 15(4) (2017) 122.

[25] S. You, C. Yang, H. Lee, B.-Y. Lee, Molecular characteristics of partially hydrolyzed fucoidans from sporophyll of Undaria Pinnatifida and their in vitro anticancer activity, Food Chemistry 119(2) (2010) 554-559.

[26] J.-i. Choi, H.-J. Kim, J.-H. Kim, M.-W. Byun, B. Soo Chun, D. Hyun Ahn, Y.-J. Hwang, D.-J. Kim, G.H. Kim, J.-W. Lee, Application of gamma irradiation for the enhanced physiological properties of polysaccharides from seaweeds, Applied Radiation and Isotopes 67(7) (2009) 1277-1281.

[27] A. Synytsya, W.-J. Kim, S.-M. Kim, R. Pohl, A. Synytsya, F. Kvasnička, J. Čopíková, Y. Il Park, Structure and antitumour activity of fucoidan isolated from sporophyll of Korean brown seaweed Undaria pinnatifida, Carbohydrate Polymers 81(1) (2010) 41-48.

[28] S.-M. Kang, K.-N. Kim, S.-H. Lee, G. Ahn, S.-H. Cha, A.-D. Kim, X.-D. Yang, M.-C. Kang, Y.-J. Jeon, Anti-inflammatory activity of polysaccharide purified from AMG-assistant extract of Ecklonia cava in LPS-stimulated RAW 264.7 macrophages, Carbohydrate Polymers 85(1) (2011) 80-85.

[29] S. Koyanagi, N. Tanigawa, H. Nakagawa, S. Soeda, H. Shimeno, Oversulfation of fucoidan enhances its anti-angiogenic and antitumor activities, Biochemical Pharmacology 65(2) (2003) 173-179.

[30] S. Soeda, Y. Shibata, H. Shimeno, Inhibitory Effect of Oversulfated Fucoidan on Tube Formation by Human Vascular Endothelial Cells, Biological & Pharmaceutical Bulletin 20(11) (1997) 1131-1135.

[31] S. Zorofchian Moghadamtousi, H. Karimian, R. Khanabdali, M. Razavi, M. Firoozinia, K. Zandi, H. Abdul Kadir, Anticancer and Antitumor Potential of Fucoidan and Fucoxanthin, Two Main Metabolites Isolated from Brown Algae, The Scientific World Journal 2014 (2014) 10.

[32] C. Oliveira, A.S. Ferreira, R. Novoa-Carballal, C. Nunes, I. Pashkuleva, N.M. Neves, M.A. Coimbra, R.L. Reis, A. Martins, T.H. Silva, The Key Role of Sulfation and Branching on Fucoidan Antitumor Activity, Macromolecular Bioscience 17(5) (2017) 1600340.

[33] T. Nishino, C. Nishioka, H. Ura, T. Nagumo, Isolation and partial characterization of a noval amino sugar-containing fucan sulfate from commercial Fucus vesiculosus fucoidan, Carbohydrate Research 255 (1994) 213-224.

[34] M. Nagaoka, H. Shibata, I. Kimura-Takagi, S. Hashimoto, K. Kimura, T. Makino, R. Aiyama, S. Ueyama, T. Yokokura, Structural study of fucoidan from Cladosiphon okamuranus tokida, Glycoconjugate Journal 16(1) (1999) 19-26.

[35] B. Li, F. Lu, X. Wei, R. Zhao, Fucoidan: Structure and Bioactivity, Molecules 13(8) (2008) 1671-95.

[36] A. Ahmadi, S. Zorofchian Moghadamtousi, S. Abubakar, K. Zandi, Antiviral Potential of Algae Polysaccharides Isolated from Marine Sources: A Review, BioMed Research International 2015 (2015) 10.

[37] M. Witvrouw, E. De Clercq, Sulfated Polysaccharides Extracted from Sea Algae as Potential Antiviral Drugs, General Pharmacology: The Vascular System 29(4) (1997) 497-511.

[38] J.-B. Lee, K. Hayashi, M. Hashimoto, T. Nakano, T. Hayashi, Novel Antiviral Fucoidan from Sporophyll of Undaria pinnatifida (Mekabu), Chemical and Pharmaceutical Bulletin 52(9) (2004) 1091-1094.

[39] P. Mandal, C.G. Mateu, K. Chattopadhyay, C.A. Pujol, E.B. Damonte, B. Ray, Structural Features and Antiviral Activity of Sulphated Fucans from the Brown Seaweed Cystoseira Indica, Antiviral Chemistry and Chemotherapy 18(3) (2007) 153-162.

[40] T.T.T. Thuy, B.M. Ly, T.T.T. Van, N. Van Quang, H.C. Tu, Y. Zheng, C. Seguin-Devaux, B. Mi, U. Ai, Anti-HIV activity of fucoidans from three brown seaweed species, Carbohydrate Polymers 115 (2015) 122-128.

[41] H. Li, J. Li, Y. Tang, L. Lin, Z. Xie, J. Zhou, L. Zhang, X. Zhang, X. Zhao, Z. Chen, D. Zuo, Fucoidan from Fucus vesiculosus suppresses hepatitis B virus replication by enhancing extracellular signal-regulated Kinase activation, Virology journal 14(1) (2017) 178-178.

[42] C.A. Feghali, T.M. Wright, Cytokines in acute and chronic inflammation, Frontiers in bioscience : a journal and virtual library 2 (1997) d12-26.

[43] M.J. Abad, 10 - Anti-inflammatory properties of algae, in: H. Domínguez (Ed.), Functional Ingredients from Algae for Foods and Nutraceuticals, Woodhead Publishing2013, pp. 338-368.

[44] I.P.S. Fernando, J.-W. Nah, Y.-J. Jeon, Potential anti-inflammatory natural products from marine algae, Environmental Toxicology and Pharmacology 48 (2016) 22-30.

[45] A.C. Carvalho, R.B. Sousa, A.X. Franco, J.V. Costa, L.M. Neves, R.A. Ribeiro, R. Sutton, D.N. Criddle, P.M. Soares, M.H. de Souza, Protective effects of fucoidan, a P- and L-selectin inhibitor, in murine acute pancreatitis, Pancreas 43(1) (2014) 82-7.

[46] Q.Y. Lean, R.D. Eri, J.H. Fitton, R.P. Patel, N. Gueven, Fucoidan Extracts Ameliorate Acute Colitis, PloS one 10(6) (2015) e0128453-e0128453.

[47] H.-H. Yu, E. Chengchuan Ko, C.-L. Chang, K.S.-P. Yuan, A.T.H. Wu, Y.-S. Shan, S.-Y. Wu, Fucoidan Inhibits Radiation-Induced Pneumonitis and Lung Fibrosis by Reducing Inflammatory Cytokine Expression in Lung Tissues, Marine drugs 16(10) (2018) 392.

[48] J.-H. Yang, Topical Application of Fucoidan Improves Atopic Dermatitis Symptoms in NC/Nga Mice, Phytotherapy Research 26(12) (2012) 1898-1903.

[49] Y. Xu, J. Xu, K. Ge, Q. Tian, P. Zhao, Y. Guo, Anti-inflammatory effect of low molecular weight fucoidan from Saccharina japonica on atherosclerosis in apoE-knockout mice, International Journal of Biological Macromolecules 118 (2018) 365-374.

[50] P. Carmeliet, R.K. Jain, Angiogenesis in cancer and other diseases, Nature 407(6801) (2000) 249-57.

[51] M. Potente, H. Gerhardt, P. Carmeliet, Basic and therapeutic aspects of angiogenesis, Cell 146(6) (2011) 873-87.

[52] N.E. Ustyuzhanina, N.E. Nifantiev, A.I. Usov, M.I. Bilan, N.A. Ushakova, M.V. Kiselevskiy, Fucoidans: Pro- or antiangiogenic agents?, Glycobiology 24(12) (2014) 1265-1274.

[53] D. Ribatti, The crucial role of vascular permeability factor/vascular endothelial growth factor in angiogenesis: a historical review, British journal of haematology 128(3) (2005) 303-9.

[54] B.S. Kim, S.S. Yang, H.K. You, H.I. Shin, J. Lee, Fucoidan-induced osteogenic differentiation promotes angiogenesis by inducing vascular endothelial growth factor secretion and accelerates bone repair, Journal of tissue engineering and regenerative medicine 12(3) (2018) e1311-e1324.

[55] N. Marinval, P. Sabboural, O. Haddad, M. Maire, K. Bassand, F. Geinguenaud, N. Djaker, K. Ben Akrout, M. Lamy de la Chapelle, R. Robert, O. Oudar, E. Guyot, C. Laguillier-Morizot, A. Sutton, C. Chauvierre, F. Chaubet, N. Charnaux, H. Hlawaty, Identification of a Pro-Angiogenic Potential and Cellular Uptake Mechanism of a LMW Highly Sulfated Fraction of Fucoidan from Ascophyllum nodosum, Marine drugs 14(10) (2016) 185.

[56] M. Dithmer, A.-M. Kirsch, E. Richert, S. Fuchs, F. Wang, H. Schmidt, S.E. Coupland, J. Roider, A. Klettner, Fucoidan Does Not Exert Anti-Tumorigenic Effects on Uveal Melanoma Cell Lines, Marine drugs 15(7) (2017) 193.

[57] D.O. Croci, A. Cumashi, N.A. Ushakova, M.E. Preobrazhenskaya, A. Piccoli, L. Totani, N.E. Ustyuzhanina, M.I. Bilan, A.I. Usov, A.A. Grachev, G.E. Morozevich, A.E. Berman, C.J. Sanderson, M. Kelly, P. Di Gregorio, C. Rossi, N. Tinari, S. Iacobelli, G.A. Rabinovich, N.E. Nifantiev, I. Consorzio

Interuniversitario Nazionale per la Bio-Oncologia, Fucans, but not fucomannoglucuronans, determine the biological activities of sulfated polysaccharides from Laminaria saccharina brown seaweed, PloS one 6(2) (2011) e17283-e17283.

[58] M.-C. Chen, W.-L. Hsu, P.-A. Hwang, T.-C. Chou, Low Molecular Weight Fucoidan Inhibits Tumor Angiogenesis through Downregulation of HIF-1/VEGF Signaling under Hypoxia, Marine drugs 13(7) (2015) 4436-4451.

[59] M. Dithmer, S. Fuchs, Y. Shi, H. Schmidt, E. Richert, J. Roider, A. Klettner, Fucoidan reduces secretion and expression of vascular endothelial growth factor in the retinal pigment epithelium and reduces angiogenesis in vitro, PloS one 9(2) (2014) e89150-e89150.

[60] F. Wang, H. Schmidt, D. Pavleska, T. Wermann, A. Seekamp, S. Fuchs, Crude Fucoidan Extracts Impair Angiogenesis in Models Relevant for Bone Regeneration and Osteosarcoma via Reduction of VEGF and SDF-1, Marine drugs 15(6) (2017) 186.

[61] C. GM, The Cell: A Molecular Approach. 2nd edition. Sunderland (MA): Sinauer Associates, (2000).

[62] M. Arruebo, N. Vilaboa, B. Sáez-Gutierrez, J. Lambea, A. Tres, M. Valladares, A. González-Fernández, Assessment of the evolution of cancer treatment therapies, Cancers 3(3) (2011) 3279-3330.

[63] K. Sak, Chemotherapy and dietary phytochemical agents, Chemotherapy research and practice 2012 (2012) 282570.

[64] U. Testa, E. Pelosi, G. Castelli, Colorectal cancer: genetic abnormalities, tumor progression, tumor heterogeneity, clonal evolution and tumor-initiating cells, Medical sciences (Basel, Switzerland) 6(2) (2018) 31.

[65] M. Ellouali, C. Boisson-Vidal, P. Durand, J. Jozefonvicz, Antitumor activity of low molecular weight fucans extracted from brown seaweed Ascophyllum nodosum, Anticancer Res 13(6a) (1993) 2011-9.

[66] H. Lemjabbar-Alaoui, O.U. Hassan, Y.-W. Yang, P. Buchanan, Lung cancer: Biology and treatment options, Biochimica et biophysica acta 1856(2) (2015) 189-210.

[67] C. Zappa, S.A. Mousa, Non-small cell lung cancer: current treatment and future advances, Translational lung cancer research 5(3) (2016) 288-300.

[68] T. Marudhupandi, T.T. Ajith Kumar, S. Lakshmanasenthil, G. Suja, T. Vinothkumar, In vitro anticancer activity of fucoidan from Turbinaria conoides against A549 cell lines, International Journal of Biological Macromolecules 72 (2015) 919-923.

[69] H. Lee, J.-S. Kim, E. Kim, Fucoidan from Seaweed Fucus vesiculosus Inhibits Migration and Invasion of Human Lung Cancer Cell via PI3K-Akt-mTOR Pathways, PLOS ONE 7(11) (2012) e50624.

[70] H.-J. Boo, J.-H. Hyun, S.-C. Kim, J.-I. Kang, M.-K. Kim, S.-Y. Kim, H. Cho, E.-S. Yoo, H.-K. Kang, Fucoidan from Undaria pinnatifida Induces Apoptosis in A549 Human Lung Carcinoma Cells, Phytotherapy Research 25(7) (2011) 1082-1086.

[71] C. Yang, D. Chung, I.-S. Shin, H. Lee, J. Kim, Y. Lee, S. You, Effects of molecular weight and hydrolysis conditions on anticancer activity of fucoidans from sporophyll of Undaria pinnatifida, International Journal of Biological Macromolecules 43(5) (2008) 433-437.

[72] H.-Y. Hsu, T.-Y. Lin, M.-K. Lu, P.-J. Leng, S.-M. Tsao, Y.-C. Wu, Fucoidan induces Toll-like receptor 4-regulated reactive oxygen species and promotes endoplasmic reticulum stress-mediated apoptosis in lung cancer, Scientific reports 7 (2017) 44990-44990.

[73] H.-Y. Hsu, T.-Y. Lin, C.-H. Hu, D.T.F. Shu, M.-K. Lu, Fucoidan upregulates TLR4/CHOP-mediated caspase-3 and PARP activation to enhance cisplatin-induced cytotoxicity in human lung cancer cells, Cancer Letters 432 (2018) 112-120.

[74] R.V. Usoltseva, S.D. Anastyuk, V.V. Surits, N.M. Shevchenko, P.D. Thinh, P.A. Zadorozhny, S.P. Ermakova, Comparison of structure and in vitro anticancer activity of native and modified fucoidans from Sargassum feldmannii and S. duplicatum, International Journal of Biological Macromolecules 124 (2019) 220-228.

[75] Y.S. Han, J.H. Lee, S.H. Lee, Fucoidan inhibits the migration and proliferation of HT-29 human colon cancer cells via the phosphoinositide-3 kinase/Akt/mechanistic target of rapamycin pathways, Mol Med Rep 12(3) (2015) 3446-3452.

[76] Y.-S. Han, J.H. Lee, S.H. Lee, Antitumor Effects of Fucoidan on Human Colon Cancer Cells via Activation of Akt Signaling, Biomolecules & therapeutics 23(3) (2015) 225-232.

[77] K. Azuma, T. Ishihara, H. Nakamoto, T. Amaha, T. Osaki, T. Tsuka, T. Imagawa, S. Minami, O. Takashima, S. Ifuku, M. Morimoto, H. Saimoto, H. Kawamoto, Y. Okamoto, Effects of Oral Administration of Fucoidan Extracted from Cladosiphon okamuranus on Tumor Growth and Survival Time in a Tumor-Bearing Mouse Model, Marine Drugs 10(10) (2012) 2337-48.

[78] E.J. Kim, S.Y. Park, J.-Y. Lee, J.H.Y. Park, Fucoidan present in brown algae induces apoptosis of human colon cancer cells, BMC Gastroenterology 10(1) (2010) 96.

[79] I.-H. Kim, M.-J. Kwon, T.-J. Nam, Differences in cell death and cell cycle following fucoidan treatment in high-density HT-29 colon cancer cells, Molecular medicine reports 15(6) (2017) 4116-4122.

[80] M.I. Bilan, A.A. Grachev, N.E. Ustuzhanina, A.S. Shashkov, N.E. Nifantiev, A.I. Usov, A highly regular fraction of a fucoidan from the brown seaweed Fucus distichus L, Carbohydr Res 339(3) (2004) 511-7.

[81] C. DeSantis, J. Ma, L. Bryan, A. Jemal, Breast cancer statistics, 2013, CA Cancer J Clin 64(1) (2014) 52-62.

[82] M.I. Nounou, F. ElAmrawy, N. Ahmed, K. Abdelraouf, S. Goda, H. Syed-Sha-Qhattal, Breast Cancer: Conventional Diagnosis and Treatment Modalities and Recent Patents and Technologies, Breast cancer : basic and clinical research 9(Suppl 2) (2015) 17-34.

[83] C.W.S. Tong, M. Wu, W.C.S. Cho, K.K.W. To, Recent Advances in the Treatment of Breast Cancer, Frontiers in oncology 8 (2018) 227-227.

[84] A.M. Banafa, S. Roshan, Y.-y. Liu, H.-j. Chen, M.-j. Chen, G.-x. Yang, G.-y. He, Fucoidan induces G1 phase arrest and apoptosis through caspases-dependent pathway and ROS induction in human breast

cancer MCF-7 cells, Journal of Huazhong University of Science and Technology [Medical Sciences] 33(5) (2013) 717-724.

[85] Z. Zhang, K. Teruya, H. Eto, S. Shirahata, Induction of Apoptosis by Low-Molecular-Weight Fucoidan through Calcium- and Caspase-Dependent Mitochondrial Pathways in MDA-MB-231 Breast Cancer Cells, Bioscience, Biotechnology, and Biochemistry 77(2) (2013) 235-242.

[86] J. Lu, K.K. Shi, S. Chen, J. Wang, A. Hassouna, L.N. White, F. Merien, M. Xie, Q. Kong, J. Li, T. Ying, W.L. White, S. Nie, Fucoidan Extracted from the New Zealand Undaria pinnatifida-Physicochemical Comparison against Five Other Fucoidans: Unique Low Molecular Weight Fraction Bioactivity in Breast Cancer Cell Lines, Marine drugs 16(12) (2018) 461.

[87] X. He, M. Xue, S. Jiang, W. Li, J. Yu, S. Xiang, Fucoidan Promotes Apoptosis and Inhibits EMT of Breast Cancer Cells, Biol Pharm Bull 42(3) (2019) 442-447.

[88] R.-H. Chen, S.-M. Tsao, H.-Y. Hsu, T.-Y. Lin, P.-A. Hwang, L.-M. Tseng, J. Hsu, Fucoidan induces changes in the epithelial to mesenchymal transition and decreases metastasis by enhancing ubiquitin-dependent TGFβ receptor degradation in breast cancer, Carcinogenesis 34(4) (2012) 874-884.

[89] M. Xue, Y. Ge, J. Zhang, Q. Wang, L. Hou, Y. Liu, L. Sun, Q. Li, Anticancer Properties and Mechanisms of Fucoidan on Mouse Breast Cancer In Vitro and In Vivo, PLOS ONE 7(8) (2012) e43483.

[90] Z. Zhang, K. Teruya, T. Yoshida, H. Eto, S. Shirahata, Fucoidan extract enhances the anti-cancer activity of chemotherapeutic agents in MDA-MB-231 and MCF-7 breast cancer cells, Marine drugs 11(1) (2013) 81-98.

[91] M.A. Linares, A. Zakaria, P. Nizran, Skin Cancer, Primary Care: Clinics in Office Practice 42(4) (2015) 645-659.

[92] Z. Apalla, D. Nashan, R.B. Weller, X. Castellsagué, Skin Cancer: Epidemiology, Disease Burden, Pathophysiology, Diagnosis, and Therapeutic Approaches, Dermatology and therapy 7(Suppl 1) (2017) 5-19.

[93] V. Thakur, J. Lu, G. Roscilli, L. Aurisicchio, M. Cappelletti, E. Pavoni, W.L. White, B. Bedogni, The natural compound fucoidan from New Zealand Undaria pinnatifida synergizes with the ERBB inhibitor lapatinib enhancing melanoma growth inhibition, Oncotarget 8(11) (2017) 17887-17896.

[94] M.T. Ale, H. Maruyama, H. Tamauchi, J.D. Mikkelsen, A.S. Meyer, Fucoidan from Sargassum sp. and Fucus vesiculosus reduces cell viability of lung carcinoma and melanoma cells in vitro and activates natural killer cells in mice in vivo, International Journal of Biological Macromolecules 49(3) (2011) 331-336.

[95] M.T. Ale, H. Maruyama, H. Tamauchi, J.D. Mikkelsen, A.S. Meyer, Fucose-containing sulfated polysaccharides from brown seaweeds inhibit proliferation of melanoma cells and induce apoptosis by activation of caspase-3 in vitro, Marine drugs 9(12) (2011) 2605-2621.

[96] Z.-J. Wang, W. Xu, J.-W. Liang, C.-S. Wang, Y. Kang, Effect of fucoidan on B16 murine melanoma cell melanin formation and apoptosis Afr J Tradit Complement Altern Med 14(4) (2017) 149-155.

[97] C.C. Beaver, M.A. Magnan, Managing Chemotherapy Side Effects: Achieving Reliable and Equitable Outcomes, Clin J Oncol Nurs 20(6) (2016) 589-591.

[98] W.H. De Jong, P.J. Borm, Drug delivery and nanoparticles:applications and hazards, Int J Nanomedicine 3(2) (2008) 133-49.

[99] J.W. Nichols, Y.H. Bae, Odyssey of a cancer nanoparticle: from injection site to site of action, Nano Today 7(6) (2012) 606-618.

[100] E. Pérez-Herrero, A. Fernández-Medarde, Advanced targeted therapies in cancer: Drug nanocarriers, the future of chemotherapy, European Journal of Pharmaceutics and Biopharmaceutics 93 (2015) 52-79.

[101] S. Senapati, A.K. Mahanta, S. Kumar, P. Maiti, Controlled drug delivery vehicles for cancer treatment and their performance, Signal Transduction and Targeted Therapy 3(1) (2018) 7.

[102] V. Agrahari, V. Agrahari, A.K. Mitra, Nanocarrier fabrication and macromolecule drug delivery: challenges and opportunities, Ther Deliv 7(4) (2016) 257-78.

[103] M. Emeje, Recent Applications of Natural Polymers in Nanodrug Delivery, Journal of Nanomedicine & Nanotechnology s4(01) (2011).

[104] L. Chollet, P. Sabboural, C. Chauvierre, J.-N. Villemin, D. Letourneur, F. Chaubet, Fucoidans in Nanomedicine, Marine Drugs 14(8) (2016) 145.

[105] V.K. Pawar, Y. Singh, K. Sharma, A. Shrivastav, A. Sharma, A. Singh, J.G. Meher, P. Singh, K. Raval, A. Kumar, H.K. Bora, D. Datta, J. Lal, M.K. Chourasia, Improved chemotherapy against breast cancer through immunotherapeutic activity of fucoidan decorated electrostatically assembled nanoparticles bearing doxorubicin, International Journal of Biological Macromolecules 122 (2018) 1100-1114.

[106] K.-Y. Lu, R. Li, C.-H. Hsu, C.-W. Lin, S.-C. Chou, M.-L. Tsai, F.-L. Mi, Development of a new type of multifunctional fucoidan-based nanoparticles for anticancer drug delivery, Carbohydrate Polymers 165 (2017) 410-420.

[107] P. Manivasagan, S. Bharathiraja, N.Q. Bui, B. Jang, Y.-O. Oh, I.G. Lim, J. Oh, Doxorubicin-loaded fucoidan capped gold nanoparticles for drug delivery and photoacoustic imaging, International Journal of Biological Macromolecules 91 (2016) 578-588.

[108] H. Kim, V.P. Nguyen, P. Manivasagan, M.J. Jung, S.W. Kim, J. Oh, H.W. Kang, Doxorubicin-fucoidan-gold nanoparticles composite for dual-chemo-photothermal treatment on eye tumors, Oncotarget 8(69) (2017) 113719-113733.

[109] P. Wang, R.K. Kankala, J. Fan, R. Long, Y. Liu, S. Wang, Poly-L-ornithine/fucoidan-coated calcium carbonate microparticles by layer-by-layer self-assembly technique for cancer theranostics, Journal of Materials Science: Materials in Medicine 29(5) (2018) 68.

[110] C. Oliveira, N.M. Neves, R.L. Reis, A. Martins, T.H. Silva, Gemcitabine delivered by fucoidan/chitosan nanoparticles presents increased toxicity over human breast cancer cells, Nanomedicine 13(16) (2018) 2037-2050.

[111] P. Wang, R.K. Kankala, B. Chen, R. Long, D. Cai, Y. Liu, S. Wang, Poly-allylamine hydrochloride and fucoidan-based self-assembled polyelectrolyte complex nanoparticles for cancer therapeutics, Journal of Biomedical Materials Research Part A 107(2) (2019) 339-347.

[112] Y. Shamay, M. Elkabets, H. Li, J. Shah, S. Brook, F. Wang, K. Adler, E. Baut, M. Scaltriti, P.V. Jena, E.E. Gardner, J.T. Poirier, C.M. Rudin, J. Baselga, A. Haimovitz-Friedman, D.A. Heller, P-selectin is a nanotherapeutic delivery target in the tumor microenvironment, Science translational medicine 8(345) (2016) 345ra87.

[113] S.-W. Shin, W. Jung, C. Choi, S.-Y. Kim, A. Son, H. Kim, N. Lee, C.H. Park, Fucoidan-Manganese Dioxide Nanoparticles Potentiate Radiation Therapy by Co-Targeting Tumor Hypoxia and Angiogenesis, Marine Drugs 16(12) (2018) 510.

[114] M.S. Deepika, R. Thangam, T.S. Sheena, R. Sasirekha, S. Sivasubramanian, M.D. Babu, K. Jeganathan, R. Thirumurugan, A novel rutin-fucoidan complex based phytotherapy for cervical cancer through achieving enhanced bioavailability and cancer cell apoptosis, Biomedicine & Pharmacotherapy 109 (2019) 1181-1195.

[115] J. Venkatesan, K.S. Singh, S. Anil, S.-K. Kim, S.M. Shim, Preparation, Characterization and Biological Applications of Biosynthesized Silver Nanoparticles with Chitosan-Fucoidan Coating, Molecules 23(6) (2018) 1429.

[116] B. Jang, M.S. Moorthy, P. Manivasagan, L. Xu, K. Song, K.D. Lee, M. Kwak, J. Oh, J.-O. Jin, Fucoidan-coated CuS nanoparticles for chemo-and photothermal therapy against cancer, Oncotarget 9(16) (2018) 12649-12661.

[117] M.R.A. Abdollah, T.J. Carter, C. Jones, T.L. Kalber, V. Rajkumar, B. Tolner, C. Gruettner, M. Zaw-Thin, J. Baguña Torres, M. Ellis, M. Robson, R.B. Pedley, P. Mulholland, R. T. M. de Rosales, K.A. Chester, Fucoidan Prolongs the Circulation Time of Dextran-Coated Iron Oxide Nanoparticles, ACS Nano 12(2) (2018) 1156-1169.

[118] K.W. Lee, D. Jeong, K. Na, Doxorubicin loading fucoidan acetate nanoparticles for immune and chemotherapy in cancer treatment, Carbohydr Polym 94(2) (2013) 850-6.

[119] M. Tengdelius, D. Gurav, P. Konradsson, P. Pahlsson, M. Griffith, O.P. Oommen, Synthesis and anticancer properties of fucoidan-mimetic glycopolymer coated gold nanoparticles, Chem Commun (Camb) 51(40) (2015) 8532-5.

[120] R. Kimura, T. Rokkaku, S. Takeda, M. Senba, N. Mori, Cytotoxic Effects of Fucoidan Nanoparticles against Osteosarcoma, Marine Drugs 11(11) (2013) 4267-4278.

[121] R. Li, S. Pavuluri, K. Bruggeman, B.M. Long, A.J. Parnell, A. Martel, S.R. Parnell, F.M. Pfeffer, A.J.C. Dennison, K.R. Nicholas, C.J. Barrow, D.R. Nisbet, R.J. Williams, Coassembled nanostructured bioscaffold reduces the expression of proinflammatory cytokines to induce apoptosis in epithelial cancer cells, Nanomedicine: Nanotechnology, Biology and Medicine 12(5) (2016) 1397-1407.

[122] M. Tengdelius, D. Gurav, P. Konradsson, P. Påhlsson, M. Griffith, O.P. Oommen, Synthesis and anticancer properties of fucoidan-mimetic glycopolymer coated gold nanoparticles, Chemical Communications 51(40) (2015) 8532-8535.

SECTION 2

EXPERIMENTAL PLAN

Chapter II

Materials & Methods

Chapter II

Materials and Methods

OVERVIEW

This chapter provides a detailed description of the materials, methodologies and procedures that were used for the work presented in Chapters III to VIII of this thesis, complementing the specific information on "Materials and Methods" for each of those chapters included in the respective sections. A description of the main polymers used can be found in the first part of this section. Then, the methods for the production of nanoparticles and nanofiber mesh will be described. The different characterization techniques applied to assess the physico-chemical properties of the materials and systems will be addressed. Moreover, the *in vitro* and/or *in vivo* assays performed to validate the developed systems will be discussed. The specifications of the materials and equipments are also specified in this section.

II-1. MATERIALS

II-1.1. Fucoidan

Fucoidan is a sulfated polysaccharide present in the cell wall of different species of brown algae, being *Fucus vesiculosus* the most common and well-studied [1]. Fucoidan is mainly composed of sulfated fucose residues, although other monosaccharides may also be present like mannose, galactose, glucose, xylose and uronic acids [2, 3]. The chemical structure of fucoidan is usually composed of residues of α-L-fucopiranose interconnected by links (1 → 3) or alternating (1 → 3) and (1 → 4) (**Figure II-1**). Polymer branching is also possible with other sugars being related to the species of brown seaweed.

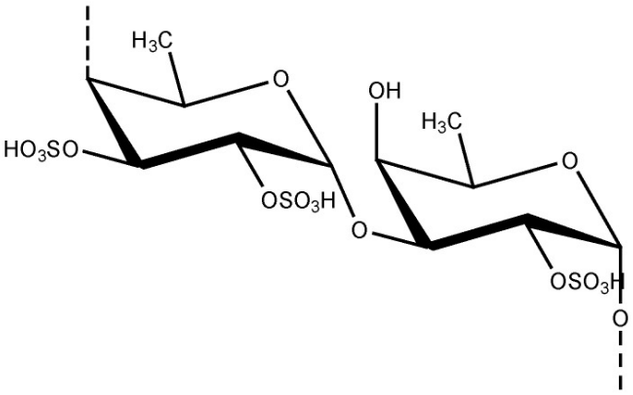

Figure II-1 Fucoidan chemical structure from *Fucus vesiculosus*, representing the (1 → 3) and (1 → 4) alternating bonds.

Crude and purified fucoidan extracts are commercially available. In this thesis, different fucoidan extracts were tested and used on the studies discussed in the chapters III to VIII, all from *Fucus vesiculosus* and purchased to Sigma-Aldrich (USA) or Marinova (Australia). Despite other biological activities of fucoidan, this works is mainly focused on its antitumor capability. Each extract was tested over human cancer and non-cancer cells to assess its antitumor behavior, selecting the extract for each work according to the results (**Table II-1**). Indeed, three distinct biological behaviors were observed for the different extracts (Chapter III). Some of the extracts (Marinova, batch: DPFVF2015505) presented cytotoxic effects over normal cells at lower concentrations than cancer cells (for high concentrations). Therefore, this extract did not show a direct antitumor activity over the cells tested. In this sense, this extract was used to develop nanoparticles systems for the delivery of a chemotherapeutic drug (gemcitabine) (Chapter VI) and, further, on the development of functionalized nanoparticles to specifically target ErbB-2 positive breast cancers (Chapter VII). On the other hand, an extract from Sigma (batch: 081M7672V) presented toxicity to both cancer and normal cells for the same concentrations, which was

reported in Chapter III. With this extract no further assays were conducted. Extracts from Sigma (batches: SLBC6348V and SLBP3196V) presented the desire behavior of an effective antitumor bioactive agent, since they were able to present a selective behavior, presenting toxicity over the cancer cells without affecting normal cells, at a defined concentration. These extracts were used to study the anti-angiogenic potential of an effective antitumor fucoidan (Chapter IV) and to develop a nanofibrous mesh with immobilized fucoidan to treat melanoma (Chapter V). With all these systems and strategies it was possible to explore and potentiate fucoidan usage aiming to develop more effective antitumor therapies.

Table II-1 Fucoidan chemical structure from *Fucus vesiculosus*.

Company	Batch	Mw (kDa)	Biological outcome	Chapter
Marinova (Pharmaceutical Grade)	DPFVF2015505	91	Toxic to normal cells at lower dosages than to cancer cells (high concentrations)	III VI VII
Sigma (Crude)	SLBC6348V	60	Toxic to cancer cells but not toxic to normal cells	III
	081M7672V	42	Toxic to both cancer and normal cells	III
	SLBP3196V	108	Toxic to cancer cells but not to normal cells	IV V

II-1.2. Chitosan

Chitosan, a natural linear and cationic polysaccharide, is the alkaline deactylated product of chitin, which can be found in the exoskeleton of invertebrates such as crustaceans, insects and spiders, as well as in the cell walls of fungi [4, 5]. Chitin is the second most abundant polysaccharide, both in terms of usage and distribution, right after cellulose. Chitosan is mainly composed of randomly distributed (1-4)-linked D-glucosamine (deacetylated unit, more abundant) and N-acetyl-D-glucosamine (acetylated unit) (**Figure II-2**). The molecular weight (Mw) and the degree of deacetylation (DD) are key parameters that influence chitosan's characteristics [6]. Chitosan presents unique properties such as biocompatibility,

biodegradability and bioactivity [7]. This make it a promising polymer to be used for different applications, namely for the development of drug delivery systems [8].

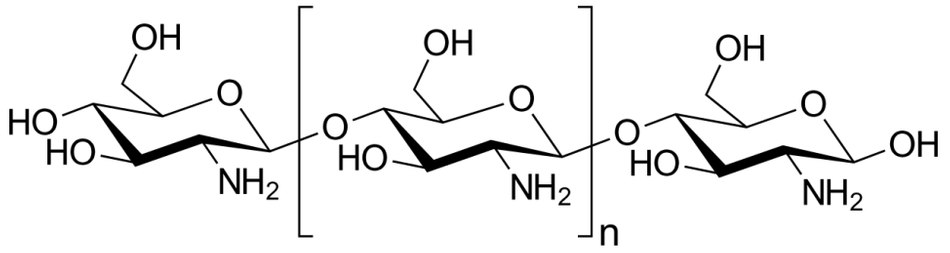

Figure II-2 Chitosan chemical structure if the DD=100%.

In the scope of this thesis, chitosan was used due to its origin and cationic nature (since most of the polysaccharides are usually either neutral or negatively charged), aiming to develop marine-based nanoparticles by polyelectrolyte complexation with fucoidan (negatively charged) [9]. Chitosan-based drug delivery systems for cancer treatment have been extensively studied, namely in the form of nanoparticles for the release of different chemotherapeutic drugs [10]. **Table II-2** presents some examples and the effects of the systems when compared with the free drug.

Table II-2 Chitosan-based nanoparticles for the release of chemotherapeutic drugs.

DRUG	CANCER TYPE	OUTCOMES	REF
DOXORUBICIN	Breast Colon	enhanced cellular accumulation and cellular uptake of the chemotherapeutic drug	[11]
	Breast	enhance chemo-radiotherapeutic effect affecting cancer cells viability, inducing necrosis at a very low radiation	[12]
	Liver	cells apoptosis and cell cycle arrest at G2/M phase	[13]
PACLITAXEL	Breast	higher percentages of late apoptotic cells than unloaded nanoparticles and naïve drug	[14]
	Breast	higher internalization index, cytotoxic effects and cells apoptotic ratio than non-loaded NPs *in vitro*	[15]
	Lung	increase in the uptake of the NPs was verified and apoptosis was enhanced inducing cell cycle arrest at G2/M phase.	[16]

	Lung	inhibited lung cancer cells proliferation and enhanced apoptosis	[17]
GEMCITABINE	Pancreas	increased cytotoxicity over cancer cells when compared with free drug	[18]
	Breast	pH related release profile and increased cytotoxicity and cellular uptake than free gemcitabine	[19]
	Pancreas	inhibiting pancreatic cancer cells invasion and migrations in nude mice, promoting their apoptosis and enhancing the efficacy of the chemotherapeutic agent	[20]

The medical grade chitosan 95/20 (batch number: 212-261115-04, DD=97,6%), used in Chapters VI and VII, was purchased from Heppe Medical Chitosan GmbH (Germany). It presents a molecular weight of 40–150 kDa by GPC, as provided by the manufacture.

II-1.3. Polycaprolactone

The chemical structure of polycaprolactone (PCL), an hydrophobic and biodegradable synthetic polyester, is shown in **Figure II-3**. PCL is produced by chemical synthesis from crude oil and can be degraded by hydrolysis of its ester bonds in physiological conditions. PCL has been extensively used in different biomedical fields namely as drug delivery systems, sutures and scaffolds, mainly due to its biocompatibility and ability to form blends and copolymers with a wide range of other polymers, being Food and Drug Administration (FDA) for applications in the human body [21, 22]. Moreover, PCL is commonly used in biomedical applications also due to its biodegradability, relatively inexpensive cost, and easy modification and functionalization [23]. Due to these reasons and to the relatively easy processability by electrospinning (section II-3.1.1), PCL was the chosen polymer to produce the nanofiber meshes that were used as a patch for fucoidan immobilization in Chapter V. The PCL (Mw 70,000-90,000 by GPC) was purchase from Sigma Aldrich (USA).

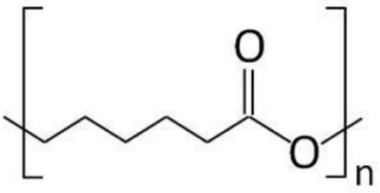

Figure II-3 Polycaprolactone chemical structure.

II-2. REAGENTS

Unless stated otherwise, all the reagents used in this thesis were purchased from Sigma-Aldrich (USA) for analysis and used as received.

II-3. PRODUCTION TECHNIQUES

II-3.1. Nanofibrous mesh production, activation and functionalization

II-3.1.1. Electrospinning technique

The nanofibrous meshes (NFMs) were produced by the electrospinning technique. This is an efficient and versatile technique that produces ultrafine fibers that can range from nano to micro scales [24]. The typical electrospinning setup comprises a spinneret coupled to a polymeric solution reservoir, a high voltage power source and a collector, as it is possible to observe in **Figure II-4 A)**. The solution is ejected through the needle by applying an high voltage that opposes the surface tension of the polymeric solution, leading to the initiation of a jet. The solvent partially evaporates, as the jet travels from the needle to the collector, and a nanofibrous mesh is formed in the conductive collector [25, 26]. The electrospinning apparatus, used in Chapter V of this thesis has been previously developed in house and comprises: one semi-commercial high-voltage power supplier (Genvolt, UK), a precision syringe pump (KDScientific, USA), a ground collector, a cuboid chamber and an isolation transformer (**Figure II-4 B**).

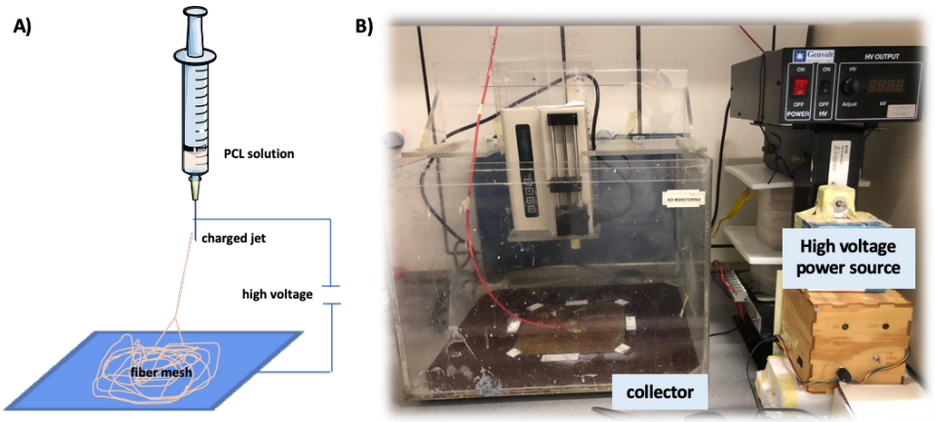

Figure II-4 Schematic representation of the electrospinning A) and the home-made setup.

The production of the nanofibrous meshes was performed inside a chemical wood, due to the release of solvents needed to dissolve polycaprolactone. This technique results in NFM characterized by a high specific surface area that in combination with the microporous structure facilitates cell adhesion, proliferation, migration and differentiation [27]. NFMs typically mimic the extracellular matrix of many tissues, by imitating its fibrils morphology and by the diameter of the fibers, providing an adequate microenvironment for cell-cell and cell-biomaterial interactions.

Briefly, a 15% (w/v) PCL solution was prepared with an organic solvent mixture of chloroform and dimethylformamide (DMF) at a 7:3 ratio. This solution was placed in a 5 mL plastic syringe with a metallic blunted end needle, with an internal diameter of 0.8 mm, coupled. The PCL solution was electrospun by applying a voltage of 11.1 kV, a needle tip to ground collector distance of 18 cm, and a flow rate of 1 mL h^{-1}. After the complete processing of 1 mL of PCL solution, the nanofiber mesh (NFM) was allowed to dry for 1 day. This processed NFM was cut into samples of 1 × 1 cm^2 for further assays. Temperature and humidity, two important parameters that can influence this process, were kept under control. All the electrospinning experiments were performed at 22 ˚C, as well as the subsequently drying of the electrospun nanofiber meshes.

II-3.1.2. Nanofibrous meshes activation, aminolysis and fucoidan immobilization

Another important aspect, besides the peculiar morphological features, is that this NFM can be easily functionalized, namely aiming the immobilization of fucoidan.

For the activation of the nanofibers surface, an ultraviolet–ozone (UV–ozone) cleaner system was used (ProCleaner 220, Bioforce Nanoscience, USA). The UV-O method is a photo-sensitized oxidation

process in which the molecules are excited and/or dissociated by the absorption of short-wavelength UV radiation [28]. The products of this excitation reaction with the atmospheric oxygen are simpler volatile molecules which desorbs from the surface. When both UV wavelengths (184.9 nm and 253.7 nm) are presented, atomic oxygen (O) is continuously generated, as well as ozone is formed and destroyed, simultaneously. This is a versatile technique used to sterilize, activate and clean samples, increasing surface wettability. In chapter V, both sides of the electrospun NFMs were exposed for 90 seconds to UV–ozone irradiation.

After this, the insertion of amine groups (NH_2) was performed by aminolysis (**Figure II-5**). This chemical reaction can modify the surface charge, chemical groups and wettability of the NFM. PCL contains ester groups (-COO-) that can be hydrolyzed to carboxylic acid groups under environmental alkaline conditions. Moreover, it is possible that amino groups can be introduced at the polyester surface by a reaction with hexanediamide (HMD; Sigma Aldrich), providing that one amino group reacts with the - COO- group to form a covalent bond (-CONH-), while the other amino group is unreactive and free. The addition of amine groups can provide a non-toxic platform for cells and decreases the surface hydrophobicity. It also allows an easier functionalization, since it will provide active sites for the linkage of other biomolecules and polymers. Methodologically, electrospun nanofibers were immersed in a 1 M HMD solution for 1h at 37°C. After this process, nanofibers were washed 3 times to remove all unreactive HMD solution.

For the fucoidan immobilization, the polysaccharide was dissolved in 0.1 M NaCl. Different concentrations of fucoidan were prepared (Fu 2.5; Fu 5; Fu 7.5 and Fu 10 mg mL^{-1}) and 200 µL of each solution was added over each NFM sample in a 24 well-plate. The reaction was performed during 8h and after that the solutions were removed and the NFM were left to dry overnight. In the following day, NFM were washed twice. All those steps were performed under sterile conditions.

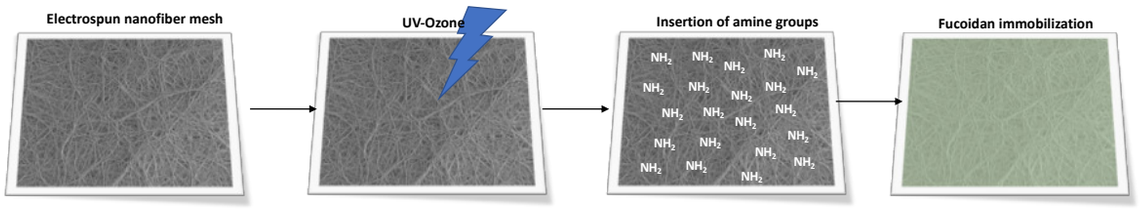

Figure II-5 Schematic representation of NFMs activation, aminolysis and fucoidan immobilization.

II-3.1.3. Quantification of immobilized fucoidan

Toluidine blue (TB) was discovered by William H. Perkin in 1856 and is used to detect glycosaminoglycans (GAGs) [29]. TB staining is based on metachromasia, a principle in which the dye reacts with electronegative groups in tissues to produce colors of different wavelengths according to the GAG concentration. The negatively charged sulfates in the GAGs neutralize the positive charge of toluidine blue, leading to dye aggregation by hydrophobic bonding and van der Waals interactions [30]. In the case of this work, and since toluidine blue is often used to quantify sulfated polysaccharides, it was chosen to quantify the amount of fucoidan immobilized on the NFMs developed in Chapter V. Briefly, each sample was immersed in 500 µL of TB solution (0.1 M HCl, 20 mg NaCl and 4 mg toluidine blue O chloride) for 4 h at room temperature (**Figure II-6**). This solution was removed and the biofunctionalized NFMs were washed to ensure the removal of unreacted TB solution. Afterwards, the biofunctionalized NFMs were immersed in 500 µL of a solution containing 0.1M NaCl and ethanol (1:4) until complete decoloration. The amount of TBO was assessed by measuring the absorbance at 530 nm using a microplate reader. The amount of fucoidan immobilized at the surface of each NFM was calculated by performing a standard curve with fucoidan. For that, different concentrations of fucoidan (Fu 2.5; Fu 5; Fu 7.5 and Fu 10 mg mL^{-1}) were quantified by the method described above, with little modifications. After the incubation with TB, the solutions were centrifuged and the unreacted TB was removed. The pellet was then resuspended with the above mentioned 0.1M NaCl and ethanol solution, and read at 530 nm. Each condition was read in triplicate.

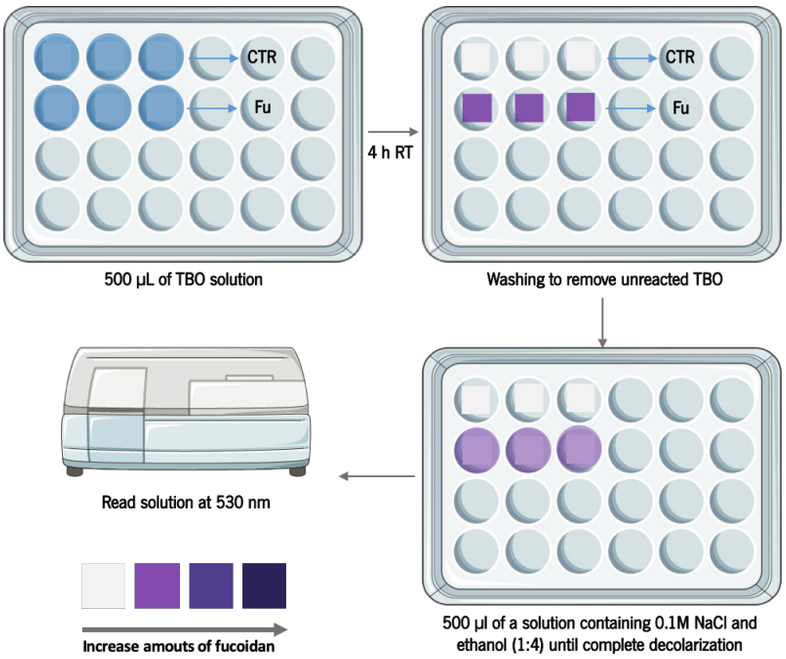

Figure II-6 Schematic representation of the TB quantification.

II-3.2. Drug delivery systems

II-3.2.1. Nanoparticles production

Marine-origin polymeric nanoparticles were prepared by polyelectrolyte complexation. Polyelectrolyte complexes (PECs) are formed due to electrostatic interactions between oppositely charged molecules (e.g. polymer-polymer, polymer-drug and polymer-drug-polymer) [31]. This is a cost-effective and easy method to produce nanoparticles, which avoids the use of chemical cross-linking agents that may present unwanted cytotoxic effects. Different parameters are known to influence the formation of PECs, namely charge density, polyelectrolytes concentration, pH, ionic strength and solvents [32]. The use of PECs for the development of drug delivery systems has been extensively described during the last couple of decades. These drug delivery systems are able to encapsulate different compounds, like chemotherapeutic drugs, into the polymer matrix at the molecular level. This DDS offer great advantages by improving drugs' stability and protecting them from enzymatic degradation, a controlled release profile of the drug, as well as an higher surface area that allows an easier functionalization. However, some limitations may be also present, related with a limited drug-loading capacity, drug loss during nanoparticles' circulation and poor-site specific accumulation [33].

In Chapter VI and VII, fucoidan (negatively charged) was complexed with chitosan (positively charged), with a polymeric solution being added drop-by-drop into the other solution and a spontaneously formation of the nanoparticles occurs (**Figure II-7**).

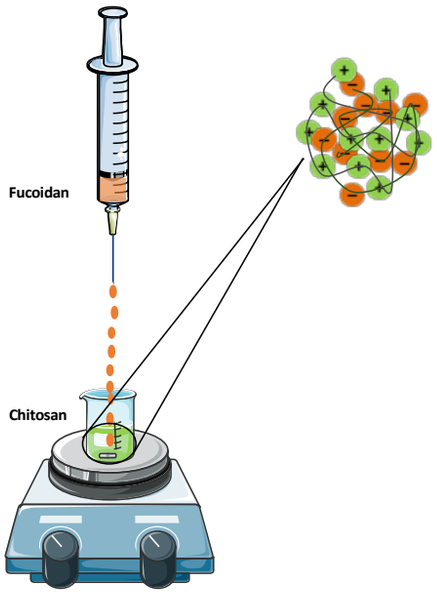

Figure II-7 Fucoidan/chitosan nanoparticles production.

Different parameters were evaluated regarding nanoparticles production to assess the optimal production conditions, both in terms of size and polydispersive index (Pdi) (**Table II-3**). Each parameter was evaluated separately while all the others were kept constant. After all the optimization steps, nanoparticles parameters were maintained for all further assays.

Table II-3 Parameters optimization for nanoparticles production.

Parameter	Fu/CH conc (mg mL $^{-1}$)	Ratio	pH (solutions)	Solvents	EDC/NHS conc (mM)
Tested conditions	0.25/0.25	1:2	3	UPW	600/240
	0.5/0.5	1:1	5	Osmotized W	300/120
	0.75/0.75	2:1	7	0.9% NaCl	150/60
	1/1		9		

Fu: fucoidan; CH: chitosan; UPW (ultra-pure water); W (water); NaCl (sodium chloride)

Nanoparticles final formulation resulted from chitosan dissolved in 1% v/v acetic acid solution at 0.5 mg mL ^{1} concentration, whereas the polyanion (fucoidan) was prepared in ultra-pure water to reach a final concentration of 0.5 mg mL $^{-1}$. Chitosan and fucoidan solutions acidity adjusted by the addition of 1M HCl and/or 1 M NaOH, depending on the desired pH. Chitosan solution was adjusted to pH=5, whereas the pH of fucoidan solution was adjusted if it was not as expected (pH=9). The solutions were kept at a final theoretical ratio (v/v) of 1:1 and a spontaneous formation of nanoparticles occurs. Right after, 300 mM EDC + 120 mM NHS was added to the nanoparticles solution and left under stirring for 2 hours at 600 rpm. After that, nanoparticles were collected using 300 kDa vivaspin filters for 15 minutes at 4000 rpm. Nanoparticles were washed twice with ultra-pure water and, finally, were filtered with 0.22 μm filters. Glucose was added in all centrifugation steps to avoid nanoparticles aggregation. For gemcitabine (Gem) encapsulation, all the previous steps were performed, but with Gem being added to the CH solution, maintaining the same production conditions (CH:Fu:Gem ratio 1:1:0.3). The entrapment efficiency (EE) was calculated by measuring the initial concentration and non-encapsulated Gem, according to the following formula:

Equation II-1 Equation for the determination of the entrapment efficiency.

$$\%EE = \frac{(\text{initial concentration-non-entrapped drug})}{\text{initial concentration}} x100$$

II-3.2.2. Production of the ErbB-2 targeting system

Antibodies have two different regions: a variable region that is specific of each antibody and a non-variable region that is common for each type of antibody. The specific and variable region is also known as the antigen binding site where only a specific antigen can be linked. Typically, there is a carboxyl group (-COOH) in the antibodies structure at the end of their non-variable region. This antibody group can react with free amine groups (-NH_2), as the ones present on chitosan (**Figure II-9**).

For the functionalization of the previously developed NPs with an ErbB-2 antibody (clone 7H3L20, Thermo Fisher, USA), some additional steps were performed. After centrifugation and purification, the nanoparticles were re-suspended in Ultra-pure water (UPW) and added to the antibody solution, previously activated with EDC/NHS (50 mM/200 mM). Nanoparticles were left under stirring for 2 h, followed by a washing step to remove unbound antibody. A wide range of ErbB-2 antibody concentrations (from 0 to 20 μg mL^{-1}) were tested to determine the maximum immobilization capacity of the nanoparticles. In order

to determine the degree of immobilization, an indirect method was used to quantify the fluorescence of unbound secondary antibody solution (*n* = 3 samples, read in triplicate). Alexa Fluor 488 (1:100; Molecular Probes, USA) was added for 1 h at RT, with the reading parameters of 495 nm for the absorption and 519 nm for the emission. Negative control samples were also prepared, where all the antibody immobilization steps were performed with the exception of the primary antibody incubation, which was substituted with UPW.

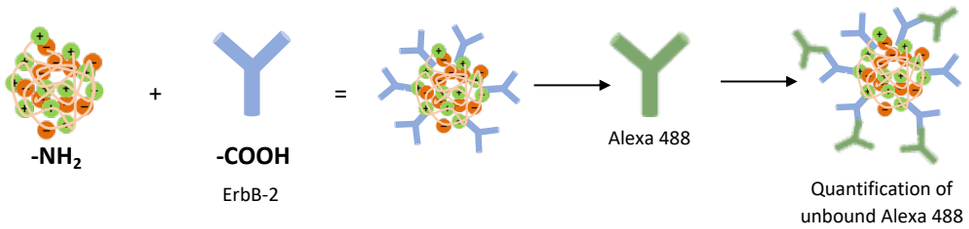

Figure II-8 Schematic representation of ErbB-2 antibody immobilization.

II-3.2.3. EDS/NHS chemistry

EDC is a crosslinking agent used to couple carboxyl groups to primary amines. Although NHS (N-hydroxysuccinimide) is not required for carbodiimide reactions, its use greatly enhances the coupling efficiency, leading to a two-step reaction (**Figure II-9**) [34]. Since EDC/NHS is a zero-length cross-linker (do not become part of the final crosslink), this chemical reaction does not present cytotoxic concerns. With the combination of EDC/NHS, amine reactive NHS esters can be available to react with any carboxyl-containing molecule (-COOH). This reaction was performed in Chapter VI and VII, namely for the production and stabilization of the NPs and the immobilization of the ERbB-2 antibody ate the surface of the developed NPs. EDC/NHS was dissolved in 0.1 MES(2-N-morpholino) ethanesulfonic acid) buffer with 0.9% (wt/wt) NaCl, following pH adjustment to pH=4.7. The concentration for NPs has been optimized as described above. The concentration used for the activation of the antibody has been already reported by our group and used accordingly [35].

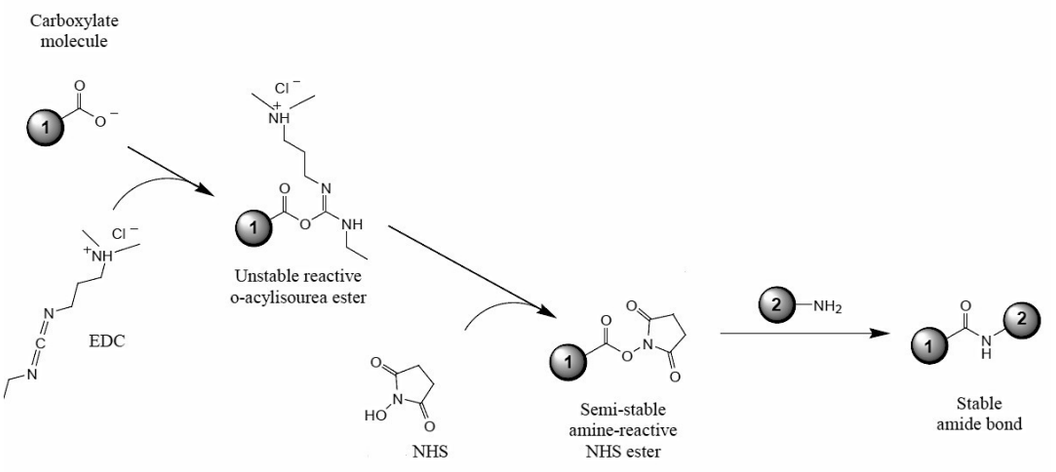

Figure II-9 EDC/NHS chemistry [34].

II-3.2.4. Gemcitabine

Gemcitabine (Gem) is a chemotherapeutic drug often used in the treatment of different types of cancer such as lung, ovary, pancreatic and breast, being used as a single agent or in combination with other chemotherapeutic drugs (**Figure II-10**) [36-38]. This chemotherapeutic drug is a nucleoside analog and incorporates into DNA, inhibiting DNA synthesis, blocking cell proliferarion at G1/S-phase. It presents a rapid metabolization and short-half-life that requires increased levels of Gem to get higher therapeutic efficacy, but consequently associayed to severe side effects [39, 40]. In the work herein presented, Gem was selected due to its usage in the treatment of breast cancer making it a good candidate for the development of drug delivery and targeting systems. Its hydrophilic nature is of great interest to allow an easier encapsulation into the developed marine-origin polymeric nanoparticles. The Gem used in Chapters VI and VII of this thesis (Gemcitabine (2'-Deoxy-2',2'-difluorocytidine)) was purchased from Carbosynth (United Kingdom).

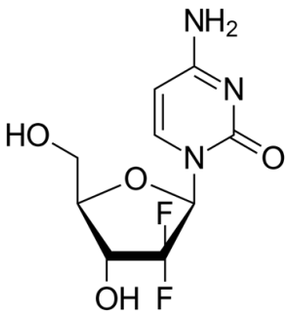

Figure II-10 Gemcitabine chemical structure.

II-3.2.4.1 *Gemcitabine Release Studies*

By using Beer-Lambert law, it is possible to determine concentrations of an absorbing chemical in solution. This is based in the principle that the absorbance of a solution is directly proportional to the concentration of the absorbing species in the solution and the light path length. The concentration of the chemical can be determined using a calibration curve. The release kinetics of Gem, in Chapter VI, was measured by placing 1.5 mL of drug-loaded NPs into dialysis membranes, and this system into 50 mL of 0.9% NaCl at 37°C under 60 rpm stirring. At predetermined time periods (0, 5, 15, 30, 45 min; 1, 1.5, 2, 3, 4, 5, 6, 8, 12, 24, 48 and 72 h), an aliquot of 2 mL of the release solution was taken and immediately analyzed to measure the maximum absorbance at 268 nm by Ultra-violet-visible spectroscopy (UV-Vis) (Shimadzu).

UV-Vis spectrophotometry refers to absorption or reflectance spectroscopy of photons in the UV-visible region. This spectroscopic technique uses light in the visible and adjacent regions near ultraviolet (UV) and near infrared (NIR) ranges [41].

II-4. PHYSICOCHEMICAL CHARACTERIZATION

II-4.1. Chemical characterization

II-4.1.1. Proton-Nuclear Magnetic Resonance analysis (^{1}H-NMR)

Proton-Nuclear Magnetic Resonance (^{1}H-NMR) is widely used to identify polymers and analyze their chemical modifications [42]. The magnetic resonance of protons, which is obtained by the small magnetic

fields produced by the movement of electrons, is measured and the distribution of electrons in molecules is distinct for different chemical groups. If a chemical group is modified it results in the modification of its magnetic resonance and a new peak or chemical shift appears in the ^{1}H-NMR spectrum.

This technique was used to observe chemical differences between the different fucoidan extracts in Chapter III. Briefly, NMR experiments were acquired on a Bruker AVANCE 400 (Bruker, USA) spectrometer using D_2O as solvent. The residual HOD signal was used as reference for the chemical shifts that are reported in ppm. Mnova Software 9.0 (Mestrelab Research) was used for spectral processing. Sulfation position and branching was qualitatively analyzed based on the chemical shifts previously described [43, 44].

II-4.1.2. Gel permeation chromatography

Gel Permation Chromatography (GPC) is used to determine the distribution of the molecular weight of a polymer [45]. This type of exclusion chromatography involves the use of a stationary phase column, enabling the separation of analytes dispersed in the mobile phase from a sample according to their size (smaller analytes are retained for longer periods of time). When compared to standard samples with known molecular weight, the molecular weight of the analytes can be determined.

This technique was performed to compare the molecular weights of different fucoidan extracts in Chapter III. GPC measurements were performed with a Malvern Viscotek TDA 305 (Malvern, UK) with refractometer, right angle light scattering and viscometer detectors on a set of four columns: pre-column Suprema 5 µm 8x50 S/N 3111265, Suprema 30 Å 5 µm 8x300 S/N 3112751, Suprema 1000 Å 5 µm 8x300 S/N 3112851 PL and Aquagel-OH MIXED 8 µm 7.5x300 S/N 8M-AOHMIX-46-51, with refractive index detection (RI-Detector 8110, Bischoff). The system was kept at 30 °C using a solution of 0.1 M NaN_3 and 0.01 M NaH_2PO_4 (pH = 6.6) as eluent at rate of 1 mL min^{-1}. The elution times from the RI detector signal were calibrated with a commercial polysaccharide set from Varian® that contains 10 Pullulans with narrow polydispersity and Mp (molecular mass at the peak maximum) ranging from 180 Da to 708 kDa.

II-4.1.3. Depolymerization of fucoidan extract FE1 by acid hydrolysis

Hydrolyzed fucoidan has been described to present increased cytotoxicity over cancer cells [46]. Different methods can be applied, namely by hydrolyzing fucoidan under mild (boiling water with HCl) or harsh conditions (microwave) [47]. Since mild conditions have been reported to yield hydrolysates presenting increased cytotoxic effects over cancer cells, this was the chosen method to depolymerize fucoidan, aiming to obtain lower molecular weight fucoidan in Chapter III (**Figure II-11**).

Briefly, hydrolyzed fucoidan was obtained by dissolving 20 mg of fucoidan in 1 mL of 0.01 M HCl at 100 °C for 10 min, followed by neutralization with 1 mL of 0.01 M NaOH. A control was performed by dissolving 20 mg of fucoidan in 1 mL of 0.01 M HCl without heat treatment, followed by neutralization with 1 mL of 0.01 M NaOH. The depolymerization was confirmed by measuring the molecular weight as described in the previous section.

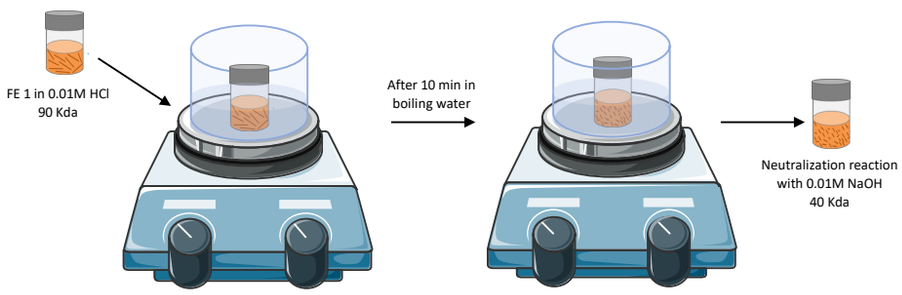

Figure II-11 Schematic representation of fucoidan depolymerization

II-4.1.4. Carbohydrates composition by Gas chromatography

Fucoidan composition was assessed to understand whether its monosaccharides could be related with the antitumor behavior. The neutral monosaccharides composition can be determined by first hydrolyzing the polysaccharides to their constituent monosaccharides with strong acid and, then, converted to alditol acetates by reduction with sodium borohydride to the corresponding aditol, followed by acetylation of the hydrolysis on each aditol. The resultant aditol acetates are volatile, and can be identified and quantified by gas chromatography (GC). GC is a common type of chromatographic technique commonly used in analytical chemistry for separating and analyzing compounds that can be vaporized without decomposition [48]. Typical uses of GC include testing the purity of a particular substance, or separating the different components of a mixture (the relative amounts of such components can also be determined).

In Chapter III, neutral monosaccharides were determined as alditol acetates as described elsewhere [49]. Briefly a pre-hydrolysis of fucoidan was performed, with 72% sulfuric acid for 3 h at RT. Afterwards, the fucoidan extracts were submitted to a hydrolysis with sulfuric acid 1 M at 100°C for 2.5 h. 2-Deoxyglucose was used as an internal standard. Monosaccharides were reduced with sodium borohydride and acetylated by acetic anhydride using methylimidazole as a catalyst. The formed alditol acetate derivatives were analyzed by GC with a 30 m column DB-225 (J&W Scientific, Folsom, CA, USA) (0.25 mm internal diameter, and 0.15 mm film thickness), and using a flame ionization detector (Perkin Elmer, Clarus 400). The hydrolysis of all samples was performed in duplicate and each one was injected twice. A third analysis was done for the few samples with higher variability. Uronic acids were quantified by a modification of the 3-phenylphenol colorimetric method [49]. Samples were prepared by hydrolysis with 72% sulfuric acid for 3h at RT followed by 1 h in sulfuric acid 1 M at 100°C. A calibration curve was made with D-galacturonic acid. The hydrolysis and analysis of the samples was done in triplicate.

II-4.1.5. Sulfation Degree: ester sulfate determination

One of the most significant parameters reported to influence fucoidan antitumor behavior is the sulfation degree [50]. Higher sulfation has been related with enhanced biological properties. Having this in mind, this parameter was studied in Chapter III, to compare the different fucoidan extracts.

The content of ester sulfates in the fucoidan extracts was determined by the turbidimetric method proposed by Dodgson and Price [51, 52]. The fucoidan extracts were accurately weighed (usually 2-4 mg) and dissolved in the respective amount of N-hydrochloric acid 1 M. The mixture was submitted to a hydrolysis at 105-110 °C for 5 h. A portion (0.2 mL) was transferred to a tube containing 3.8 mL of 3% (w/v) trichloroacetic acid. Barium chloride-gelatin reagent (1 mL) was added and, after mixing, the whole was kept at RT for 15-20 min. The barium chloride-gelatin reagent was previously prepared by mixing gelatin (1 g) with 200 mL of hot water (60-70°C) and allowed to stand at 4°C overnight. Barium chloride (1 g) was dissolved in the semi-gelatinous fluid and the resultant cloudy solution was allowed to stand for 2-3 h before use. The solution was then analyzed at 360 nm (Jenway 6405 UV/Vis) against reagent blank containing distilled water instead of the sample.

A second 0.2 mL portion of the hydrolysate was mixed with 3.8 mL of trichloroacetic acid, as described above, and with 1 mL of gelatin solution (i.e. containing no barium chloride). The extinction of this "control" solution was then measured at 360 nm against a reagent blank consisting on distilled water

instead of sample and 1 mL of gelatin solution. The concentration of sulfate esters was determined from a calibration curve built with K_2SO_4 solutions, containing between 20 and 200 µg of SO_4^{2-} ion.

II-4.1.6. Desulfation and Methylation analysis by GC-qMS

The same sulfation degree can correspond to different sulfates position, which may present different biological outcomes. Methylation analysis, before and after desulfation, allow to know the substitution of sugar residues, corresponding to branching points and the substitution by sulfate esters [53]. When a position is acetylated in the native polysaccharide and become methylated after desulfation, it is indication that this position contains a sulfate residue. However, when a position is acetylated even after desulfation of the polysaccharide, it can be inferred that it is a branching point. These important parameters, the sulfates position and polymer branching, were both analyzed in Chapter III.

The glycosidic-substitution analysis was determined by gas chromatography-quadrupole mass spectrometry (GC-qMS) of the partially methylated alditol acetates, based on Ciucanu and Kerek [54] and Coelho, Rocha, and Coimbra [55]. The native and desulfated samples (1–2 mg) were dissolved in 1 mL of anhydrous dimethylsulfoxide (DMSO) and, then, powdered NaOH (40 mg) were added under an argon atmosphere. For polysaccharide desulfation, 10 mg were dissolved in 1.8 mL of dried dimethyl sulfoxide. Then, 0.1 mL pyridine was added, followed by 13 mg of pyromellitic acid, 12 mg of NaF, and 0.2 mL of pyridine. The mixture was stirred at 120 °C for 3 h, cooled and poured into 1 mL of 3% of $NaHCO_3$ aqueous solution. The solution containing the desulfated polysaccharide was dialysed and freeze-dried. The procedure was repeated in order to guarantee the complete desulfation.

Afterward, the desulfated polysaccharide was submitted to methylation analysis. The samples were methylated with CH_3I (80 µL) during 20 min with stirring, followed by a second and third addition of 80 µL CH_3I and stirred for another 20 min. $CHCl_3$/MeOH (1:1, v/v, 3 mL) was added, and the solution was dialyzed (membrane with a pore diameter of 12–14 kDa) against 50% EtOH. The dialysate was evaporated to dry and the material was remethylated using the same procedure. The remethylated material was hydrolyzed with 2 M TFA (1 mL) at 120°C for 1 h and, then, reduced and acetylated as previously described for neutral sugar analysis (using $NaBD_4$ instead of $NaBH_4$). The partially methylated alditol acetates (PMAA) were separated and analyzed by GC–qMS (GC-2010 Plus, Shimadzu, Japan). The GC was equipped with a DB-1 (J&W Scientific, Folsom, CA, USA) capillary column (30 m length, 0.25 mm of internal diameter, and 0.10 µm of film thickness). The samples were injected in “split” mode with the

injector temperature at 250°C. The temperature program used was the follow: 1) an initial temperature of 80°C; 2) an increase of 7.5°C/min until 140°C and a holding time of 5 min; 3) an increase of 0.2°C/min until 143.2°C; 4) an increase of 12°C/min until 200°C; 5) an increase of 50°C/min until 250°C and a hold time of 5 min. The helium carrier gas was settled at a total flow rate of 8.5 mL/min. The GC was connected to GCMS-QP 2010 Ultra Shimadzu mass quadrupole selective detector, operating with an electron impact mode at 70 eV and scanning the range m/z 50–700 in a 1 s cycle in a full scan mode acquisition.

II-4.1.7. X-ray Photoelectron Spectroscopy

X-ray Photoelectron Spectroscopy (XPS) is a surface-sensitive quantitative spectroscopic technique that allows to measure the surface energy of a substrate by assessing its surface chemistry, based in photoelectric effct [56]. XPS spectra are obtained by irradiating the sample with a beam of X-rays that measure the kinetic energy and the number of electrons that scape from the top 0 to 10 nm of the material surface.

The chemical state of the different elements present in the material can be detected through this analysis, before and/or after surface treatments. Therefore, to confirm fucoidan immobilization at the surface of NFMs, XPS analysis was performed in Chapter V. It was expected that by the immobilization of fucoidan, a sulphur peak would be detected due to the sufate groups from fucoidan and not present on the other materials. A Kratos Axis-Supra instrument equipped with aluminium Kα monochromatized radiation at 1486.6 eV X-ray source, within ESCApe software was used. The residual vacuum in the X-Ray analysis chamber was maintained at around $4.5x10^{-8}$ torr. The samples were fixed to the sample holder with double sided carbon tape.Due to the non-conductive nature of the samples it was necessary to use a co-axial electron neutralizer to minimize surface charging due to the removal electrons from the susbtrate. The XPS measurements were carried out using monochromatic Al-Kα radiation (1486.6 eV). Photoelectrons were collected from a take-off angle of 90° relative to the sample surface. The measurement was done in a Constant Analyser Energy mode (CAE) with a 160 eV pass energy and 15 mA of emission current for survey spectra and 40 eV pass energy for high resolution spectra, also using and emission current of 15 mA. The binding energies (BEs) positions were referenced to the C1s on unsputtered surfaces. Charge referencing was done by setting the lower binding energy C1s photo peak at 285.0 eV C1s hydrocarbon peak and the survey spectra of C1s, O1s, S2p were recorded [57].

II-4.2. Physical characterization

II-4.2.1. Contact angle

Contact angle (θ) measurements were performed to evaluate the wettability of NFMs with or without fucoidan immobilized at their surface, in Chapter V. The contact angle refers to the angle formed when a liquid interacts with the solid surface (**Figure II-12**) [58]. If the water contact angle is <90°, the surface is considered hydrophilic (high wetting), whereas if it is >90° the surface is considered hydrophobic (low wetting). The contact angle depends on several interrelated parameters, such as, surface chemistry, roughness/topography and crystallinity.

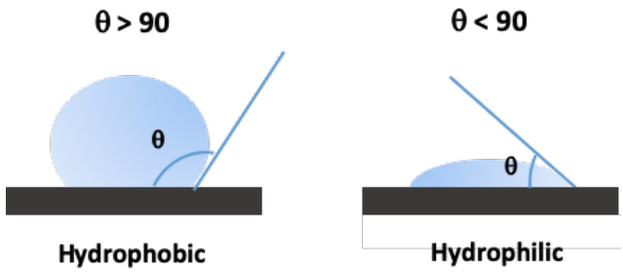

Figure II-12 Schematic representation of an hydrophiid and hydrophilic surface.

Surface hydrophilicity of NFM with and without fucoidan was measured as the static contact angle of a standard liquid (ultra-pure water, 3 µL), at room temperature, using a Contact Angle Equipment (OCA 15plus equipment, Germany and SCA-20 software). During every determination, a motor driven syringe was used to deposit a drop of water over the NFM surface. Measurements were recorded for each sample and the determinations were performed in triplicate.

II-4.2.2. Dynamic light scattering

Dynamic light scattering (DLS) is a technique for measuring the size of particles, typically at the submicron range. This technique presents the ability to make measurements in native environments, it is sensitive to small sample volumes and user friendly commercially available operating instruments are availble [59]. A typical DLS system comprises the following components: a laser that provides a light source to illuminate the sample contained into a cell, a detector (173°) used to measure the scattered light; and an attenuator used to reduce the intensity of the laser source and hence reduce the intensity of scattering. The DLS analysis relies on the follow functioning: when a particle is suspended in a solution

and is illuminated by light, it scatters light providing that its refraction index differs from that of the suspending solvent. DLS measures Brownian motion and relates this to the size of the particles. Brownian motion is the random movement of particles in relation to the solvent molecules that surround them [60]. The larger the particle, the slower the Brownian motion will be. The average size and distribution (measured as the polydispersive index, Pdi) of the nanoparticles produced in this work were determined by dynamic light scattering (DLS) using a Zetasizer Nano ZS (Malvern Instruments, Malvern, UK), in Chapters VI and VII (**Figure II-13 A**). Samples were diluted in UPW and the size analysis lasted 180 s and performed at 25°C, in triplicate. The zeta potential measurements were performed by a dip cell in automatic mode (**Figure II-13 B**).

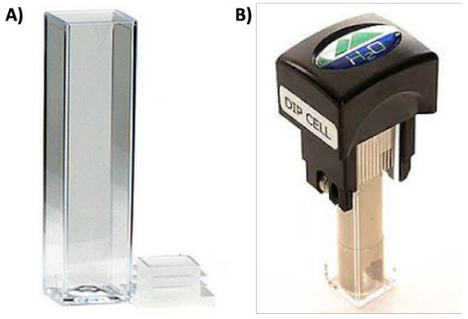

Figure II-13 Cuvette used for size measurements A) and Dip cell used for zeta-potential analysis B).

The zeta-potential is an essential and easily measurable physical property related to the surface charge of materials in solution and to their electrophoretic mobility [61]. The magnitude of the zeta-potential gives an indication of the potential stability of the NPs, in the case of this thesis. If all the particles in suspension have a high negative or positive zeta potential, then they tend to repel each other. If the particles have low zeta potential values, the particles tend to aggregate. The defined stability of the nanoparticles in relation to the zeta-potential is stated in **Table II-4**.

Table II-4 Zeta-potential values and stability [61]

Values (mV)	Stability
± 0 - 10	Highly unstable
± 10 - 20	Relatively stable
± 20 - 30	Moderately stable
> ±30	Highly stable

II-4.2.3. Nanoparticle Tracking Analysis (NTA)

NP tracking analysis (NTA) experiments were performed using a NanoSight NS500 instrument (Malvern Panalytical, UK). Nanosight is an easy-to-use and reproducible technique for nanoparticles characterization. In addition to measuring the size, nanosight can also calculate NPs concentration, reason why this equipment was used in Chapter VI. It allows the visualization of the NPs motion in solution, which is registered by CCD camera, due to scattering of a laser beam [59]. This system includes a charge-coupled device camera that allows visualization and tracking of Brownian motion of laser-illuminated particles in suspension. Video images were analyzed using NTA analytical software version 2.3. The measurements were made at room temperature and each video sequence was captured over 60 s.

Despite these interesting features, the referred techniques based on light scattering do not provide information regarding NPs morphology, reason why additional techniques were considered, as assessed in the following sections.

II-4.2.4. Scanning electron microscopy and scanning transmission electron microscopy

Scanning Electron Microscopy (SEM) is a precise imaging technique to acquire high-resolution 2D images of a sample [62]. This is an interesting microscopic technique that uses high magnifications to study the morphology and topography of different materials and structures, allowing the observation of the details at the sub-micron level. A focused beam of electrons scans the samples' surface by interacting with its atoms, producing several signals which are detectable by the SEM equipment, and transformed into a 2D image [63]. Since the electron beam can be scattered only on conductive samples, polymeric samples are usually sputtered with a thin layer of conductive materials, such as gold, platinium or carbon. Scanning transmission electron microscopy (STEM) combines the principles of transmission electron microscopy (TEM) and SEM. TEM uses the electrons which are passing through the sample (transmitted electrons) before they are collected. As a result, TEM offers information on the inner structure of the sample, while SEM provides information on the sample's surface and composition. One advantage of STEM over conventional SEM images is the improvement in spatial resolution.

Measurement of particles' size and morphology observation were obtained using High Resolution-SEM (Auriga, Carl Zeiss, Germany), in Chapter VI. A drop of nanoparticles solution was placed in a glass

slide glued to the stub and left to dry overnight. Afterwards, the samples were vacuum-coated with a gold-platinum mixture. STEM analysis was also performed with the same equipment.

II-4.2.5. Atomic Force Microscopy

Atomic Force Microscopy (AFM) technique allows the analysis of the samples' surface with high resolution and accuracy [64]. Unlike electron or optical microscopy, AFM does not acquire images by focusing the light or electrons onto the surface. Instead, approaches the height and topography of the samples surface with a sharp probe or cantilever, which deflection due to force interaction between the sample surface and the cantilever allows the evaluation of suface roughness and (nano)topography. Furthermore, besides being an imaging tool, AFM has several spectroscopic modes that measure other samples properties, such as the height, at the nanoscale.

Morphological analysis of the develop targeting NPs, in Chapter VII, was obtained using a MultiMode STM microscope controlled by a NanoScope III from Digital Instruments system, operating in tapping mode at a frequency of 1 Hz. Prior to the analysis, a drop of NPs solution was placed in a glass slide and left to dry overnight.

II-5. *IN VITRO* BIOLOGICAL CHARACTERIZATION

II-5.1. Cell sources – The tumor microenvironment

The tumor microenvironment (TME) comprises not only cancer cells but also normal cells and tissues (**Figure II-14**) [65]. Despite the cancer cells, cells of the immune system, cells characteristic of the tissue, fibroblasts, as well as endothelial cells are part of the TME. It is also known that, when a therapeutic strategy aims to be intravenously injected, the first biological barrier will be the blood vessels endothelium [66]. As so, the effect of potentially antitumor compounds over normal cells should always be studied, an aspect that is missing in most reported studies regarding fucoidan usage. In the context of this thesis, besides breast cancer and melanoma cells, as models of cancer cells, different normal cells were always used depending on the targeting tumor and final application.

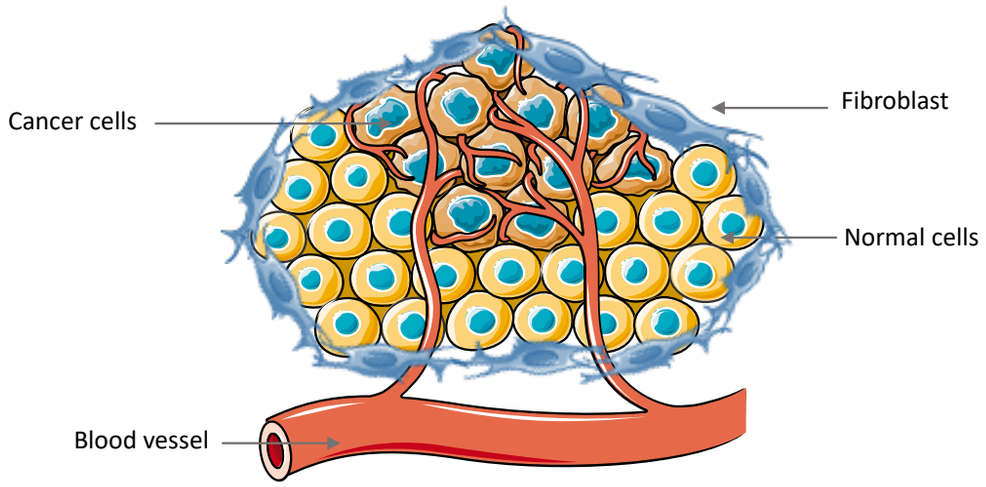

Figure II-14 The different cell types of the tumor microenvironment.

Regarding the chosen cell sources for the development of these studies, only cells from human origin were used. Primary cells are directly isolated from human or animal tissues using enzymatic or mechanical methods. The primary cells are sensitive and often require additional supplementation of the culture medium, having a limited lifespan. Despite some difficulties in working with primary cells, the results obtained with this type of cells can be more representative of the *in vivo* environment [67]. By its side, cell lines are immortalized cells that present the ability to proliferate indefinitely either due to a genetic mutation or artificial modification [68]. Cell lines are easy to culture and useful cell models, presenting reliable experimental results. Therefore, cell lines were the most used type of cells in this thesis. There were two exceptions: human dermal fibroblasts and keratinocytes, since there are no well-established cells lines in these two cases.

II-5.1.1. Breast cancer cells

Like most cancers, breast cancer is a complex and heterogenous disease. It can be divided in different sub-types namely, luminal A (around 40%), luminal B (around 20%), triple negative (15-20%) and HER2-positive (10-15%), according to their immunoprofile [69]. The cell sub-types studied and the corresponding cell lines used in this work are summarized in **Table II-5**, trying to address breast cancer heterogeneity.

Table II-5 Breast cancer cell lines immuneprofile used in the different studies

Molecular Subtype	Immuneprofile	Studied Cell Lines	Prognosis	Chapter
Luminal A	ER+, PR+/-, HER2-	MCF-7	Good	III
Her2+	ER-, PR-, HER2+	SKBR3	Medium	VII
Triple negative	ER-, PR-, HER2-	MDA-MB-231	Poor	III and VI

II-5.1.1.1 *MCF-7 cell line*

One of the most common used breast cancer cell line is MCF-7. It was established in 1973 at the Michigan Cancer Foundation [70]. MCF-7 cells were isolated from the pleural effusion of a 69-year-old woman with metastatic disease. It proves to be a suitable model cell line for breast cancer investigations worldwide, including those regarding anticancer drugs. It is ER-positive and progesterone receptor (PR)-positive and belongs to the luminal A molecular subtype. MCF-7 is a poorly-aggressive and non-invasive cell line, normally being considered to have low metastatic potential [71]. This cell line was used as model of breast cancer cell line when studying the effects of different fucoidans over cancer and non-cancer cells in Chapter III.

II-5.1.1.2 *SKBR3 cell line*

This cell line was established in 1970 from the pleural effusion of a 43-year-old Caucasian female with malignant adenocarcinoma of the breast [72]. SK-BR-3 is a human breast cancer cell line that overexpresses Her2 (ErbB-2). Her-2 is overexpressed in about 30% of breast cancer cells and poorly expressed in normal cells offering an opportunity to use this gene expression as biomarker of breast cancer [73]. In addition, this cell line is also a useful preclinical model to screen for therapeutic agents targeting Her2 and to delineate mechanisms of resistance to Her2-targeted therapies. In this sense, this cell line was used as model to assess nanoparticles targeting efficiency in chapter VII.

II-5.1.1.3 *MDA-MB-231 cell line*

MDA-MB-231 cell line is one of the most commonly used breast cancer cell lines and was established from a pleural effusion of a 51-year-old Caucasian female with a metastatic mammary adenocarcinoma [74]. This is an highly aggressive and invasive cell type, being designated as triple-negative since it lacks estrogen and progesterone receptors, as well as Her2 expression. Triple-negative breast cancer are the most aggressive and the ones with poorest diagnosis, with limited treatment options [75]. Since this cell line represents the most aggressive type of breast cancer it was the most studied in this thesis. In Chapter III, it was used to assess the effects of different fucoidans over different cancer cells. In Chapter IV, it was used to study the anti-tumor and anti-angiogenic potential of fucoidan. In another study, and trying to develop more effective treatments for this type of breast cancer, the nanoparticle drug delivery system efficiency was assessed over this cell line in Chapter VI.

All these breast cancer cell lines were cultured in D-MEM high glucose medium supplemented with 10% Fetal Bovine Serum (FBS) (Biochrom, Germany), 1% Pen/Strep (100 U/100 g mL^{-1}; Life Technologies, USA) and 1% of MEM sodium pyruvate solution (Life Technologies, USA). Cells were incubated at 37°C in a humidified 5% CO_2 atmosphere. The medium was changed every 2-3 days, until cells reached a 80-90% confluence. Cells were trypsinized with TripLE express (Life Technologies, USA) for 5 minutes at 37°C, centrifuged at 300 g for 5 minutes (Eppendorf 5810R centrifuge equipped with an A-4-62 rotor), and re-suspended in cell culture flasks (BD Biosciences, USA).

II-5.1.2. Melanoma cells

WM115, a human metastatic melanoma cell line derived from the primary tumor, was purchased from ATCC (USA) [76]. This cell line was used in Chapter V to assess the efficacy of the developed nanofiber meshes comprising fucoidan to treat melanoma. WM115 cells were cultured in Eagle's Minimum Essential Medium (EMEM 30-2003, ATCC) with 10% FBS (Biochrom, Germany), Pen/Strep (100 U/100 g mL^{-1}; Life Technologies, USA) and 1% 100 mM MEM sodium pyruvate solution (Life Technologies, USA). Cells were incubated at 37°C in a humidified 5% CO_2 atmosphere. The medium was changed every 2-3 days, until cells reached 80-90% confluence. Cells were trypsinized with TripLE express (Life Technologies, USA) for 5 minutes at 37°C and centrifuged at 300 *g* for 5 minutes (Eppendorf 5810R centrifuge equipped with an A-4-62 rotor), and re-suspended in cell culture flasks (BD Biosciences, USA).

II-5.1.3. Endothelial cells

II-5.1.3.1 *HPMEC-ST1.6R cell line*

A human pulmonary microvascular endothelial cell line (HPMEC-ST1.6R) was used to study the angiogenic potential of fucoidan, in Chapter IV. This cell line is commonly used to study the angiogenic process *in vitro* [77]. Cells were cultured in M199 medium supplemented with 20% FBS (Biochrom, Germany), 2 mM Glutamax (Life Technologies), Pen/Strep (100 U/100 g mL^{-1}; Life Technologies) and endothelial cell growth supplement (ECGS - 25 μg mL^{-1}; Becton Dickinson). Cells were incubated at 37°C in a humidified 5% CO_2 atmosphere. Medium was changed every 2-3 days, until cells reached a 80-90% confluence. Cells were trypsinized with TripLE express (Life Technologies) for 5 minutes at 37°C and centrifuged at 300 *g* for 5 minutes (Eppendorf 5810R centrifuge equipped with an A-4-62 rotor), and re-suspended in cell culture flasks (BD Biosciences, USA).

II-5.1.3.2 *EA.hy.926 cell line*

The human umbilical vein cell line, EA.hy926, was established by fusing primary human umbilical vein cells with a thioguanine-resistant clone of A549 by exposure to polyethylene glycol (PEG) [78]. This cell line was used as model of normal cells in Chapter VI and VII. These endothelial cells were cultured in D-MEM Low Glucose medium supplemented with 10% FBS (Biochrom, Germany) and 1% Pen/Strep (100 U/100 g mL^{-1}; Life Technologies, USA). Cells were incubated at 37°C in a humidified 5% CO_2 atmosphere. The medium was changed every 2-3 days, until cells reached a 80-90% confluence. Cells were trypsinized with TripLE express (Life Technologies, USA) for 5 minutes at 37°C and centrifuged at 300 *g* for 5 minutes (Eppendorf 5810R centrifuge equipped with an A-4-62 rotor), and re-suspended in cell culture flasks (BD Biosciences, USA).

II-5.1.4. Fibroblasts

II-5.1.4.1 *MRC-5 cell line*

The MRC-5 cells (Medical Research Council cell strain 5) were isolated in 1966 by J.P. Jacobs from lung tissue of a 14 week old aborted caucasian male fetus [79]. It is a fibroblast-like cell line and was

used in Chapter III of this thesis as a model of normal cells. Fibroblast cells were cultured in D-MEM Low Glucose medium supplemented with 10% FBS (Biochrom, Germany) and 1% Pen/Strep (100 U/100 g mL^{-1}; Life Technologies, USA). Cells were incubated at 37°C in a humidified 5% CO_2 atmosphere. The medium was changed every 2-3 days, until cells reached 80-90% confluence. Cells were trypsinized with TripLE express (Life Technologies, USA) for 5 minutes at 37°C and centrifuged at 300 g for 5 minutes (Eppendorf 5810R centrifuge equipped with an A-4-62 rotor), and re-suspended in cell culture flasks (BD Biosciences, USA).

II-5.1.4.2 *Primary Human Dermal Fibroblasts*

Primary Human Dermal Fibroblasts (hDFs) were purchased from Gibco, Thermo Fisher (USA). hDFs were used in Chapter V since fibroblasts are the most abundant cells in the dermal layer of the skin. Cells were cultured in Medium 106 (Gibco, USA) supplemented with 10% FBS (Biochrom, Germany), 1% Pen/Strep (100 U/100 g mL^{-1}; Life Technologies, USA) and 2% Low Serum Growth Supplement (Life Technologies, USA). Cells were incubated at 37°C in a humidified 5% CO_2 atmosphere. Medium was changed every 2-3 days, until cells reached a 80-90% confluence. Cells were trypsinized with TripLE express (Life Technologies, USA) for 5 minutes at 37°C and centrifuged at 300 g for 5 minutes (Eppendorf 5810R centrifuge equipped with an A-4-62 rotor), and re-suspended in cell culture flasks (BD Biosciences, USA).

II-5.1.5. Isolation of Human Keratinocytes

Human primary keratinocytes (hKCs) were obtained from samples from the Hospital da Prelada (Porto, Portugal), under an established protocol. Skin tissues were cut into small fragments (1-2 cm^2) and incubated overnight at 4°C with 2.5 U/mL dispase (BD Biosciences, USA). Epidermis was peeled off and digested at 37°C for 8 minutes using 0.05 % w/v Trypsin-EDTA (Invitrogen, UK). After inhibiting the digestion with an equal amount of FBS, cells were scraped, ant the digested epidermis was filtered through a sterile 100 µm cell strainer. After centrifugation (300 *g*, 5 minutes), the cells were resuspended in Keratinocyte Serum free medium (Life Technologies, Scotland), supplemented with Bovine Pituitary Extract (Life Technologies, Scotland), recombinant EGF (Life Technologies, Scotland) and 1% Pen/Strep solution (100 U/100 g mL^{-1}; Life Technologies, USA) and maintained at 37°C in a humidified tissue culture incubator with 5% CO_2 atmosphere. hKCs were trypsinized with TrypIE Express (Life Technologies,

USA) for 2-4 minutes at 37°C, incubated for further 5 min without TrypIE Express and centrifuged at 300 *g* for 5 minutes (Eppendorf 5810R centrifuge equipped with an A-4-62 rotor), and re-suspended in cell culture flasks (BD Biosciences, USA). Keratinocytes are the main component of the epidermis layer of the skin and were used in Chapter V as model of normal cells.

II-5.2. Cell seeding procedures

II-5.2.1. Seeding on the bottom of well-plates

2D cultures are important assays, as a first screening, to study the cytotoxicity of drugs/compounds [80]. In the context of this thesis, and to assess the cytotoxic effects of the different fucoidan extracts, mono-cultures were established for normal and cancer cells. The different cells were harvested, and 15 000 cells were cultured per well in 24-well Clear Flat Bottom TC-treated Multiwell Cell Culture Plates (Corning, USA). The cells were left to adhere for 4h and, after that, fucoidan extracts or nanoparticles were to the culture. Fucoidan extracts were dissolved in the corresponding culture medium at different concentrations (ranging from 0 to 1 mg mL^{-1}). For all the assays a positive control was performed (no fucoidan or NPs in the culture medium). After 1, 2 and 3 days of culture, a cell viability assay was performed. Each experimental condition was tested in triplicate and three independent assays were performed for each type of cells.

II-5.2.2. Seeding on top of electrospun nanofibrous mehes

The efficacy of the developed nanofiber meshes systems was assessed by testing different cell types, namely keratinocytes, fibroblast and melanoma cells (Chapter V). Cells were harvested and seeded onto fucoidan immobilized electrospun NFMs. Cell seeding was performed by dropping a 50 µL suspension containing 50 000 cells per NFM, and the cells were left to adhere for 4h. After cell attachment, culture medium was added. NFMs subjected to surface activation, and aminolysis, but no fucoidan immobilization were used as control condition. After 1, 3 and 7 days of culture, samples were collected for the cell viability assay and SEM observation. Triplicates of each condition were used in three independent assays.

II-5.2.3. Co-culture system

To validate the targeting capability of the ErbB-2 nanoparticles, a co-culture system was established with EA.hy.926 and SKBR3 cell lines (Chapter VII). Co-culture systems are more informative than 2D mono-cultures, since it can better represent the tumor microenvironment that comprises not only cancer cell but also healthy tissues [65]. The co-culture system was established using Nunc Polycarbonate Cell Culture Inserts in Multi-Well Plates (Thermo Fischer, USA) (**Figure II-15**). Endothelial cells were seeded at $3x10^4$ cells/insert and cultured for 3 days to allow cells proliferation and the formation of an endothelial monolayer. After that, the ErbB-2 positive breast cancer cells (SKBR3 cell line) were cultured as $1.5x10^4$ cells at the bottom of 24 well-plates. The culture medium of each cell type was maintained separatly. In the following day, the developed targeting system (NPs+Gem+Ab) and the control conditions (NPs+Gem or free Gem) were added over the endothelial cells layer, at a previously defined concentration (50 µl NPs mL^{-1}) [81]. MTS assay and live/dead stainning was performed 1, 2 and 3 days after co-culture establishment.

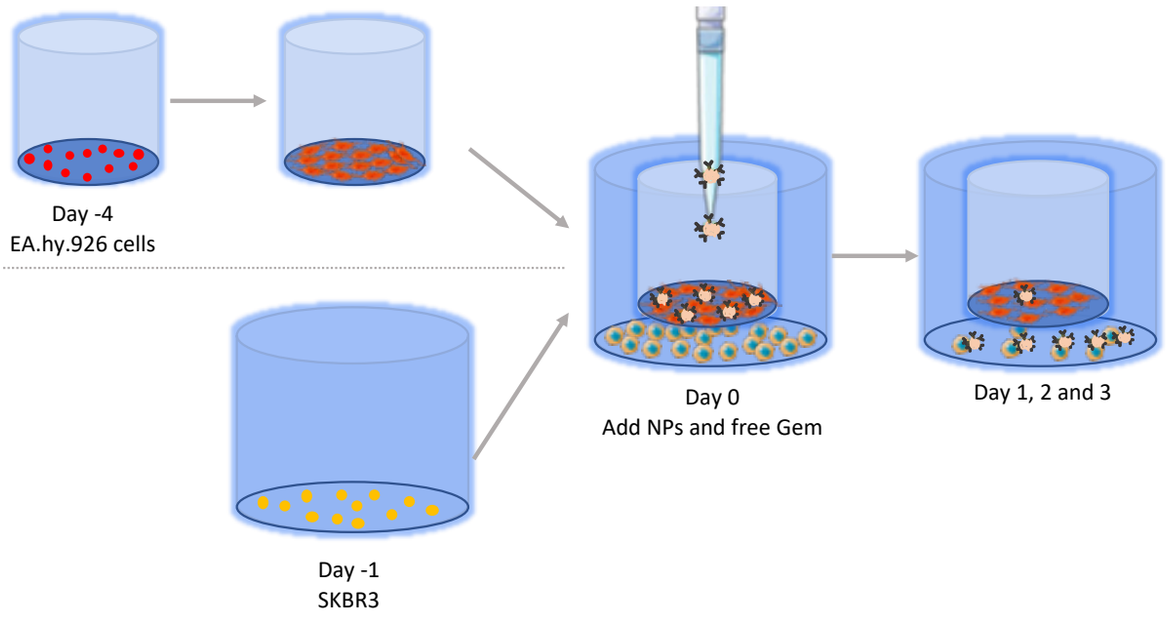

Figure II-15 Schematic representation of the co-culture system setup with endothelial (EA.hy.926) and ErbB-2 positive breast cancer cells (SKBR3)

II-5.3. Metabolic activity and cell viability

II-5.3.1. Metabolic activity assay

The cytotoxicity of a material/compound can be evaluated by changes in the cell's metabolic activity, which is assessed by the overall metabolic activity of the cell through enzymatic cleavage of colorimetric of fluorescent substrates. MTS is a colorimetric assay that quantifies cell metabolic activity and is generally used to study the cytotoxicity of a compound [82]. The principle of this assay is based on the reduction of a tetrazolium compound (MTS) into colored formazan by cells in culture, presumably by the action of NADH or similar reducing molecules that transfer electrons to MTS. The color intensity reflects the number of viable cells, as dying cells lose the capacity to reduce MTS. The CellTiter 96 AQueous One Solution cell proliferation assay (Promega, USA) was performed at the previously defined time points. The culture medium was removed from each well and the samples rinsed with sterile phosphate-buffered saline (PBS). A mixture of culture medium (without Fetal Bovine Serum and phenol red) and MTS reagent (5:1 ratio) was added to each well and left to incubate for 3 h, at 37◦C, in a humidified 5% CO_2 atmosphere. Thereafter, the absorbance of the MTS reaction medium from each sample was read in triplicate at 490 nm in a microplate reader (Synergy HT, Bio-TEK; USA). All experiments were performed three times, independently. MTS assay was perfomed in Chapters III, IV, V, VI and VII of this thesis.

II-5.3.2. Cell viability assay

Calcein-AM/Propidium iodide (PI) staining is a qualitative method for the visualization of cells' viability and death [83]. Calcein acetoxymethyl (Calcein AM), which is a non-fluorescent reagent that is a derivative of calcein, is transported through the cellular membrane inside the cells. It is converted to a green-fluorescent calcein after acetoxymethyl ester hydrolysis by intracellular esterases, in live cells. This process does not occur in dead cells, where intracellular esterases are inactive and the acetoxymethyl ester stays intact. Fluorescent propidium iodide (PI) is used for the visualization of dead cells. PI is a red-fluorescent nuclear and chromosome counterstain, which only binds to cytoplasmatic DNA of dead cells (whre the cellular membrane is disrupted)

In Chapter VII**,** the cell viability of the established co-culture system was assessed by staining the cells with calcein-AM (1 μg mL^{-1}, 1:500, Invitrogen, USA) and PI (2 μg mL^{-1}, 1:1000, Invitrogen, USA). Briefly, cells were immersed in a calcein AM/propidium iodide (PI) solution in culture medium for 10 minutes and incubated at 37 °C in an atmosphere of 5% CO_2, protected from light. Viable cells metabolize calcein

AM into green fluorescent calcein (Ex/Em ≈ 495/515 nm), while dead cells find their DNA stained red by PI (Ex/Em ≈ 493/636 nm). Samples were imaged using a Transmitted and Reflected Light Microscope (Zeiss Axio Imager.Z1m, Zeiss, Germany) at 5x magnification.

II-5.3.3. Tube formation assay

Tube formation assay is a well-established method used to screen the angiogenic activity of compounds/drugs [84]. It is a quick, easy to set up, and highly reproducible assay. Briefly, when cultured on top of Matrigel, a natural ECM-based hydrogel, endothelial cells are induced to differentiate and form tube-like structures [85]. If a compound presents anti-angiogenic behavior, it disrupts the tubular-like structures, whereas if it is angiogenic it maintains or enhances the tubular-like network. The tube formation occurs quite fast, within 2-6 h, depending on the quantity and type of angiogenic stimuli. Different types of endothelial cells can be used for this assay, from primary cells to cell lines.

In Chapter IV, human endothelial cells (HPMEC-ST-1.6R) were used to perform the tube formation assay. Briefly, the bottom of 96 well-plates were pre-coated with 100 µL of Matrigel (Corning Matrigel Basement Membrane, Corning, USA) and left to solidify for 1 h at 37°C (**Figure II-16**). Afterwards, 15 000 cells were seeded on top of it. Two different assays were conducted: one where fucoidan was added at the time of cell seeding and another where fucoidan was only added 4 h after endothelial cells organization. These two assays allowed to see whether fucoidan inhibited the formation of new blood vessels and/or was able to destroy a pre-formed network. Samples were analyzed in an inverted microscope (Axiovert 40–Zeiss, Germany) and photos were acquired using a digital camera (G11, Canon, Japan) at different time points: 0, 4, 8, 12 and 16 h.

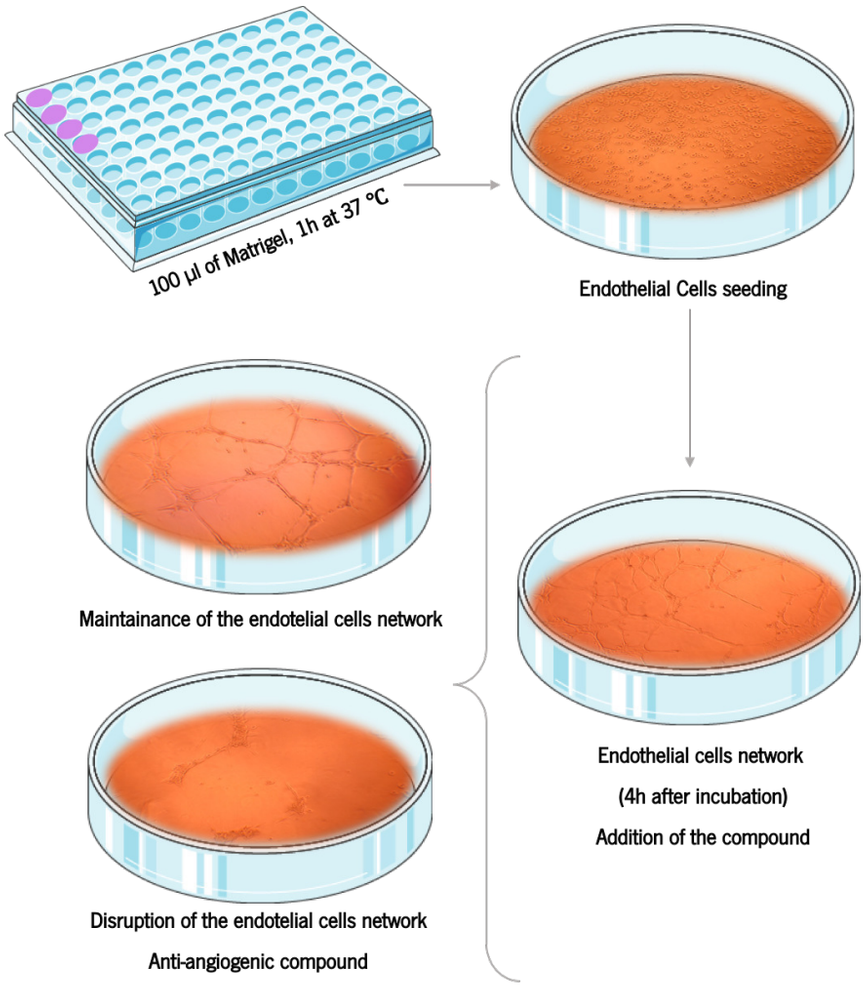

Figure II-16 Schematic representation of the tube formation assay.

II-5.3.4. Enzyme-Linked Immunosorbent Assay

ELISA (enzyme-linked immunosorbent assay) is a versatile, simple and sensitive assay designed for the quantification of specific antigens (peptides, proteins, antibodies and hormones). ELISAs operate on principles similar to other immunoassays. Basically, ELISA relies on the specific binding between the antibody and the target antigen, and a detection system that allows to indicate the presence and quantity of binding antigen. Usually, a specific primary antibody is attached to the surface of a 96 well-plate that will bind to the antigen. This step is followed by the addition of a secondary antibody, an enzyme that binds this primary antibody and a substrate that links the enzyme. Color changes occurs and is measured using a spectrometer. The antigen concentration is determined by using a standard calibration curve.

In the herein thesis, ELISA was used to quantify the amount of endothelial cells-related growth factors, regarding the tube formation assay (Chapter IV). At first, the culture medium was collected at the

end of the assay and frozen at -80°C, until analysis. For the quantification of the secreted growth factors, human PDGF and VEGF development kits were both purchased from Prepotech (USA). The quantification was performed according to manufactures' protocol and the main steps can be observed in **Table II-6**. Briefly, the primary antibodies were incubated overnight in a 96-well plate (Nunc-Immuno MicroWell 96-well solid plates). Then, a blocking step was performed to assure that the antigen would specifically bind the immobilized antibody. Both the standards and the samples were incubated for 2 h at room temperature. In the last step, 100 μL of ABTS liquid substrate was added to each standard and sample, and each plate was read at 405 and 650 nm.

Table II-6 Main steps of the ELISAs procedures

	VEGF	PDGF
Capture antibody	0.50 μg mL^{-1} 100 μL/well overnight at RT	1.0 μg mL^{-1} 100 μL/well overnight at RT
Block buffer	1% BSA in PBS, 1h at RT	
Standard/Sample	100 μL, 2h at RT	
Detection antibody	Biotinylated Rabbit Anti-Human VEGF + 2.5mg D-mannitol	Biotinylated Rabbit Anti-Human PDGF-BB + 2.5mg D-mannitol
Avidin-HRP Conjugate	1:2000, 30 min at RT	
ABTS	100 μL of substrate	
Absorbance	405nm with wavelength correction set at 650nm	
Sensitivity	16–1000 pg mL^{-1}	

II-5.4. Internalization studies

II-5.4.1. DTAF-labeled fucoidan

To allow the visualization of fucoidan internalization, 5-(4,6-dichlorotriazinyl)aminofluorescein (DTAF) was used as a green fluorescent probe in Chapter III. Dichlorotriazines are among the few reactive groups that are reported to react directly with polysaccharides and other alcohols in aqueous solution [86]. DTAF is a reactive dye with absorption/emission maxima of 492/516 nm.

DTAF-labeled fucoidan was prepared as previously described [86, 87]. Briefly, DTAF was reconstituted in methanol and kept at 4 °C until further use. A 0.2 mg mL^{-1} solution of fucoidan was left to stir with DTAF 20 µg mL^{-1} for 3 h. The DTAF-labeled fucoidan was added to the cells in culture and, at days 1, 2, and 3, the samples were washed with PBS, fixed for 30 min with 10% formalin, washed again with PBS and kept in PBS at 4°C. To evaluate whether and where fucoidan has been internalized by the different cell types, the nucleus and cytoskeleton were also fluorescently labeled. Firstly, a blocking step was performed with 3% Bovine Serum Albumin (BSA) in PBS for 30 min. Then, the BSA solution was removed and the cells washed with PBS. After that, Phalloidin-Tetramethylrhodamine B isothiocyanate (1:200 in PBS) was added and left incubating for 45 min. Another washing step was performed and the same samples were incubated with 4,6-Diamidino-2-phenyindole, dilactate (1:1000 in PBS) for 15 min. Cell were washed with PBS and observed in a transmitted and reflected light microscope with Apotome 2 (Axio Imager Z1m, Zeiss, Germany).

II-5.4.2. NPs cellular uptake

The ErbB-2 nanoparticles were fluorescently labeled to allow the observation of nanoparticles internalization by endothelial and breast cancer cells in Chapter VII. Fluorescein isothiocyanate (FITC) is the most widely used fluorescent probe for the preparation of conjugates with biological molecules. FITC was added to the chitosan solution at 2 mg mL^{-1} and the nanoparticles were produced as described in a previous section. Three different cell types (MDA-MB-231, SKBR3 and EA-hy926) were seeded in tissue culture coverslips at a density of $1.5x10^4$. After cells' adherence, NPs (NPs+FITC) and NPs with immobilized ErbB-2 antibody (NPs+FITC+Ab) were added to the culture; a negative control with only cells was performed for each cell type. After 24h, the different conditions were rinsed with PBS and the cells were fixed with 10% formalin (Bio-optica, Italy). To evaluate whether and where the NPs have been

internalized, the cytoskeleton and nucleus of those cells were also fluorescent labeled. For that, phalloidin (1:250 in PBS) was added and left to incubate for 45 min. Another washing step was performed and the same samples were incubated with DAPI (1:1000 in PBS) for 15 min. Cell were washed with PBS and observed in an Inverted Confocal Microscope with Incubation (TCS SP8, Leica, Germany) at 20x magnifications.

II-6. *IN VIVO* STUDIES

Animal manipulation for *in vivo* studies was performed only by qualified personnel and following the Principle of the 3Rs. The host institution is authorized by the DGVA (Direção Geral de Alimentação e Veterinária) to perform animal experimentation. All animal protocols were conducted in accordance with the Portuguese legislation (Portaria nº1005/92) and international standards on animal welfare as defined by the EC Directive 2010/63/EU.

II-6.1. CAM Assay

The chick chorioallantoic membrane (CAM) assay is a simple, fast and cost-effective minimally invasive *in vivo* assay to screen compounds regarding its angiogenic potential [88]. The CAM assay has also been used as a model for tumor microenvironment [89]. The CAM is composed of a multilayer epithelium, including the ectoderm at the air interface, the mesoderm or stroma and the endoderm at the interface with the allantoic sac. This membrane contains ECM proteins such as fibronectin, laminin, collagen type I and integrins, and the presence of such proteins mimics the physiological cancer environment. For that reason, the CAM assay have been widely used to study tumor cell invasion and angiogenesis. Indeed, in the CAM assay, the development of the tumor is much faster being possible to observe a tumor xenograft 2-5 days after onplantation, whereas in mammal's it usually takes between 3 to 6 weeks [89].

This assay was implemented in the study reported in Chapter IV, aiming to assess the angiogenic potential of a specific fucoidan extract. Two different assays were performed: one without the tumor (CAM I) and the other with a tumor onplanted on the membrane (CAM II). The timeline of both assays is presented in **Figure II-17**. Briefly, white fertilized chicken eggs (Pintobar, Portugal) were incubated at 37 °C for 3 days. After this, a window was opened into the shell in order to evaluate embryo viability. For CAM I, a silicon ring was onplanted on the CAM at day 9 of embryo development, to define the area where

fucoidan would be injected (in the following day). Regarding CAM II, the tumor was onplantated at day 9 and fucoidan was injected at day 13. At day 17, the CAM was photographed *in ovo* and the embryos were sacrificed by incubation at -80°C for 10 min. After fixation with paraformaldehyde at 4% *ex ovo* images were captured directly from the plate. Three independent assays were performed, resulting in n=15 eggs per condition.

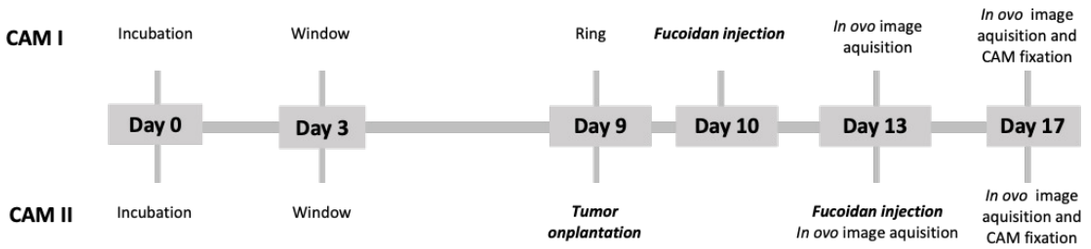

Figure II-17 Timeline of the two CAM assays performed in this study reported in Chapter IV: CAM I without tumor onplatation and CAM II with a breast cancer tumor onplanted on the membrane.

II-6.2. Early tumor animal model

In vitro studies were a powerful tool to study and validate the efficacy of the proposed compounds and developed systems. Nevertheless, they have limitations (namely regarding complexity) and the next step was to assess the efficacy of the targeting system in an *in vivo* model that mimics the tumor microenvironment. In this sense, immunocompromised mice where human cancer cells can be injected, were the chosen animal model. These are well-established models in the study of tumor growth and metastasis [90, 91]. Despite the fact that these models may also present some limitations, due to the differences in tumor histopathology between human and mice, they are a valuable and useful approach to study breast cancer genetics, biological processes, and metastatic potential.

In Chapter VII the efficacy of the developed targeting system was assessed in an early tumor mice model (**Figure II-18**). NSG (NOD.Cg-Prkdc^{scid} Il2rg^{tm1Wjl}/SzJ) immunosupressed female mice (n=12; 6 per group) were injected with 1x10^{6} breast cancer cells (SKBR3 cell line) suspended in PBS and matrigel (Corning, USA; 1:1) into the mammary fat pad (total volume of 50 µL). Mice were maintained under standard laboratory conditions, as previsously described, which included an artificial 12 h light/dark cycle, controlled ambient temperature (21 ± 1 °C) and a relative humidity of 50-60% [92]. The confirmation of specified pathogen-free health status of sentinel mice maintained within the same animal room was performed according to FELASA guidelines. Experimental mice were always manipulated in a flow hood chamber, except during the surgery.

After 5 days post-implantation, the developed targeting system (NPs+Gem+Ab) and a saline solution (control conditions) were admnistered into each animal group, every week (day 5, 12, 19 and 26). First measurement of the tumor size was possible 26 days after breast cancer cells' injection, being measured at day 29 and 32 (end of experiment). Animal body weight and tumor size (calculated by measuring the two largest side and applying the **Equation II-2**, being L1 the largest side, and L2 the other one) was measured and recorded once a week.

Equation II-2 Equation for the tumor volume measurements.

$$V = \frac{3.14 \times L1 \times L1 \times L2}{6}$$

At day 32, animals were sacrificed using CO_2 due to the tumors' size. Tumors were excised, as well as other organs of interest like lungs, liver and kidneys to assess possible metastasis. Afterwards, the tumor and organs were fixed in 4% formaldehyde and subsequently embedded in paraffin for further histological analysis. All animal procedures were conducted in accordance with the guidelines for the care and use of laboratory animals (European Directive 2010/63/EU) and approved by DGAV (reference 017761), the competent national authority for animal protection.

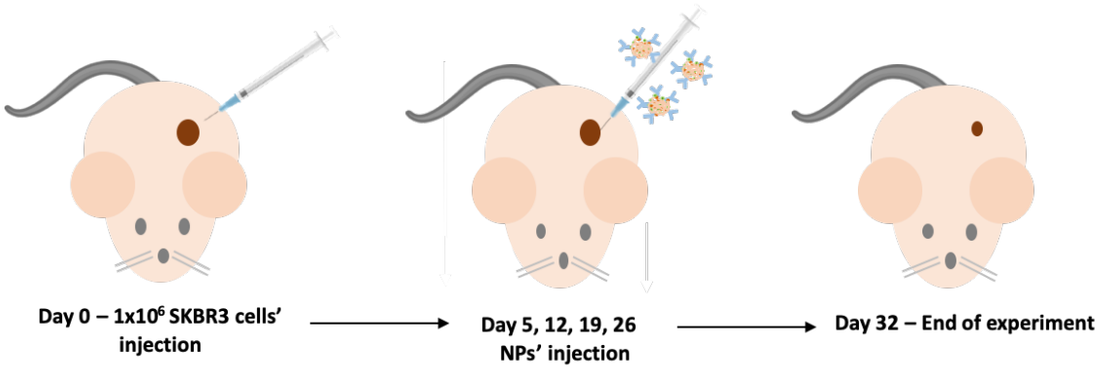

Figure II-18 Steps of the *in vivo* assay using immunosuppressed mice to test the efficiency of targeting on a cancer model.

II-7. HISTOLOGICAL PROCEDURES

In Chapter IV and VII, histological analysis was performed to the samples from CAM assay and from the *in vivo* mice models. After retrieving the samples, they were fixed with 10% (v/v) formalin, dehydrated in a graded series of ethanol baths and xylene, in a Spin Tissue Processor (STP120-2, Thermo Fisher, USA) and embedded in paraffin. Sections of 4 µm thick were cut using a microtome (HM355S, Thermo Fisher, USA). Paraffin-embedded sections were deparaffinized in xylene and rehydrated in an automatic

stainer (HMS740, Microm, Germany) and stained following the protocols described below. As last step, sections were washed in distilled water, dehydrated and mounted. The histological sections were analyzed under Leica DM750 microscope.

II-7.1. Hematoxylin & eosin staining

Hematoxylin and eosin (H&E) is one of the most used staining in histology. This staining allows the visualization of different cell components [93]. Hematoxylin is a base that preferentially stains the acidic components of cells in blue, including some proteins, nuclei, DNA and RNA, or the endoplasmic reticulum. Eosin, as an acid, dyes the basic components of cells with a pink color, such as, the cytoplasm or collagen fibrils. H&E staining was used in Chapter IV and VII to analyze representative CAM sections and tumor and other organs, respectively.

II-7.2. Immunohistochemistry – Lectin

Immunohistochemistry (IHC) is a method for the detection and visualization of specific antigens. The principle of this technique relies in the specific binding of an antibody to an antigen. IHC detection methods vary and can be based on the nature of reporting and binding chemistry [94]. 3,3'-diaminobenzidine (DAB) is often used in IHC staining as a chromogen. DAB is oxidized in the presence of peroxidase and hydrogen peroxide resulting in a dark brown reaction product at the site of enzymatic activity. Herein, immunohistochemistry was used to stain lectins in the CAM sections (Chapter IV). *Sambucus Nigra* Lectin (SNA, EBL; Vector Labs, USA) has been used to identify vascular beds in chick CAMs. It specifically binds to the endothelial cells that surround and infiltrate the CAM implants, being useful for angiogenesis assays.

Sections of 4 μm thickness were deparaffinized and rehydrated in an automatic stainer. Immunohistochemical analysis was performed according to the streptavidin-biotin peroxidase complex system (UltraVision Large Volume Detection System Anti-Polyvalent, HRP; LabVision Corporation, UK). Briefly, after rehydration, slides were subjected to heat-induced antigen-retrieval with 10 mM citrate buffer at pH=6 for 20 min at 98 °C. The slides were washed with PBS and then incubated with 3% (v/v) hydrogen peroxide (H_2O_2) for 10 min at RT to inactivate endogenous peroxidases, which may induce a non-specific background when using HRP conjugated antibodies. Another washing step with PBS was performed and slides were incubated with an UV block solution for 10 min, before incubation with biotinylated primary

antibody (anti-lectin 1:500) for 1h at RT. The sections were washed with PBS and incubated with streptavidine-peroxidase from the UltraVision Detection System kit, for 10 min at RT. The DAB (Vector Labs, USA) solution was prepared according to the manufactures' indications (DAB Solution: 5 mL of distilled water, 2 drops of buffer stock solution, 4 drops of DAB stock solution, 2 drops of H_2O_2) and incubated for 2-3 minutes at RT. Then, the sections were washed for 5 minutes in running water, to completely remove the DAB solution, and counterstained with Gill-2 hematoxylin (dilution 1:1 in distilled water; Merck, Germany). As negative control, the primary antibody incubation step was replaced by the antibody diluent solution alone. Images were acquired using Leica DM750 (Leica, Germany) at different magnifications 4×, 10× and 40×.

II-8. STATISTICAL ANALYSIS

Statistical analysis was performed using a GraphPad Prism 5.0 software (GraphPad Software, USA) where statistical significance was set to * ($p < 0.05$). Data was analyzed by a Shapiro-Wilk test to assess data normality. Data that followed a normal distribution was analyzed using a one-way analysis of variance, followed by Turkey multiple comparison test, when more than two groups were compared. Data that did not follow a normal distribution was analyzed using the Kruskal-Wallis test, followed by Dunn's multiple comparison test, when more than two groups were compared. The quantitative results are presented as mean ± standard deviation.

II-9. REFERENCES

[1] M.T. Ale, A.S. Meyer, Fucoidans from brown seaweeds: an update on structures, extraction techniques and use of enzymes as tools for structural elucidation, RSC Advances 3(22) (2013) 8131-8141.

[2] B. Li, F. Lu, X. Wei, R. Zhao, Fucoidan: Structure and Bioactivity, Molecules 13(8) (2008) 1671-95.

[3] H.J. Fitton, N.D. Stringer, S.S. Karpiniec, Therapies from Fucoidan: An Update, Marine Drugs 13(9) (2015) 5920-5946.

[4] M.H. Periayah, A.S. Halim, A.Z.M. Saad, Chitosan: A Promising Marine Polysaccharide for Biomedical Research, Pharmacognosy reviews 10(19) (2016) 39-42.

[5] Martins A., ML, Costa-Pinto A. R., Reis R. L., and Neves N. M., Bio-Inspired Integration of Natural Materials, in: a.C.K.M. Anthony B. B. (Ed.), Bio-Inspired Materials for Biomedical Engineering, Wiley Library2014 125-150.

[6] I. Younes, M. Rinaudo, Chitin and chitosan preparation from marine sources. Structure, properties and applications, Mar Drugs 13(3) (2015) 1133-74.

[7] S. Kim, Competitive Biological Activities of Chitosan and Its Derivatives: Antimicrobial, Antioxidant, Anticancer, and Anti-Inflammatory Activities, International Journal of Polymer Science 2018 (2018) 13.

[8] J. Li, C. Cai, J. Li, J. Li, J. Li, T. Sun, L. Wang, H. Wu, G. Yu, Chitosan-Based Nanomaterials for Drug Delivery, Molecules (Basel, Switzerland) 23(10) (2018) 2661.

[9] R.C.F. Cheung, T.B. Ng, J.H. Wong, W.Y. Chan, Chitosan: An Update on Potential Biomedical and Pharmaceutical Applications, Marine drugs 13(8) (2015) 5156-5186.

[10] S.-C. Hong, S.-Y. Yoo, H. Kim, J. Lee, Chitosan-Based Multifunctional Platforms for Local Delivery of Therapeutics, Marine Drugs 15(3) (2017) 60.

[11] A. Khdair, I. Hamad, H. Alkhatib, Y. Bustanji, M. Mohammad, R. Tayem, K. Aiedeh, Modified-chitosan nanoparticles: Novel drug delivery systems improve oral bioavailability of doxorubicin, European Journal of Pharmaceutical Sciences 93 (2016) 38-44.

[12] M.M. Fathy, F.S. Mohamed, N. Elbialy, W.M. Elshemey, Multifunctional Chitosan-Capped Gold Nanoparticles for enhanced cancer chemo-radiotherapy: An invitro study, Physica Medica 48 (2018) 76-83.

[13] C. Wang, Z. Zhang, B. Chen, L. Gu, Y. Li, S. Yu, Design and evaluation of galactosylated chitosan/graphene oxide nanoparticles as a drug delivery system, Journal of Colloid and Interface Science 516 (2018) 332-341.

[14] U. Gupta, S. Sharma, I. Khan, A. Gothwal, A.K. Sharma, Y. Singh, M.K. Chourasia, V. Kumar, Enhanced apoptotic and anticancer potential of paclitaxel loaded biodegradable nanoparticles based on chitosan, International Journal of Biological Macromolecules 98 (2017) 810-819.

[15] H. Yang, C. Tang, C. Yin, Estrone-modified pH-sensitive glycol chitosan nanoparticles for drug delivery in breast cancer, Acta Biomaterialia 73 (2018) 400-411.

[16] A. Babu, N. Amreddy, R. Muralidharan, G. Pathuri, H. Gali, A. Chen, Y.D. Zhao, A. Munshi, R. Ramesh, Chemodrug delivery using integrin-targeted PLGA-Chitosan nanoparticle for lung cancer therapy, Scientific Reports 7(1) (2017) 14674.

[17] J. Jiang, Y. Liu, C. Wu, Y. Qiu, X. Xu, H. Lv, A. Bai, X. Liu, Development of drug-loaded chitosan hollow nanoparticles for delivery of paclitaxel to human lung cancer A549 cells, Drug Dev Ind Pharm 43(8) (2017) 1304-1313.

[18] M.R. Zeiderman, D.E. Morgan, J.D. Christein, W.E. Grizzle, K.M. McMasters, L.R. McNally, Acidic pH-targeted chitosan capped mesoporous silica coated gold nanorods facilitate detection of pancreatic tumors via multispectral optoacoustic tomography, Acs Biomater Sci Eng 2(7) (2016) 1108-1120.

[19] M. Parsian, G. Unsoy, P. Mutlu, S. Yalcin, A. Tezcaner, U. Gunduz, Loading of Gemcitabine on chitosan magnetic nanoparticles increases the anti-cancer efficacy of the drug, European Journal of Pharmacology 784 (2016) 121-128.

[20] H. Yu, H. Song, J. Xiao, H. Chen, X. Jin, X. Lin, B. Pan, W. Ji, The effects of novel chitosan-targeted gemcitabine nanomedicine mediating cisplatin on epithelial mesenchymal transition, invasion and metastasis of pancreatic cancer cells, Biomedicine & Pharmacotherapy 96 (2017) 650-658.

[21] R. Xue, Y. Qian, L. Li, G. Yao, L. Yang, Y. Sun, Polycaprolactone nanofiber scaffold enhances the osteogenic differentiation potency of various human tissue-derived mesenchymal stem cells, Stem Cell Res Ther 8(1) (2017) 148-148.

[22] D. Mondal, M. Griffith, S.S. Venkatraman, Polycaprolactone-based biomaterials for tissue engineering and drug delivery: Current scenario and challenges, International Journal of Polymeric Materials and Polymeric Biomaterials 65(5) (2016) 255-265.

[23] E. Malikmammadov, T.E. Tanir, A. Kiziltay, V. Hasirci, N. Hasirci, PCL and PCL-based materials in biomedical applications, Journal of biomaterials science. Polymer edition 29(7-9) (2018) 863-893.

[24] A. Martins, R.L. Reis, N.M. Neves, Electrospinning: processing technique for tissue engineering scaffolding, International Materials Reviews 53(5) (2008) 257-274.

[25] J. Xue, T. Wu, Y. Dai, Y. Xia, Electrospinning and Electrospun Nanofibers: Methods, Materials, and Applications, Chem Rev 119(8) (2019) 5298-5415.

[26] A. Valizadeh, S. Mussa Farkhani, Electrospinning and electrospun nanofibres, IET nanobiotechnology 8(2) (2014) 83-92.

[27] R. Ng, R. Zang, K.K. Yang, N. Liu, S.-T. Yang, Three-dimensional fibrous scaffolds with microstructures and nanotextures for tissue engineering, RSC Advances 2(27) (2012) 10110-10124.

[28] F. Darain, W.Y. Chan, K.S. Chian, Performance of Surface-Modified Polycaprolactone on Growth Factor Binding, Release, and Proliferation of Smooth Muscle Cells, Soft Materials 9(1) (2010) 64-78.

[29] G. Sridharan, A.A. Shankar, Toluidine blue: A review of its chemistry and clinical utility, J Oral Maxillofac Pathol 16(2) (2012) 251-5.

[30] F. Kubaski, H. Osago, R.W. Mason, S. Yamaguchi, H. Kobayashi, M. Tsuchiya, T. Orii, S. Tomatsu, Glycosaminoglycans detection methods: Applications of mass spectrometry, Molecular Genetics and Metabolism 120(1) (2017) 67-77.

[31] S. Lankalapalli, V.R.M. Kolapalli, Polyelectrolyte Complexes: A Review of their Applicability in Drug Delivery Technology, Indian journal of pharmaceutical sciences 71(5) (2009) 481-487.

[32] M.G. Carneiro-da-Cunha, M.A. Cerqueira, B.W.S. Souza, J.A. Teixeira, A.A. Vicente, Influence of concentration, ionic strength and pH on zeta potential and mean hydrodynamic diameter of edible polysaccharide solutions envisaged for multinanolayered films production, Carbohydrate Polymers 85(3) (2011) 522-528.

[33] A.C. Lima, P. Sher, J.F. Mano, Production methodologies of polymeric and hydrogel particles for drug delivery applications, Expert Opinion on Drug Delivery 9(2) (2012) 231-248.

[34] Z. Ahmad, J.H. Shepherd, D.V. Shepherd, S. Ghose, S.J. Kew, R.E. Cameron, S.M. Best, R.A. Brooks, J. Wardale, N. Rushton, Effect of 1-ethyl-3-(3-dimethylaminopropyl) carbodiimide and N-

hydroxysuccinimide concentrations on the mechanical and biological characteristics of cross-linked collagen fibres for tendon repair, Regen Biomater 2(2) (2015) 77-85.

[35] C. Oliveira, A.R. Costa-Pinto, R.L. Reis, A. Martins, N.M. Neves, Biofunctional nanofibrous substrate comprising immobilized antibodies and selective binding of autologous growth factors, Biomacromolecules 15(6) (2014) 2196-205.

[36] G.N. Hortobagyi, Treatment of advanced breast cancer with gemcitabine and vinorelbine, Oncology (Williston Park, N.Y.) 15(2 Suppl 3) (2001) 15-7.

[37] S. Modi, A.D. Seidman, Single-agent gemcitabine in the treatment of advanced breast cancer, Clinical breast cancer 4 Suppl 3 (2004) S101-6.

[38] H. Sakamoto, M. Kitano, Y. Suetomi, Y. Takeyama, H. Ohyanagi, T. Nakai, C. Yasuda, M. Kudo, Comparison of standard-dose and low-dose gemcitabine regimens in pancreatic adenocarcinoma patients: a prospective randomized trial, Journal of Gastroenterology 41(1) (2006) 70-76.

[39] L.W. Hertel, G.B. Boder, J.S. Kroin, S.M. Rinzel, G.A. Poore, G.C. Todd, G.B. Grindey, Evaluation of the antitumor activity of gemcitabine (2',2'-difluoro-2'-deoxycytidine), Cancer research 50(14) (1990) 4417-22.

[40] W. Plunkett, P. Huang, Y.Z. Xu, V. Heinemann, R. Grunewald, V. Gandhi, Gemcitabine: metabolism, mechanisms of action, and self-potentiation, Semin Oncol 22 (1995) 3-10.

[41] J.D.a.C. Ingle, Stanley R, Spectrochemical analysis, 1988.

[42] O.W. Sørensen, James Keeler. Understanding NMR Spectroscopy, Magnetic Resonance in Chemistry 44(8) (2006) 820-820.

[43] M.J. Clement, B. Tissot, L. Chevolot, E. Adjadj, Y. Du, P.A. Curmi, R. Daniel, NMR characterization and molecular modeling of fucoidan showing the importance of oligosaccharide branching in its anticomplementary activity, Glycobiology 20(7) (2010) 883-94.

[44] M.I. Bilan, A.A. Grachev, A.S. Shashkov, N.E. Nifantiev, A.I. Usov, Structure of a fucoidan from the brown seaweed Fucus serratus L, Carbohydrate Research 341(2) (2006) 238-245.

[45] D. Berek, Size exclusion chromatography – A blessing and a curse of science and technology of synthetic polymers, Journal of Separation Science 33(3) (2010) 315-335.

[46] F. Atashrazm, R.M. Lowenthal, G.M. Woods, A.F. Holloway, J.L. Dickinson, Fucoidan and Cancer: A Multifunctional Molecule with Anti-Tumor Potential, Marine Drugs 13(4) (2015) 2327-2346.

[47] C. Yang, D. Chung, I.-S. Shin, H. Lee, J. Kim, Y. Lee, S. You, Effects of molecular weight and hydrolysis conditions on anticancer activity of fucoidans from sporophyll of Undaria pinnatifida, International Journal of Biological Macromolecules 43(5) (2008) 433-437.

[48] D. French, Chapter Five - Advances in Clinical Mass Spectrometry, in: G.S. Makowski (Ed.), Advances in Clinical Chemistry, Elsevier2017, pp. 153-198.

[49] C. Nunes, L. Silva, A.P. Fernandes, R.P.F. Guiné, M.R.M. Domingues, M.A. Coimbra, Occurrence of cellobiose residues directly linked to galacturonic acid in pectic polysaccharides, Carbohydrate Polymers 87(1) (2012) 620-626.

[50] S. Koyanagi, N. Tanigawa, H. Nakagawa, S. Soeda, H. Shimeno, Oversulfation of fucoidan enhances its anti-angiogenic and antitumor activities, Biochemical Pharmacology 65(2) (2003) 173-179.

[51] K.S. Dodgson, Determination of inorganic sulphate in studies on the enzymic and non-enzymic hydrolysis of carbohydrate and other sulphate esters, The Biochemical journal 78(2) (1961) 312-319.

[52] K.S. Dodgson, R.G. Price, A note on the determination of the ester sulphate content of sulphated polysaccharides, The Biochemical journal 84(1) (1962) 106-110.

[53] G. Jiao, G. Yu, J. Zhang, H.S. Ewart, Chemical Structures and Bioactivities of Sulfated Polysaccharides from Marine Algae, Marine Drugs 9(2) (2011) 196-223.

[54] I. Ciucanu, F. Kerek, A simple and rapid method for the permethylation of carbohydrates, Carbohydrate Research 131(2) (1984) 209-217.

[55] S. Vincenzi, A. Crapisi, A. Curioni, Foamability of Prosecco wine: Cooperative effects of high molecular weight glycocompounds and wine PR-proteins, Food Hydrocolloids 34 (2014) 202-207.

[56] H.-L. Lee, N.T. Flynn, X-ray photoelectron spectroscopy, Handbook of Applied Solid State Spectroscopy (2006) 485-507.

[57] A. Taylor, Practical surface analysis, 2nd edn., vol I, auger and X-ray photoelectron spectroscopy. Edited by D. Briggs & M. P. Seah, John Wiley, New York, 1990, 657 pp., price: £86.50. ISBN 0471 92081 9, Journal of Chemical Technology & Biotechnology 53(2) (1992) 215-215.

[58] S. Kertész, T. Freitas, C. Hodúr, Characterization of polymer membranes by contact angle goniometer, Analecta Technica Szegedinensia 8 (2014) 18-22.

[59] M.Y. Chan, Q.M. Dowling, S.J. Sivananthan, R.M. Kramer, Particle Sizing of Nanoparticle Adjuvant Formulations by Dynamic Light Scattering (DLS) and Nanoparticle Tracking Analysis (NTA), Methods Mol Biol 1494 (2017) 239-252.

[60] G. Metcalfe, M.F.M. Speetjens, D.R. Lester, H.J.H. Clercx, Beyond Passive: Chaotic Transport in Stirred Fluids, in: E. van der Giessen, H. Aref (Eds.), Advances in Applied Mechanics, Elsevier2012, pp. 109-188.

[61] S. Bhattacharjee, DLS and zeta potential – What they are and what they are not?, Journal of Controlled Release 235 (2016) 337-351.

[62] D. McMullan, Scanning electron microscopy 1928–1965, Scanning 17(3) (1995) 175-185.

[63] S. Khan, Scanning Electron Microscopy: Principle and Applications in Nanomaterials Characterization, 2018.

[64] P. Klapetek, M. Valtr, D. Nečas, O. Salyk, P. Dzik, Atomic force microscopy analysis of nanoparticles in non-ideal conditions, Nanoscale research letters 6(1) (2011) 514-514.

[65] F.R. Balkwill, M. Capasso, T. Hagemann, The tumor microenvironment at a glance, Journal of cell science 125(Pt 23) (2012) 5591-6.

[66] M. Hu, K. Polyak, Microenvironmental regulation of cancer development, Current Opinion in Genetics & Development 18(1) (2008) 27-34.

[67] G. Stacey, C. MacDonald, Immortalisation of primary cells, Cell biology and toxicology 17(4-5) (2001) 231-46.

[68] G. Kaur, J.M. Dufour, Cell lines: Valuable tools or useless artifacts, Spermatogenesis 2(1) (2012) 1-5.

[69] D.L. Holliday, V. Speirs, Choosing the right cell line for breast cancer research, Breast cancer research : BCR 13(4) (2011) 215-215.

[70] H.D. Soule, J. Vazguez, A. Long, S. Albert, M. Brennan, A human cell line from a pleural effusion derived from a breast carcinoma, J Natl Cancer Inst 51(5) (1973) 1409-16.

[71] S. Comsa, A.M. Cimpean, M. Raica, The Story of MCF-7 Breast Cancer Cell Line: 40 years of Experience in Research, Anticancer Res 35(6) (2015) 3147-54.

[72] J. Fogh, J.M. Fogh, T. Orfeo, One hundred and twenty-seven cultured human tumor cell lines producing tumors in nude mice, J Natl Cancer Inst 59(1) (1977) 221-6.

[73] N. Iqbal, N. Iqbal, Human Epidermal Growth Factor Receptor 2 (HER2) in Cancers: Overexpression and Therapeutic Implications, Molecular biology international 2014 (2014) 852748.

[74] R. Cailleau, M. Olive, Q.V. Cruciger, Long-term human breast carcinoma cell lines of metastatic origin: preliminary characterization, In vitro 14(11) (1978) 911-5.

[75] K.J. Chavez, S.V. Garimella, S. Lipkowitz, Triple negative breast cancer cell lines: one tool in the search for better treatment of triple negative breast cancer, Breast disease 32(1-2) (2010) 35-48.

[76] B. Westermark, A. Johnsson, Y. Paulsson, C. Betsholtz, C.H. Heldin, M. Herlyn, U. Rodeck, H. Koprowski, Human melanoma cell lines of primary and metastatic origin express the genes encoding the chains of platelet-derived growth factor (PDGF) and produce a PDGF-like growth factor, Proceedings of the National Academy of Sciences 83(19) (1986) 7197.

[77] V. Krump-Konvalinkova, F. Bittinger, R.E. Unger, K. Peters, H.A. Lehr, C.J. Kirkpatrick, Generation of human pulmonary microvascular endothelial cell lines, Laboratory investigation; a journal of technical methods and pathology 81(12) (2001) 1717-27.

[78] C.J. Edgell, C.C. McDonald, J.B. Graham, Permanent cell line expressing human factor VIII-related antigen established by hybridization, Proc Natl Acad Sci U S A 80(12) (1983) 3734-7.

[79] J.P. Jacobs, C.M. Jones, J.P. Baille, Characteristics of a Human Diploid Cell Designated MRC-5, Nature 227(5254) (1970) 168-170.

[80] R. Edmondson, J.J. Broglie, A.F. Adcock, L. Yang, Three-dimensional cell culture systems and their applications in drug discovery and cell-based biosensors, Assay Drug Dev Technol 12(4) (2014) 207-218.

[81] C. Oliveira, N.M. Neves, R.L. Reis, A. Martins, T.H. Silva, Gemcitabine delivered by fucoidan/chitosan nanoparticles presents increased toxicity over human breast cancer cells, Nanomedicine 13(16) (2018) 2037-2050.

[82] T. Mosmann, Rapid colorimetric assay for cellular growth and survival: Application to proliferation and cytotoxicity assays, Journal of immunological methods 65(1) (1983) 55-63.

[83] T. Riss, A. Niles, R. Moravec, N. Karassina, J. Vidugiriene, Cytotoxicity Assays: In Vitro Methods to Measure Dead Cells, in: G.S. Sittampalam, A. Grossman, K. Brimacombe, M. Arkin, D. Auld, C. Austin, J. Baell, B. Bejcek, J.M.M. Caaveiro, T.D.Y. Chung, N.P. Coussens, J.L. Dahlin, V. Devanaryan, T.L. Foley, M. Glicksman, M.D. Hall, J.V. Haas, S.R.J. Hoare, J. Inglese, P.W. Iversen, S.D. Kahl, S.C. Kales, S. Kirshner, M. Lal-Nag, Z. Li, J. McGee, O. McManus, T. Riss, O.J. Trask, Jr., J.R. Weidner, M.J. Wildey, M. Xia, X. Xu (Eds.), Assay Guidance Manual, Bethesda (MD), 2004.

[84] M.L. Ponce, Tube Formation: an In Vitro Matrigel Angiogenesis Assay, in: C. Murray, S. Martin (Eds.), Angiogenesis Protocols: Second Edition, Humana Press, Totowa, NJ, 2009, pp. 183-188.

[85] K.L. DeCicco-Skinner, G.H. Henry, C. Cataisson, T. Tabib, J.C. Gwilliam, N.J. Watson, E.M. Bullwinkle, L. Falkenburg, R.C. O'Neill, A. Morin, J.S. Wiest, Endothelial cell tube formation assay for the in vitro study of angiogenesis, Journal of visualized experiments : JoVE (91) (2014) e51312-e51312.

[86] S. Prigent-Richard, M. Cansell, J. Vassy, A. Viron, E. Puvion, J. Jozefonvicz, D. Letourneur, Fluorescent and radiolabeling of polysaccharides: Binding and internalization experiments on vascular cells, Journal of Biomedical Materials Research 40(2) (1998) 275-281.

[87] M. Ellouali, C. Boisson-Vidal, P. Durand, J. Jozefonvicz, Antitumor activity of low molecular weight fucans extracted from brown seaweed Ascophyllum nodosum, Anticancer Res 13(6A) (1993) 2011-2019.

[88] D. Ribatti, The chick embryo chorioallantoic membrane (CAM). A multifaceted experimental model, Mech Dev 141 (2016) 70-77.

[89] D. Ribatti, The chick embryo chorioallantoic membrane as a model for tumor biology, Experimental Cell Research 328(2) (2014) 314-324.

[90] K. Sakamoto, J.W. Schmidt, K.-U. Wagner, Mouse models of breast cancer, Methods in molecular biology (Clifton, N.J.) 1267 (2015) 47-71.

[91] I. Holen, V. Speirs, B. Morrissey, K. Blyth, In vivo models in breast cancer research: progress, challenges and future directions, Dis Model Mech 10(4) (2017) 359-371.

[92] C.S. Gonçalves, J. Vieira de Castro, M. Pojo, E.P. Martins, S. Queirós, E. Chautard, R. Taipa, M.M. Pires, A.A. Pinto, F. Pardal, C. Custódia, C.C. Faria, C. Clara, R.M. Reis, N. Sousa, B.M. Costa, WNT6 is a novel oncogenic prognostic biomarker in human glioblastoma, Theranostics 8(17) (2018) 4805-4823.

[93] A.H. Fischer, K.A. Jacobson, J. Rose, R. Zeller, Hematoxylin and eosin staining of tissue and cell sections, CSH protocols 2008 (2008) pdb.prot4986.

[94] Immunocytochemistry and Immunohistochemistry, Essential Guide to Reading Biomedical Papers, pp. 117-127.

SECTION 3

EXPERIMENTAL STUDIES

CHAPTER III

The key role of sulfation and branching on fucoidan antitumor activity

Chapter III

The key role of sulfation and branching on fucoidan antitumor activity†

ABSTRACT

There is an urgent need for antitumor bioactive agents with minimal or no side effects over normal adjacent cells. Fucoidan is a marine-origin polymer with known antitumor activity. However, there are still some concerns about its application due to the inconsistent experimental results, specifically its toxicity over normal cells and the mechanism behind its action. Herein we have tested three fucoidan extracts (FEs) over normal and breast cancer cell lines. From cytotoxicity results, only one of the extracts showed selective antitumor behavior (at 0.2 mg mL^{-1}), despite similarities in sulfation degree and carbohydrates composition. Although the three FEs present different molecular weights, depolymerization of selected samples discarded Mw as the key factor in the antitumor activity. Significant differences in sulfates position and branching were observed, presenting FE 2 the higher branching degree. Based on all these experimental data, we believe these last two properties are the ones that influence the cytotoxic effects of fucoidan extracts.

† This chapter is based on the following publication:

Oliveira C., Ferreira, A. S., Novoa-Carballal R., Nunes C., Pashkuleva I., Neves N. M., Coimbra M. A., Reis R. L., Martins A., Silva T. H. The Key Role of Sulfation and Branching on Fucoidan Antitumor Activity. Macromolecular Bioscience, 2017, 17, 1600340. doi:10.1002/mabi.201600340

.

III-1. INTRODUCTION

Cancer can have various origin-factors, being characterized by uncontrolled cell growth and spread [1]. Cancer therapeutics aim to increase the survival time and the quality-of-life of the patients. The goal of cancer treatment is the extinction of tumor cells, ideally with minimal damage to healthy tissues. The toxic effects over normal cells often limit the current chemotherapeutic agents used in cancer treatments, which conduct to reduced dosage and, consequently, efficacy of the treatment [2, 3].

Breast cancer is the second most frequent diagnosed cancer and the first among females [4]. If breast cancer is detected in an early stage, there is a possibility to be treated and removed surgically. However, the treatment of the advanced stage breast cancer is often followed by reoccurrence and can become fatal, even when chemotherapeutic agents are administered. There are several factors like tumors heterogeneity, drug resistance, side effects and toxicity to healthy tissues, that diminish the efficacy and usefulness of this treatment [5, 6].Therefore, there is a strong interest in developing better-tolerated anti-cancer agents and treatment modalities [7].

Because of the side effects of many current treatments, the use of natural substances with low toxicity is of great interest [8]. Natural-derived polymers are of special interest due to their biological and chemical similarities to natural tissues composition. Marine organism are valuable sources of materials with intriguing properties and characteristics [9]. Among marine-origin materials, fucoidan is a polysaccharide that consists of sulfated fucose residues and is possible to be extracted from brown seaweeds of different species such as *Fucus vesiculosus*, *Laminaria japonica*, *Undaria pinnatifida* [10-12].Fucoidan has been reported to have various biological activities including antibacterial, antioxidant, antiviral, and antitumor [13, 14].

Fucoidan antitumor behavior has been demonstrated *in vitro* and *in vivo* for different type of cancers such as breast, lung, prostate, colon, and melanoma [7, 15-18]. It retards tumor development, eradicating tumor cells by targeting key apoptotic molecules. Furthermore, the synergistic effect of fucoidan with current anticancer agents has also been reported [8, 19]. Despite the promising results about its anticancer effects, the fucoidan mechanism of action is not clearly understood and thus, fucoidan has not yet been developed as a regulated therapeutic agent [20, 21]. The main barriers to its utilization in clinic are: i) its toxicity to normal cells, and ii) the variable and contradictory results in fucoidan usage [8, 22]. In addition, there are a huge variety of algae fucoidan sources, which implies various extraction and purification methods that may influence fucoidan's intrinsic properties and its bioactivity

such as molecular weight, carbohydrates composition and sulfation. Molecular weight has been reported as one of the main factors influencing fucoidan antitumor behavior. From previously reported works, lower molecular weight fucoidan presents higher antitumor effects whereas higher sulfation degree has been related with enhanced bioactivity responses [8, 23]. However, most studies analyzing antitumor activity did not characterize in detail the composition of the used fucoidan and this is probably the cause of some contradictory findings [10, 13, 14].

An effective cancer therapeutic strategy is characterized by the ability to eliminate tumors without damaging healthy tissues. Due to the different properties affecting fucoidan bioactivity, there is the need to evaluate the antitumor effects of a certain extract and characterize which feature(s) is (are) playing the major role. For that purpose, herein, three different extracts from the same species (i.e. *F. vesiculosus*) were tested with human breast cancer cells, and normal endothelial and fibroblastic cells. From these biological data we were able to observe three completely different bioactive responses and, in that sense, we decided to carry out structure-activity relationship (SAR) studies.

III-2. EXPERIMENTAL SECTION

III-2.1. Materials

Fucoidan Extract 1 (FE 1) was purchased from Marinova, whereas Fucoidan Extract 2 (FE 2 – batch SLBC6348V) and Fucoidan Extract 3 (FE 3 – batch 081M7672V), were purchased from Sigma-Aldrich, all used as received. The human vascular endothelial growth factor (VEGF) ELISA kit was purchased from Peprotech (Rochy Hill, USA) and kept at 4°C until used. Phalloidin–Tetramethylrhodamine B isothiocyanate (Texas Red - Phalloidin), 5-([4,6-Dichlorotriazin-2-yl]amino)fluorescein hydrochloride (DTAF) were both purchased from Sigma. 4,6-Diamidino-2-phenyindole, dilactate (DAPI) was purchased from Biotium (Hayward, CA; USA).

III-2.2. Biological assays

III-2.2.1. Cell expansion

Human fibroblasts (MRC-5 cell line) and pulmonary microvascular endothelial cells (HPMEC-ST1.6R cell line) were used as non-cancer cells. Fibroblast cells were cultured in D-MEM low glucose medium

(Sigma Aldrich) supplemented with 10 % FBS (Alfagene) and Pen/Strep (100 U/100 g mL^{-1}; Life Technologies). Fibroblasts were used at passages 14-16. Endothelial cells were cultured in M199 medium (Sigma Aldrich) supplemented with 20% FBS (Alfagene), 2 mM Glutamax (Life Technologies), Pen/Strep (100 U/100 g mL^{-1}; Life Technologies), endothelial cell growth supplement (ECGS - 25 µg mL^{-1}; Becton Dickinson). Endothelial cells were used at passages 38-40. Human breast adenocarcinoma cells (MCF-7 and MDA-MB-231 cell lines) were used to assess the effect of different fucoidan's concentrations over these cancer cells models. Both cell lines were cultured in D-MEM high glucose medium (Sigma Aldrich) supplemented with 10% FBS (Alfagene), Pen/Strep (100 U/100 g mL^{-1}; Life Technologies) and 1% MEM sodium pyruvate solution 100 mM (Alfagene). The MCF-7 cell line was used at passages 16-18, whereas the MDA-MB-231 cell line was used at passages 42-44. The four types of cells were incubated at 37°C in a humidified 5% CO_2 atmosphere. Media were exchanged every 2-3 days until cells reached a 90% confluence.

III-2.2.2. Cell Culture

Non-cancer and cancer cells were harvested and 15 000 cells were cultured in 24 well-plates. The cells were left to adhere for 4 hours and, after that, fucoidan extracts were added to adherent cells. Fucoidan extracts were dissolved in the culture medium at different concentrations: for FE 1 the concentrations tested were 0.1 mg mL^{-1}, 0.5 mg mL^{-1}, 1 mg mL^{-1}, 2 mg mL^{-1}, 3 mg mL^{-1}, 4 mg mL^{-1} and 5 mg mL^{-1}, whereas for FE 2 and FE 3 the concentrations were 0.1 mg mL^{-1}, 0.2 mg mL^{-1}, 0.3 mg mL^{-1}, 0.4 mg mL^{-1} and 0.5 mg mL^{-1}. For all the assays a positive control was performed (no fucoidan in the culture medium). Each experimental condition was tested in triplicate and two independent assays were performed for each type of cells and fucoidan extracts.

III-2.2.3. Cell Viability

The metabolic activity of non-cancer and cancer cells, cultured at different fucoidan extracts' concentrations and time points, was determined by the MTS assay (CellTiter 96 ® AQueous One Solution, Promega). The MTS assay is a colorimetric method commonly used for cytotoxicity assays or for determining the number of viable cells in proliferation. Basically, the quantity of formazan product is directly proportional to the number of living cells in culture [24]. At days 1, 2 and 3, the culture medium was removed and the testing conditions were rinsed with sterile PBS. A mixture of culture medium

(without FBS and phenol red) and MTS reagent (5:1 ratio) was added to each well and left to incubate for 3 h, at 37 °C, in a humidified 5% CO_2 atmosphere. Thereafter, the absorbance of the MTS reaction medium from each sample was read in triplicate at 490 nm in a microplate reader (Synergy HT, Bio-TEK). All experiments were performed in triplicate.

III-2.2.4. DTAF-labeled fucoidan and morphological observation

DTAF-labeled fucoidan was prepared as described elsewhere [25, 26]. Briefly, DTAF was reconstituted in methanol and kept at 4 °C until further use. A 0.2 mg mL^{-1} solution of FE 1 and FE 2 was left to stir with DTAF for 3 h (20 µg/ml). The procedure described in sections 5.2.2 and 5.2.3 were followed, but was added DTAF-labeled FE 1 and FE 2 instead of the pure FE. At days 1, 2 and 3, samples were washed with PBS, fixed for 30 min with 10% formalin, washed again with PBS and kept in PBS at 4°C.

To evaluate whether and where fucoidan has been internalized by the different cell types, the nucleus and cytoskeleton of those cells were also fluorescent labeled. First, a blocking step was performed with 3% BSA in PBS for 30 min. Then, the BSA solution was removed and cells were washed with PBS. After that, Phalloidin-Tetramethylrhodamine B isothiocyanate (1:200 in PBS) was added and left incubating for 45 min. Another washing step was performed and the same samples were incubated with 4,6-Diamidino-2-phenyindole, dilactate (1:1000 in PBS) for 15 min. Cell were washed with PBS and observed in a Transmitted and Reflected Light Microscope with Apotome 2 (Axio Imager Z1m, Zeiss).

III-2.3. Fucoidan characterization

III-2.3.1. Molecular weight determination by Gel permeation chromatography (GPC)

GPC measurements were performed with a Malvern Viscotek TDA 305 with refractometer, right angle light scattering and viscometer detectors on a set of four columns: pre-column Suprema 5 µm 8x50 S/N 3111265, Suprema 30 Å 5 µm 8x300 S/N 3112751, Suprema 1000 Å 5 µm 8x300 S/N 3112851 PL and Aquagel-OH MIXED 8 µm 7.5x300 S/N 8M-AOHMIX-46-51, with refractive index detection (RI-Detector 8110, Bischoff). The system was kept at 30 °C using 0.1 M NaN_3, 0.01 M NaH_2PO_4 (pH = 6.6) as eluent at rate of 1 mL min^{-1}. The elution times of the RI detector signal were calibrated with a

commercial polysaccharide set from Varian that contains 10 Pullulans with narrow polydispersity and Mp (molecular mass at the peak maximum) ranging from 180 Da to 708 kDa.

III-2.3.2. Depolymerization of fucoidan extract FE1 by acid hydrolysis

FE 1 was hydrolyzed to obtain lower molecular weight fucoidan, following a procedure described previously [38]. Briefly, partially hydrolyzed fucoidan was obtained by hydrolyzing FE 1 (20 mg) with 1 mL of 0.01 M HCl at 100 °C for 10 min, followed by neutralization with 1 mL of 0.01 M NaOH. The resulting hydrolyzed fucoidan FE1* was analyzed by GPC. A control was performed by dissolving FE 1 (20 mg) in 1 mL of 0.01 M HCl without heat treatment, followed by neutralization with 1 mL of 0.01 M NaOH. The procedures described in sections 5.2.2 and 5.2.3 were followed, but, instead of FE 1, hydrolyzed fucoidan was added at different concentrations (0.2 mg mL^{-1}, 0.5 mg mL^{-1} and 1 mg mL^{-1}). A positive control with untreated cells and controls with HCl and NaOH without fucoidan were also performed.

III-2.3.3. Carbohydrates composition: determination of neutral and acidic monosaccharides

Neutral monosaccharides were determined as alditol acetates as described elsewhere [27]. Briefly a pre-hydrolysis of fucoidans was performed, with 72% sulfuric acid for 3 h at room temperature (RT). Afterwards, the fucoidan extracts were submitted to a hydrolysis with sulfuric acid 1 M at 100°C for 2.5 h. 2-Deoxyglucose was used as an internal standard. Monosaccharides were reduced with sodium borohydride and acetylated by acetic anhydride using methylimidazole as a catalyst. The formed alditol acetate derivatives were analyzed by gas chromatography (GC) with a 30 m column DB-225 (J&W Scientific, Folsom, CA, USA), internal diameter, and film thickness of 0.25 mm and 0.15 mm, respectively, and using a flame ionization detector (Perkin Elmer, Clarus 400). The hydrolysis of all samples was performed in duplicate and each one was injected twice. A third analysis was done for the few samples with higher variability. Uronic acids were quantified by a modification of the 3-phenylphenol colorimetric method [27]. Samples were prepared by hydrolysis with 72% sulfuric acid for 3h at RT followed by 1 h in sulfuric acid 1 M at 100°C. A calibration curve was made with D-galacturonic acid. The hydrolysis and analysis of the samples was done in triplicate.

III-2.3.4. NMR spectroscopy

NMR experiments were acquired on a Bruker AVANCE 400 spectrometer using D_2O as solvent. The residual HOD signal was used as reference for the chemical shifts that are reported in ppm. Mnova Software 9.0 (Mestrelab Research) was used for spectral processing. Sulfation position and branching was qualitatively analyzed based on the chemical shifts described previously [28, 29].

III-2.3.5. Sulfation Degree: ester sulfate determination

The content of ester sulfates in the fucoidan extracts was determined by the turbidimetric method proposed by Dodgson and Price [30, 31]. The fucoidan extracts were accurately weighed (usually 2-4 mg) and dissolved in the respective amount of N-hydrochloric acid 1 M. The mixture was submitted to a hydrolysis at 105-110 °C for 5 h. A portion (0.2 mL) was transferred to a tube containing 3.8 mL of 3% (w/v) trichloroacetic acid. Barium chloride-gelatin reagent (1 mL) was added and, after mixing, the whole was kept at RT for 15-20 min. The barium chloride-gelatin reagent was previously prepared by mixing gelatin (1 g) with 200 mL of hot water (60-70°C) and was allowed to stand at 4°C overnight. Barium chloride (1 g) was dissolved in the semi-gelatinous fluid and the resultant cloudy solution was allowed to stand for 2-3 h before use. The solution was then analyzed at 360 nm (Jenway 6405 UV/Vis) against reagent blank containing distilled water instead of sample.

A second 0.2 mL portion of the hydrolysate was mixed with 3.8 mL of trichloroacetic acid, as described above, and with 1 mL of gelatin solution (i.e. containing no barium chloride). The extinction of this "control" solution was then measured at 360 nm against a reagent blank consisting on distilled water instead of sample and 1 mL of gelatin solution. The concentration of sulfate esters was determined by building a K_2SO_4 calibration curve, containing between 20 and 200 µg of SO_4^{2-} ion.

III-2.3.6. Desulfation

For polysaccharide desulfation, 10 mg were dissolved in 1.8 mL of dried dimethyl sulfoxide. Then, 0.1 mL pyridine was added, followed by 13 mg of pyromellitic acid, 12 mg of NaF, and 0.2 mL of pyridine. The mixture was stirred at 120 °C for 3 h, cooled and poured into 1 mL of 3% of $NaHCO_3$ aqueous solution. The solution containing the desulfated polysaccharide was dialysed and freeze-dried. The

procedure was repeated in order to guarantee the complete desulfation. Afterwards, the desulfated polysaccharide was submitted to methylation analysis [32, 33].

III-2.3.7. Methylation analysis

Glycosidic-substitution analysis was determined by gas chromatography-quadrupole mass spectrometry (GC-qMS) of the partially methylated alditol acetates based on Ciucanu and Kerek [34] and Coelho, Rocha, and Coimbra [35]. The native and desulfated samples (1–2 mg) were dissolved in 1 mL of anhydrous dimethylsulfoxide (DMSO), and then powdered NaOH (40 mg) were added under an argon atmosphere. The samples were methylated with CH_3I (80 µL) during 20 min with stirring, following by a second and third addition of 80 µL CH_3I and stirring for another 20 min. $CHCl_3$/MeOH (1:1, v/v, 3 mL) was added, and the solution was dialyzed (membrane with a pore diameter of 12–14 kDa) against 50% EtOH. The dialysate was evaporated to dryness and the material was remethylated using the same procedure. The remethylated material was hydrolyzed with 2 M TFA (1 mL) at 120°C for 1 h, and then reduced and acetylated as previously described for neutral sugar analysis (using $NaBD_4$ instead of $NaBH_4$). The partially methylated alditol acetates (PMAA) were separated and analyzed by GC–qMS (GC-2010 Plus, Shimadzu). The GC was equipped with a DB-1 (J&W Scientific, Folsom, CA, USA) capillary column (30 m length, 0.25 mm of internal diameter, and 0.10 µm of film thickness). The samples were injected in "split" mode with the injector temperature at 250°C. The temperature program used was as follows: 1) an initial temperature of 80°C; 2) an increase of 7.5°C/min until 140°C and a hold time of 5 min; 3) an increase of 0.2°C/min until 143.2°C; 4) an increase of 12°C/min until 200°C; 5) an increase of 50°C/min until 250°C and a hold time of 5 min. The helium carrier gas had a total flow rate of 8.5 mL/min. The GC was connected to GCMS-QP 2010 Ultra Shimadzu mass quadrupole selective detector operating with an electron impact mode at 70 eV and scanning the range m/z 50–700 in a 1 s cycle in a full scan mode acquisition.

III-2.4. Statistical analysis

Statistical analysis was performed using Graph Pad Prism Software. Differences between the different conditions of the cellular assays were analyzed using non-parametric test (Kruskal-Wallis test) and a $p<0.05$ was considered significant. Data are presented as mean ± standard deviations.

III-3. RESULTS

III-3.1. Cytotoxicity of fucoidan extracts

III-3.1.1. FE 1 does not present toxic effects over cancer cells and shows toxicity for normal cells

FE 1 presents cytostatic effects at day 2 and day 3 for MDA-MB-231 cell line as demonstrated by the inhibited cells growth when compared to the control and lower concentrations (Figure III-1 A). Regarding MCF-7 cell line, fucoidan presents toxic effects only at day 3 and at concentration of 5 mg mL^{-1} (Figure III-1 B). Cytotoxic assays for the normal cells showed cytotoxic effect at day 2 for concentrations above 2 mg mL^{-1} (**Figure III-1- C** and **D**).

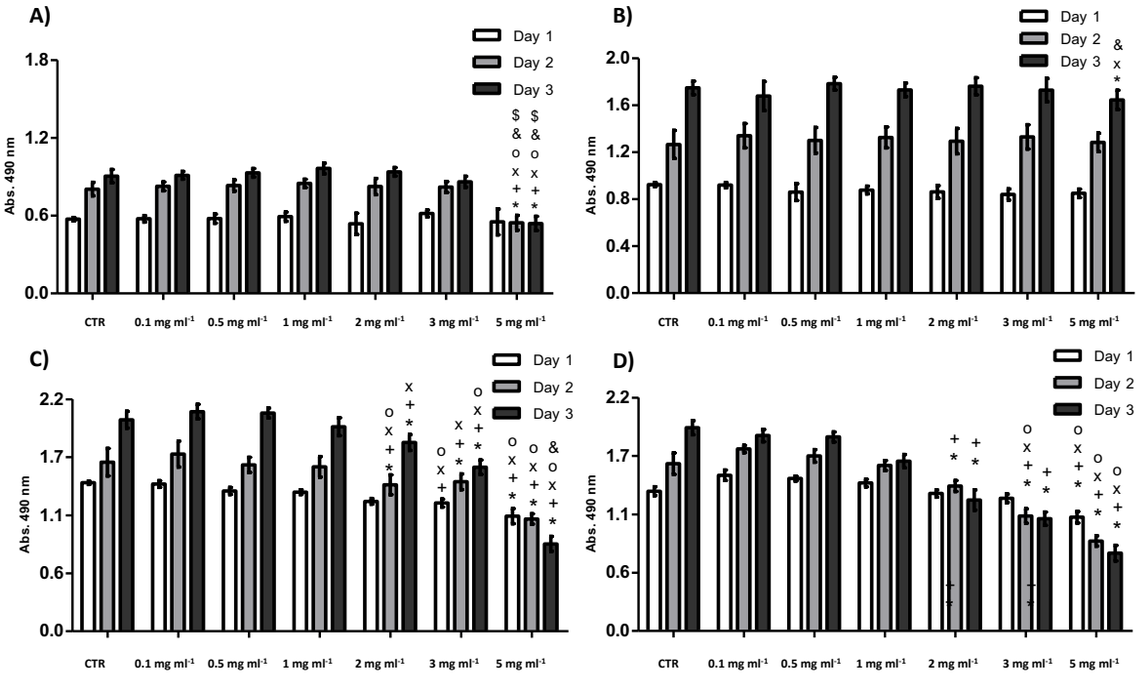

Figure III-1 Cytotoxicity of FE 1, at different concentrations and time-points (1, 2 and 3 days), over human cell lines A) MDA-MB-231, B) MCF-7, C) HPMEC-ST1.6R and D) MRC-5. Data was considered statistically different if $p < 0.05$. * indicates significant differences when compared to CTR; +, when compared to 0.1 mg mL^{-1}; x, when compared to 0.5 mg mL^{-1}; ○, when compared to 1 mg mL^{-1}; &, when compared to 2 mg mL^{-1} and $, when compared to 3 mg mL^{-1}.

III-3.1.2. FE2 induces cancer cells death but does not affect the viability of normal cells at 0.2mg mL^{-1}

We began to test FE2 at the same concentrations as the FE1. However, a significant effect of fucoidan over the breast cancer cell lines was revealed at low concentrations: at day 2 and at concentration of 0.2

mg mL^{-1}, the fucoidan induces cell death for both MDA-MB-231 and MCF-7 cell lines (**Figure III-2 A** and **B**). This effect become more pronounced at higher fucoidan concentrations. The two types of normal cells show distinct behavior: cytostatic effect for the endothelial cells was observed at day 2 and at concentration of 0.5 mg mL^{-1} (**Figure III-2 C**), while, for fibroblastic cells this effect was seen above concentration of 0.3 mg mL^{-1} (**Figure III-2 D**).

These results demonstrated that FE2 induces apoptosis for the two types of tumor cells above 0.2 mg mL^{-1} and maintains the viability of normal endothelial and fibroblastic cells at the same concentration.

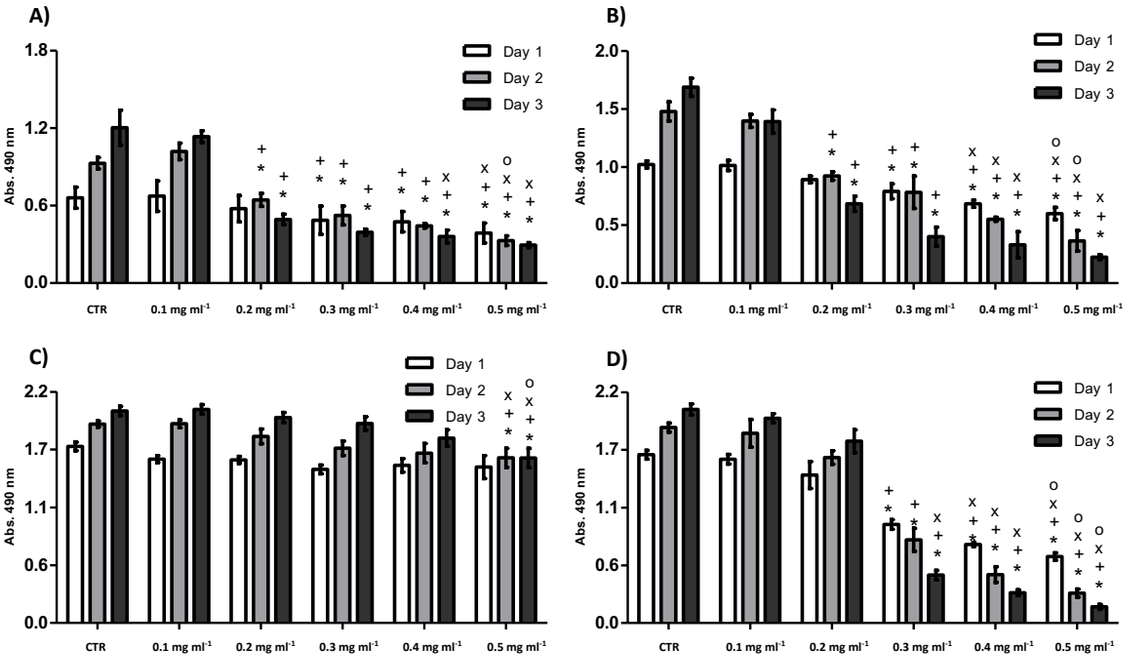

Figure III-2 Cytotoxicity of FE 2, at different concentrations and time-points (1, 2 and 3 days), over human cell lines A) MDA-MB-231, B) MCF-7, C) HPMEC-ST1.6R and D) MRC-5. Data was considered statistically different if $p < 0.05$. * indicates significant differences when compared to CTR; +, when compared to 0.1 mg mL^{-1}; x, when compared to 0.2 mg mL^{-1}; ◦ , when compared to 0.3 mg mL^{-1} and &, when compared to 0.4 mg mL^{-1}.

III-3.1.3. FE3 is toxic to both cancer and normal cells

Similar to FE2, FE3 induces cancer cells death at day 1 for concentrations above 0.2 mg mL^{-1} (**Figure III-3 A and B**). However, FE 3 affects also the normal cells at this concentration and thus, its effect differs from FE2. Stronger cytostatic effect was observed for endothelial cells (**Figure III-3 C**): significantly diminished proliferation was measured for the cells at 0.1 mg mL^{-1} concentration and significant cytotoxic effect is observed above concentration of 0.3 mg mL^{-1}. Concerning the fibroblastic cells, fucoidan has

severe consequences over this cell type and the cytotoxic effect is observed for concentration above 0.2 mg mL^{-1} (**Figure III-3 D**).

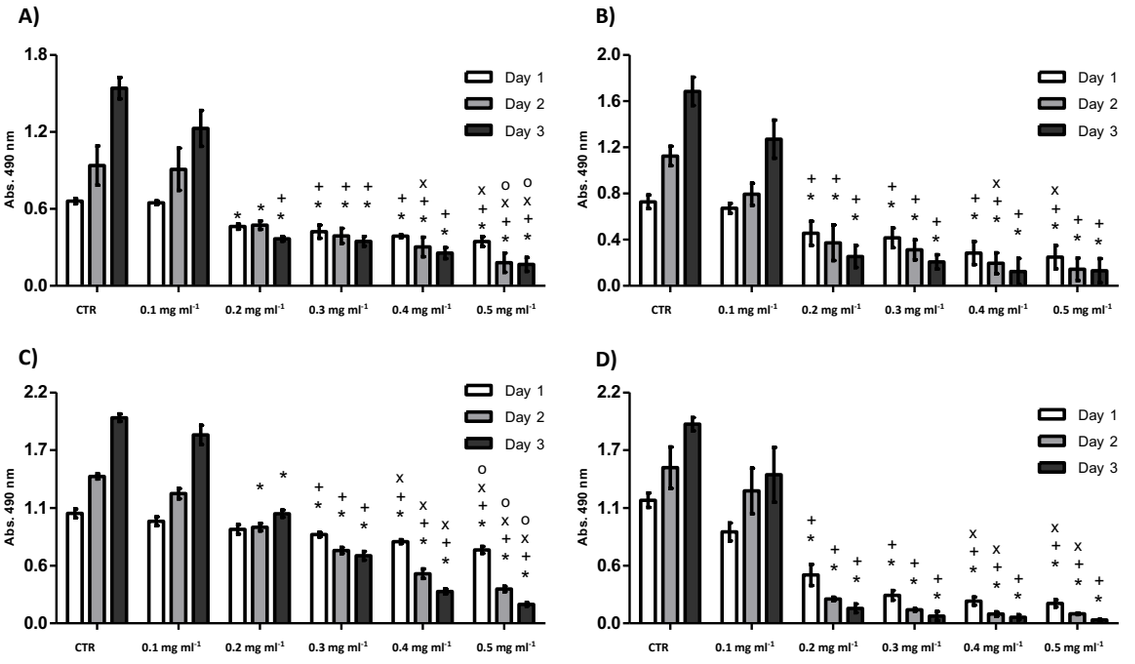

Figure III-3. Cytotoxicity of FE 3, at different concentrations and time-points (1, 2 and 3 days), over human cell lines A) MDA-MB-231, B) MCF-7, C) HPMEC-ST1.6R and D) MRC-5. Data was considered statistically different if $p < 0.05$. * indicates significant differences when compared to + control; +, when compared to 0.1 mg mL^{-1}; x, when compared to 0.2 mg mL^{-1}; ∘ , when compared to 0.3 mg mL^{-1} and &, when compared to 0.4 mg mL^{-1}.

III-3.2. Physicochemical characterization of the different fucoidan extracts

III-3.2.1. Molecular weight

The GPC analysis showed that the three extracts have significantly different molecular weight. A smallest retention volume (longer chain) was determined for FE 1 (**Figure III-4 B**). The molecular weight of FE 1 is two times higher when compared with FE 3. All the three extracts have a very similar Mw/Mn (polydispersity) (**Figure III-4 A**).

A)

	MOLECULAR WEIGHT (Mw)	Mw/Mn
FE 1	91	1.8
FE 2	60	1.7
FE 3	42	1.8

B)

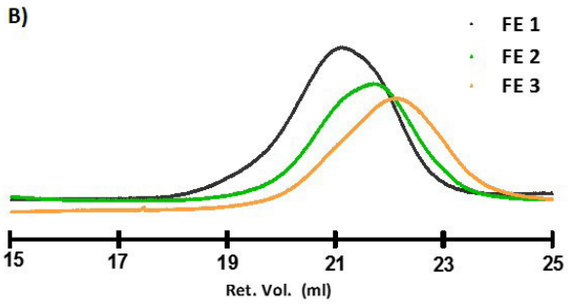

Figure III-4. A) Molecular weight (Mw) and Mw/Mn of FE 1, FE 2 and FE 3 measured by GPC, B) molecular weight chromatograms.

III-3.2.2. DTAF-labeled fucoidans' cellular internalization

An internalization assay was performed to assess if cancer cells were able to internalize the FE based on its molecular weight. In that sense FE 2 (the one with selective bioactivity) was compared with FE 1 (no bioactive activity and higher molecular weight). No green labelling is observed for the positive controls and DTAF (**Figure III-5**) showing that DTAF alone is not internalized by breast cancer and endothelial cells. Endothelial cells cultured with labelled FE 1 and FE 2 do not present any green fluorescence, i.e DTAF-labeled fucoidan was not internalized by these cells. On the other hand, breast cancer cells internalized the labeled fucoidan: green staining localized near to the nucleus is visible in Figure III-5 for both FE 1 and FE 2.

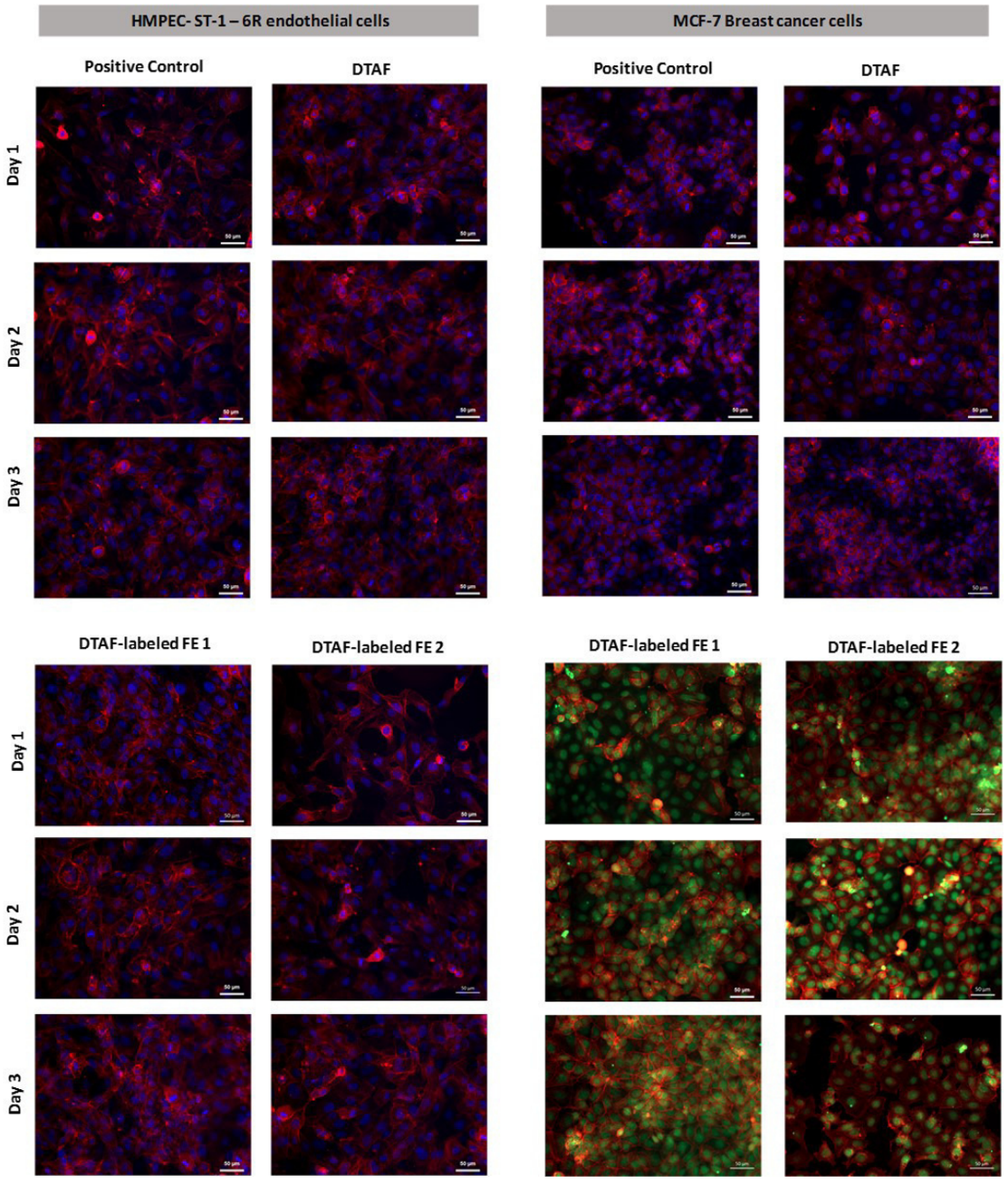

Figure III-5. Internalization of DTAF-labeled FE 1 and FE 2 by HPMEC-ST-1.6R and MCF-7 cell lines. In MCF-7 cultures, the nucleus staining by DAPI was omitted in face of the co-localization of internalized DATF-labeled fucoidans.

III-3.2.3. FE 1 hydrolysis

The above results (**Figures III-4** and **III-5**) did not lead straightforward to any conclusions about the significance of molecular weights on fucoidans bioactivity. However, since many authors related the Mw with the antitumor activity we performed further analysis about its influence the FE 1 (the one with higher molecular weight) was hydrolyzed by an acidic reaction in boiling water to lower molecular weight polymer

and we further analyzed it. We obtained a polymer with molecular weight of 40 kDa (Figure III-6 A). This molecular weight is similar to the one of FE 3, that has toxic effect over both cancer and normal cells. The toxicity of this new polymer (FE 1*) was evaluated with breast cancer and endothelial cells and demonstrated no significant differences as compared with the initial FE1 (**Figure III-6 C**) and **D**) vs **Figure III-1 B** and **C**).

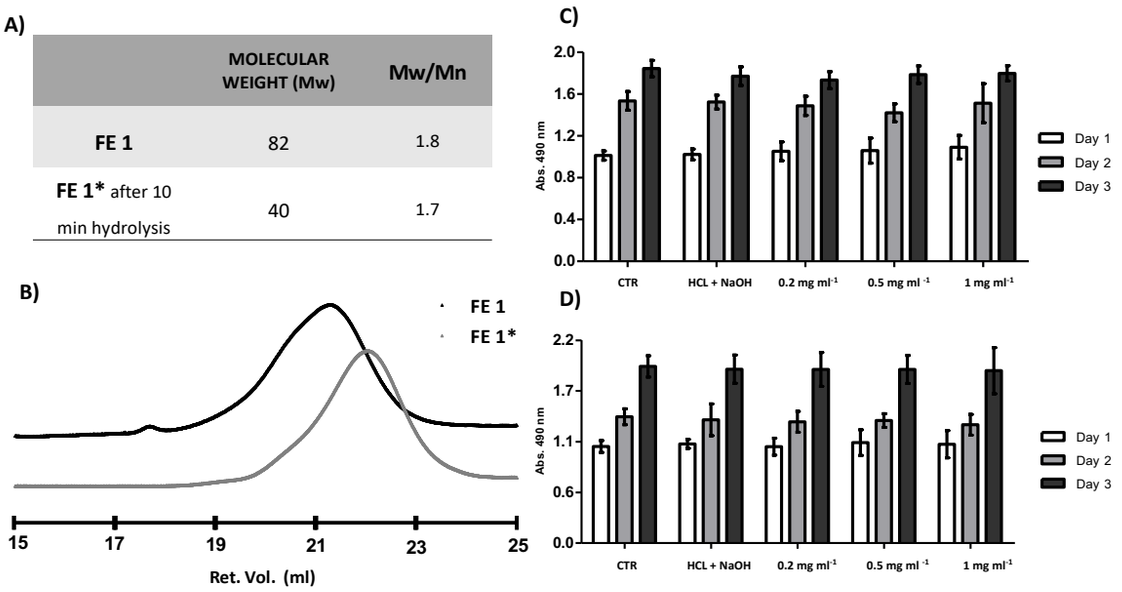

Figure III-6. A) molecular weight (Mw) and Mw/Mn measured by GPC, B) molecular weight chromatogram. Cytotoxicity of FE 1* over C) MCF-7 and D) HPMEC-ST-1.6R cell lines. No statistically significant differences were observed.

III-3.2.4. Carbohydrates composition

The obtained results for the monomeric composition of the analyzed sulfated-polysaccharides showed that the predominant sugar was the fucose (71.2 - 79.1% mol), as expected. The following sugars are the uronic acids (9.8 – 15.3% mol), xylose (3.9 – 8% mol), galactose (3.5% - 5.5% mol) and minor amounts of mannose and glucose (**Table III-1**). It seemed that there are not many differences between the analyzed fucoidan extracts. When comparing one of the previous referred extracts with FE 1 (no toxicity over cancer cells) we often find comparable values, with at least one of the extracts (FE 2 and FE 3). The total sugar mass per extract mass is also very similar for the three extracts. Having a closer look into the quantification of neutral sugars and uronic acids, and having in mind that FE 2 and FE 3 are the

ones that present toxicity to cancer cells, it is not possible to find any correlation between these sugar components and the anti-cancer activity.

Table III-1 Carbohydrates composition of the three fucoidan extracts

	% TOTAL SUGAR MASS/ EXTRACT MASS	% MOLAR OF NEUTRAL SUGARS					% MOLAR OF URONIC ACIDS
		Fucose	Xylose	Mannose	Galactose	Glucose	
FE 1	52.5 ± 2.5	73.1 ± 0.4	8.0 ± 0.1	1.3 ± 0.2	3.5 ± 0.3	0.7 ± 0.1	13.3 ± 0.3
FE 2	52.2 ± 1.9	79.1 ± 0.6	3.9 ± 0.0	0.8 ± 0.0	5.5 ± 0.1	0.8 ± 0.0	9.8 ± 0.5
FE 3	50.5 ± 2.7	71.2 ± 0.5	5.3 ± 0.1	1.5 ± 0.3	5.4 ± 0.0	1.3 ± 0.9	15.3 ± 0.8

III-3.2.5. NMR spectroscopy

The differences in the biological activity observed in FE seems to be unrelated to the Mw and sugars composition therefore we decided to analyze in detail the sulfation and branching of the samples. The fastest way to compare the 3 extracts and obtain a general idea of the differences in composition is ^{1}H NMR. The ^{1}H NMR of the 3 samples at 400 MHz is included in **Figure III-7**.

The spectra correspond to the previously described for fucoidan samples with the isolated regions of the fucose methyl protons (H6, 1-1.5 ppm), acetyl protons (at 2.2 ppm with a small proportion 0.5 to 1 acetyl groups per every 10 fucose residues) and anomeric (5.0-5.5 ppm) and a highly overlapped region corresponding to all other signals in the fucose ^{1}H NMR [26]. The strong overlap hampers a very detailed information but the 3 extracts show enough differences to expect considerable different composition. Especially interesting was difference the region around 3.9-4.3 ppm that contains signals attributed to branched fucose [29]. In light of these results a detailed study of sulfation position and branching was performed by methylation analysis.

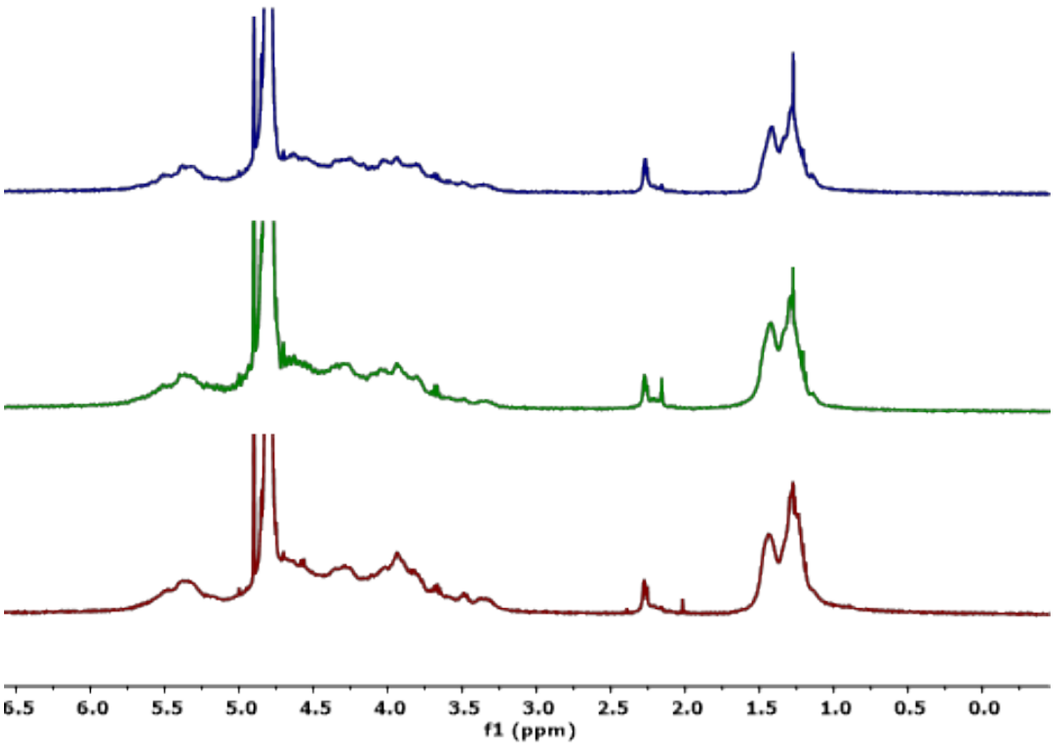

Figure III-7 1H NMR spectra (400 MHz, D2O, 25 °C) of the Fucoidan extracts: FE1 bottom, FE 2 middle and FE 3 top.

III-3.2.6. Sulfation degree and methylation analysis

Sulfation is another key factor in fucoidan bioactivity: higher sulfation degree is often associated with greater bioactivity [36]. Quantification results demonstrate that the studied extracts have a very similar total percentage of sulfates, which varies between 28.0 and 29.3%. The analysis of partially methylated alditol acetates before (native) and after desulfation (desulfated) of fucoidans allow to know the substitution of sugar residues, corresponding to branching points and the substitution by sulfate esters. When a position is acetylated in the native polysaccharide and become methylated after desulfation, it is indication that this position contains a sulfate residue. However, when a position is acetylated even after desulfation of the polysaccharide, it can be inferred that it is a branching point. The results are shown in **Table III-2**.

In native fucoidan extracts, 2,3,4-Fuc was the major residue for the three extracts, followed by 2,4- and 2,3-Fuc (co-eluated peaks) residues, indicating a high percentage of substituted fucose. After desulfation it was observed the decrease of these specific residues (75-80% for 2,3,4-Fuc and 46-61% for 2,4-Fuc + 2,3-Fuc), meaning that part of the substituents was sulfate esters that were removed with the

desulfation procedure. An increase mainly of the 4-Fuc and 3-Fuc residues after desulfation allowed to infer that the fucoidan backbone was constituted by these linkages, which is in accordance with literature, reporting that *F. vesiculosus* fucoidan main chain is composed of alternating 4-O and 3-O fucose linkages [37, 38]. These results allowed also to conclude that sulfate esters were mainly linked in 2-O fucose. However, the observation of the 2-O linkage in the desulfated sample shows that this linkage should be also a characteristic of the fucoidan structure. The increase of 3,4-Fuc residues after desulfation, as well as the maintenance of about 10% of 2,3,4-Fuc, 2,4-Fuc, and 2,3-Fuc branched residues, corroborate the presence of a branched fucoidan structure mainly in 3-O or 4-O positions. As the sum of all branched residues is equal to the sum of terminal residues of Fuc, Xyl and UA (GlcA and GalA), it can be inferred that the fucoidan had a polymeric nature (no extra Fuc terminal residues), containing fucose, xylose, and uronic acids as side chains terminal residues.

The branching degree (sum of branched Fuc/(total Fuc minus the terminal Fuc), indicates the frequency (%) of side chain residues present in the backbone. Therefore, this structural feature of the polysaccharides was determined for FE 1, FE 2, and FE 3 and allowed to show that FE 2 was more branched (83.4%) than FE 1 (67.5%) or FE 3 (60.4%) (Table 2).

The percentage of sulfate present in each fucose position (4-,3-, and 2-O linkage) was determined based on the increase of each fucose linkage after desulfation in relation to the native fucoidan (**Table III-2)**. The major percentage of sulfate esters was present in the 2-O-Fuc for all extracts (51-60%), which is in agreement with literature [37, 38]. In addition, it is also possible to observe the presence of sulfates in 3-O position (28-35%) and 4-O position (27-36%). The FE 2 showed the presence of fewer sulfate esters in 4-O and 2-O positions when compared with the other extracts, in opposite to FE 3 that had a higher percentage of sulfates in 4-O and 2-O positions. FE 1 had a higher content of sulfate in 3-O position.

Table III-2 Sulfation degree (%), glycosidic-substitution composition (%) of fucoidan samples in fractions FE 1, FE 2, and FE 3, before and after desulfation.

		FE 1		FE 2		FE 3	
Sulfation Degree (% Sulfate mass/extract mass)		**28.0 ± 1.4**		**29.3 ± 2.8**		**28.6 ± 1.9**	
Sugar residues and substitution positions		**Native**	**Desulfated**	**Native**	**Desulfated**	**Native**	**Desulfated**
t-Fuc		5.5	14.2	4.2	13.1	4.7	13.4
4-Fuc		0.9	10.6	1.9	7.6	1.5	11.0
3-Fuc		1.5	9.3	1.2	7.3	1.5	13.6
2-Fuc		5.1	8.8	3.9	5.2	4.1	5.7
3,4-Fuc		3.9	12.3	7.3	11.2	5.8	9.2
2,4-Fuc + 2,3-Fuc		19.1	10.3	24.8	10.6	27.6	10.7
2,3,4-Fuc		42.8	9.1	42.9	11.3	34.8	6.8
Total Fuc		**78.8**	**74.6**	**86.3**	**66.3**	**79.9**	**70.4**
t-Xyl		6.8	9.1	3.3	7.7	4.4	8.2
t-GlcA + t-GalA		14.5	16.3	10.4	26.0	15.6	21.4
Branching degree (%)		**67.5**		**83.4**		**58.9**	
Sulphate (%)	4-*O* linkage	30.5		27.4		38.5	
	3-*O* linkage	34.9		29.4		27.7	
	2-*O* linkage	55.6		50.9		60.3	

III-4. DISCUSSION

Fucoidan has been reported to inhibit the growth of cancer cells, having a great interest in the development of new cancer therapies [8]. When considering a cancer therapy, the ultimate goal is to affect cancer cells without damaging the surrounding healthy environment, having non or minimal side-effects [39]. The tumor microenvironment comprises not only the cancer cells but also the non-cancerous

cells which includes endothelial cells, fibroblasts and circulating immune cells [40, 41]. For this reason, it is of utmost importance to test whether fucoidan can only damage the tumor cells and not the healthy surrounding tissues. The three fucoidan extracts were tested with endothelial, fibroblastic and breast cancer cells. When designing a blood administered drug, there is a need to assure that its circulation will not affect the blood vessels. Therefore, we tested the cytotoxicity of fucoidan over human endothelial cells (HPMEC-ST-1.6R cell line). The healthy tissue around the tumor should not be affected when the drug enters into the interstitial fluid. Therefore, fucoidan should not affect this type of cells as well, herein represented by human fibroblasts (MRC-5 cell line). Breast cancer is one of the most frequent cancers and, as many other types of cancer, presents heterogeneous behavior. We used two different breast cancer cells lines to depict this tumor heterogeneity. MCF-7 cell line is an ideal cell model to study hormone responsive tumors since it is estrogen receptor (ER)-positive cells and forms tumors in the presence of estrogen. On the other hand, MDA-MB-231 cell line is ER-negative and have been shown to be tumorigenic [42, 43].

As previously stated, the desired effect of a cancer therapeutic strategy is that fucoidan has toxicity over cancer cell and no or diminished effects over non-cancer cells. Some publications only show the effects of fucoidan over cancer cells [19, 44]. However, this can lead to some misinterpretation of fucoidans' antitumor activity, since it could also have toxic effects over normal cells. In the present study, we denoted that not all fucoidan extracts present this desired behavior. Specifically, FE 1, despite the wide range of concentrations, showed toxicity to normal cells at lower concentrations than cancer cells, resulting in an extract without antitumor features and not suitable for cancer therapies. On the other hand, both FE 2 and FE 3 presented toxicity to cancer cells, although FE 3 also presented toxicity to normal fibroblast cells at the same concentrations. Therefore, FE 3 has to be used with extreme careful and in a more target and precise way to try to affect only the cancer cells and diminished the toxic effects over non-cancer cells, by not affecting the surrounding environment. The FE 2 is the one with the desired anti-tumor behavior, since it showed toxicity effects over cancer cells at 0.2 mg mL^{-1} and, at this concentration, neither endothelial nor fibroblastic cells were affected. From this first group of results, we conclude that not all fucoidans present desirable features, leading to different toxic profiles when in contact with the same cells.

After this biological screening, the next step was focused on the physicochemical characterization of the three extract, trying to understand which feature(s) play(s) a pivotal role in this antitumor behavior. As previously reported, the physicochemical factors that may influence fucoidan bioactivity are the

molecular weight, monosaccharide composition, sulfates degree and sulfates position. Nevertheless, despite not being directly related with fucoidan intrinsic structure the source and extraction method have also been described to influence its bioactive behavior. The effect of molecular weight has been reported as the crucial factor for the fucoidan bioactivity. Previous *in vitro* studies showed that lower molecular weight fucoidan significantly increased the anticancer activity of fucoidan [23, 44, 45]. Furthermore, it has been described that even with higher amounts of sulfation, molecular weight plays a more decisive role [8]. Among the fucoidans studied in the present work, FE 1 has the highest molecular weight when compared with FE 2 and FE 3, but the latter are the ones presenting toxicity to breast cancer cells. Molecular weight is known to be associated with cell internalization, among other factors, from which we hypothesized that when comparing FE 2 with FE 1, only FE 2 (lower molecular weight) would be internalized by cancer cells and exert its antitumor action [46, 47]. However, as illustrated in Figure III-5, no differences were observed in the cellular internalization of FE 1 and FE 2. Thus, these results do not give any conclusions regarding the relationship between cellular internalization and the molecular weight for the studied system.

It has been described that hydrolyzed fucoidan exhibited a higher percentage of anticancer activity [8, 48]. In particular, hydrolyzed fucoidan under mild conditions (in boiling water with HCl) showed higher anti-tumor activity whereas hydrolyzed fucoidan generated under harsh conditions (microwave) slightly enhanced the anti-cancer effects [8]. In this sense, FE 1 was hydrolyzed by acidic reaction to assess if the resulting fucoidan, FE 1*, with lower molecular weight, would present toxicity over cancer cells. However, as seen in Figure III-6, this lower molecular weight extract did not present toxicity to normal and cancer cells. It has been described that acidic hydrolysis can reduce also sulfate content and depolymerization could change monosaccharides ratio, as e.g. decreasing the level of uronic acids [45, 49]. Besides, by comparing FE 1* and FE 3 it is possible to conclude that despite having similar molecular weight the two extracts present significant differences in their bioactivity response. These results suggest that the antitumor behavior may be related with other factors and not directly associated with fucoidans' molecular weight

The studied fucoidan extracts have a total percentage of carbohydrates between 50.5 and 52.5 and of sulfates between 28.0 and 29.3, which means that the total amount of polysaccharides present in the samples varies between 78.5 and 81.8%. These results confirm that fucose and sulfates are the main components of fucoidan from *F. vesiculosus*, as described elsewhere [13, 50]. The uronic acids content has been determined in fucoidan composition, although we need to be cautious in assuming that the full

uronic acid measured is contained within the fucoidan polymers, as has been described elsewhere [51]. The carbohydrates composition did not indicate any clear relation structure-activity.

Higher sulfation is related with greater molecular bioactivity and thus researchers have produced over-sulfated fucoidans to enhance its biological properties [37]. It has been suggested that over-sulfation causes higher negative charge in the molecule, which facilitate formation of fucoidan-protein complexes involved in cell proliferation [39]. Sulfate mass quantification, of the three fucoidan extracts did not present significant variation. Despite these results, sulfates can still play a role in the antitumor activity, since the same sulfation degree can correspond to different sulfates position, i.e. sulfation distribution along fucoidan backbone, presenting distinct biological response. Thus, both sulfates position and polymer branching were assessed to better understand the role of the chemical structure on the exhibited biological activity. The FE 2 was the polysaccharide with higher percentage of fully branched chains (together in 3-O and 4-O-Fuc) and, as a consequence, it is a more branched structure than the other ones. Also, as all hydroxyl groups are linked, they could not have sulfates in these residues. The sulfates occur mainly in 2-O-Fuc. In comparison with FE 2, FE 1 had higher sulfation in 4-O-Fuc and 3-O-Fuc while FE 3 had higher sulfation in 4-O-Fuc. Consequently, the sulfates position is different for the three fucoidans. It is possible that these structural differences may influence their cytotoxicity response, particularly regarding the breast cancer cell lines tested.

It is thus shown here that the antitumor behavior is not ubiquitous, as could be inferred from the published reports, but dependent on their chemical structure, being also important to highlight that the same fucoidan extract can present different effects over different types of cells and cancers [15].

As referred before, the source (original species) and extraction method are two factors that may affect fucoidan intrinsic properties and that are commonly associated with fucoidans' bioactivity. Fucoidan preparations isolated from different sources have shown differential anti-cancer effects *in vivo* due to corresponding structural properties [22]. Since the source of fucoidan is the same for the three extracts (i.e. *F. vesiculosus*), the extraction method may be the factor influencing fucoidan intrinsic properties and thus the different antitumor behavior. Even from the same company, we have different batches that can present different behaviors. The preservation of the fucoidan molecules' structural integrity essentially depends on the extraction methodology which has a crucial, but partly ignored, significance for obtaining the relevant structural features required for specific biological activities and for elucidating structure-function relations [14].

To be suited to a regulated product, fucoidan extracts must be defined and reproducible. Sustainable, clean and regulated harvesting, or culturing of a single type of seaweed are required. In order to meet therapeutic regulatory requirements, common extraction methods and distribution of fully characterized fucoidans needs to be taken into consideration. This is particularly relevant when trying to take a product from a preclinical concept to clinical trials. The development and use of such consistent extraction procedures would also help in achieving a better understanding of structure-function relationship of fucoidan extracts.

III-5. CONCLUSIONS

Despite the promising results about the anti-cancer effects of fucoidan, some variability impedes its utilization in the clinic. Specifically, contradictory experimental results influenced by endogenous and exogenous factors in fucoidan usage are the main barriers. It is also important to have in mind that the ultimate goal of an effective cancer therapy is to damage cancer cells without negatively affect the surrounding healthy environment. This distinctive action mode was only observed with the FE 2 being important to characterize the physicochemical properties of the different extracts. The present results allow to infer that the molecular weight, monosaccharides composition and content of sulfates could not be related with the cytotoxicity of FE 1, FE 2, and FE 3 extracts. From our results, we can conclude that the branching degree of the fucoidans may be the most obvious cause of the different biological behavior of the three extracts.

In this sense, more focus should be direct to the optimization and standardization of the extraction and purification processes to obtain consistent protocols that account for the biodiversity of fucoidan extracts, from different seaweeds, and to retain the structural features of significance for specific bioactivity of fucoidan extracts. Furthermore, the determination and clarification of the structural characteristics responsible for antitumor activities of fucoidan will be essential for its potential as a marine-origin drug.

III-6. ACKNOWLEDGEMENTS

The authors would like to thank the funding from projects 0687_NOVOMAR_1_P, co-funded by INTERREG 2007-2013/POCTEP, CarbPol_u_Algae (EXPL/MAR-BIO/0165/2013)

and IF/00376/2014/CP1212/CT0015, funded by the Portuguese Foundation for Science and Technology, FCT, and ComplexiTE (ERC-2012-ADG 20120216-321266), funded by the European Research Council under the European Union's Seventh Framework Programme for Research and Development. The authors would like to thank also FCT, Portugal, for the scholarship of ASF (SFRH/BD/102471/2014), fellowship of CN (SFRH/BPD/100627/2014), Investigator grants of AM (IF/00376/2014), RNC (IF/00373/2014) and IP (IF/00032/2013) and the financial support to CICECO- Aveiro Institute of Materials (POCI-01-0145-FEDER-007679, FCT UID/CTM/50011/2013) and QOPNA (UID/QUI/00062/2013), through national founds and co-financed by the FEDER, within the PT2020 Partnership Agreement.

III-7. REFERENCES

[1] C. GM, The Cell: A Molecular Approach. 2nd edition. Sunderland (MA): Sinauer Associates, (2000).

[2] K. Sak, Chemotherapy and dietary phytochemical agents, Chemotherapy research and practice 2012 (2012) 282570.

[3] A. Gennari, M. D'Amico, D. Corradengo, Extending the duration of first-line chemotherapy in metastatic breast cancer: a perspective review, Therapeutic advances in medical oncology 3(5) (2011) 229-232.

[4] C. DeSantis, J. Ma, L. Bryan, A. Jemal, Breast cancer statistics, 2013, CA Cancer J Clin 64(1) (2014) 52-62.

[5] U.N.C.C.f.C.U. National Collaborating Centre for Cancer, (2009).

[6] M.M. Gottesman, Mechanisms of cancer drug resistance, Annual review of medicine 53 (2002) 615-27.

[7] H.-Y. Hsu, T.-Y. Lin, Y.-C. Wu, S.-M. Tsao, P.-A. Hwang, Y.-W. Shih, J. Hsu, Fucoidan inhibition of lung cancer in vivo and in vitro : role of the Smurf2-dependent ubiquitin proteasome pathway in TGF β receptor degradation, Oncotarget 5(17) (2014) 7870-7885.

[8] F. Atashrazm, R.M. Lowenthal, G.M. Woods, A.F. Holloway, J.L. Dickinson, Fucoidan and Cancer: A Multifunctional Molecule with Anti-Tumor Potential, Marine Drugs 13(4) (2015) 2327-2346.

[9] T.H. Silva, A. Alves, B.M. Ferreira, J.M. Oliveira, L.L. Reys, R.J.F. Ferreira, R.A. Sousa, S.S. Silva, J.F. Mano, R.L. Reis, Materials of marine origin: a review on polymers and ceramics of biomedical interest, International Materials Reviews 57(5) (2012) 276-306.

[10] J.H. Fitton, D.N. Stringer, S.S. Karpiniec, Therapies from Fucoidan: An Update, Marine Drugs 13(9) (2015) 5920-5946.

[11] L. Yang, P. Wang, H. Wang, Q. Li, H. Teng, Z. Liu, W. Yang, L. Hou, X. Zou, Fucoidan derived from Undaria pinnatifida induces apoptosis in human hepatocellular carcinoma SMMC-7721 cells via the ROS-mediated mitochondrial pathway, Marine drugs 11(6) (2013) 1961-1976.

[12] N. Li, Q. Zhang, J. Song, Toxicological evaluation of fucoidan extracted from Laminaria japonica in Wistar rats, Food and Chemical Toxicology 43(3) (2005) 421-426.

[13] B. Li, F. Lu, X. Wei, R. Zhao, Fucoidan: Structure and Bioactivity, Molecules 13(8) (2008).

[14] M.T. Ale, J.D. Mikkelsen, A.S. Meyer, Important Determinants for Fucoidan Bioactivity: A Critical Review of Structure-Function Relations and Extraction Methods for Fucose-Containing Sulfated Polysaccharides from Brown Seaweeds, Marine Drugs 9(10) (2011) 2106-2130.

[15] G. Moussavou, H.D. Kwak, W.B. Obiang-Obonou, A.C. Maranguy, S.-D. Dinzouna-Boutamba, H.D. Lee, G.O. Pissibanganga, K. Ko, I.J. Seo, K.Y. Choo, Anticancer Effects of Different Seaweeds on Human Colon and Breast Cancers, Marine Drugs 12(9) (2014) 4898-911.

[16] M.T. Ale, H. Maruyama, H. Tamauchi, J.D. Mikkelsen, A.S. Meyer, Fucoidan from Sargassum sp. and Fucus vesiculosus reduces cell viability of lung carcinoma and melanoma cells in vitro and activates natural killer cells in mice in vivo, International Journal of Biological Macromolecules 49(3) (2011) 331-336.

[17] H.-J. Boo, J.-H. Hyun, S.-C. Kim, J.-I. Kang, M.-K. Kim, S.-Y. Kim, H. Cho, E.-S. Yoo, H.-K. Kang, Fucoidan from Undaria pinnatifida Induces Apoptosis in A549 Human Lung Carcinoma Cells, Phytotherapy Research 25(7) (2011) 1082-1086.

[18] H.-J. Boo, J.-Y. Hong, S.-C. Kim, J.-I. Kang, M.-K. Kim, E.-J. Kim, J.-W. Hyun, Y.-S. Koh, E.-S. Yoo, J.-M. Kwon, H.-K. Kang, The anticancer effect of fucoidan in PC-3 prostate cancer cells, Marine drugs 11(8) (2013) 2982-2999.

[19] Z. Zhang, K. Teruya, T. Yoshida, H. Eto, S. Shirahata, Fucoidan extract enhances the anti-cancer activity of chemotherapeutic agents in MDA-MB-231 and MCF-7 breast cancer cells, Marine drugs 11(1) (2013) 81-98.

[20] H. Lee, J.-S. Kim, E. Kim, Fucoidan from seaweed Fucus vesiculosus inhibits migration and invasion of human lung cancer cell via PI3K-Akt-mTOR pathways, PloS one 7(11) (2012) e50624-e50624.

[21] K. Senthilkumar, P. Manivasagan, J. Venkatesan, S.-K. Kim, Brown seaweed fucoidan: Biological activity and apoptosis, growth signaling mechanism in cancer, International Journal of Biological Macromolecules 60 (2013) 366-374.

[22] J.-Y. Kwak, Fucoidan as a Marine Anticancer Agent in Preclinical Development, Marine Drugs 12(2) (2014) 851-70.

[23] A. Kasai, S. Arafuka, N. Koshiba, D. Takahashi, K. Toshima, Systematic synthesis of low-molecular weight fucoidan derivatives and their effect on cancer cells, Organic & Biomolecular Chemistry 13(42) (2015) 10556-10568.

[24] T.M. Buttke, J.A. McCubrey, T.C. Owen, Use of an aqueous soluble tetrazolium/formazan assay to measure viability and proliferation of lymphokine-dependent cell lines, Journal of immunological methods 157(1-2) (1993) 233-40.

[25] S. Prigent-Richard, M. Cansell, J. Vassy, A. Viron, E. Puvion, J. Jozefonvicz, D. Letourneur, Fluorescent and radiolabeling of polysaccharides: Binding and internalization experiments on vascular cells, Journal of Biomedical Materials Research 40(2) (1998) 275-281.

[26] M. Ellouali, C. Boisson-Vidal, P. Durand, J. Jozefonvicz, Antitumor activity of low molecular weight fucans extracted from brown seaweed Ascophyllum nodosum, Anticancer Res 13(6A) (1993) 2011-2019.

[27] C. Nunes, L. Silva, A.P. Fernandes, R.P.F. Guiné, M.R.M. Domingues, M.A. Coimbra, Occurrence of cellobiose residues directly linked to galacturonic acid in pectic polysaccharides, Carbohydrate Polymers 87(1) (2012) 620-626.

[28] M.J. Clement, B. Tissot, L. Chevolot, E. Adjadj, Y. Du, P.A. Curmi, R. Daniel, NMR characterization and molecular modeling of fucoidan showing the importance of oligosaccharide branching in its anticomplementary activity, Glycobiology 20(7) (2010) 883-94.

[29] M.I. Bilan, A.A. Grachev, A.S. Shashkov, N.E. Nifantiev, A.I. Usov, Structure of a fucoidan from the brown seaweed Fucus serratus L, Carbohydrate Research 341(2) (2006) 238-245.

[30] K.S. Dodgson, Determination of inorganic sulphate in studies on the enzymic and non-enzymic hydrolysis of carbohydrate and other sulphate esters, The Biochemical journal 78(2) (1961) 312-319.

[31] K.S. Dodgson, R.G. Price, A note on the determination of the ester sulphate content of sulphated polysaccharides, The Biochemical journal 84(1) (1962) 106-110.

[32] I.J. Miller, J.W. Blunt, Desulfation of algal galactans, Carbohydrate Research 309(1) (1998) 39-43.

[33] S. Geresh, S. Arad, O. Levy-Ontman, W. Zhang, Y. Tekoah, R. Glaser, Isolation and characterization of poly- and oligosaccharides from the red microalga Porphyridium sp, Carbohydrate Research 344(3) (2009) 343-349.

[34] I. Ciucanu, F. Kerek, A simple and rapid method for the permethylation of carbohydrates, Carbohydrate Research 131(2) (1984) 209-217.

[35] S. Vincenzi, A. Crapisi, A. Curioni, Foamability of Prosecco wine: Cooperative effects of high molecular weight glycocompounds and wine PR-proteins, Food Hydrocolloids 34 (2014) 202-207.

[36] S. Koyanagi, N. Tanigawa, H. Nakagawa, S. Soeda, H. Shimeno, Oversulfation of fucoidan enhances its anti-angiogenic and antitumor activities, Biochemical Pharmacology 65(2) (2003) 173-179.

[37] L. Chevolot, B. Mulloy, J. Ratiskol, A. Foucault, S. Colliec-Jouault, A disaccharide repeat unit is the major structure in fucoidans from two species of brown algae, Carbohydrate Research 330(4) (2001) 529-535.

[38] V.H. Pomin, P.A. Mourao, Structure, biology, evolution, and medical importance of sulfated fucans and galactans, Glycobiology 18(12) (2008) 1016-27.

[39] S. Zorofchian Moghadamtousi, H. Karimian, R. Khanabdali, M. Razavi, M. Firoozinia, K. Zandi, H. Abdul Kadir, Anticancer and Antitumor Potential of Fucoidan and Fucoxanthin, Two Main Metabolites Isolated from Brown Algae, The Scientific World Journal 2014 (2014) 10.

[40] K. Wang, L.-H. Cai, B. Lan, J.J. Fredberg, Hidden in the mist no more: physical force in cell biology, Nature methods 13(2) (2016) 124-125.

[41] F.R. Balkwill, M. Capasso, T. Hagemann, The tumor microenvironment at a glance, Journal of cell science 125(Pt 23) (2012) 5591-6.

[42] D.L. Holliday, V. Speirs, Choosing the right cell line for breast cancer research, Breast cancer research : BCR 13(4) (2011) 215-215.

[43] A.S. Levenson, V.C. Jordan, MCF-7: the first hormone-responsive breast cancer cell line, Cancer research 57(15) (1997) 3071-8.

[44] R. Kimura, T. Rokkaku, S. Takeda, M. Senba, N. Mori, Cytotoxic Effects of Fucoidan Nanoparticles against Osteosarcoma, Marine Drugs 11(11) (2013) 4267-4278.

[45] J.-i. Choi, H.-J. Kim, Preparation of low molecular weight fucoidan by gamma-irradiation and its anticancer activity, Carbohydrate polymers 97(2) (2013) 358-362.

[46] L. Zhang, S. Bhatnagar, E. Deschenes, G.M. Thurber, Mechanistic and quantitative insight into cell surface targeted molecular imaging agent design, Scientific Reports 6 (2016) 25424.

[47] M.M. Schmidt, K.D. Wittrup, A modeling analysis of the effects of molecular size and binding affinity on tumor targeting, Molecular cancer therapeutics 8(10) (2009) 2861-2871.

[48] C. Yang, D. Chung, I.-S. Shin, H. Lee, J. Kim, Y. Lee, S. You, Effects of molecular weight and hydrolysis conditions on anticancer activity of fucoidans from sporophyll of Undaria pinnatifida, International Journal of Biological Macromolecules 43(5) (2008) 433-437.

[49] L.-E. Rioux, S.L. Turgeon, M. Beaulieu, Structural characterization of laminaran and galactofucan extracted from the brown seaweed Saccharina longicruris, Phytochemistry 71(13) (2010) 1586-1595.

[50] T. Nishino, C. Nishioka, H. Ura, T. Nagumo, Isolation and partial characterization of a noval amino sugar-containing fucan sulfate from commercial Fucus vesiculosus fucoidan, Carbohydrate Research 255 (1994) 213-224.

[51] M. Nagaoka, H. Shibata, I. Kimura-Takagi, S. Hashimoto, K. Kimura, T. Makino, R. Aiyama, S. Ueyama, T. Yokokura, Structural study of fucoidan from Cladosiphon okamuranus tokida, Glycoconjugate Journal 16(1) (1999) 19-26.

Chapter IV

Fucoidan from *Fucus vesiculosus* inhibits new blood vessel formation and breast tumor growth *in vivo*

Chapter IV

Fucoidan from *Fucus vesiculosus* inhibits new blood vessel formation and breast tumor growth *in vivo* ‡

ABSTRACT

Fucoidan is a marine-origin sulfated polysaccharide that can show anticancer activity, to which both pro- and anti-angiogenic responses have been reported. Due to this unpredictability, the angiogenic potential of an effective anticancer crude fucoidan (CF), at a concentration of 0.5 mg mL^{-1}, was evaluated. Tube formation assay demonstrated that CF, either administered while endothelial cells seeding or after cells' adhesion, inhibited or disrupted the formation of tubular-like structures. Although CF did not significantly reduced VEGF secretion, it significantly reduced the expression of PDGF. Two Chicken Embryo Chorioallantoic membrane (CAM) assays were performed: one without tumor (CAM I) and the other with an onplanted tumor mass (CAM II). CF injection reduced the number of blood of vessels and significantly decreased the size of the tumor, respectively. *In vitro* and *in vivo* results support the effectiveness of fucoidan as a natural antitumor therapeutic agent.

‡ This chapter is based on the following publication:

Oliveira C., Granja S., Neves N.M., Reis R.L., Baltazar F., Silva T.H., Martins A., *Fucoidan from Fucus vesiculosus inhibits new blood vessel formation and breast tumor growth in vivo*, Carbohydrate Polymers. (2019) 223. doi: 10.1016/j.carbpol.2019.115034

.

IV-1. INTRODUCTION

Angiogenesis is the physiological process that comprises the formation of new blood vessels from pre-existing ones, a process mediated by endothelial cells. This process encompasses different phases: sprout formation (initiated with the release of enzymes from the endothelial cells), cell proliferation and migration and formation of tubular-like structures [1, 2]. Angiogenesis requires several regulating molecules that may trigger this process. Between them, growth factors (GFs) are the key players, namely vascular endothelial growth factor (VEGF) that induces endothelial cells proliferation and migration, and platelet-derived growth factor (PDGF) related with blood vessels maturation [1, 3]. These growth factors are essential in many physiological processes like embryonic development, tissue regeneration and wound healing, where angiogenesis is temporary and highly regulated. Nevertheless, there are some pathological conditions where angiogenesis is an unregulated process, such as tumor growth and cancer metastases [4, 5]. Angiogenesis does not promote cancer appearance but enables tumor progression and metastasis [6].Tumor growth comprises two different stages: the first stage does not involve blood vessels formation, whereas the second stage requires the formation of new capillaries for the exchange of nutrients/waste and cancer cells' survival. These new blood vessels are also a mean for tumor cells circulation [4, 7, 8]. Therefore, blocking angiogenesis in the tumor microenvironment has become a promising approach for the development of effective anticancer therapies [9, 10].

Most of the current anti-cancer drugs used in cancer therapeutics affects both cancer and healthy cells, resulting in severe adverse effects. Anti-angiogenic compounds may present less side effects since neoangiogenesis is not common in healthy adults. Blocking VEGF pathway is the most common approach to limit tumor angiogenesis and has been reported for different types of cancers [11]. However, there are some limitations since VEGF blockage may also damage healthy vessels and resistance to VEGF inhibitors may occur, resulting in adverse side effects [12]. Recent findings may use other mechanisms, independently or in combination with VEGF-blockage, trying to improve current anti-angiogenic treatments for cancer [13]. Different strategies based on natural compounds have been reported to present these anti-angiogenic activity, increasing bioavailability and the delivery of drugs to the sites of tumor angiogenesis [14].

Fucoidan is a marine-origin sulfated polysaccharide that can be extracted from different brown algae species, such as *F. vesiculosus*, which is the most common. Fucoidan from this species presents a relatively simple composition and is mainly composed of fucose and sulfate residues. The main component unit is 1,2-α-fucose and most of sulfate groups are located at position C-4 of the fucose units.

Fucoidan structure may also be composed of other monosaccharides as glucose, xylose, galactose and mannose [15]. Fucoidan may present diversified biological activities including antibacterial, antioxidant, antiviral and antitumor, depending on their chemical features [16, 17]. Some of these biological activities are still controversial, since not all fucoidans present the same biological responses [15]. In a previous work, we related the antitumor activity of CF with its chemical structure, highlighting the relevance of structure-activity relationship (SAR) [18]. Considering the angiogenic potential of fucoidan, both pro- and anti-angiogenic responses have been reported in the literature [19]. Fucoidan was reported to limit angiogenesis in osteosarcoma, associated with a decrease in VEGF and SDF-1 (stromal derived factor-1) [20]. In another attempt, an anti-angiogenic sulfated fucoidan was reported, presenting its biological activity by blocking VEGF signaling to inhibit human lung cancer cells growth [21]. Low molecular weight fucoidan suppressed HIF-1/VEGF signaling pathway using human bladder cancer cells [22]. The same signaling pathway was investigated with human multiple myeloma cells and fucoidan presented anti-angiogenic properties [23]. Regarding prostate cancer, fucoidan was reported to inhibit human cancer cells proliferation by reducing specific endothelial markers like VEGF [24]. Fucoidan from *F. vesiculosus* inhibited the growth of human thyroid cancer cells and suppressed angiogenesis [25]. There is only one study that relates breast cancer and anti-angiogenic potential of fucoidan. In this case, micro-vessels reduction was observed in a mouse breast cancer cell model when fucoidan was injected [26]. Despite the demonstrated anti-angiogenic activity, other studies were not able to reach the same conclusions. In human hepatocarcinoma cells lines treated with different doses of fucoidan, angiogenesis was not affected and there was no decrease in VEGF expression [27]. In another attempt, fucoidan did not present antitumor activity for uveal melanoma cells lines, demonstrating a pro-angiogenic potential instead [28].

The pro-angiogenic activity of fucoidan has been most studied for non-tumor pathologies. Fucoidan was evaluated in ischemic tissues, showing its capability for revascularization by triggering mobilization of endothelial progenitor cells [29]. The angiogenic effect of fucoidan for inducing osteoblastic differentiation through VEGF secretion, resulted in enhanced angiogenesis and bone repair [30]. Some studies have already reported that different fucoidan extracts, regarding their chemical features, may present different angiogenic biological effects [31].

An effective anticancer CF presents toxicity to cancer cells without affecting normal cells, as previously reported by us [32]. Considering that fucoidan can exert an anti-cancer response through different mechanisms, including by inhibiting the formation of blood vessels, but also that the angiogenic potential of fucoidan is still controversial, we hypothesized that a CF similar to the one used in the previous

work has also an anti-angiogenic effect. The tube formation assay evaluated the effect of fucoidan on the formation/inhibition of tubular like structures. These findings were correlated with the secretion of VEGF and PDGF, two important GFs secreted by human endothelial cells and involved in angiogenesis. Furthermore, CAM assay was performed as a model to study angiogenesis *in vivo*. With this model two different approaches were carried out: one without tumor cells (CAM I) to ascertain about the effect of fucoidan over the vasculatures and other where tumor cells were onplanted into the chick membrane (CAM II) to assess the influence of fucoidan in a simulated tumor microenvironment.

IV-2. EXPERIMENTAL SECTION

IV-2.1. Materials

Crude fucoidan from *F. vesiculosus* (batch number: SLBP3196V) was purchased from Sigma-Aldrich and used as received. Fucoidan molecular weight is 107 800 Da, was measured by Gel Permeation Chromatography - Multi-angle Laser Light Scattering (from the certificate of analysis). The sulfation degree was determined as 15%, based on S:C atomic ratio of 0.025 obtained from XPS analysis. Human breast adenocarcinoma cells (MDA-MB-231) and cell culture medium (M199 and D-MEM high glucose) were purchased from Sigma-Aldrich whereas endothelial cell growth supplement (ECGS) and matrigel were both acquired from Corning. Fetal bovine serum (FBS) and MEM sodium pyruvate were purchased from Life Technologies. Biotinylated Sambucus Nigra Lectin (SNA, EBL) was purchased from Vector Laboratories. MTS assay (CellTiter 96® AQueous One Solution) was bought from Promega. VEGF and PDGF Development ELISA kits were both purchased from Prepotech. 96-well plate (Nunc-Immuno MicroWell 96-well solid plates) and 2,2′-azino-bis(3-ethylbenzthiazoline-6-sulfonic acid) (ABTS) were purchased from Sigma-Aldrich.

IV-2.2. Fucoidan extract assay to assess antitumor activity as cytotoxic agent

IV-2.2.1. Cell expansion

Human endothelial cells (HPMEC-ST1.6R) were cultured in M199 medium supplemented with 20% FBS, 2 mM Glutamax, Pen/Strep (100 U/100 g mL^{-1}), ECGS (25 µg mL^{-1}). Cells were used at passages 38-40. Human breast adenocarcinoma cells (MDA-MB-231) were cultured in D-MEM high glucose

medium supplemented with 10% FBS, Pen/Strep (100 U/100 g mL^{-1}) and 1% MEM sodium pyruvate solution. Breast cancer cells were used at passages 41-43.

IV-2.2.2. Cell seeding and culture

Human endothelial and cancer cells were harvested and 15 000 cells were seeded in 24 well-plates. After 4h of adherence, crude fucoidan (CF) was added at different concentrations (0.1, 0.2, 0.3, 0.4, 0.5, 0.75 and 1 mg mL^{-1}). A control, without fucoidan in the culture medium, was performed for all the assays. Each experimental condition was tested in triplicate and two independent assays were performed for each type of cells.

IV-2.2.3. Cell Viability

The metabolic activity of human cell lines was determined by MTS assay. After 1, 2 and 3 days, the culture medium was removed and the testing conditions were rinsed with sterile PBS. A mixture of culture medium (without FBS and phenol red) and MTS reagent (5:1 ratio) was added to each well and left to incubate for 3 h, at 37 °C, in a humidified 5% CO_2 atmosphere. Thereafter, the absorbance of the MTS reaction medium from each sample was read at 490 nm in a microplate reader (Synergy HT, Bio-TEK).

IV-2.3. *In vitro* evaluation of CF angiogenic potential

IV-2.3.1. Tube formation assay (TFA)

Human endothelial cells were used for the tube formation assay. The bottom of 96 well-plates were pre-coated with 100 µL of matrigel and left to solidity for 1 h at 37 °C. Afterwards, 15 000 cells were seeded on top of the matrigel. Two different assays were conducted: one where CF was added at the time of cell seeding (tube formation assay I - TFA I); and another where CF was only added 4h after cells adherence (tube formation assay II – TFA II). Samples were analyzed in an inverted microscope (Axiovert 40 – Zeiss) and photos were acquired using a digital camera (G11, Canon) at different time points: 0 h, 4 h, 8 h, 12 h and 16 h.

IV-2.3.2. Quantification of secreted VEGF and PDGF

For the quantification of secreted growth factors, human PDGF and VEGF development ELISA kits were used according to manufactures' protocol. Briefly, the primary antibodies were incubated overnight in a 96-well plate (Nunc-Immuno MicroWell 96-well solid plates). Both the standards and the samples were incubated, and the assay was conducted according to the manufacturer's protocol. In the last step, 100 µL of ABTS liquid substrate was added to each sample, and each plate was read at 405 and 650 nm.

IV-2.4. *In vivo* evaluation of CF angiogenic potential

IV-2.4.1. Chick Embryo Chorioallantoic membrane I

White fertilized chicken eggs were incubated at 37 °C for 3 days (**Figure IV-1**). After this, a window was opened into the shell in order to evaluate embryo viability. A silicon ring was onplanted on the CAM, at day 9 of embryo development, to determine the area where 0.5 mg mL^{-1} CF was injected (injection of water was used as control group), and the eggs were returned to the incubator at 37°C until day 13 for *in-ovo* images acquisition. At day 17, CAM was photographed *in-ovo* and embryos were sacrificed by incubation at -80 °C for 10 min. After fixation with paraformaldehyde at 4% (PFA4%) *ex-ovo* images were captured directly from the plate. Three independent assays were performed, resulting in n=15 eggs per condition.

IV-2.4.2. Chick Embryo Chorioallantoic membrane II

The same protocol of CAM I was followed until day 9 of embryonic development. At that day, instead of inserting a ring into the CAM, a tumor was injected. For tumor development, $1x10^6$ human breast cancer cells were re-suspended in matrigel and onplanted into the CAM, allowing–tumor development until day 13. At this time point, *in-ovo* photos were acquired and 20 µl of fucoidan was injected in the tumor. At day 17, CAM was photographed *in-ovo* and embryos were sacrificed by incubation at -80°C for 10 min. After fixation with paraformaldehyde at 4% (PFA4%) CAM *ex-ovo* images were captured directly from the plate. Three independent assays were performed, resulting in n=15 eggs per condition.

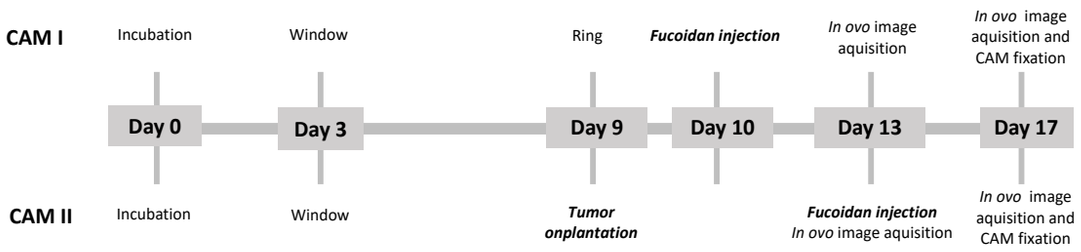

Figure IV-1 Timeline of CAM assay. CAM I without tumor and CAM II with tumor.

IV-2.4.3. Histological analysis

The excised membranes were transferred to histological cassettes, embedded in paraffin and serially sectioned for H&E and immunohistochemical analysis of an endothelial marker, lectin.

IV-2.4.3.1 *H&E staining*

Hematoxylin and eosin (H&E) staining was performed in CAM sections of 4 μm thickness. Briefly, sections were deparaffinized with xylene, rehydrated in ethanol and stained with hematoxylin and eosin. Afterwards, sections were dehydrated and mounted with resinous mounting medium. The histological sections were analyzed under Leica DM750 microscope at 4×, 10× and 40× magnifications.

IV-2.4.3.2 *Immunohistochemistry – Lectin*

CAM sections of 4 μm thickness were deparaffinized and rehydrated in an automatic stainer. Immunohistochemical analysis was performed according to the streptavidin-biotin peroxidase complex system (UltraVision Large Volume Detection System Anti-Polyvalent, HRP; LabVision Corporation). Briefly, after rehydration, slides were subjected to heat-induced antigen-retrieval with 10 mM citrate buffer at pH=6 for 20 min at 98°C. The slides were washed with PBS and then incubated with 3% hydrogen peroxide for 10 min to inactivate endogenous peroxidases. Another washing step was performed and slides were incubated with UV block solution for 10 min, before incubation with biotinylated primary antibody (anti-lectin 1:500) for 1h at RT. Section were washed with PBS and incubated with streptavidine-peroxidase for 10 min, followed by 3,3'diaminobenzidine (DAB) incubation. All sections were counterstained with Gill-2 hematoxylin. For negative controls, primary antibody incubation step was

replaced with antibodies diluent solution alone. Images were acquired using Leica DM750 at different magnifications 4×, 10× and 40×.

IV-2.5. Statistical analysis

Statistical analysis was performed using Graph Pad Prism Software 5. Differences between testing conditions of the cellular assays were analyzed using non-parametric test (Kruskal-Wallis test) and a $p < 0.05$ was considered significant. Data are presented as mean ± standard deviations.

IV-3. RESULTS

IV-3.1. Cytotoxicity of CF

The effect of CF at different concentrations was evaluated over human endothelial (HPMEC-ST1.6R) and breast cancer (MDA-MB-231) cells lines. CF presented toxic effects for breast cancer cells at lower concentrations (0.5 mg mL^{-1}) than endothelial cells (**Figure IV-2**). Statistically significant differences start to be observed at day 2 for 0.4 mg mL^{-1} regarding cancer cells. For endothelial cells, these differences are just observed at day 2 for 0.75 mg mL^{-1}. Therefore, 0.5 mg mL^{-1} was set as the selective fucoidan concentration to conduct all further assays.

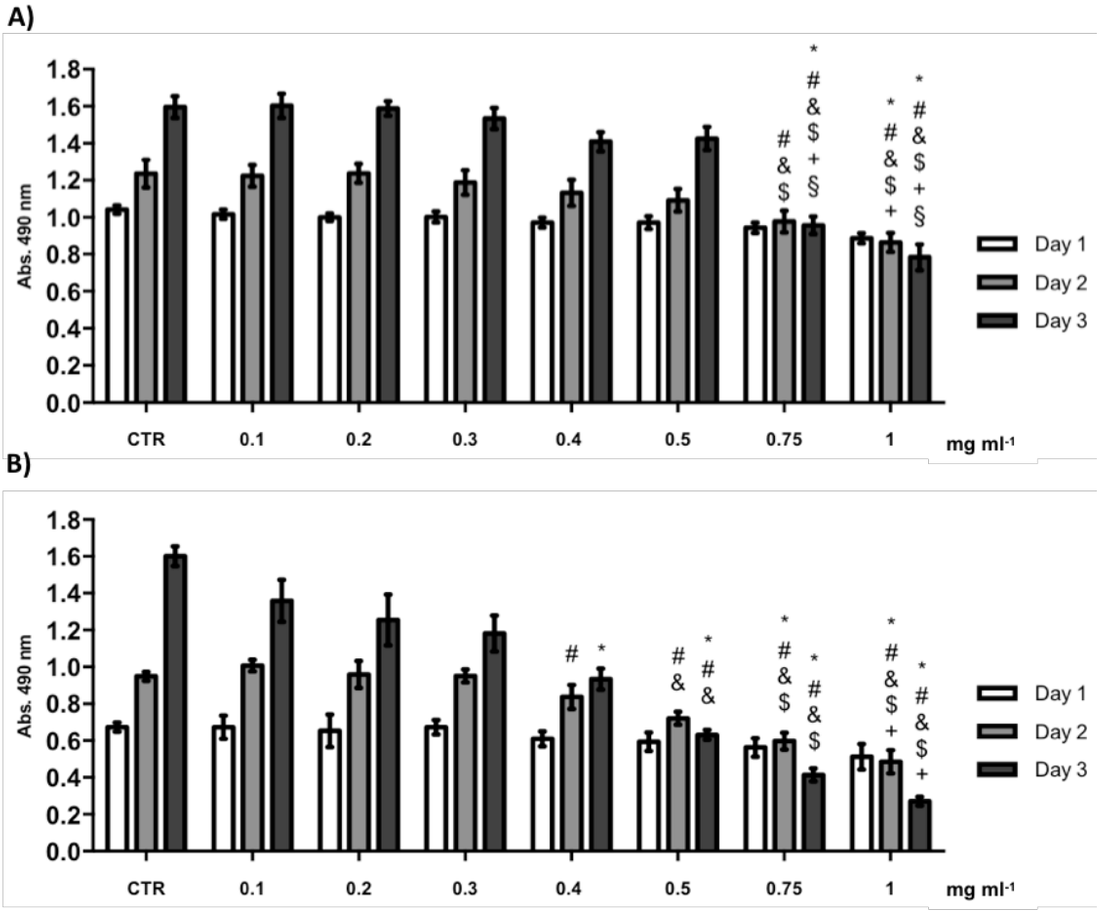

Figure IV-2 Cytotoxicity of CF, at different concentrations and time-points (1, 2 and 3 days), over human cell lines A) HPMEC.ST1.6R and B) MDA-MB-231. Data was considered statistically different if $p < 0.05$. * when compared to CTR; # when compared to 0.1 mg mL−1; & when compared to 0.2 mg mL−1; $ when compared to 0.3 mg mL−1 and + when compared to 0.4 mg mL−1.

IV-3.2. Tube formation assay

IV-3.2.1. Influence of CF over angiogenesis

In TFA I, CF at 0.5 mg mL^{-1} was added at the same time of endothelial cells seeding. In the control conditions without CF, cells adhered on top of matrigel and it was possible to observe the formation of tubular-like structures, after 4h (**Figure IV-3, CTR**). For later time points, these tubular-like structures were even more evident and dense. In the presence of CF (**Figure IV-3, Fucoidan**), endothelial cells aglomerated instead of forming tubular-like structures, even for later time points.

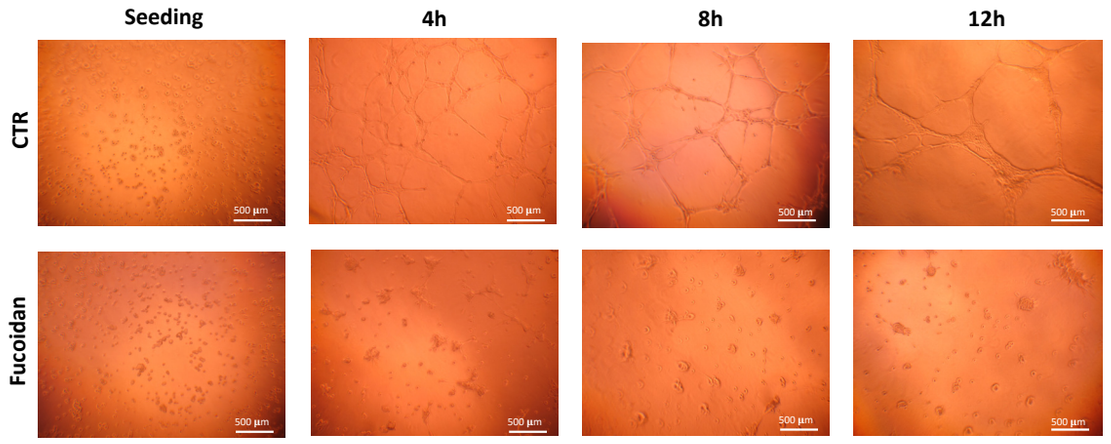

Figure IV-3 Tube formation assay I (TFA I). Photos taken at different time points for both the control and fucoidan conditions. Total magnification 35x.

IV-3.2.2. Influence of CF over an existing vascular network

In another assay (TFA II), CF was only added 4h after endothelial cells seeding, when the formation of the capilary-like structures was already observed (**Figure IV-4 , 4 h**). In control conditions, it was possible to observe the same behavior described in TFA I. The addition of fucoidan, destroyed a pre-formed endothelial network. This behavior started to be observed at 8h, being more evident in the later time points (12h and 16h), where the endothelial network was completely destroyed and cells tended to aglomerate.

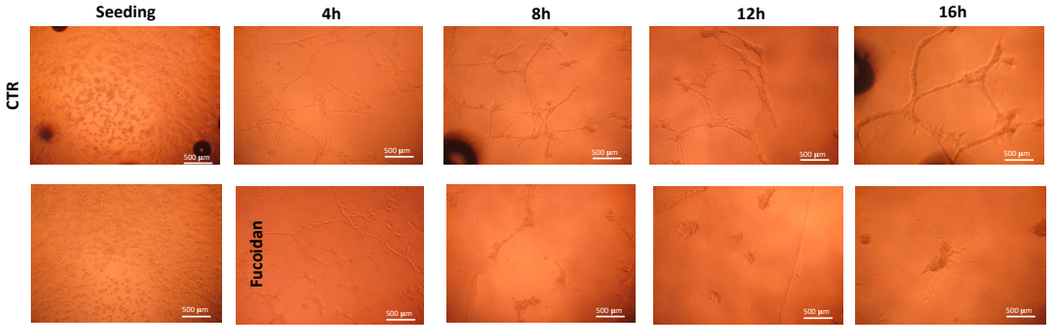

Figure IV-4 Tube formation assay I (TFA I). Photos taken at different time points for both the control and fucoidan conditions. Total magnification 35x.

IV-3.2.3. Secreted VEGF and PDGF

To give a quantitative perspective of TFA assays, secreted VEGF and PDGF were quantified by ELISA. Regarding VEGF quantification, both TFA assays presented similar values (**Figure IV-5 A**). The controls

secreted around 2.88±0.13 pg mL^{-1} and 2.63±0.20 pg mL^{-1}, for TFA I and TFA II, respectively, whereas in the presence of CF, endothelial cells secreted 2.37±0.19 pg mL^{-1} (TFA I) and 2.39±0.37 pg mL^{-1} (TFA II). Although a slightly decrease of VEGF concentration was observed for CF, no statistically significant differences were observed when compared to control conditions. Regarding PDGF quantification, both tube formation assays present statistically significant differences, when comparing control with fucoidan conditions (**Figure IV-5 B**). In TFA I, the controls present values around 0.39±0.09 pg mL^{-1}, whereas samples with CF present values around 0.12±0.03 pg mL^{-1}, indicating a reduction of around 70%. For TFA II, the presence of CF reduced the secretion of PDGF (0.51±0.13 pg mL^{-1}) around 41%, when compared with control conditions (0.30±0.07 pg mL^{-1}). In summary, CF at 0.5 mg mL^{-1} did not significantly reduce VEGF secretion, but significantly affect the secretion of PDGF, when compared to the control conditions (without fucoidan).

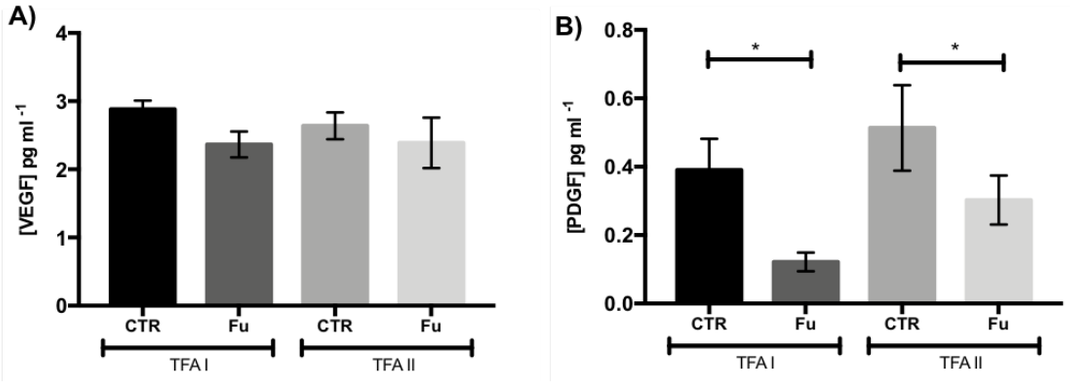

Figure IV-5 Quantification of secreted VEGF A) and PDGF B). Tube formation assay I – TFA I (CF added at cell seeding) and TFA II (CF added 4 h after cell seeding). Data was considered statistically different (*) if $p < 0.05$. The two assays were analyzed separately.

IV-3.3. Influence of CF over angiogenesis *in vivo*

IV-3.3.1. Blood vessel quantification

Following the previous *in-vitro* results, the anti-angiogenic activity of fucoidan was also assessed *in-vivo*, in a CAM assay. For that, the number of blood vessels converging into the study area (the ring) was evaluated 7 days after CF injection (day 17 - end of experiment). **Figure IV-6 A)** presents *in-ovo* images at two different time points: 3 and 7 days after CF injection. The CAM developed as expected along time but no conclusive differences could be observed between conditions with added CF and control. Thus, CAM was retrieved and *ex-ovo* photos, at day 7, were obtained, where fucoidan condition seemed to present a

less vascularized CAM around the site of CF injection (ring). This observation was confirmed by counting the blood vessels of all photos (n=15), CTR condition presented 25.5 ± 3.5 vessels whereas fucoidan condition presented around 22±4.2 vessels. **In Figure IV-6 B)**, it was possible to observe a significant decrease in the number of blood vessels, in the presence of fucoidan, when compared to control condition.

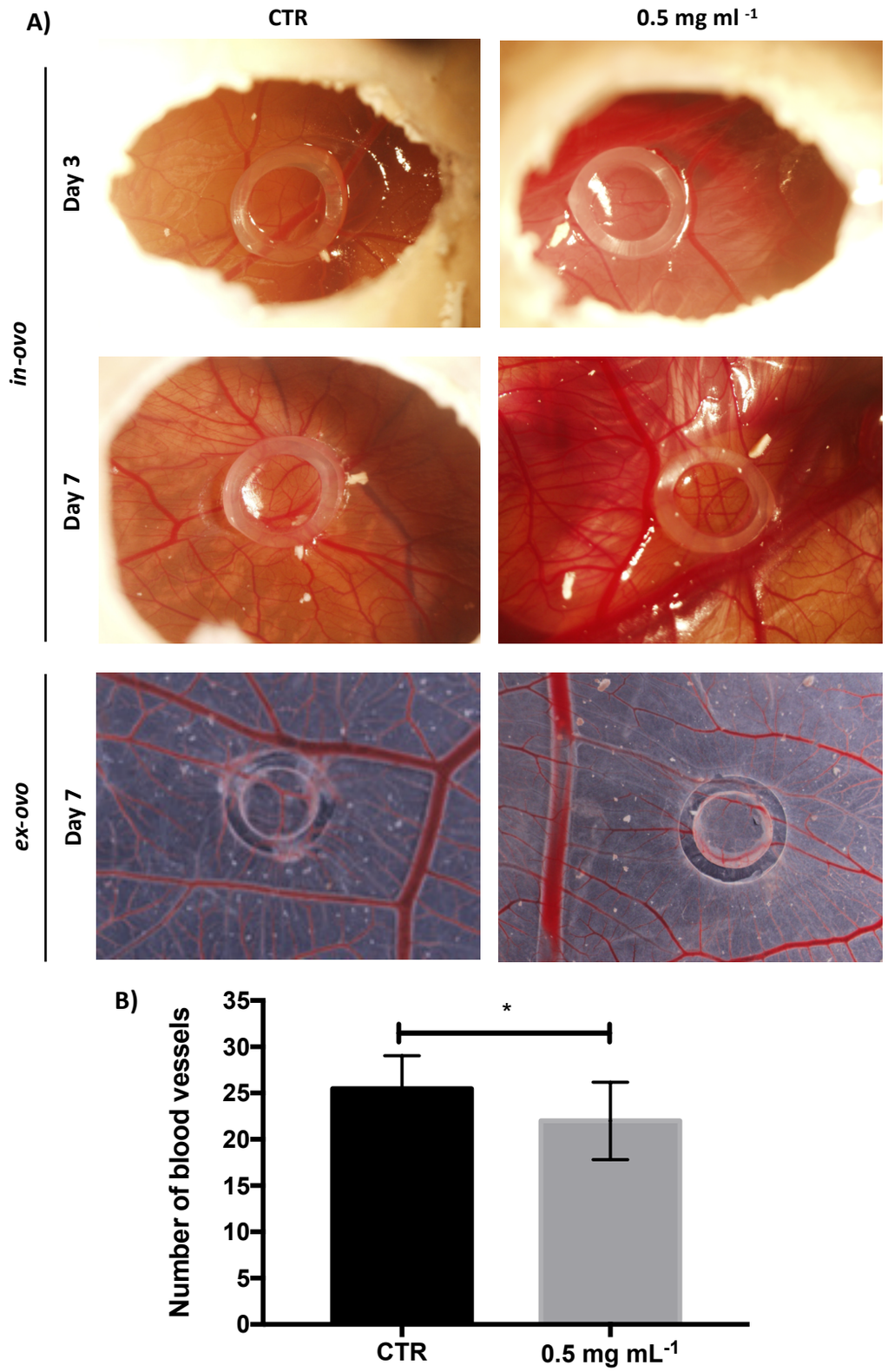

Figure IV-6 CAM assay I. A) In-ovo and ex-ovo photos of the control and fucoidan conditions at different times points – 3 and 7 days – after fucoidan injection. Ex-ovo photos were cropped into 500x500 size photos around the ring, and B) the number of blood vessels

IV-3.3.2. H&E staining and immunohistochemistry

Figure I-7 shows photomicrographs of excised CAM histological sections stained with H&E and SNA-lectin, after 7 days of CF injection. H&E staining allows the observation of the blood vessel morphology present in the CAM. Several microscopic and macroscopic blood vessels could be observed along the CAM in all tested conditions. Blood vessels presented their typical round shape and no morphological differences were observed between the control and fucoidan conditions. Regarding SNA-lectin staining (brown staining – lectins specifically binds to chick endothelial cells), it seems to be less lectins for the fucoidan conditions, than the control condition.

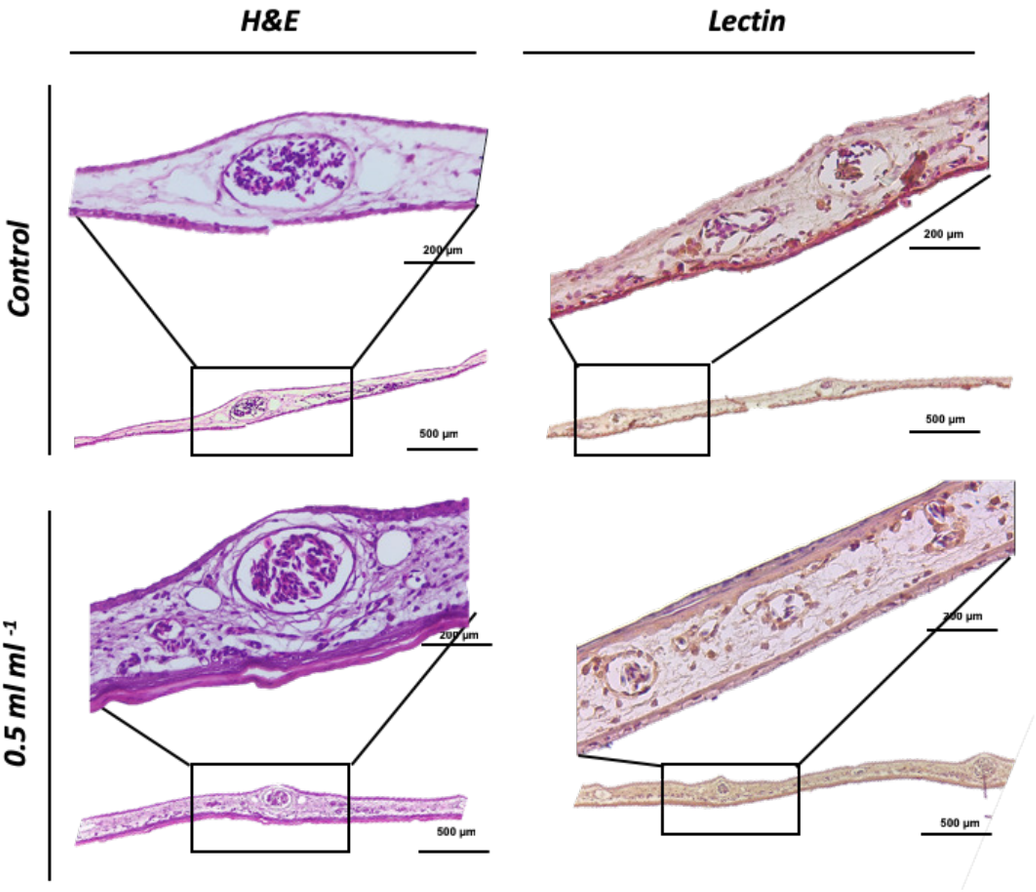

Figure IV-7 Photomicrographs of the excised CAM histological sections, obtained 7 days after FE injection, stained with H&E and immunostained for lectin.

IV-3.4. Influence of CF on the tumor microenvironment

IV-3.4.1. Blood vessel quantification and tumor size

In the CAM II assay, human breast cancer cells were re-suspended in matrigel and onplanted into the chick membrane. **In Figure IV-8 A)**, it is possible to observe the successful development of a tumor mass 4 days after tumor onplantation. The tumor spheroids kept their integrity along the 8 days of experiment. From day 8 *ex-ovo* photos, the area occupied by the tumor was measured and the number of blood vessels was determined as in the previous CAM assay. **Figure IV-8 B)** shows that the number of blood vessels was similar between control and fucoidan conditions. On the other hand, the administration of CF induced a decrease in the tumor area to 2.4±0.5 mm^2 (0.5 mg mL^{-1}) when compared with the control 3.1±0.5 mm^2 (**Figure IV-8 C**).

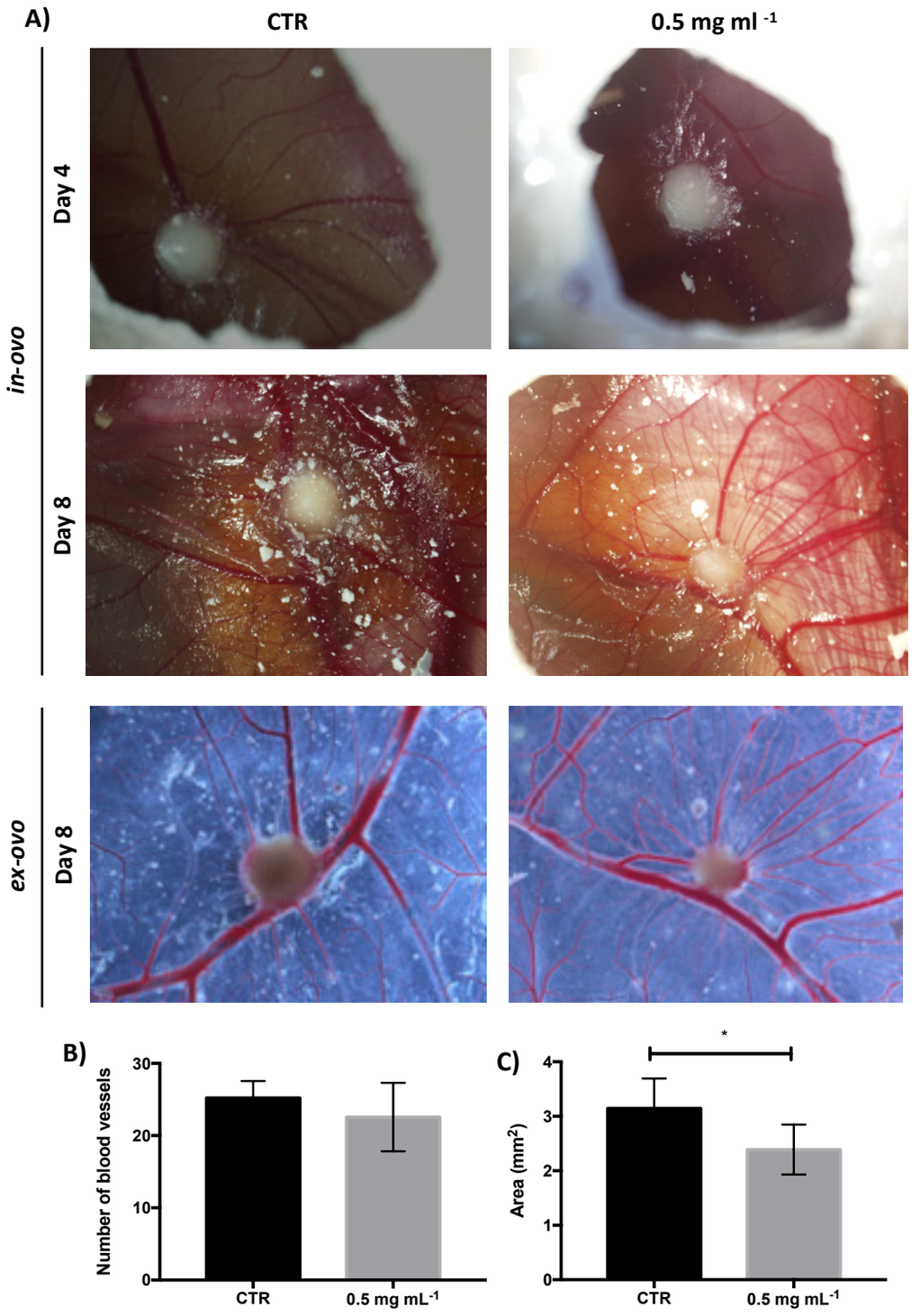

Figure IV-8 CAM assay I. A) *In-ovo* and *ex-ovo* photos of the control and fucoidan conditions at different times points – 4 and 8 days– after tumor onplantation. *Ex-ovo* photos were cropped into 500×500 size photos around the ring, and B) the number of blood vessels was counted and C) the tumor size was measured. Data was considered statistically different (*) if $p < 0.05$.

IV-3.4.2. H&E staining and Lectin immunoexpression

In this CAM assay, the H&E staining and the expression of SNA-lectin was performed as for CAM I. In the H&E staining it was possible to observe the integration of the tumor within the CAM. As expected, most of the blood vessel distribution was observed in the area under the tumor, presenting their typical round morphology (**Figure IV-9 – H&E**). These blood vessels presented a small diameter maybe due to the pressure caused by the presence of the tumor mass. SNA-lectin (**Figure IV-9 – Lectin**) seemed to present some differences when CF was administered into the tumor, showing decreased lectins immunoexpression for the fucoidan conditions tested [33].

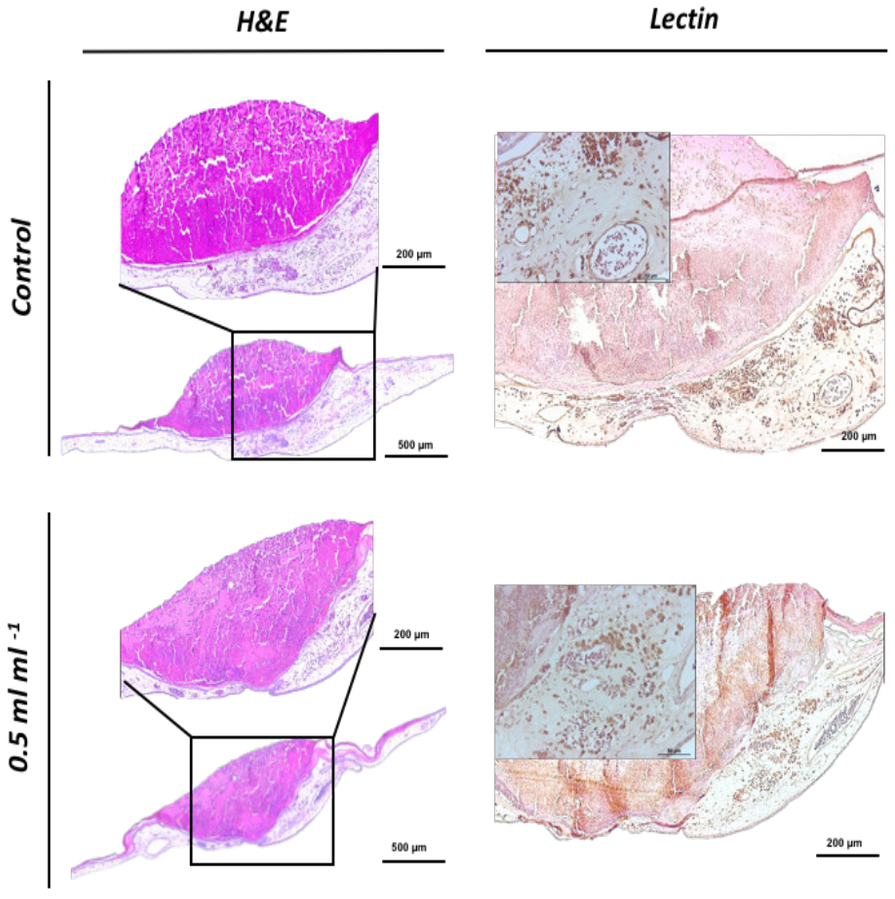

Figure IV-9 Photomicrographs of the excised CAM sections, stained with H&E and immunostained for lectin.

IV-4. DISCUSSION

Fucoidan's potential as an agent for the regulation of angiogenesis has been described in the literature, reporting both pro- and anti-angiogenic properties [19]. To clarify its bioactivity, the cytotoxicity

of a specific CF was evaluated over two different human cells lines, since the main goal of an effective anti-cancer therapy is to induce cancer cells death without affecting normal cells. Accordingly, human breast adenocarcinoma cells (MDA-MB-231) were used as a model of cancer cells. Whereas, human pulmonary microvascular endothelial cells (HPMEC-ST1.6R) were used as model of normal cells due to the context of the present work, namely the role of angiogenesis in the tumor microenvironment/development. In a therapeutic perspective, endothelial cells are the first barrier that fucoidan will face when intravenously injected. From the experimental results, it was possible to observe that, at 0.5 mg mL^{-1}, CF presented toxic effects over breast cancer cells without affecting normal endothelial cells. This is the selective concentration of interest when aiming to develop an effective antitumor strategy, affecting only tumor cells without damaging the surrounding healthy tissues [34]. Knowing that tumors require a vascular network to growth, it is important to study as well the effects of fucoidan over angiogenesis [24, 35]. If exerting an anti-angiogenic effect as hypothesized in the present work, this CF will hamper the formation of that vascular network, limiting tumor progression and thus showing a double anticancer activity.

Different *in vitro* and *in vivo* experimental methods have been developed to study the different steps of angiogenesis, as well as to assess the influence of a certain compound in that process. Tube formation assay is a well-established method to study angiogenesis *in vitro* [36, 37]. In this sense, we evaluated the influence of a selective CF over the formation of tubular-like structures. Results point out that, when CF was administered at the same time of endothelial cells seeding, these cells were no longer capable of forming tubular-like structures, indicating that CF was an inhibitor of angiogenesis *in vitro*. In a different attempt, when CF was only added 4h after endothelial cells seeding, this polysaccharide destroyed the already pre-formed tubular-like network, indicating that CF also inhibited vascularization *in vitro*. This is aligned with Liu *et al.* findings, where fucoidan affects tube formation *in vitro* (HUVEC) by reducing tubular-like structures in a dose dependent manner [23].

The formation of new vascular network requires its initiation by a proangiogenic growth factor, VEGF, and subsequent vessel stabilization by PDGF [1, 3]. VEGF is a potent angiogenic factor, highly expressed by endothelial cells, that is required for cells adhesion, migration, proliferation and survival [38]. Considering the enrolment of these two GFs in the vascular development and blood vessels maturation, their expression was quantified. Although the secretion of VEGF was not statistically different between control and fucoidan conditions, PDGF was significantly lower expressed in the fucoidan conditions for both tube formation assays (TFA I and TFA II). The higher expression of PDGF in the control condition of

TFA II may be related with the fact that CF was added 4h later than in the TFA I. In the presence of this selective CF, endothelial cells were metabolically active and expressing VEGF, despite not being capable of forming mature tubular-like structures (TFA I). This same behavior was also previously reported, showing that the addition of CF resulted in a reduction of angiogenic structures, maintaining cells viability [39]. Furthermore, even when a pre-vascular network is present (TFA II), fucoidan is capable of destroying it. By the combination of these results, the anti-angiogenic potential of this CF was established *in vitro*.

Despite the evidences provided by *in vitro* experiments, *in vivo* assays are considered to be more informative. Among the *in vivo* experiments, the chick embryo chorioallantoic membrane (CAM) assay represents a rapid, simple and cost-effective screening of biomaterials or compounds biocompatibility. The CAM assay has also been established as an experimental system for research in tumor biology. Despite the presented advantages, it also presents some limitations, such as difficulties in distinguishing new capillaries from the existing ones, it is a time restricted experiment, and some unspecific interactions with endogenous factors may affect angiogenesis process. Nevertheless, the CAM assay is a well-established method to easily study the angiogenic potential of different compounds [40-42]. Accordingly, we evaluated the angiogenic potential of CF, for the selective concentration defined *in vitro* (0.5 mg mL^{-1}). Angiogenesis response usually occurs after 72-96 h of a stimulus, but longer periods may be considered. When blood vessels converge towards the onplanted compound and there is an increase in the number of surrounding vessels, it is a signal of neoangiogenesis. Otherwise, when vessels become less dense or disappear around the studied area, it is considered a angiostatic compound [41]. The number of blood vessels around the ring, where CF was injected, was quantified and significantly lower values were observed when compared with the control condition, indicating that fucoidan affects angiogenesis *in-ovo*, corroborating the previous *in vitro* results. A decrease in the number of blood vessels with a sulfated fucoidan was also observed by other researchers [21].

CAM has also been used as a model for tumor microenvironment [43, 44]. In this sense, another CAM assay was conducted with the onplantation of a tumor mass, aiming to study the effect of CF in an *in vivo* tumor microenvironment. In this CAM assay, the development of the tumor is much faster and the tumor xenograft is visible 2-5 days after onplantation, whereas in mammal's models the tumor growth takes between 3 and 6 weeks [41]. Experimental results point out that the number of blood vessels was very similar to the assay without the tumor, although there were no significant differences between the control and fucoidan conditions. The differences between the two assays may be related with the fact that in CAM II, FE is only injected 4 days after tumor onplantation, presenting its activity for an additional 4

days, when compared with CAM I (7 days). We must have in consideration that CF only exerts its biological activity for a relatively short time to expect to see significant differences. The area of the tumor was also quantified 8 days after tumor onplantation (last day of the assay - day 17), in the *ex-ovo* photos. With the local injection of CF, the size of the tumors decreased significantly.

To complement these quantitative results, histological analysis was performed for both CAM I and CAM II. This provides useful qualitative information on blood vessels morphology and specific endothelial marker (SNA-Lectin) expression. Lectins are specific carbohydrate-binding proteins that allows the visualization of the vasculature and the interaction of lectins with endothelial cells is frequently species-specific [33]. Lectins are of great value for the observation of blood vessels, sites of leakage/increased permeability, to identify vascular hierarchies and are also a valuable tool for the isolation of endothelial cells [45, 46]. Microscopically by H&E staining, it was possible to observe the blood vessel distribution along the CAM for all the conditions. Differences between controls and fucoidan conditions are not that clear, for both CAM I and CAM II. Complementarily, the immunohistochemical analysis of endothelial cells of excised CAM revealed the presence of endothelial cells surrounding the blood vessels and the tumor. Despite no significant differences being observed in the number of blood vessels for CAM II, angiogenesis may be impaired because lectin is less expressed in the presence of FE. This observation may be related with a decrease of blood vessel stability, as previously reported in the TFA II, particularly by the lower secretion of PDGF.

IV-5. CONCLUSIONS

It is known that some compounds exert their anticancer activity by limiting angiogenesis, which would hamper tumor progression. A CF at a selective concentration of 0.5 mg ml^{-1} (toxic over cancer cells without affecting normal cells) was able to inhibit and destroy tubular-like structures *in vitro.* Furthermore, CF injected in the CAM compromised angiogenesis *in vivo* by reducing the number of blood vessels. When CF was injected in a CAM onplanted with a tumor, tumor shrinkage was observed. Taken together, these results demonstrate the anti-angiogenic potential of this selective FE both in-vitro and in-vivo. This CF has thus a two-fold anticancer therapeutic potential: having toxic effect over cancer cells and hampering tumor growth by exerting a negative effect on tumor vascularization.

IV-6. ACKNOWLEDGMENTS

This work was developed under the scope of the Structured projects for R&D&I NORTE-01-0145-FEDER-000013, NORTE-01-0145-FEDER-000021 and NORTE-01-0145-FEDER-000023, supported by the Northern Portugal Regional Operational Programme (NORTE 2020), under the Portugal 2020 Partnership Agreement, through the European Regional Development Fund (FEDER), and through the Competitiveness Factors Operational Programme (COMPETE), and by National funds, through the Portuguese Foundation for Science and Technology (FCT), under the scope of the project POCI-01-0145-FEDER-007038. The authors would like also to thank Norte 2020, for financing the PhD scholarship of C.O. "Norte-08-5369-000037" and FCT for the grant of S.G. (SFRH/BPD/117858/2016) and the Investigator grant of A.M. (IF/00376/2014).

IV-7. REFERENCES

[1] R.R. Chen, E.A. Silva, W.W. Yuen, D.J. Mooney, Spatio-temporal VEGF and PDGF delivery patterns blood vessel formation and maturation, Pharm Res 24(2) (2007) 258-64.

[2] P. Carmeliet, R.K. Jain, Molecular mechanisms and clinical applications of angiogenesis, Nature 473(7347) (2011) 298-307.

[3] E. di Tomaso, N. London, D. Fuja, J. Logie, J.A. Tyrrell, W. Kamoun, L.L. Munn, R.K. Jain, PDGF-C induces maturation of blood vessels in a model of glioblastoma and attenuates the response to anti-VEGF treatment, PLoS One 4(4) (2009) e5123.

[4] D.S. Winlaw, Angiogenesis in the pathobiology and treatment of vascular and malignant diseases, Ann Thorac Surg 64(4) (1997) 1204-11.

[5] M. Klagsbrun, P.A. D'Amore, Regulators of angiogenesis, Annu Rev Physiol 53 (1991) 217-39.

[6] N.J. Nelson, Inhibitors of angiogenesis enter phase III testing, J Natl Cancer Inst 90(13) (1998) 960-3.

[7] P. Carmeliet, Angiogenesis in life, disease and medicine, Nature 438(7070) (2005) 932-6.

[8] J. Folkman, Tumor angiogensis: role in regulation of tumor growth, Symp Soc Dev Biol 30(0) (1974) 43-52.

[9] N. Petrovic, Targeting Angiogenesis in Cancer Treatments: Where do we Stand?, J Pharm Pharm Sci 19(2) (2016) 226-38.

[10] F.Z. Shahneh, B. Baradaran, F. Zamani, L. Aghebati-Maleki, Tumor angiogenesis and anti-angiogenic therapies, Hum Antibodies 22(1-2) (2013) 15-9.

[11] Y. Kubota, Tumor angiogenesis and anti-angiogenic therapy, Keio J Med 61(2) (2012) 47-56.

[12] F. Azam, S. Mehta, A.L. Harris, Mechanisms of resistance to antiangiogenesis therapy, Eur J Cancer 46(8) (2010) 1323-32.

[13] W.H. Yang, J. Xu, J.B. Mu, J. Xie, Revision of the concept of anti-angiogenesis and its applications in tumor treatment, Chronic Dis Transl Med 3(1) (2017) 33-40.

[14] M.K. Shanmugam, S. Warrier, A.P. Kumar, G. Sethi, F. Arfuso, Potential Role of Natural Compounds as Anti-Angiogenic Agents in Cancer, Curr Vasc Pharmacol 15(6) (2017) 503-519.

[15] M.T. Ale, J.D. Mikkelsen, A.S. Meyer, Important Determinants for Fucoidan Bioactivity: A Critical Review of Structure-Function Relations and Extraction Methods for Fucose-Containing Sulfated Polysaccharides from Brown Seaweeds, Marine Drugs 9(10) (2011) 2106-2130.

[16] J.H. Fitton, D.N. Stringer, S.S. Karpiniec, Therapies from Fucoidan: An Update, Mar Drugs 13(9) (2015) 5920-46.

[17] F. Atashrazm, R.M. Lowenthal, G.M. Woods, A.F. Holloway, J.L. Dickinson, Fucoidan and Cancer: A Multifunctional Molecule with Anti-Tumor Potential, Marine Drugs 13(4) (2015) 2327-2346.

[18] C. Oliveira, A.S. Ferreira, R. Novoa-Carballal, C. Nunes, I. Pashkuleva, N.M. Neves, M.A. Coimbra, R.L. Reis, A. Martins, T.H. Silva, The Key Role of Sulfation and Branching on Fucoidan Antitumor Activity, Macromol Biosci 17(5) (2017) 1600340.

[19] N.E. Ustyuzhanina, M.I. Bilan, N.A. Ushakova, A.I. Usov, M.V. Kiselevskiy, N.E. Nifantiev, Fucoidans: pro- or antiangiogenic agents?, Glycobiology 24(12) (2014) 1265-74.

[20] F. Wang, H. Schmidt, D. Pavleska, T. Wermann, A. Seekamp, S. Fuchs, Crude Fucoidan Extracts Impair Angiogenesis in Models Relevant for Bone Regeneration and Osteosarcoma via Reduction of VEGF and SDF-1, Mar Drugs 15(6) (2017).

[21] H. Chen, Q. Cong, Z. Du, W. Liao, L. Zhang, Y. Yao, K. Ding, Sulfated fucoidan FP08S2 inhibits lung cancer cell growth in vivo by disrupting angiogenesis via targeting VEGFR2/VEGF and blocking VEGFR2/Erk/VEGF signaling, Cancer Lett 382(1) (2016) 44-52.

[22] M.C. Chen, W.L. Hsu, P.A. Hwang, T.C. Chou, Low Molecular Weight Fucoidan Inhibits Tumor Angiogenesis through Downregulation of HIF-1/VEGF Signaling under Hypoxia, Mar Drugs 13(7) (2015) 4436-51.

[23] F. Liu, G. Luo, Q. Xiao, L. Chen, X. Luo, J. Lv, L. Chen, Fucoidan inhibits angiogenesis induced by multiple myeloma cells, Oncol Rep 36(4) (2016) 1963-72.

[24] X. Rui, H.F. Pan, S.L. Shao, X.M. Xu, Anti-tumor and anti-angiogenic effects of Fucoidan on prostate cancer: possible JAK-STAT3 pathway, BMC Complement Altern Med 17(1) (2017) 378.

[25] H.Y. Shen, L.Z. Li, K.C. Xue, D.D. Hu, Y.J. Gao, Antitumor activity of fucoidan in anaplastic thyroid cancer via apoptosis and anti-angiogenesis, Mol Med Rep 15(5) (2017) 2620-2624.

[26] M. Xue, Y. Ge, J. Zhang, Q. Wang, L. Hou, Y. Liu, L. Sun, Q. Li, Anticancer properties and mechanisms of fucoidan on mouse breast cancer in vitro and in vivo, PLoS One 7(8) (2012) e43483.

[27] C. Zhu, R. Cao, S.X. Zhang, Y.N. Man, X.Z. Wu, Fucoidan inhibits the growth of hepatocellular carcinoma independent of angiogenesis, Evid Based Complement Alternat Med 2013 (2013) 692549.

[28] M. Dithmer, A.M. Kirsch, E. Richert, S. Fuchs, F. Wang, H. Schmidt, S.E. Coupland, J. Roider, A. Klettner, Fucoidan Does Not Exert Anti-Tumorigenic Effects on Uveal Melanoma Cell Lines, Mar Drugs 15(7) (2017).

[29] C. Boisson-Vidal, F. Zemani, G. Caligiuri, I. Galy-Fauroux, S. Colliec-Jouault, D. Helley, A.M. Fischer, Neoangiogenesis induced by progenitor endothelial cells: effect of fucoidan from marine algae, Cardiovasc Hematol Agents Med Chem 5(1) (2007) 67-77.

[30] B.S. Kim, S.S. Yang, H.K. You, H.I. Shin, J. Lee, Fucoidan-induced osteogenic differentiation promotes angiogenesis by inducing vascular endothelial growth factor secretion and accelerates bone repair, Journal of tissue engineering and regenerative medicine 12(3) (2018) e1311-e1324.

[31] M.T. Ale, J.D. Mikkelsen, A.S. Meyer, Important determinants for fucoidan bioactivity: a critical review of structure-function relations and extraction methods for fucose-containing sulfated polysaccharides from brown seaweeds, Mar Drugs 9(10) (2011) 2106-30.

[32] C. Oliveira, A.S. Ferreira, R. Novoa-Carballal, C. Nunes, I. Pashkuleva, N.M. Neves, M.A. Coimbra, R.L. Reis, A. Martins, T.H. Silva, The Key Role of Sulfation and Branching on Fucoidan Antitumor Activity, Macromolecular Bioscience 17(5) (2017) 1600340.

[33] S.M. Jilani, T.J. Murphy, S.N. Thai, A. Eichmann, J.A. Alva, M.L. Iruela-Arispe, Selective binding of lectins to embryonic chicken vasculature, J Histochem Cytochem 51(5) (2003) 597-604.

[34] D. Anastasiou, Tumour microenvironment factors shaping the cancer metabolism landscape, Br J Cancer 116(3) (2017) 277-286.

[35] J. Folkman, Proceedings: Tumor angiogenesis factor, Cancer research 34(8) (1974) 2109-13.

[36] R.E. Unger, V. Krump-Konvalinkova, K. Peters, C.J. Kirkpatrick, In vitro expression of the endothelial phenotype: comparative study of primary isolated cells and cell lines, including the novel cell line HPMEC-ST1.6R, Microvasc Res 64(3) (2002) 384-97.

[37] K.L. DeCicco-Skinner, G.H. Henry, C. Cataisson, T. Tabib, J.C. Gwilliam, N.J. Watson, E.M. Bullwinkle, L. Falkenburg, R.C. O'Neill, A. Morin, J.S. Wiest, Endothelial cell tube formation assay for the in vitro study of angiogenesis, J Vis Exp (91) (2014) e51312.

[38] N. Ferrara, H.P. Gerber, J. LeCouter, The biology of VEGF and its receptors, Nat Med 9(6) (2003) 669-76.

[39] M. Dithmer, S. Fuchs, Y. Shi, H. Schmidt, E. Richert, J. Roider, A. Klettner, Fucoidan reduces secretion and expression of vascular endothelial growth factor in the retinal pigment epithelium and reduces angiogenesis in vitro, PloS one 9(2) (2014) e89150-e89150.

[40] C. Storgard, D. Mikolon, D.G. Stupack, Angiogenesis assays in the chick CAM, Methods Mol Biol 294 (2005) 123-36.

[41] D. Ribatti, The chick embryo chorioallantoic membrane (CAM). A multifaceted experimental model, Mech Dev 141 (2016) 70-7.

[42] D. Ribatti, Chick embryo chorioallantoic membrane as a useful tool to study angiogenesis, Int Rev Cell Mol Biol 270 (2008) 181-224.

[43] O. Martinho, S. Granja, T. Jaraquemada, C. Caeiro, V. Miranda-Goncalves, M. Honavar, P. Costa, M. Damasceno, M.R. Rosner, J.M. Lopes, R.M. Reis, Downregulation of RKIP is associated with poor outcome and malignant progression in gliomas, PLoS One 7(1) (2012) e30769.

[44] D. Ribatti, The chick embryo chorioallantoic membrane as a model for tumor biology, Exp Cell Res 328(2) (2014) 314-24.

[45] M.G. Gabrielli, G. Materazzi, A.M. Bondi, G. Menghi, Developmental expression of glycocomponents in the chick chorioallantoic membrane, Anat Embryol (Berl) 207(1) (2003) 63-71.

[46] C.B.S. Henry, D.O. DeFouw, Differential Lectin Binding to Microvascular Endothelial Glycoconjugates during Normal Angiogenesis in the Chick Chorioallantoic Membrane, Microvascular Research 49(2) (1995) 201-211.

Chapter V

Effective fucoidan-based therapeutic strategies to treat melanoma

Chapter V

Effective fucoidan-based therapeutic strategies to treat melanoma §

ABSTRACT

Melanoma is one of the rarest but most aggressive skin cancer. The current limitations of cancer treatments lead to the need to develop alternative strategies that may be more efficient. Herein, we propose the use of a marine-origin polymer, fucoidan as a natural bioactive agent against melanoma. Fucoidan in its soluble form presented increased cytotoxicity over melanoma cells when comparing with the toxic effects over human dermal fibroblasts and keratinocytes. Fucoidan was also immobilized at the surface of electrospun nanofiber mesh (NFM) at a maximum concentration of 1.2 mg ml $^{-1}$ (NFM_Fu), as confirmed by XPS, envisioning the development of a therapeutic patch. Contact angle measurement showed that NFM_Fu is more hydrophilic than NFM, presenting a contact angle of 32°, lower than the 108° of the control condition. As for soluble fucoidan, NFM_Fu was able to reduce human melanoma cells viability by 50% without affecting dermal fibroblasts and keratinocytes. Taken together, this strategy may set the basis for a valuable approach to treat melanoma.

§ This chapter is based on the following publication:

Oliveira C., Soares A, I., Neves N. M., Reis R. L., Marques A. P., Silva T. H., Martins A. *Effective fucoidan-based therapeutic strategies to treat melanoma.* (Submitted)

V-1. INTRODUCTION

Current treatment modalities for cancer do not achieve the ideal therapeutic outcomes due to severe side effects experienced by cancer patients [1]. In this sense, alternative approaches are required and, between the possibilities, there is an increasing interest in the use of natural compounds from marine resources as biologically active products. Brown algae are a source of polysaccharides that may present several biological responses [2-4]. Among these marine origin materials, fucoidan has attracted enormous interest in the last recent years [5]. Fucoidan is a polysaccharide consisting in a sequence of sulfated fucose residues, together with other sugars, namely uronic acids, with chemical structure depending on the species and its life cycle, and extraction parameters [6]. Different physicochemical properties such as molecular weight, carbohydrates composition, sulfation degree and pattern along fucoidan backbone have been related with its biological activities [6-8], such as antitumor, anti-angiogenic and anti-inflammatory [5, 9]. Regarding particularly its antitumor activity, fucoidan has been recognized as a potential antitumor agent in different types of cancer like breast, lung, colon and melanoma [10-14].

Melanoma is a relatively rare form of cancer, representing about 1% of all skin tumours but is the most aggressive and deadliest form of skin cancer, having a very poor prognosis when it becomes metastatic [15-17]. Risk factors for melanoma include sunburns during childhood, genetic family history and intermittent exposure to strong sunlight [18]. Current treatment modalities may be surgical resection, chemotherapy, immunotherapy and targeted therapy, depending on the characteristics of the tumour (size, site and genetic profile) [19, 20]. To improve survival rates, the combination of different therapies is often recommended. The lack of specificity to tumour cells is one of the major limitations of current therapies that may result in adverse effects and reduced efficiency [21].

Trying to overcome these limitations, the need for testing alternative strategies and compounds offers interesting possibilities [22]. Fucoidan has been reported to inhibit melanoma development and progression namely in its soluble form. Crude commercial fucoidan extracts from *Fucus vesiculosus* and *Sargassum sp*. showed that despite the demonstrated cell growth inhibition at low dosages, both extracts presented very similar cytotoxic profiles over melanoma cells [23]. In another attempt, similar extracts were studied, with a comparable anti-proliferative trend, being crude commercial fucoidan more cytotoxic than the extracted fucoidan, for higher doses [24]. It was also demonstrated that fucoidan reduced the proliferation of melanoma cells and melanin production in a dose-dependent manner, producing alterations in cells morphology [25]. The antitumor activity and the relation with the chemical features of fucoidan extracted from *Undaria pinnatifida* and *Fucus evanescens* was evaluated over different human

cancer cell lines, namely colon, breast and melanoma [13]. No cytotoxic effects were observed over a non-cancer mouse epidermal cell line, whereas more pronounced growth inhibition was observed for breast and melanoma cells lines. A recent study evaluated the toxicity of fucoidan from *Fucus vesiculosus* over B16 murine melanoma cells, showing an inhibition of melanoma cells growth by regulating specific proteins/enzymes expression levels [14]. However, as previously reported by our group, not all fucoidan extracts present this interesting and promising antitumor activity, relating its biological activity with its chemical structure [7, 26]. In fact, despite the reports of cytotoxicity of different fucoidan extracts over melanoma cells, another commercially available fucoidan from *Fucus vesiculosus* was evaluated over five different uveal melanoma cells lines, not showing anti-tumorigenic effects [27].

In this study, we evaluate the toxicity of soluble fucoidan over human melanoma cells and non-tumor dermal fibroblasts and keratinocytes as models of the main cell types characterizing the tumor microenvironment. Additionally, we propose an alternative approach to treat melanoma by developing a tailored nanofiber mesh functionalized with fucoidan (NFM_Fu), aimed to be used as a skin patch to treat melanoma in a more local, precise and effective way, as well as a complementary treatment after tumor excision.

V-2. MATERIALS AND METHODS

V-2.1. Materials

Polycaprolactone (PCL; batch number: MKBP7389V; Mw = 70 000–90 000), chloroform, N,N-dimethylformamide (DMF), 1,6-hexanediamine (HMD) and fucoidan from *Fucus vesiculosus* (Fu; batch number: SLBP3196V; Mw = 107 800) were purchased from Sigma-Aldrich and used as received.

V-2.2. Production of Nanofibrous Meshes

A 15% (w/v) PCL solution was prepared with an organic solvent mixture of chloroform and DMF at a 7:3 ratio. The PCL solution was electrospun by applying a voltage of 11.1 kV, a needle tip to ground collector distance of 18 cm, and a flow rate of 1 mL h^{-1}. After the complete processing of 1 mL of PCL solution, the nanofibrous mesh (NFM) was allowed to dry for 1 day [28]. This processed NFMs were cut into samples of 1 × 1 cm^2 for further assays.

V-2.3. Ultraviolet–Ozone Irradiation and Aminolysis

For the activation of the NFM, an ultraviolet–ozone (UV–ozone) cleaner system was used (ProCleaner 220, Bioforce Nanoscience). Both sides of the electrospun NFMs were exposed for 90 seconds to UV-ozone irradiation. After this surface activation, amine groups ($-NH_2$) were inserted at the surface of NFM by immersion in a 1 M HMD solution for 1 h at 37 °C. Finally the functionalized NFM were washed 3x with PBS [29].

V-2.4. Fucoidan immobilization of NFM

Fucoidan was dissolved in 0.1 M NaCl at different concentrations (Fu 2.5; Fu 5; Fu 7.5 and Fu 10 mg mL^{-1}) and 200 µl of each solution was added over functionalized NFM in a 24 well-plate. This reaction was performed during 8h and, after that, the solutions were removed and the biofunctionalized NFM were left to dry overnight. In the following day, NFM were washed twice. All steps were performed under sterile conditions.

V-2.5. Quantification of immobilized fucoidan - Toluidine Blue Assay

Toluidine Blue (TBO) was used to quantify the amount of fucoidan immobilized into each NFM [30]. Each sample was immersed in 500 µL of TBO solution (0.1 M HCl, 20 mg NaCl, and 4 mg toluidine blue O chloride) for 4 h at room temperature. The TBO solution was removed and the biofunctionalized NFMs were washed until all unreacted TBO solution was removed. Afterwards, the biofunctionalized NFMs were immersed in 500 µL of a solution containing 0.1M NaCl and ethanol (1:4) for complete decoloration. The amount of TBO was assessed by measuring the absorbance of the supernatant at 530 nm using a microplate reader. The amount of fucoidan immobilized at the surface of each NFM was calculated from a standard curve established with fucoidan solutions at different concentrations (Fu 2.5; Fu 5; Fu 7.5 and Fu 10 mg mL^{-1}). In this sense, after incubating fucoidan with TBO, the solutions were centrifuged and the unbound TBO was removed. The pellet was then resuspended with the above mentioned 0.1M NaCl and ethanol solution and read at 530 nm. Each condition was read in triplicate.

V-2.6. Contact angle

Surface hydrophilicity of NFM and NFM_Fu was measured as the static contact angle of a standard liquid (ultra-pure water, 3 μL), at room temperature, using a Contact Angle Equipment (OCA 15plus equipment, Germany and SCA-20 software). During every determination, a motor driven syringe was used to deposit a drop of liquid over the NFM surface. Measurements were recorded for each sample and the determinations were performed in triplicate.

V-2.7. XPS analysis

Analysis of the samples was performed using a Kratos Axis-Supra instrument controlled with ESCApe software. Due to the non-conductive nature of the samples it was necessary to use a co-axial electron neutralizer to minimize surface charging. The XPS measurements were carried out using monochromatic Al-Kα radiation (1486.6 eV). Photoelectrons were collected from a take-off angle of 90° relative to the sample surface. The measurement was done in a Constant Analyser Energy mode (CAE) with a 160 eV pass energy and 15 mA of emission current for survey spectra and 40 eV pass energy for high resolution spectra, also using an emission current of 15 mA. Charge referencing was done by setting the lower binding energy C1s photo peak at 285.0 eV C1s hydrocarbon peak [31]. The chemical composition of the samples was examined by XPS surface measurements. The C1s, O1s, S2p and survey spectra were recorded using a Kratos Axis-Supra instrument. The residual vacuum in the X-Ray analysis chamber was maintained at around $4.5x10^{8}$ torr. The samples were fixed to the sample holder with double sided carbon tape.

V-2.8. Biological assays

V-2.8.1. Cell Culture

Human melanoma cells (WM-115 cell line, ATCC) were cultured in Eagle's Minimum Essential Medium (EMEM 30-2003, ATCC), supplemented with 10% FBS (Alfagene), 1% pen/strep (100 U/100 μg mL^{-1}; Life Technologies) and incubated at 37 °C in a humidified 5% CO_2 atmosphere. Human dermal fibroblasts (hDFs, Gibco) were cultured in Medium 106 (Gibco) supplemented with 10% FBS (Alfagene), Pen/Strep (100 U/100 g mL^{-1}; Life Technologies) and 2% Low Serum Growth Supplement (Life Technologies). Human keratinocytes (hKCs) were isolated as previously published by our group [32].

hKCs were cultured in Keratinocyte-SFM (Life technologies) supplemented with 1% Pen/Strep (100 U/100 g mL^{-1}; Life Technologies). The medium was changed every two days until cells reached confluence.

V-2.8.2. Cell seeding for soluble fucoidan test

Melanoma and normal skin cells were cultured at a density of 15 000 cells and were cultured in 24 well-plates. The cells were left to adhere for 4h and, after that, fucoidan extracts were added to adherent cells. Fucoidan extracts were dissolved in the corresponding culture medium at different concentrations (i.e. 0.25, 0.5, 0.75 and 1 mg mL^{-1}). For all the assays a positive control was performed without fucoidan. Each experimental condition was tested in triplicate and three independent assays were performed.

V-2.8.3. Cell seeding on top of NFM

Cell seeding was performed onto fucoidan immobilized electrospun NFMs (NFM_Fu) by dropping a 50 µL cell suspension containing 50 000 cells per NFM_Fu. Cells were left to adhere for 4h. before culture medium was added. NFMs subjected to surface activation, aminolysis, but without fucoidan immobilization were used as control (NFM_CTR). After 1, 3 and 7 days of culture, samples were collected for cell viability assay and SEM observation. Triplicates of each condition were used in three independent assays (n=3).

V-2.8.4. Viability assays

The metabolic activity was determined by the MTS assay (CellTiter 96 AQueous One Solution, Promega). Briefly, at days 1, 3 and 7, the culture medium was removed and the samples were rinsed with sterile PBS. A mixture of culture medium and MTS reagent (5:1 ratio) was added to each condition as well as to the negative control comprising no cells. Samples were left to incubate for 3 h at 37 °C in a humidified 5% CO2 atmosphere. Thereafter, the absorbance of the MTS reaction medium from each sample was read in triplicate at 490 nm (Synergy HT, BioTEK).

V-2.8.5. Scanning Electron Microscopy analysis

The morphology and distribution of cells seeded on top of the NFM_Fu or NFM_CTR was analyzed by Scanning Electron Microscopy (SEM). At each time point (1, 3 and 7 days), samples were collected and fixed with 2.5% glutaraldehyde. After fixation, samples were washed with PBS and dehydrated with increasing concentrations of ethanol, until 100% was reached. Samples were then left to dry overnight. In the following day, all samples were vacuum-coated with platinum mixture and observed at the SEM (JSM-6010 LV, JEOL, Japan). Photographs at x150 and x1000 magnifications were obtained.

V-2.9. Statistical Analysis

Statistical analysis was performed using Graph Pad Prism Software. Differences between the testing conditions were analyzed using nonparametric test (Kruskal–Wallis test), since data did not follow a normal distribution and a $p < 0.05$ was considered significant. Data are presented as mean ± standard deviations.

V-3. RESULTS

V-3.1. Cytotoxicity effects of soluble fucoidan over human melanoma, keratinocytes and dermal fibroblasts

The toxicity of fucoidan over melanoma cells started to be observed at day 1 for concentrations above 0.5 mg mL^{-1}. At day 3, melanoma cells viability reached values below 20% for those fucoidan concentrations (**Figure V-1 A**). Regarding noncancerous cells, namely keratinocytes, fucoidan presented significant toxicity at day 2 for 0.25 mg mL^{-1} and above, presenting a toxicity between 40-55% at day 3 when compared with the CTR, being dose-independent (**Figure V-1 B**). For dermal fibroblasts, fucoidan presented significant cytotoxicity for day 2 and 3, when comparing the different concentrations with the control, presenting a maximum toxicity around 25-30%, which was also independent of the dosage (**Figure V-1 C**).

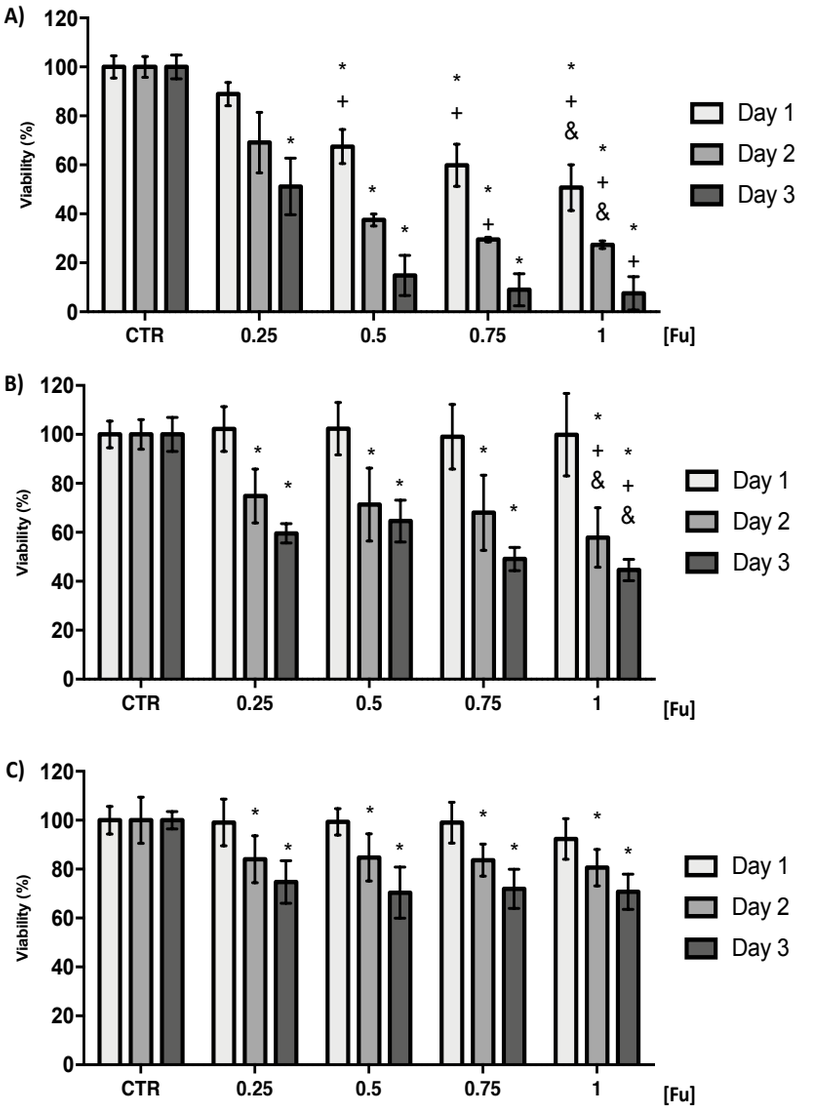

Figure V-1 Viability of human melanoma cells (WM-115 cell line) (A), human keratinocytes (B) and human dermal fibroblasts (C). Data was considered statistically different if $p < 0.05$. * indicates significant differences when compared to CTR; +, when compared to 0.25 mg mL^{-1}, and & when compared to 0.5 mg mL^{-1}.

V-3.2. Quantification of fucoidan immobilized on NFM

Different concentrations of fucoidan were immobilized at the surface of NFM until the saturation concentration was reached (10 mg mL^{-1}, according to the manufacture information). After optimizing a standard curve, the different concentrations were calculated and it was possible to observe that by increasing the initial concentration of fucoidan, higher amounts are immobilized. The maximum immobilization capacity was around 1.2 mg mL^{-1} for Fu10, twice the concentration of Fu2.5 with a minimum immobilization of around 0.6 mg mL^{-1} (**Figure V-2 A**). the lower concentrations Fu5 and Fu2.5

are the ones with higher immobilization percentages when compared to the initial concentration, 16% and 26% respectively. Fu10 and Fu7.5 have similar immobilization percentages of around 12%. Nevertheless, these are the two concentrations with more fucoidan immobilized on the NFM (Fu 7.5 – 0.9 mg ml^{-1}). In **Figure V-2 B**) It is possible to confirm the presence of fucoidan by observing the color change of the NFMs. Fucoidan in solution presents a light brown color and the membranes with fucoidan are more yellowish than the controls, that present its original white color. After toluidine blue staining (**Figure V-2 C**) it is clear that the NFMS that contain fucoidan are purple, whereas the control is not stained.

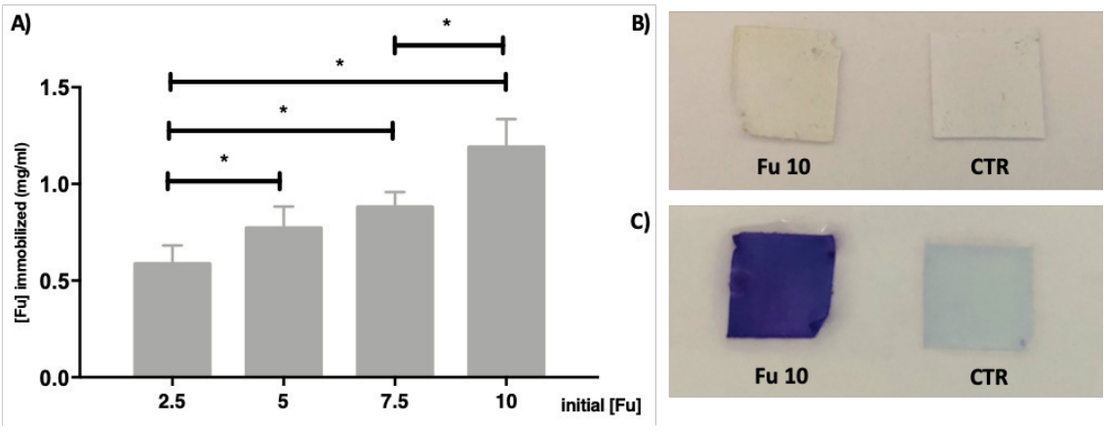

Figure V-2 Quantification of immobilized fucoidan on the NFMs A). Change of colour after fucoidan immobilization B) and after Toluidine Blue assay C).

V-3.3. Characterization of bare and fucoidan-functionalized NFM

V-3.3.1. Contact Angle

The hydrophilicity of NFM with or without immobilized fucoidan was determined by the water contact angle. In the table from **Figure V-3**, it is possible to observe that by increasing the concentration of immobilized fucoidan, NFMs presented a lower contact angle, being more hydrophilic. Electrospun NFMs without fucoidan presented a water contact angle of 121±8°. On the other hand, NFMs with immobilized fucoidan (Fu10) were much more hydrophilic, presenting a water contact angle of 36±8°.

CONDITION	CTR	Fu 2.5	Fu 5	Fu 7.5	Fu 10
CONTACT ANGLE	121± 8°	91± 11°	48± 9°	42± 9°	36± 8°

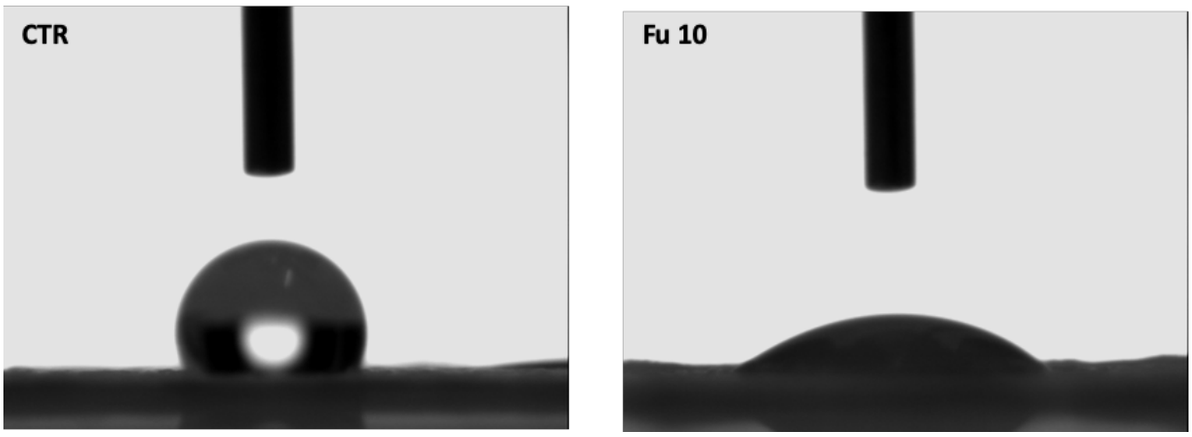

Figure V-3 Water contact angle measurements for the CTR NFM and the different concentrations of immobilized fucoidan. Representative images for CTR and Fu10.

V-3.3.2. XPS analysis

XPS was used to analyse the surface chemistry of the different NFMs with or without immobilized fucoidan. From the quantitative analysis (**Table V-1**) it is possible to observe that carbon and oxygen were present in all the nanofiber meshes with immobilized fucoidan, as well as in the control (without fucoidan), as expected since both elements are constituents of PCL and fucoidan chemical structure. With increasing fucoidan concentration on the solutions used for the functionalization of NFMs, there was a decrease in the atomic concentration of carbon and an increase of oxygen and particularly of sulphur, originated from the sulphate groups present on immobilized fucoidan.

Table V-1 Elemental quantitative analysis of the surface of NFMs functionalized with different fucoidan concentrations.

mg ml $^{-1}$		Atomic conc. [%]	Error [%]	Mass conc. [%]	Error [%]
CTR	S 2p	-	-	-	-
	O 1s	24.03	0.38	29.65	0.44
	C 1s	75.97	0.38	70.35	0.44
Fu 2.5	O 1s	25.29	0.38	30.90	0.43
	S 2p	0.39	0.05	0.95	0.13
	C 1s	74.32	0.38	68.15	0.44
Fu 5	O 1s	28.98	0.49	34.89	0.54
	S 2p	0.60	0.07	1.44	0.18
	C 1s	70.43	0.50	63.66	0.56
Fu 7.5	O 1s	28.91	0.55	34.57	0.61
	S 2p	1.07	0.09	2.56	0.22
	C 1s	70.02	0.57	62.86	0.63
Fu 10	O 1s	36.14	0.50	42.10	0.53
	S 2p	1.41	0.09	3.28	0.21
	C 1s	62.46	0.51	54.62	0.54

A general spectrum of the control condition (**Figure V-4 A**) indicates the presence of two main peaks for carbon (291.40 eV) and oxygen (537.12 eV). For Fu10 (**Figure V-4 B**), three main peaks are detected: carbon (297.70 eV), oxygen (544.47) and sulphur (176.0). After fucoidan immobilization, a peak starting

at 177.95 eV and ending at 167.51 eV appears, which is attributed to the sulphur element (S2p) from the fucoidan chain, confirming fucoidan immobilization (**Figure V-4 C**).

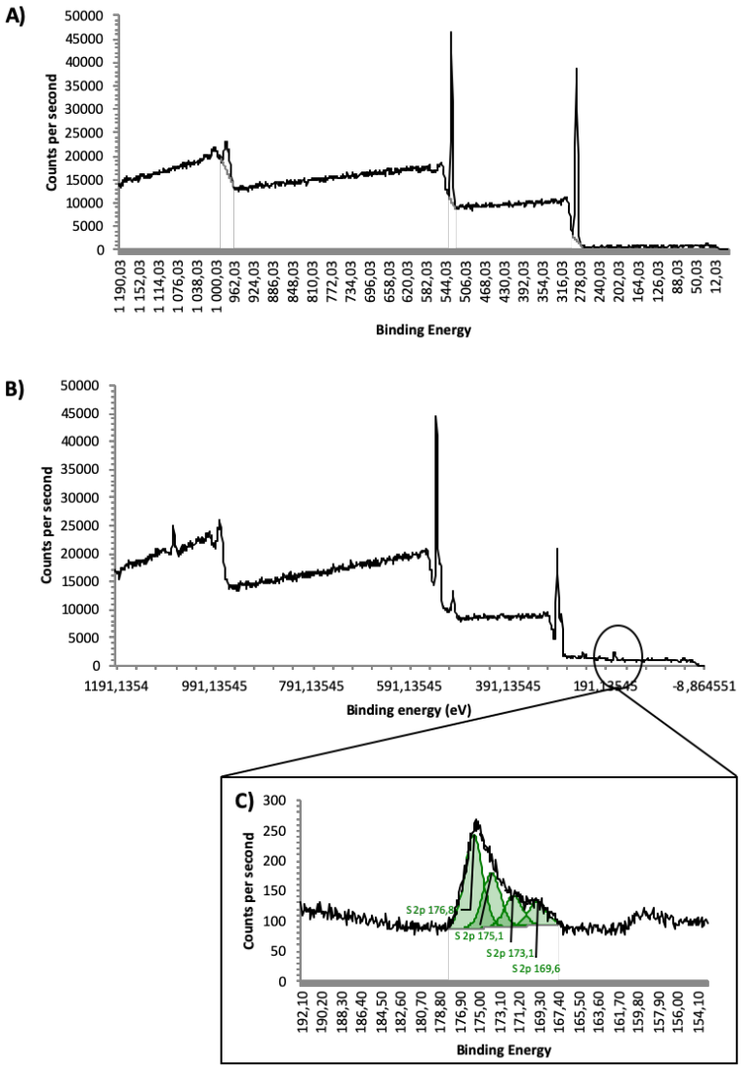

Figure V-4 XPS analysis: survey spectrum of CTR A); general spectra of Fu 10 B) and sulphur spectra of Fu 10 C).

V-3.4. Biological response

V-3.4.1. Cytotoxicity over human melanoma cells

The viability of the melanoma cells was lower on the NFM_Fu condition than on the CTR from day 3 onward. At days 3 and 7, NFM_Fu induced decreased viability (**Figure V-5 A**). Specifically, at day 3, around 70% of melanoma cells are viable, whereas at day 7 there is a viability of around 50% when compared with the CTR. These observations were corroborated by the SEM micrographs (**Figure V-5 B**). Cells were

able to colonize in the control NFM, covering its surface by showing increasing number of cells along the course of the 7 days. Oppositely, in the case of NFM_Fu condition this colonization of the mesh was not observed.

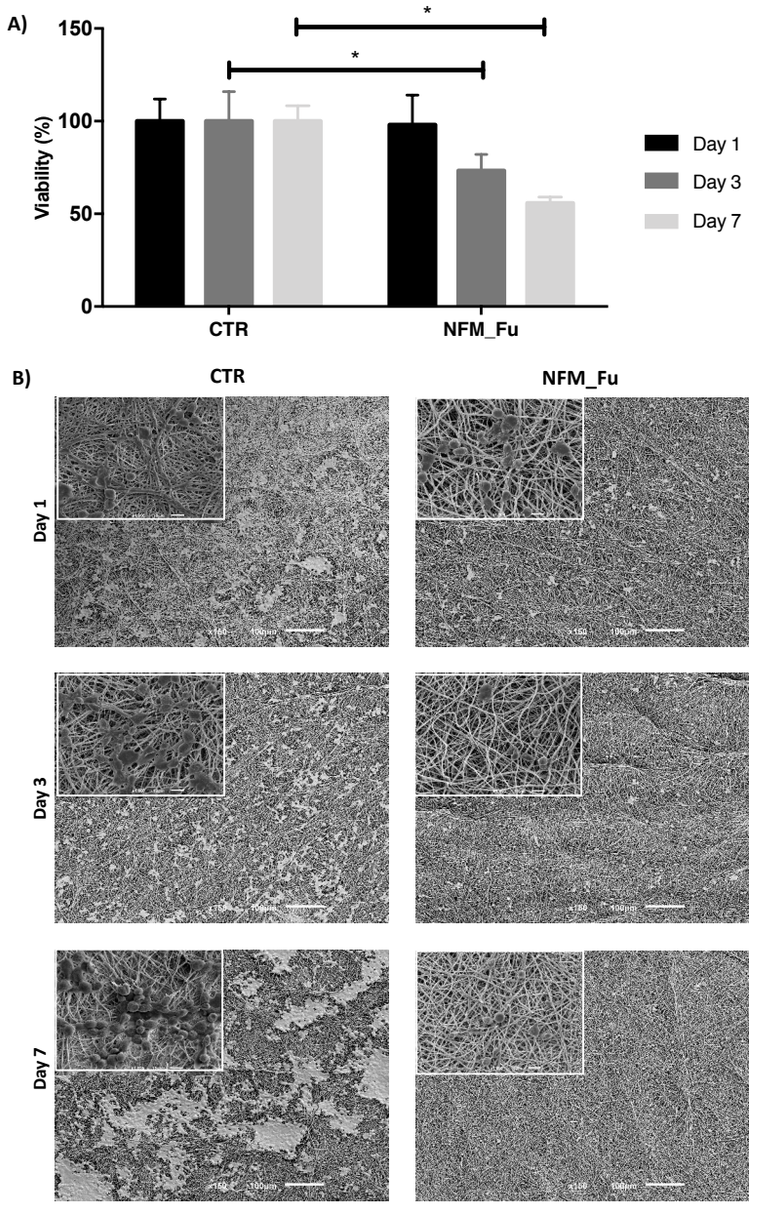

Figure V-5 Cell viability A) and representative SEM images B) of human melanoma cells cultured on NFMs with and without (CTR) fucoidan. Data were considered statistically different if $p < 0.05$.

V-3.4.2. Cytotoxicity over human keratinocytes

The immobilization of fucoidan on the NFM did not present cytotoxic effects over seeded keratinocytes (**Figure V-6 A**). No significant differences were observed between the CTR and NFM_Fu for all time points. When analysing the SEM micrographs, keratinocytes covered the NFMs surface, presenting no morphological differences between the CTR condition and NFM_Fu, along the 7 days of culture (**Figure V-6 B**).

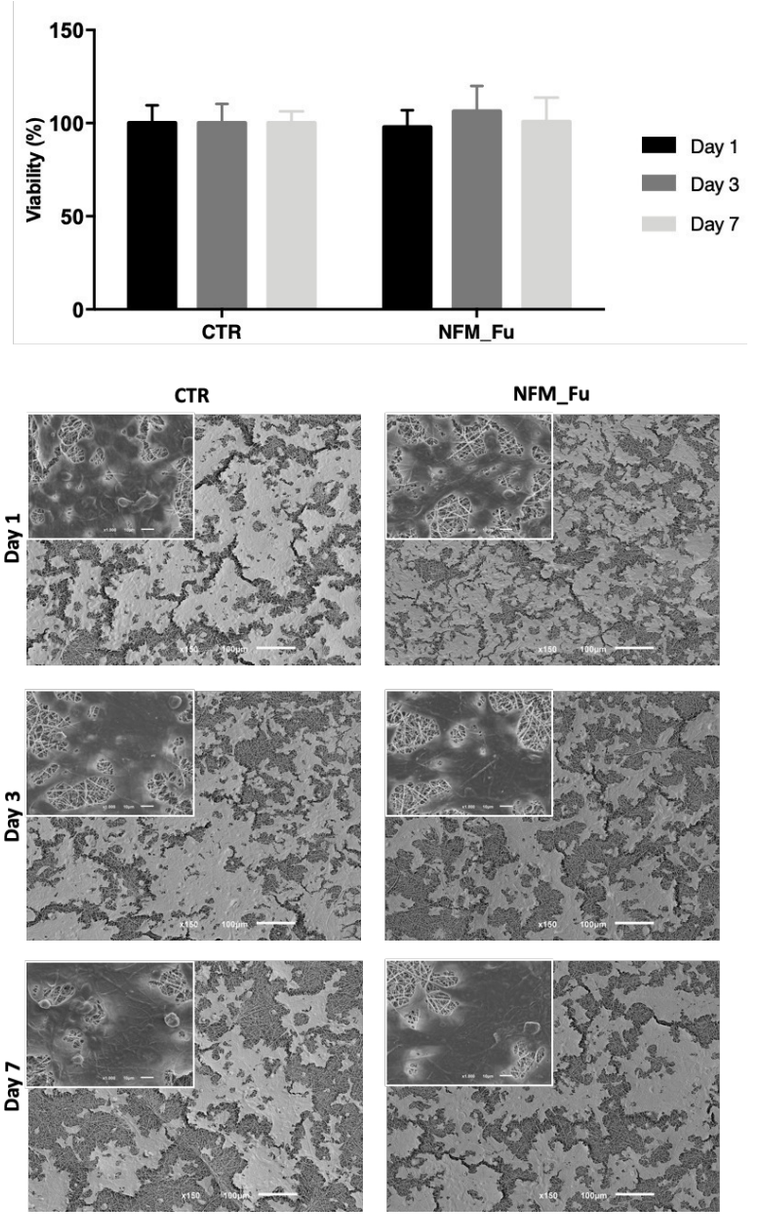

Figure V-6 Cell viability A) and representative SEM images B) of human keratinocytes cultured on NFMs with and without (CTR) fucoidan. Data was considered statistically different if $p < 0.05$.

V-3.4.3. Cytotoxicity over human dermal fibroblast

NFM_Fu was also not cytotoxic for the dermal fibroblasts (**Figure V-7**). There were no significant differences between the CTR and NFM_Fu regarding the viability, for all time points. When analysing the SEM micrographs, it is possible to observe that cells covered the surface of the NFMs, forming a dense cell layer along time, and presenting no morphological differences between the two conditions.

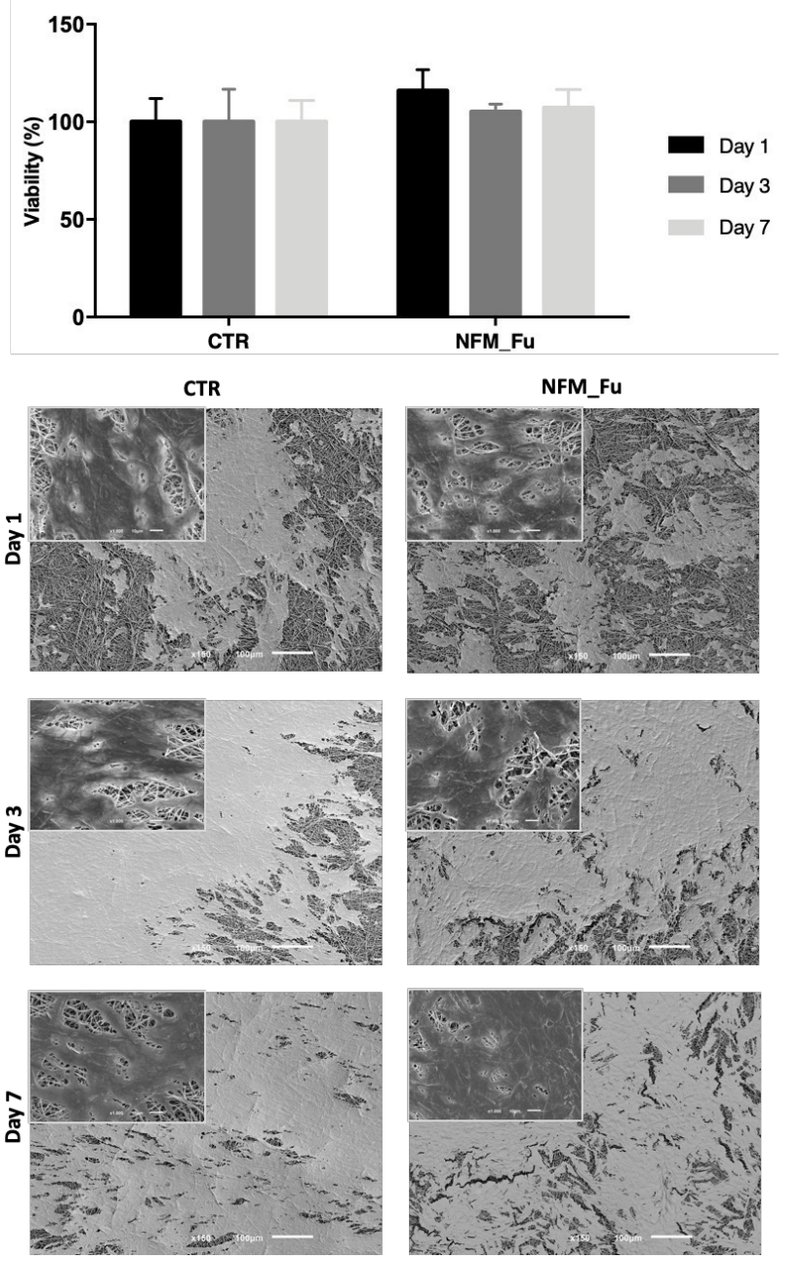

Figure V-7 Cell viability A) and SEM observation B) of human dermal fibroblasts (hDFs) cultured on NFMs with or without (CTR) fucoidan. Data was considered statistically different if $p < 0.05$.

V-4. DISCUSSION

Melanoma is a relatively rare form of skin cancer in most countries of the world but is considered one of the most aggressive and deadthly [17]. If detected and treated at an early stage, melanoma presents a high survival rate. However, when melanoma is diagnosed in a late stage, the survival goes down to 15-20% at 5 years [15]. Although some recent advances in the field, there is still no effective therapeutic for this type of cancer. Due to an increasing incidence of this cancer, the use of natural compounds, namely the ones extracted from seaweeds, has been attracting a growing interest. It has been hypothesised that the consumption of brown seaweeds can be somehow related with the low incidence of melanoma in oriental countries [22, 33]. The best-known antitumor seaweed extract is fucoidan. Fucoidan in the soluble form has been reported to inhibit different types of cancer, including melanoma [22-24]. Herein, despite testing fucoidan in its soluble form as a bioactive agent, an alternative and innovative therapeutic strategy is proposed, by incorporating fucoidan on an electrospun nanofibrous mesh, aiming to act as a skin patch able to be easily and locally applied at the tumor sites.

Firstly, we evaluated the toxicity of fucoidan at different concentrations over different cell types. Besides the testing in human melanoma cells (WM-115 cell line), human dermal fibroblasts and keratinocytes were used as models of non-cancer cells since they are the main cellular components of skin dermis and epidermis, respectively [34]. As described by others, soluble fucoidan is highly cytotoxic for melanoma cells. Fucoidan from different species cultured with melanoma cell lines showed a decrease in cells viability between 40-60%, depending on the extracts [13]. In another study, the effects of native and over-sulfated fucoidan were studied in tumor xenografts, where lung and melanoma cells were injected into mice. Both fucoidan extracts were able to reduce the tumor size after 21 days of daily injections [26]. From our results, the viability of cancer cells was below 20% for concentrations of 0.5 mg mL^{-1} and above. For this same concentration of fucoidan (0.5 mg ml^{-1}), keratinocytes presented viability around 60%, whereas dermal fibroblasts present viability around 70%. Integrating these results, soluble fucoidan is a good candidate to treat melanoma since it has increased toxicity over melanoma cells with low effects over non-cancer cells.

Aiming to further decrease these cytotoxic side effects, we proposed the immobilization of fucoidan at the surface of nanofibrous meshes. Electrospun nanofibrous meshes are of special interest due to an easy functionalization, a high specific surface area and porosity and a pore size that is smaller than the size of most cells [35, 36]. The production, activation and insertion of amine groups at surface of electrospun PCL nanofibrous meshes has been previously described and optimized by our group [28,

29]. Few studies have been reported using nanofibrous-based systems to treat melanoma, namely by the incorporation of chemotherapeutic drugs (i.e. doxorubicin and imiquimod) [37, 38]. The use of fucoidan, a natural compound, has never been reported to be immobilized at the surface of electrospun nanofiber meshes. In fact, there are only a few reports were fucoidan has been combined with other polymers during the electrospinning process for tissue regeneration purposes [39-41].

To quantify the immobilized fucoidan, Toluidine Blue assay was established [42, 43]. As observed it was possible to observe, control NFMs are not stained, whereas the ones with immobilized fucoidan are stained in blue, with increasing intensity with fucoidan content (data not shown). The system seems not to have reached its maximum immobilization capacity (maximum fucoidan concentration tested was 10 mg mL^{-1}, which is the maximum solubility of fucoidan), but different initial concentrations lead to different percentages of immobilization.

The immobilization of fucoidan on electrospun NFMs was validated by contact angle and XPS analysis. As expected, the highest fucoidan concentrations presented the highest percentage of sulphur atoms, meaning that a higher concentration of fucoidan has been immobilized. Furthermore, the immobilization of fucoidan also increased the oxygen content due to the presence of this element in functional groups within polysaccharide structure, including the sulfates [44].

One of the major disadvantages of some current cancer treatments is the fact that, besides affecting the tumor, they also have severe toxic effects over many healthy tissues [45]. Therefore, when developing systems for melanoma treatment, there is the need to evaluate their cytotoxic effects not only over melanoma cells, but also over adjacent non-cancer cells. *In vitro* results revealed a 50% decrease on melanoma cells viability while maintain the viability of normal cells, which is an indication of the selectiveness and effectiveness of the developed functionalized nanofibrous membranes. To the best of our knowledge, despite few studies regarding fucoidan usage as a bioactive agent, there is only one fucoidan-based system reported in the literature that aims to treat melanoma. Fucoidan-based nanoparticles with affinity to P-selectin and incorporating different chemotherapeutic drugs were developed presenting increased toxicity when compared with untargeted drugs and nanoparticles [46]. In this sense, by the development and promising results of the proposed nanofibrous system, the basis of a new and innovative therapeutic approach to tackle melanoma were established, namely envisioning its use as adjuvant system in the form of patch applied after tumor excision.

V-5. CONCLUSIONS

The antitumor features of fucoidan in its soluble form or immobilized on an electrospun nanofibrous mesh appears as an original and effective therapeutic alternative to treat melanoma. In its soluble form, fucoidan was more effective over melanoma cells, although it presented some toxicity over non-cancerous cells. To try to overcome these cytotoxic side effects, fucoidan was immobilized at the surface of NFM. Indeed, the cytotoxic effects of NFM_Fu over melanoma cells along with the non-toxicity over keratinocytes and dermal fibroblasts, allows its application as a skin patch without causing adverse effects on surrounding healthy tissues. Therefore, it may be considered an adjuvant after tumour excision to tackle eventual remaining melanoma cells. Furthermore, this therapy can be personalized according to the tumour characteristics by changing its size, shape and treatment time.

V-6. ACKNOWLEDGEMENTS

This work was developed under the scope of the Structured Projects for R&D&I NORTE-01-0145-FEDER-000021 and NORTE-01-0145-FEDER-000023 supported by the Northern Portugal Regional Operational Programme (NORTE 2020), under the Portugal 2020 Partnership Agreement. The authors would like also to thank NORTE 2020 for financing the PhD scholarship of C.O. "Norte-08-5369-000037" and FCT for the Investigator grant of A.M. (IF/00376/2014). Dr. Luísa Rodrigues is acknowledged by the XPS analysis.

V-7. REFERENCES

[1] M. Arruebo, N. Vilaboa, B. Sáez-Gutierrez, J. Lambea, A. Tres, M. Valladares, A. González-Fernández, Assessment of the evolution of cancer treatment therapies, Cancers 3(3) (2011) 3279-3330.

[2] G.M. Cragg, D.J. Newman, Natural products: a continuing source of novel drug leads, Biochimica et biophysica acta 1830(6) (2013) 3670-3695.

[3] M.F. de Jesus Raposo, A.M.B. de Morais, R.M.S.C. de Morais, Marine Polysaccharides from Algae with Potential Biomedical Applications, Marine Drugs 13(5) (2015) 2967-3028.

[4] T.H. Silva, A. Alves, E.G. Popa, L.L. Reys, M.E. Gomes, R.A. Sousa, S.S. Silva, J.F. Mano, R.L. Reis, Marine algae sulfated polysaccharides for tissue engineering and drug delivery approaches, Biomatter 2(4) (2012) 278-289.

[5] J.H. Fitton, D.N. Stringer, S.S. Karpiniec, Therapies from Fucoidan: An Update, Marine Drugs 13(9) (2015) 5920-5946.

[6] M.T. Ale, J.D. Mikkelsen, A.S. Meyer, Important Determinants for Fucoidan Bioactivity: A Critical Review of Structure-Function Relations and Extraction Methods for Fucose-Containing Sulfated Polysaccharides from Brown Seaweeds, Marine Drugs 9(10) (2011) 2106-2130.

[7] C. Oliveira, A.S. Ferreira, R. Novoa-Carballal, C. Nunes, I. Pashkuleva, N.M. Neves, M.A. Coimbra, R.L. Reis, A. Martins, T.H. Silva, The Key Role of Sulfation and Branching on Fucoidan Antitumor Activity, Macromol Biosci 17(5) (2017) 1600340.

[8] B. Li, F. Lu, X. Wei, R. Zhao, Fucoidan: Structure and Bioactivity, Molecules 13(8) (2008) 1671-95.

[9] J. Wang, Q. Zhang, Z. Zhang, H. Song, P. Li, Potential antioxidant and anticoagulant capacity of low molecular weight fucoidan fractions extracted from Laminaria japonica, International Journal of Biological Macromolecules 46(1) (2010) 6-12.

[10] A. Aisha, A.B. Jelili, S. Salem, B. Rolene, H. Donavon, Effects of Fucoidan and Chemotherapeutic Agent Combinations on Malignant and Non-malignant Breast Cell Lines, Current Pharmaceutical Biotechnology 18(9) (2017) 748-757.

[11] M. Alwarsamy, R. Gooneratne, R. Ravichandran, Effect of fucoidan from Turbinaria conoides on human lung adenocarcinoma epithelial (A549) cells, Carbohydrate Polymers 152 (2016) 207-213.

[12] H.-L. Tsai, C.-J. Tai, C.-W. Huang, F.-R. Chang, J.-Y. Wang, Efficacy of Low-Molecular-Weight Fucoidan as a Supplemental Therapy in Metastatic Colorectal Cancer Patients: A Double-Blind Randomized Controlled Trial, Marine drugs 15(4) (2017) 122.

[13] O.S. Vishchuk, S.P. Ermakova, T.N. Zvyagintseva, The fucoidans from brown algae of Far-Eastern seas: Anti-tumor activity and structure–function relationship, Food Chemistry 141(2) (2013) 1211-1217.

[14] Z.-J. Wang, L. Zheng, J.-M. Yang, Y. Kang, Y.-D. Park, Proteomic analyses for profiling regulated proteins/enzymes by Fucus vesiculosus fucoidan in B16 melanoma cells: A combination of enzyme kinetics functional study, International Journal of Biological Macromolecules 112 (2018) 667-674.

[15] American Cancer Society available from https://www.cancer.org/cancer/melanoma-skin-cancer.html (assessed August 2019).

[16] J. Ferlay, I. Soerjomataram, R. Dikshit, S. Eser, C. Mathers, M. Rebelo, D.M. Parkin, D. Forman, F. Bray, Cancer incidence and mortality worldwide: sources, methods and major patterns in GLOBOCAN 2012, International journal of cancer 136(5) (2015) E359-86.

[17] C. Global Burden of Disease Cancer, The Global Burden of Cancer 2013, JAMA oncology 1(4) (2015) 505-527.

[18] World Health Organization available from http://www.who.int/uv/faq/skincancer/en/index1.html (assessed August 2019).

[19] C. Bertolotto, Melanoma: From Melanocyte to Genetic Alterations and Clinical Options, Scientifica 2013 (2013) 635203.

[20] M. Batus, S. Waheed, C. Ruby, L. Petersen, S.D. Bines, H.L. Kaufman, Optimal Management of Metastatic Melanoma: Current Strategies and Future Directions, American journal of clinical dermatology 14(3) (2013) 179-194.

[21] d.C.G. Widakowich C, de Azambuja E, Dinh P, Awada A, Side effects of approved molecular targeted therapies in solid cancers, Oncologist 12(12) (2007) 1443-55.

[22] J. Teas, M.R. Irhimeh, Melanoma and brown seaweed: an integrative hypothesis, Journal of Applied Phycology 29(2) (2017) 941-948.

[23] M.T. Ale, H. Maruyama, H. Tamauchi, J.D. Mikkelsen, A.S. Meyer, Fucoidan from Sargassum sp. and Fucus vesiculosus reduces cell viability of lung carcinoma and melanoma cells in vitro and activates natural killer cells in mice in vivo, International Journal of Biological Macromolecules 49(3) (2011) 331-336.

[24] M.T. Ale, H. Maruyama, H. Tamauchi, J.D. Mikkelsen, A.S. Meyer, Fucose-Containing Sulfated Polysaccharides from Brown Seaweeds Inhibit Proliferation of Melanoma Cells and Induce Apoptosis by Activation of Caspase-3 in Vitro, Marine Drugs 9(12) (2011) 2605-2621.

[25] Z.-J. Wang, W. Xu, J.-W. Liang, C.-S. Wang, Y. Kang, Effect of Fucoidan on B16 Murine Melanoma Cell Melanin Formation and Apoptosis, African Journal of Traditional, Complementary, and Alternative Medicines 14(4) (2017) 149-155.

[26] S. Koyanagi, N. Tanigawa, H. Nakagawa, S. Soeda, H. Shimeno, Oversulfation of fucoidan enhances its anti-angiogenic and antitumor activities, Biochemical Pharmacology 65(2) (2003) 173-179.

[27] M. Dithmer, A.-M. Kirsch, E. Richert, S. Fuchs, F. Wang, H. Schmidt, S.E. Coupland, J. Roider, A. Klettner, Fucoidan Does Not Exert Anti-Tumorigenic Effects on Uveal Melanoma Cell Lines, Marine Drugs 15(7) (2017) 193.

[28] A. Martins, E.D. Pinho, S. Faria, I. Pashkuleva, A.P. Marques, R.L. Reis, N.M. Neves, Surface Modification of Electrospun Polycaprolactone Nanofiber Meshes by Plasma Treatment to Enhance Biological Performance, Small 5(10) (2009) 1195-1206.

[29] N. Monteiro, A. Martins, R. Pires, S. Faria, N.A. Fonseca, J.N. Moreira, R.L. Reis, N.M. Neves, Immobilization of bioactive factor-loaded liposomes on the surface of electrospun nanofibers targeting tissue engineering, Biomaterials Science 2(9) (2014) 1195-1209.

[30] F. Kubaski, H. Osago, R.W. Mason, S. Yamaguchi, H. Kobayashi, M. Tsuchiya, T. Orii, S. Tomatsu, Glycosaminoglycans detection methods: Applications of mass spectrometry, Molecular Genetics and Metabolism 120(1) (2017) 67-77.

[31] A. Taylor, Practical surface analysis, 2nd edn., vol I, auger and X-ray photoelectron spectroscopy. Edited by D. Briggs & M. P. Seah, John Wiley, New York, 1990, 657 pp., price: £86.50. ISBN 0471 92081 9, Journal of Chemical Technology & Biotechnology 53(2) (1992) 215-215.

[32] M. Costa, M.T. Cerqueira, T.C. Santos, B. Sampaio-Marques, P. Ludovico, A.P. Marques, R.P. Pirraco, R.L. Reis, Cell sheet engineering using the stromal vascular fraction of adipose tissue as a vascularization strategy, Acta Biomaterialia 55 (2017) 131-143.

[33] C. Karimkhani, A.C. Green, T. Nijsten, M.A. Weinstock, R.P. Dellavalle, M. Naghavi, C. Fitzmaurice, The global burden of melanoma: results from the Global Burden of Disease Study 2015, The British Journal of Dermatology 177(1) (2017) 134-140.

[34] M. Boer, E. Duchnik, R. Maleszka, M. Marchlewicz, Structural and biophysical characteristics of human skin in maintaining proper epidermal barrier function, Adavances in Dermatology and Allergology 33(1) (2016) 1-5.

[35] J. Zhan, A. Singh, Z. Zhang, L. Huang, J.H. Elisseeff, Multifunctional aliphatic polyester nanofibers for tissue engineering, Biomatter 2(4) (2012) 202-212.

[36] C. Oliveira, A.R. Costa-Pinto, R.L. Reis, A. Martins, N.M. Neves, Biofunctional Nanofibrous Substrate Comprising Immobilized Antibodies and Selective Binding of Autologous Growth Factors, Biomacromolecules 15(6) (2014) 2196-2205.

[37] M. Guo, G. Zhou, Z. Liu, J. Liu, J. Tang, Y. Xiao, W. Xu, Y. Liu, C. Chen, Direct site-specific treatment of skin cancer using doxorubicin-loaded nanofibrous membranes, Science Bulletin 63(2) (2018) 92-100.

[38] W.-C. Lin, I.T. Yeh, E. Niyama, W.-R. Huang, M. Ebara, C.-S. Wu, Electrospun Poly(ε-caprolactone) Nanofibrous Mesh for Imiquimod Delivery in Melanoma Therapy, Polymers 10(3) (2018).

[39] J.S. Lee, G.H. Jin, M.G. Yeo, C.H. Jang, H. Lee, G.H. Kim, Fabrication of electrospun biocomposites comprising polycaprolactone/fucoidan for tissue regeneration, Carbohydrate Polymers 90(1) (2012) 181-188.

[40] J. Shao, N. Yu, E. Kolwijck, B. Wang, K.W. Tan, J.A. Jansen, X.F. Walboomers, F. Yang, Biological evaluation of silver nanoparticles incorporated into chitosan-based membranes, Nanomedicine (Lond) 12(22) (2017) 2771-2785.

[41] N. Goonoo, A. Bhaw-Luximon, U. Jonas, D. Jhurry, H. Schönherr, Enhanced Differentiation of Human Preosteoblasts on Electrospun Blend Fiber Mats of Polydioxanone and Anionic Sulfated Polysaccharides, ACS Biomaterials Science & Engineering 3(12) (2017) 3447-3458.

[42] G. Sridharan, A.A. Shankar, Toluidine blue: A review of its chemistry and clinical utility, Journal of Oral and Maxillofacial Pathology : JOMFP 16(2) (2012) 251-255.

[43] J.-O. Jeong, S.I. Jeong, J.-S. Park, H.-J. Gwon, S.-J. Ahn, H. Shin, J.Y. Lee, Y.-M. Lim, Development and characterization of heparin-immobilized polycaprolactone nanofibrous scaffolds for tissue engineering using gamma-irradiation, RSC Advances 7(15) (2017) 8963-8972.

[44] K. Ozaltin, M. Lehocký, P. Humpolíček, J. Pelková, P. Sáha, A New Route of Fucoidan Immobilization on Low Density Polyethylene and Its Blood Compatibility and Anticoagulation Activity, International Journal of Molecular Sciences 17(6) (2016) 908.

[45] F. Atashrazm, R.M. Lowenthal, G.M. Woods, A.F. Holloway, J.L. Dickinson, Fucoidan and Cancer: A Multifunctional Molecule with Anti-Tumor Potential, Marine Drugs 13(4) (2015) 2327-2346.

[46] Y. Shamay, M. Elkabets, H. Li, J. Shah, S. Brook, F. Wang, K. Adler, E. Baut, M. Scaltriti, P.V. Jena, E.E. Gardner, J.T. Poirier, C.M. Rudin, J. Baselga, A. Haimovitz-Friedman, D.A. Heller, P-selectin is a nanotherapeutic delivery target in the tumor microenvironment, Sci Transl Med 8(345) (2016) 345ra87.

Chapter VI

Gemcitabine delivered by fucoidan/chitosan nanoparticles presents increased toxicity over human breast cancer cells

Chapter VI

Gemcitabine delivered by fucoidan/chitosan nanoparticles presents increased toxicity over human breast cancer cells**

ABSTRACT

Marine-origin nanoparticles aiming to develop more effective and tolerated therapies for breast cancer were developed. Nanoparticles based in two marine origin polymers (fucoidan and chitosan) were prepared by polyelectrolyte complexation, for the delivery of an antitumor drug model (gemcitabine). Final formulation resulted in stable nanoparticles around 115 – 140 nm in size and a polydispersity index <0.2. Gemcitabine was encapsulated at a maximum entrapment efficiency of 35-42%. Drug release studies demonstrated that around 84% of gemcitabine is released within 4 h. Cytotoxicity results of gemcitabine-loaded nanoparticles showed increased toxicity (around 25%) when compared with free gemcitabine. The drug-loaded nanoparticles present increased toxicity over human breast cancer cells without increasing toxic effects over endothelial cells.

** This chapter is based on the following publication:

Oliveira C., Neves N. M., Reis R. L., Martins A., Silva T. H. Gemcitabine delivered by fucoidan/chitosan nanoparticles presents increased toxicity over human breast cancer cells, Nanomedicine. 2018, 13, 2037-2050. doi:10.2217/nnm-2018-0004.

VI-1. INTRODUCTION

Cancer is one of the leading causes of death worldwide and is characterized by uncontrolled and fast growth of cells. In 2012 there were around 14 million new cases of cancer and around 8 million resulted in death. By 2035 it is expected to be around 24 million new cases per year [1]. Breast cancer is the most common cancer in females and the second deadliest [2]. Surgery, radiation and systemic therapies (chemotherapy, hormonal and target) are some of the current breast cancer treatments modalities available, depending on the extent and type of cancer [3]. Some of these treatments may present some limitations since, besides affecting the tumor, they also affect the surrounding healthy environment, and may present some side effects [3, 4]. For these reasons the use of natural substances is an interesting alternative due to their low toxicity and biological and chemical similarities to native tissues composition.

Among natural substances, marine organisms are valuable sources of materials with intriguing properties and characteristics [5]. Fucoidan is a natural derived sulfated polysaccharide extracted from brown seaweed and has been extensively investigated because of its various biological properties such as anticoagulant, antiviral, antiangiogenic, anti-inflammatory, immunomodulating and, most recently, antitumor behavior [6, 7]. Looking specifically at its antitumor behavior, we recently reported that different fucoidan extracts present different biological responses over human breast cancer and non-cancer cell lines with chemical structure apparently playing an important role [8]. Some fucoidan extracts presented the desired antitumor behavior whereas other presented toxicity for both cancer and non-cancer cells or where non-toxic for both types of cells, depending on their chemical features.

In this work, we propose the use of non-toxic fucoidan to develop a natural marine origin drug delivery system (DDS) for the release of anticancer drugs. Indeed, fucoidans have been included in nanosystems for diagnostic, drug delivery and regenerative medicine [9, 10] and have been combined with chitosan, a marine-derived polycation, to prepare nanoparticles (NPs) by polyelectrolyte complexation for the delivery of growth factors drugs and other biological compounds [10-13].

Nanoparticles have been developed as DDS for the delivery of drugs or biomolecules. Nanoparticles-based DDS present attractive properties since they can pass through the smallest capillary vessels and penetrate cells/tissue gaps to arrive at the target site [14, 15]. They may also improve macromolecules stability, protecting them from enzymatic degradation, and control their release profile. However, they may present some limitations like drug loss during circulation and limited drug loading capacity.

Gemcitabine, an antitumor drug, has been applied in the treatment of different cancers such as lung, ovary and pancreatic [16-18]. It has been also used in the treatment of breast cancer, as a single therapy or in combination with other chemotherapeutic agents [19, 20]. Gemcitabine is a nucleoside analogue that inhibits DNA synthesis, by its incorporation into DNA, followed by inhibition of cell proliferation. Gemcitabine presents a short biological half-life, being rapidly metabolized. This limits its biological effectiveness, since higher doses are required to reach a therapeutic concentration, increasing the risk of side effects [21, 22]. In this sense, there is the unmet therapeutic need to try to enhance gemcitabine biological response by incorporating it into a DDS, has it has been previously reported [23, 24].

To the best of our knowledge there are no reports in the literature regarding the development of fucoidan/chitosan nanoparticles for the delivery of gemcitabine (Gem). In this sense, we propose the combination of fucoidan (negatively charged) with chitosan by polyelectrolyte complexation to produce nanoparticles for controlled release of gemcitabine as potential breast cancer therapy. Regarding nanoparticles production there are different parameters that need to be optimized such as polymers concentration and ratio; polymeric solution pH and ionic strength. Therefore, these different parameters were tested and combined to obtain the nanoparticles with smaller size and Pdi (polydispersive index). Nanoparticles stability is another important aspect that needed to be evaluated. Having in mind the tumor microenvironment, nanoparticles toxicity was evaluated over cancer and non-cancer cells. The release profile of gemcitabine was analyzed and loaded-nanoparticles tested over endothelial and breast cancer cells as an *in-vitro* assessment of antitumor efficiency through cytotoxicity.

VI-2. EXPERIMENTAL SECTION

VI-2.1. Materials

Fucoidan (Fu) from *Fucus vesiculosus* (Mw by GPC 45-75 kDa) was purchased from Marinova whereas Chitosan (CH) 95/20 (Mw by GPC 40-150 kDa) was purchased from Heppe Medical Chitosan GmbH. 1-[3-(dimethylamino)propyl]-3-ethylcarbodiimide hydrochloride (EDC) and N-Hydroxysuccinimide (NHS) were both purchased from Sigma Aldrich. Centrifugal concentrators Vivaspin 20 300 KD were purchased from Fisher Scientific. 2'-Deoxy-2',2'-difluorocytidine (gemcitabine - $C_9H_{11}F_2N_3O_4$) was purchased from Carbosynth. Human umbilical vein endothelial cells (EA.hy926) and breast cancer cells (MDA-MB-231) were both purchased from ATCC.

VI-2.2. Methods

VI-2.2.1. Preparation of nanoparticles

Marine-origin polymeric nanoparticles were prepared by polyelectrolyte complexation. Optimization was performed to study the effect of different parameters over size and Pdi. From the results obtained, for each parameter, we chose the production condition that combined the smaller size and Pdi values. Different parameters were evaluated such as: concentration of both polymers (ranging from 0.25 mg/ml to 1 mg ml^{-1}); the ratio of polymers solution (CH:Fu – 1:2; 1:1; 2:1); chitosan and fucoidan solutions pH; ionic strength (ultra-pure water, osmotized water, and 0.9% NaCl) and crosslinking agent concentrations: 600/240 mM; 300/120 mM and 150/60 mM (EDC/NHS). Each parameter was evaluated separately while all the other were kept constant.

After all the optimization steps, nanoparticles parameters were maintained for all further assays. Briefly chitosan was dissolved in 1% (v/v) acetic acid solution at 0.5 mg ml^{-1} concentration, whereas the polyanion (fucoidan) was prepared in ultra-pure water to reach a final concentration of 0.5 mg ml^{-1}. Chitosan and fucoidan solutions were adjusted with 1M HCl and 1 M NaOH, depending on the desired pH. Chitosan solution was adjusted to pH=5, whereas fucoidan solution was measured and the pH adjusted if its values were not as expected (pH=9). 3 ml of fucoidan solution (0.5 mg ml^{-1}) was added, using a precision syringe pump, to 3 ml of chitosan solution (0.5 mg ml^{-1}) leading to a final theoretical ratio (w/w) of 1:1 and a spontaneous formation of nanoparticles occurs. Right after nanoparticles production, 300 mM EDC + 120 mM NHS was added to nanoparticles solution. Nanoparticles were stirred for 2 h at 600 rpm. After that, nanoparticles were collected using 300 kDa vivaspin filters for 15 minutes at 4000 rpm. Nanoparticles were washed twice with ultra-pure water. Glucose was added in all centrifugation steps to avoid nanoparticles aggregation. Finally, nanoparticles were filtered with 0.22 μm filters.

VI-2.2.2. Characterization of nanoparticles

VI-2.2.2.1 *Dynamic Light Scattering*

Nanoparticles size and Pdi was determined by dynamic light scattering (DLS) using a Zetasizer Nano ZS (Malvern Instruments, UK). Samples were diluted in UP water and the size analysis lasted 180 s and

performed at 25°C, in triplicate. The zeta potential measurements were performed by a dip cell in automatic mode.

VI-2.2.2.2 *Nanoparticle tracking analysis (NTA)*

NTA experiments were performed using a NanoSight NS500 instrument (Salisbury, UK). This system includes a charge-coupled device camera that allows visualization and tracking of Brownian motion of laser-illuminated particles in suspension. Video images were analyzed using NTA analytical software version 2.3. The measurements were made at room temperature and each video sequence was captured over 60 s.

VI-2.2.2.3 *SEM and STEM*

Measurement of particles' size and morphology observation were obtained using FIB-SEM (Auriga, Carl Zeiss). A drop of nanoparticles solution was placed in the stub for SEM analysis and left to dry overnight. They were then vacuum-coated with a gold-platinum mixture. Scanning transmission electron microscopy (STEM) analysis was also performed with the same equipment.

VI-2.2.2.4 *Nanoparticles physiological and storage stability*

To mimic and assess the stability of nanoparticles at physiological conditions, the nanoparticles were diluted in 0.9% NaCl and kept at 37°C. The size and Pdi of nanoparticles were measured by DLS every day, until day 7.

To evaluate nanoparticles storage stability after production, nanoparticles were diluted in ultra-pure water and kept at 4°C. Nanoparticles size and Pdi was measured by DLS every week for up to 2 months.

VI-2.2.3. Nanoparticles cytotoxicity

VI-2.2.3.1 *Cell culture and cell viability*

The cytotoxicity of the optimized nanoparticles was evaluated over human umbilical vein endothelial (EA.hy926, cell line) and breast cancer (MDA-MB-231, cell line) cells. Increasing concentration of

nanoparticles were used until toxic effects were observed. MTS assay (CellTiter 96 AQueous One Solution, Promega) was performed at 24, 48 and 72 h. At these time points, the culture medium was removed and the testing samples were rinsed with sterile Phosphate-Buffered Saline (PBS). A mixture of culture medium (without FBS and phenol red) and MTS reagent (5:1 ratio) was added to each well and left to incubate for 3h, at 37°C, in a humidified 5% CO_2 atmosphere. Thereafter, the absorbance of the MTS reaction medium from each sample was read in triplicate at 490 nm in a microplate reader (Synergy HT, Bio-TEK). All experiments were performed in triplicate. This experiment was repeated with gemcitabine-loaded nanoparticles, being the amount of free-gemcitabine the same as the one loaded into the developed nanoparticles.

VI-2.2.4. Drug encapsulation and release studies

VI-2.2.4.1 *Drug entrapment efficiency*

Gemcitabine concentrations, ranging from 0.2 to 3.2 mg ml^{-1}, were encapsulated into the nanoparticles optimized formulation. Gemcitabine was added to chitosan solution and nanoparticles were produced as described in section VI.2.2.1, maintaining the same production conditions (ratio Ch:Fu:Gem - 1:1:0.3).

Entrapment efficiency was calculated by measuring the initial concentration and non-encapsulated gemcitabine, according to the following formula:

Equation VI-1 Equation for the determination of the entrapment efficiency

$$\%EE = \frac{(\text{initial concentration-non-entrapped drug})}{\text{initial concentration}} x100$$

The samples were analyzed by UV-spectroscopy (Shimadzu) at the maximum absorbance of 268 nm. All the experiments were performed in triplicate.

VI-2.2.4.2 *Gemcitabine Release studies*

The release kinetics of gemcitabine was measured by placing 1.5 mL of gem-loaded nanoparticles into dialysis membranes, and this system into 50 mL of 0.9% NaCl at 37°C under 60 rpm stirring. At

pre-determined time periods (0, 5, 15, 30, 45 min; 1, 1.5, 2, 3, 4, 5, 6, 8, 12, 24, 48 and 72 h), an aliquot of 2 mL of the release solution was taken and immediately measured at the previously defined absorbance. The experiments were performed in triplicate.

VI-2.3. Statistical analysis

Statistical analysis was performed using Graph Pad Prism Software. Differences between the different conditions of the cellular assays were analyzed using nonparametric test (Kruskal–Wallis test) and a $p < 0.05$ was considered significant. Data are presented as mean ± standard deviations.

VI-3. RESULTS

VI-3.1. Optimization of nanoparticles production parameters

To produce marine-origin polymeric nanoparticles with constant sizes, several processing parameters were tested, namely polymers concentration and ratios, pH of the solution, ionic strength and influence of the crosslinker. Experimental results point out that a decrease in polymers concentration lead to the formation of smaller nanoparticles (**Figure VI-1 A**). With the same trend, the Pdi tends to decrease for concentrations down to 0.5 mg mL^{-1}. However, for the lowest concentration, the Pdi slightly increased indicating that at this polymers concentration the nanoparticles are less homogenous. In this sense, and by the combination of these two important properties, the working concentration was set as 0.5 mg mL^{-1} for both chitosan and fucoidan When fucoidan is in excess (CH:Fu ratio 1:2) in the final formulation, the nanoparticles present a size around 500 nm and are highly polydispersive (Pdi>0.3) (**Figure VI-1 B**). For the 2:1 ratio, the nanoparticles present a higher Pdi than 1:1. Therefore, this last ratio was used for all further experiments. The influence of pH solution was evaluated for each polymer separately, maintaining the pH of the other polymer solution (**Figure VI-1 C and D**). For the chitosan solution, pH=5 was chosen, whereas for fucoidan the testing condition that presented smaller size and Pdi values was the one with pH=9 (pH of fucoidan solution). Ionic strength was also evaluated by dissolving the polymers in different solvents with increasing ionic strength: ultra-pure water (UP W), osmotized water (OW) and 0.9% NaCl. UP W was the condition where the nanoparticles presented the lower Pdi and size values (**Figure VI-1 E**). Taking together, the optimal production parameters were set as: 0.5 mg ml^{-1} of both chitosan and fucoidan; 1:1 ratio; pH (chitosan) = 5 and pH (fucoidan) = 9 and ultra-pure water as the polymer's solvent.

After setting these parameters, the concentration of a crosslinking agent was evaluated. Different concentrations of EDC/NHS were tested, being the and 300 mM of EDC and 120 mM of NHS the condition that presented the best outcomes in terms of size and Pdi (**Figure VI-1 F**).

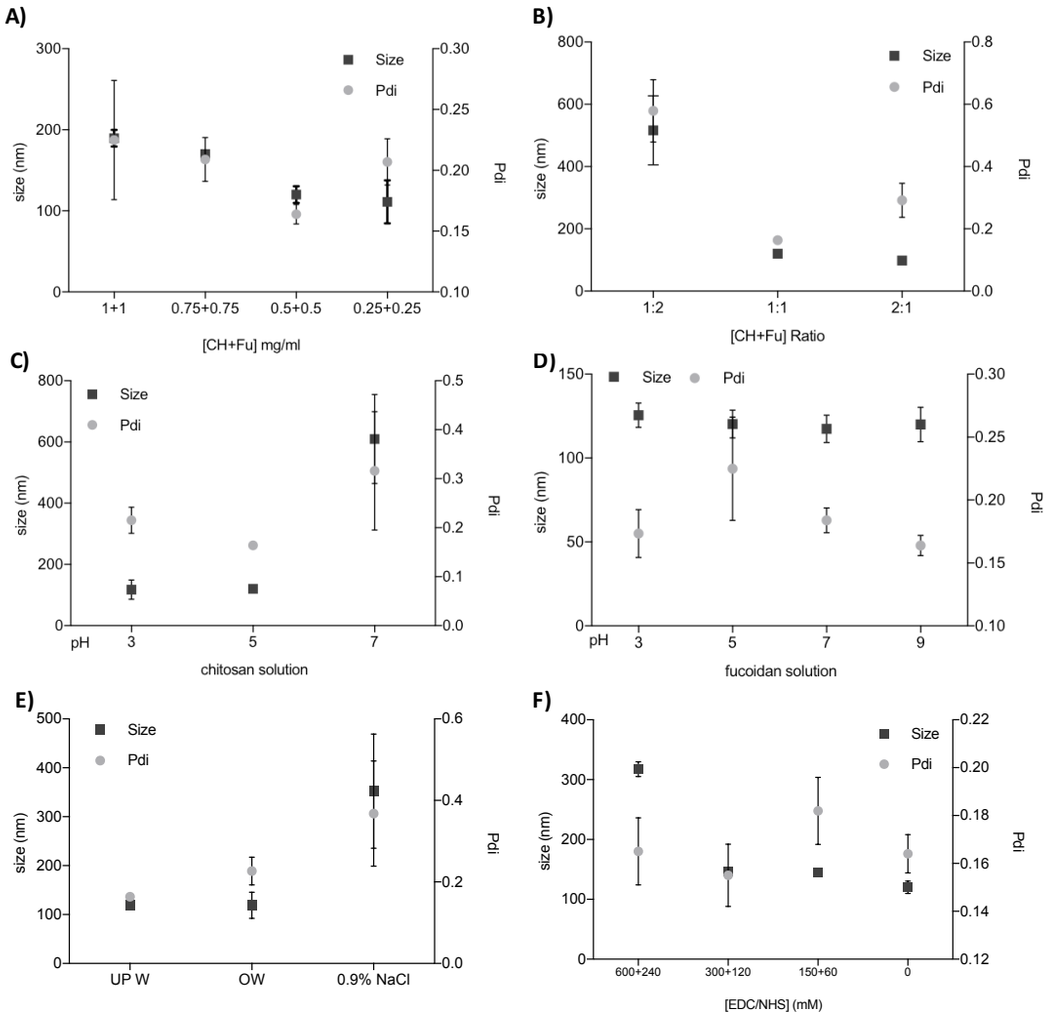

Figure VI-1 Nanoparticles' size and polydispersity index (Pdi) at different production parameters. A) and B) evaluation of chitosan (CH) and fucoidan (Fu) concentration and ratio (CH+Fu), respectively. C) and D) evaluation of the influence of chitosan and fucoidan solutions pH, respectively. E) Influence of ionic strength and F) evaluation of different crosslinker (EDC/NHS) concentrations.

VI-3.2. Nanoparticles characterization

VI-3.2.1. Nanoparticles stability

After optimizing all the production parameters, two different conditions were chosen to continue the characterization of the nanoparticles: one without crosslinking (no EDC/NHS) and the other crosslinked

with EDC/NHS (300 mM EDC + 120 mM NHS). These two conditions were used to perform stability assays, both at physiological conditions (37°C, 0.9% NaCl) (**Figure VI-2 A**) and for storage conditions (4°C, UP W) (**Figure VI-2 B**). At physiological conditions, both size and Pdi increase along the 7 days of the study, presenting values for Pdi above 0.3 from day 4 on, concerning non-crosslinked NPs. The size of crosslinked NPs was stable along the 7 days, whereas the Pdi presents some slightly variations in some time points, being these values below 0.2. For the storage condition, both types of nanoparticles present no significant variations in terms of size and Pdi up to 2 months.

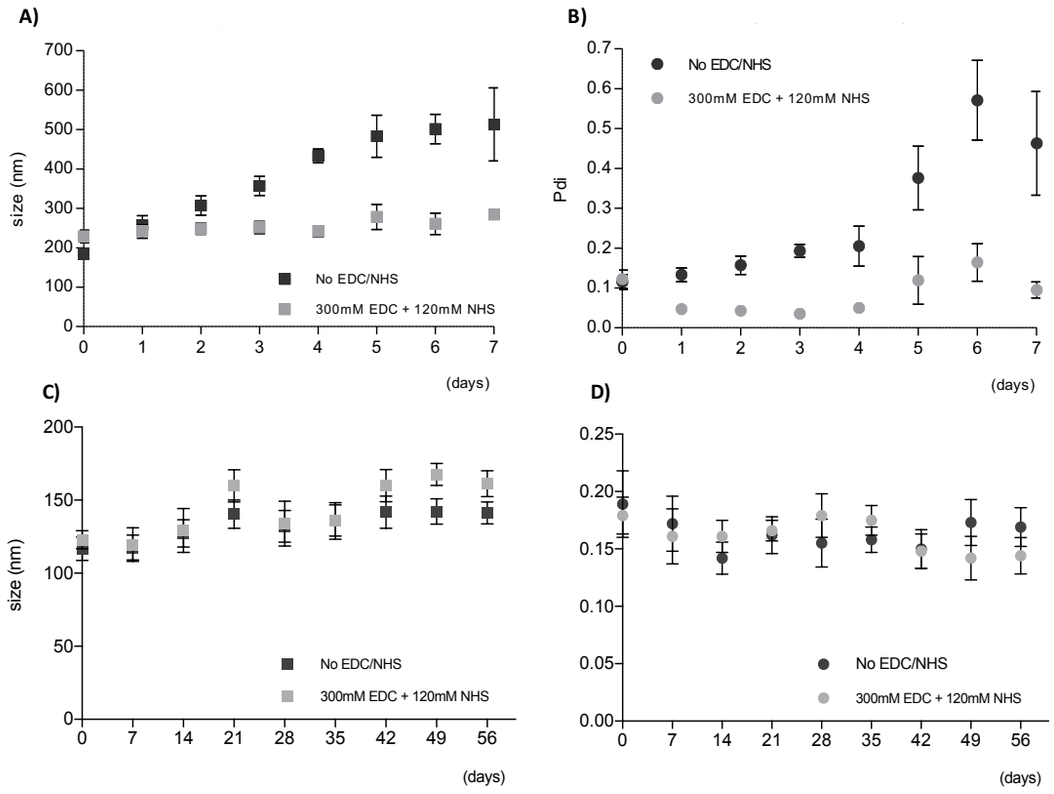

Figure VI-2 NPs stability at physiological (37°C and 0.9 % NaCl) (A and B) and storage conditions (4°C and UP W) (C and D). A) and C) regard size; B) and D) regard Pdi.

VI-3.2.2. Nanoparticles properties

Based on stability results, crosslinked nanoparticles were further characterized. NPs present a size of 140 nm, a Pdi = 0.172 and a zeta potential of 29 mV by DLS (**Table VI-1**). Nanoparticles were also evaluated by NTA, presenting presented a size around 116 nm and a final concentration of 7.81×10^{10}/ml.

Table VI-1 Nanoparticles characterization by DLS and NTA

DLS	Size (nm)	141 ± 17
	Pdi	0.172 ± 0.020
	Zeta potential (mV)	28.9 ± 3.5
NTA	Size (nm)	116 ± 17
	Concentration (particles/ml)	$7.8x10^{10} \pm 1.2x10^{10}$

Naoparticles morphology and size in dry state were also observed by SEM and STEM (**Figure VI-3 A**) and **B)**). Nanoparticles presented a round shape and a size smaller than 100 nm in both microscopic analysis.

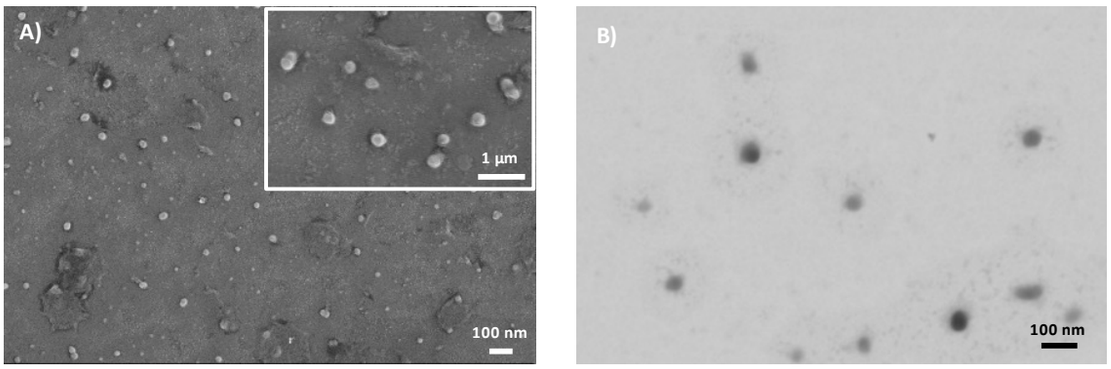

Figure VI-3 Nanoparticles morphology observation by SEM (A) and STEM (B).

VI-3.2.3. Nanoparticles cytotoxicity

After optimizing all the parameters, the cytotoxicity of the developed nanoparticles was evaluated over human endothelial (**Figure VI-4 – A**) and breast cancer (**Figure VI-4 – B**) cells. Different concentrations of NPs were tested and for concentrations above $8x10^9$ NPs mL^{-1} they start to be toxic for both cell types, despite some significant differences in previous concentrations and time points. By SEM analysis it was possible to observe the presence of the NPs at the surface of both cell types.

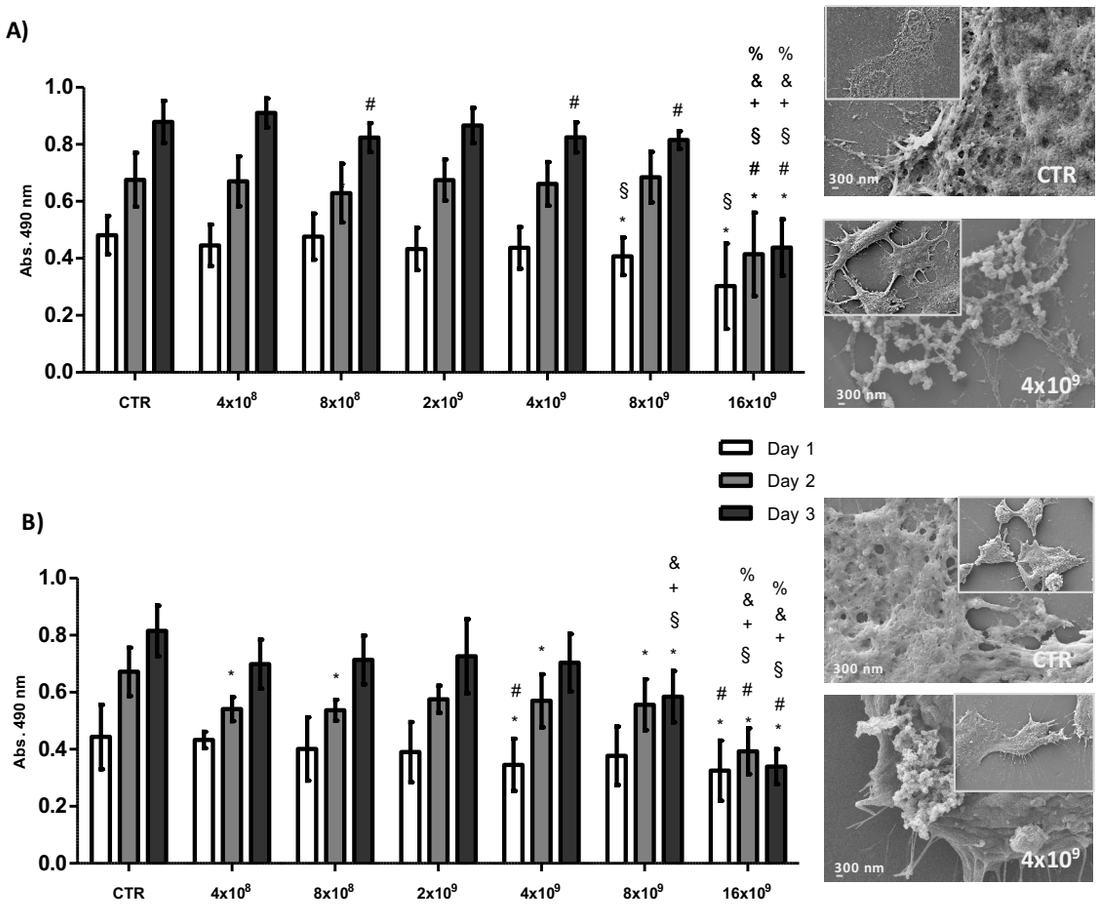

Figure VI-4 Cytotoxicity of developed NPs at different concentrations and time-points (1, 2 and 3 days), over human endothelial A) and breast cancer B) cells. Data was considered statistically significant at $p < 0.05$. * indicates significant differences compared to CTR; #, compared to 4x108; §, compared to 8x108; +, compared to 2x109; &, compared to 4x109 and % compared to 8x109. SEM observation of control and 4x109 NPs ml-1 culture conditions at day 3.

VI-3.3. Drug entrapment efficiency and release studies

VI-3.3.1. Gemcitabine entrapment efficiency

The drug entrapment efficiency was assessed by testing different gemcitabine concentrations. Concentration of 0.8 and 1.6 mg mL^{-1} present similar values and a maximum entrapment efficiency between 36 and 42%, respectively. At higher concentrations, the system saturates and the entrapment efficiency decreases to values around 30%.

In this sense, 0.8 mg/ml was the chosen concentration to evaluate the gemcitabine release profile, as well as the cytotoxic effects of gem-loaded nanoparticles over human endothelial and breast cancer

cells (**Figure VI-5 A**). Gem-loaded nanoparticles presented a size around 134 nm and a Pdi of 0.186 (**Figure VI-5 B**), similar to the values observed for the non-loaded nanoparticles (**Table I-1**).

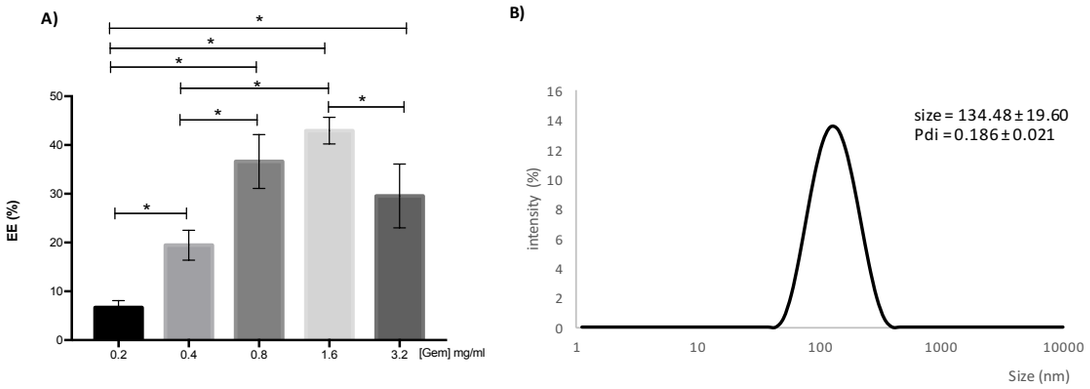

Figure VI-5 Entrapment efficiency of gemcitabine into the developed nanoparticles A); Gem-loaded NPs size distribution representation B).

VI-3.3.2. Gemcitabine release profile

The release of gemcitabine from marine-origin polymeric nanoparticles was evaluated at 37°C and 0.9% NaCl to mimic physiological conditions. Figure 6 shows that the developed system releases around 84% of the drug in a sustained way during 4 h, maintaining then a steady-state profile up to 72h (**Figure VI-6**).

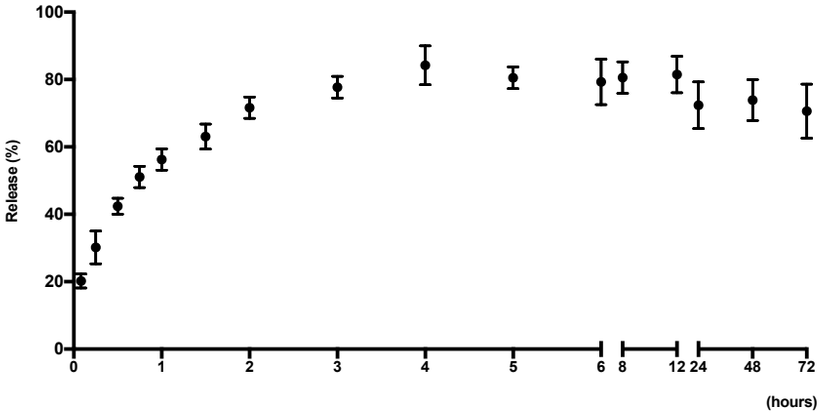

Figure VI-6 Gemcitabine release profile from marine-origin polymeric nanoparticles (0.9% NaCl, 37°C, 60 rpm).

VI-3.4. Cytotoxic effects of drug-loaded nanoparticles over cancer and non-cancer cells

Nanoparticles at $4x10^9$ NPs mL^{-1} do not present statistically significant differences when compared with the control condition for both endothelial and breast cancer cells, in all time points evaluated (**Figure VI-7**), confirming the results already reported in **Figure V-4**. However, gem-loaded nanoparticles (NPs_Gem) are cytotoxic for breast cancer cells since the first day, but being also cytotoxic at days 2 and 3 for endothelial cells. Free gemcitabine (Gem) presents also cytotoxicity to endothelial cells with similar values to the ones observed with NPs_Gem. Concerning breast cancer cells, NPs_Gem present increased toxicity at day 2 (15%) and at day 3 (25%) when comparing with free gemcitabine. Furthermore, NPs_Gem present higher toxicity over breast cancer than endothelial cells at day 3 (17%).

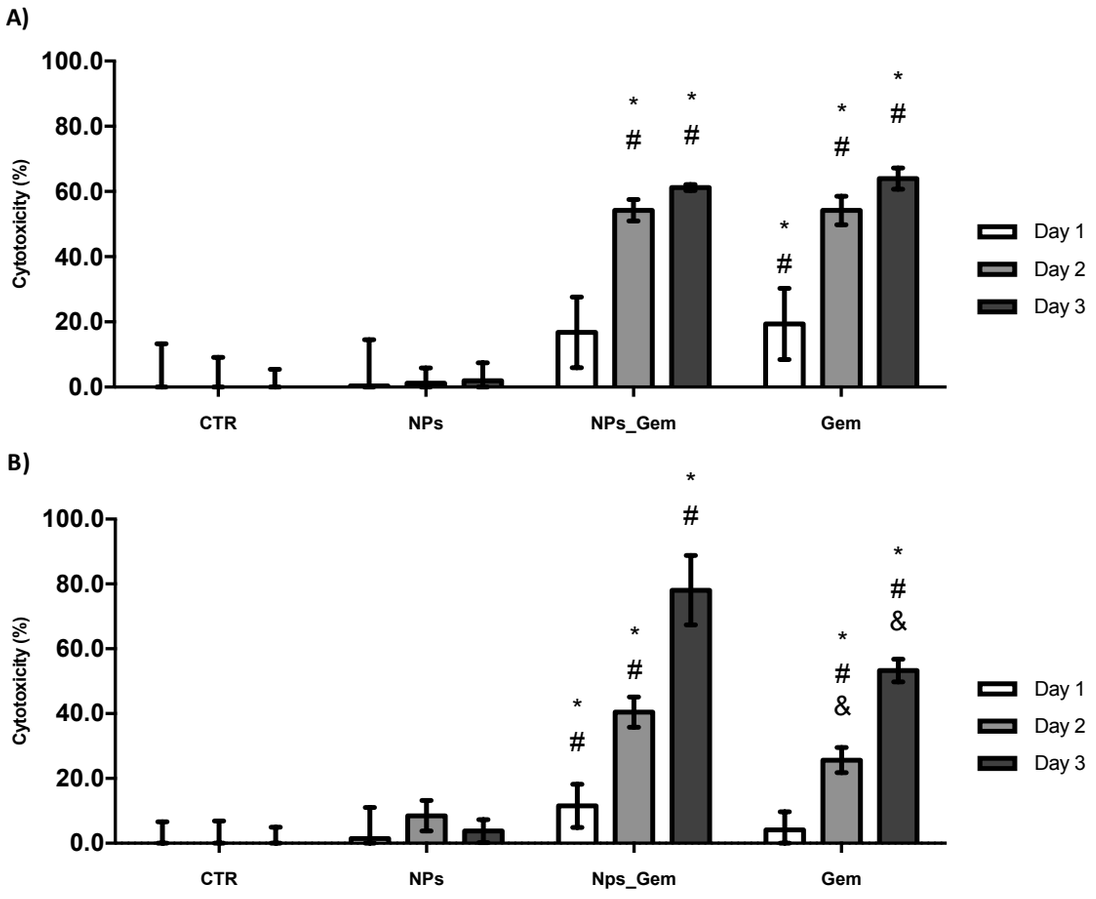

Figure VI-7 Cytotoxicity of developed Gem-loaded NPs at different time-points (1, 2 and 3 days), over human endothelial A) and breast cancer B) cells. Data was considered statistically significant when $p < 0.05$. * indicates significant differences compared to CTR; #, compared to NPs; &, compared to NPs_Gem.

VI-4. DISCUSSION

Polyelectrolyte complexation has been widely reported due to its cost-effectiveness and easy production of nanoparticles. It takes advantage of the interactions between two oppositely charged polymers and a spontaneous formation of the nanoparticles occurs [25]. There are different parameters described to affect nanoparticles size and polydispersive index, namely the polymers concentration and ratio, polymer solution pH and ionic strength [26, 27]. Our results showed that by decreasing polymers concentration, smaller nanoparticles were possible to be obtained. However, higher Pdi values are observed for both the high and low concentrations, showing obtainance of NPs with a non-homogenous size distribution. Thus, it seems that at higher concentrations there would be high entropy and at lower concentrations reduced interactions between oppositely charged polymers, resulting the influence of polymers ratio was also evaluated over NPs' size and Pdi. When higher amounts of fucoidan are present (CH:Fu_1:2), the nanoparticles present an increased size and Pdi, showing that probably there is the formation of polymeric aggregates instead of nanoparticles. Indeed, the amino groups of chitosan have a pKa ~6.5, which leads to a protonation in acidic conditions. In solutions with pH>6.5, most amino groups would be deprotonated and chitosan tends to precipitate [28]. Being deprotonated, the amine groups will be less available to form complex with fucoidan, resulting in a less controlled process, with the participation of other types of interactions gaining relevance, which will result in higher variability and consecutively high values of size and Pdi, outside the range to be considered as NPs. Chitosan at acidic pHs present protonated amines being these chemical groups more prone to form polyelectrolyte complexes with a negatively charged polymer (fucoidan), with ionic attractive interactions ruling the process, leading to the formation of the desired nanoparticles. Despite similar size values for the three other pHs, pH=5 was the one that presented more homogeneous nanoparticles' size. Fucoidan solution pH seems not to influence the development of nanoparticles size, although a low Pdi value is observed when the pH is not adjusted (pH=9). Ionic strength was analyzed by dissolving the polymers in different solvents, being ultrapure water the one that presents the better outcomes in terms of size and Pdi. As expected, 0.9% NaCl tends to form bigger and non-homogenous nanoparticles due to the presence of higher amounts of ions, which would have a charge shielding effect over the protonated groups in polyelectrolytes and thus decreasing the relevance of ionic interactions in the assembly process. Fucoidan/chitosan nanoparticles may become unstable at physiological conditions due to the deprotonation of chitosan amine groups. Trying to enhance nanoparticles stability, a crosslinking agent was tested: EDC/NHS. EDC is often used to crosslink amines (NH_2) to carboxylate groups, which activity

is enhanced by NHS through activation of the carboxylate group [29]. In the present case the rationale is to crosslink the amine groups of chitosan with the carboxylic group of the uronic acids that are present in fucoidan structure [8]. Different concentration of EDC/NHS were evaluated and the 300 mM EDC + 120 mM NHS presented the smaller Pdi. Despite 150 mM EDC + 60 mM NHS present similar results, these concentrations presented higher Pdi, reason why a higher concentration was chosen to continue the study. Higher concentrations (600 mM EDC+ 240 mM NHS), seem to start precipitating and affecting nanoparticles' size, increasing it to around 300 nm. Nanoparticles final formulation was set as: 0.5 mg/ml polymers concentration; 1:1 ratio; pH (chitosan) = 5 and pH (fucoidan) = 9 and ultra-pure as the polymer's solvent.

After this optimization process and setting all the parameters, two conditions were chosen to conduct the stability assays: one without crosslinking and the other crosslinked. Nanoparticles stability at physiological and storage conditions was assessed. Physiological conditions were mimetized by diluting the produced nanoparticles in 0.9% NaCl, which have an osmolarity similar to circulating plasma 285 - 295 mOsm/L [30]. Both nanoparticles increase their size to around 200 nm, when in contact with this isotonic solution, due to an increase in the ionic strength with associated charge shielding but also higher waster uptake (Donnan Effect) [31]. Crosslinked nanoparticles present a quite stable profile along the 7 days, whereas from day 3 on, the non-crosslinked NPs start to increase their size, indicating that they probably start to disintegrate at physiological osmolarity. We proceed the characterization of crosslinked nanoparticles which present a size around 140/115 nm (DLS/NTA), a Pdi of 0.172, which indicates that these NPs are quite homogeneous and a zeta potential of + 29 mv indicating that chitosan is at the surface of nanoparticles. By NTA, the nanoparticles presented a smaller size due to the fact that NTA is a more precise technique than DLS [32]. By SEM and STEM observation we were able to confirm the round morphology of the NPs, with a size smaller than 100 nm. The difference between DLS/NTA measurements and SEM/STEM is due to the fact that in the first characterization, NPs are measured in wet state, whereas for SEM/STEM, nanoparticles are analyzed in a dry state.

After all the optimization steps, the cytotoxicity of the developed marine-origin polymeric NPs was evaluated over human endothelial and breast cancer cells at different concentrations. NPs start to become more toxic to both cell types at the highest concentrations ($8x10^9$ NPs mL^{-1} and $16x10^9$ NPs mL^{-1}) tested. From SEM observation, we were able to observe NPs at the surface of both cells' types. From these results, $4x10^9$ NPs mL^{-1} concentration (non-toxic concentration) was selected to conduct the further experiments.

Breast cancer is sensitive to several cytotoxic drugs that may be used as single or combined therapies. In the past years new cytotoxic agents have been developed and approved to be used in cancer treatments. Gemcitabine have shown antitumor activity and good toxicity profiles to be used as single-agent therapy for advanced breast cancer. One of the drawbacks of using gemcitabine by intravenous or oral administration is related with its rapid inactivation by enzymatic delamination, low bioavailability and short half-life. These problems require an increase in dosage that may lead to unwanted side effects [19-22]. The use of nanoparticles may overcome some of these limitations since they will be able to protect the drug from enzymatic degradation, diminishing the above-mentioned efficiency problems [33].

The loading of gemcitabine on the marine-origin polymeric NPs was evaluated by testing different gemcitabine concentrations. It was possible to observe that, by increasing the concentration of the drug, there is an increase in the entrapment efficiency until it reaches a maximum concentration of 1.6 mg mL^{-1} (EE=42%). At 3.2 mg mL^{-1} the system saturates and the entrapment efficiency (EE) decreases to around 30%. Gem-loaded NPs were characterized in terms of size and Pdi, showing no significant differences. The release profile was assessed at 37°C and 0.9% NaCl to mimic physiological conditions. From the stability studies, it was observed that the nanoparticles size of the nanoparticles increased, due to the ionic strength of the solution which weakens the electrostatic interactions, leading to the release of gemcitabine from the nanoparticles [10]. Around 84% of gemcitabine was released in the first 4hours in a sustained way, reaching then a steady-state.

To assess the antitumor activity of the developed DDS, it is important to have in mind the tumor microenvironment that comprises not only cancer cells but also non-cancer cells (e.g. endothelial, fibroblasts). Indeed, being gem-loaded nanoparticles intended to be injected intravenously, the first barrier they will face is the blood vessels wall and thus endothelial cells. Different fucoidan-based nanoparticles have been developed as anticancer strategies. As example, fucoidan-cisplatin nanoparticles have been developed and evaluated for colon cancer [34], whereas fucoidan encapsulated into liposomes showed anticancer activity against osteosarcoma [35]. In another attempt, ddoxorubicin was incorporated into a protamine/fucoidan system and these loaded-nanoparticles improved inhibitory effects against a breast cancer cell line [36]. However, as far as we know there are no studies in the literature that report the use of fucoidan to develop nanoparticles for the delivery of gemcitabine. On the other hand, chitosan-based nanoparticles have been studied for the delivery of antitumoral agents, namely for the delivery of gemcitabine. For example, the loading of gemcitabine into chitosan magnetic nanoparticles increased gemcitabine efficacy when compared with free gemcitabine [37]. In other study, chitosan-based

nanoparticles were prepared by layer-by-layer technique for the incorporation of gemcitabine and platinum aiming lung cancer treatments [38]. Other studies reported the use of chitosan-based nanoparticles for the delivery of other antitumor drugs: PEG-layered chitosan nanoparticles enhanced the efficacy of ormeloxifene in breast cancer [39] and platinum-gold nanoparticles with chitosan and doxorubicin presented cell specific cytotoxicity [40].

In this sense, the combination of these two marine-origin polymers to develop nanoparticles for the delivery of gemcitabine is a novel process with potential positive outcome. We evaluated the gemcitabine loaded-nanoparticles toxicity over human endothelial and breast cancer cell lines. Regarding endothelial cells both Gem-loaded NPs and free Gem present similar cytotoxicity values. However, concerning breast cancer cells Gem-loaded NPs increased toxic effects of around 15% and 25% at day 2 and day 3, respectively, when compared with free gemcitabine. At day 3, when comparing breast cancer and endothelial cells, it was observed an increased cytotoxicity of around 17%, over breast cancer cells. The increased cytotoxicity of the Gem-loaded NPs when compared with free gemcitabine may be attributed to the cellular trafficking pathway, suggesting a more effective uptake of the drug by breast cancer cells. The encapsulation of cisplatin into chitosan lipid nanoparticles was reported, demonstrating increased apoptosis in cancer cells when compared with free cisplatin [41]. A recent paper reported that chitosan nanoparticles loaded with curcumin reduced the drug uptake in normal cells, while the same was internalized into cancer cells [42]. Another study reported the internalization of chitosan-coated nanoparticles loaded with doxorubicin into breast cancer cells cytoplasm and nucleus. The authors stated that the uptake of these nanoparticles may be attributed to the positive charge of their surface. That positively charged chitosan nanoparticles can have charge-based interaction with the cell membrane and may enter cells either by direct penetration or by endocytosis [43]. Thus, although not presenting a protective effect against the toxicity over endothelial cells, the fucoidan/chitosan nanoparticles exhibit a synergistic effect with gemcitabine resulting in a higher toxicity over breast cancer cells. Moreover, these results confirm that, by encapsulating gemcitabine into a nanoparticle, the drug is protected from enzymatic degradation, increasing its half-life and biological response.

VI-5. CONCLUSION

In conclusion, marine-origin polymeric nanoparticles were successfully produced by polyelectrolyte complexation, presenting increased at physiological conditions when crosslinked with EDC/NHS.

Gemcitabine was encapsulated in the developed nanoparticle system. This DDS increased toxicity over human breast cancer cells, when compared with free gemcitabine, without increasing their toxic effect over endothelial cells. Taken together, the herein developed DDS is an interesting strategy to be further explored on breast cancer therapies.

VI-6. ACKNOWLEDGEMENTS

The authors thank the PhD scholarship of C. Oliveira for 'NORTE-08-5369-000037' financed by NORTE 2020, Portuguese Foundation for Science and Tecnology (FCT) for the investigator grant of A Martins for (IF/00376/2014) and the support from European Research Council under the Advanced Grant ComplexiTE. The work here reported also received financial support from the European Regional Development Fund (ERDF) under the Structured Project 'Accelerating tissue engineering and personalized medicine discoveries by the integration of key enabling nanotechnologies, marine-derived biomaterials and stem cells' (NORTE-01-0145-FEDER-000021), supported by Norte Portugal Regional Operational Program (NORTE 2020), under the PORTUGAL 2020 Partnership Agreement. The authors have no other relevant affiliations or financial involvement with any organization or entity with a financial interest in or financial conflict with the subject matter or materials discussed in the manuscript apart from those disclosed.

VI-7. REFERENCES

[1] R. Siegel, J. Ma, Z. Zou, A. Jemal, Cancer statistics, 2014, CA Cancer J Clin 64(1) (2014) 9-29.

[2] C. DeSantis, J. Ma, L. Bryan, A. Jemal, Breast cancer statistics, 2013, CA Cancer J Clin 64(1) (2014) 52-62.

[3] P.G. Aftimos, A. Gombos, L. Pugliano, A. Awada, M.J. Piccart, Breast Cancer, in: M.A. Dicato (Ed.), Side Effects of Medical Cancer Therapy: Prevention and Treatment, Springer London, London, 2013, pp. 29-117.

[4] M.A. Moyad, Rapid Review of Breast Cancer Treatment Side Effects and Dietary Supplement/Integrative Options from A to Z: What Helps, Harms, or Does Nothing?, in: M.A. Moyad (Ed.), Integrative Medicine for Breast Cancer: An Evidence-Based Assessment, Springer International Publishing, Cham, 2016, pp. 225-342.

[5] T.H. Silva, A. Alves, B.M. Ferreira, J.M. Oliveira, L.L. Reys, R.J.F. Ferreira, R.A. Sousa, S.S. Silva, J.F. Mano, R.L. Reis, Materials of marine origin: a review on polymers and ceramics of biomedical interest, International Materials Reviews 57(5) (2012) 276-306.

[6] F. Atashrazm, R.M. Lowenthal, G.M. Woods, A.F. Holloway, J.L. Dickinson, Fucoidan and Cancer: A Multifunctional Molecule with Anti-Tumor Potential, Marine Drugs 13(4) (2015) 2327-2346.

[7] J.H. Fitton, D.N. Stringer, S.S. Karpiniec, Therapies from Fucoidan: An Update, Marine Drugs 13(9) (2015) 5920-5946.

[8] C. Oliveira, A.S. Ferreira, R. Novoa-Carballal, C. Nunes, I. Pashkuleva, N.M. Neves, M.A. Coimbra, R.L. Reis, A. Martins, T.H. Silva, The Key Role of Sulfation and Branching on Fucoidan Antitumor Activity, Macromolecular Bioscience 17(5) (2017) 1600340.

[9] L. Chollet, P. Sabboural, C. Chauvierre, J.-N. Villemin, D. Letourneur, F. Chaubet, Fucoidans in Nanomedicine, Marine Drugs 14(8) (2016) 145.

[10] K.-Y. Lu, R. Li, C.-H. Hsu, C.-W. Lin, S.-C. Chou, M.-L. Tsai, F.-L. Mi, Development of a new type of multifunctional fucoidan-based nanoparticles for anticancer drug delivery, Carbohydrate Polymers 165 (2017) 410-420.

[11] Y.C. Huang, Y.T. Yang, Effect of basic fibroblast growth factor released from chitosan-fucoidan nanoparticles on neurite extension, Journal of tissue engineering and regenerative medicine 10(5) (2016) 418-27.

[12] Y.-C. Huang, J.-K. Chen, U.I. Lam, S.-Y. Chen, Preparing, characterizing, and evaluating chitosan/fucoidan nanoparticles as oral delivery carriers, Journal of Polymer Research 21(5) (2014) 415.

[13] Y.-C. Huang, R.-Y. Li, Preparation and Characterization of Antioxidant Nanoparticles Composed of Chitosan and Fucoidan for Antibiotics Delivery, Marine Drugs 12(8) (2014) 4379-4398.

[14] Z. Liu, Y. Jiao, Y. Wang, C. Zhou, Z. Zhang, Polysaccharides-based nanoparticles as drug delivery systems, Adv Drug Deliv Rev 60(15) (2008) 1650-62.

[15] F. Masood, Polymeric nanoparticles for targeted drug delivery system for cancer therapy, Mater Sci Eng C Mater Biol Appl 60 (2016) 569-78.

[16] H. Hayashi, T. Kurata, K. Nakagawa, Gemcitabine: Efficacy in the Treatment of Advanced Stage Nonsquamous Non-Small Cell Lung Cancer, Clinical Medicine Insights. Oncology 5 (2011) 177-184.

[17] H. Kawaguchi, Y. Terai, A. Tanabe, H. Sasaki, M. Takai, S. Fujiwara, K. Ashihara, Y. Tanaka, T. Tanaka, S. Tsunetoh, M. Kanemura, M. Ohmichi, Gemcitabine as a molecular targeting agent that blocks the Akt cascade in platinum-resistant ovarian cancer, Journal of Ovarian Research 7 (2014) 38-38.

[18] E.M. O'Reilly, J. Roach, P. Miller, K.H. Yu, C. Tjan, M. Rosano, S. Krause, W. Avery, J. Wolf, K. Flaherty, D. Nix, D.P. Ryan, Safety, Pharmacokinetics, Pharmacodynamics, and Antitumor Activity of Necuparanib Combined with Nab-Paclitaxel and Gemcitabine in Patients with Metastatic Pancreatic Cancer: Phase I Results, The oncologist 22 (2017) 1429.

[19] L.W. Hertel, G.B. Boder, J.S. Kroin, S.M. Rinzel, G.A. Poore, G.C. Todd, G.B. Grindey, Evaluation of the antitumor activity of gemcitabine (2',2'-difluoro-2'-deoxycytidine), Cancer research 50(14) (1990) 4417-22.

[20] S. Modi, A.D. Seidman, Single-agent gemcitabine in the treatment of advanced breast cancer, Clinical breast cancer 4 Suppl 3 (2004) S101-6.

[21] V. Heinemann, Role of gemcitabine in the treatment of advanced and metastatic breast cancer, Oncology 64(3) (2003) 191-206.

[22] G.N. Hortobagyi, Treatment of advanced breast cancer with gemcitabine and vinorelbine, Oncology (Williston Park, N.Y.) 15(2 Suppl 3) (2001) 15-7.

[23] T. Santiago, R.S. DeVaux, K. Kurzatkowska, R. Espinal, J.I. Herschkowitz, M. Hepel, Surface-enhanced Raman scattering investigation of targeted delivery and controlled release of gemcitabine, Int J Nanomedicine 12 (2017) 7763-7776.

[24] M. Smith, M. Hepel, Controlled release of targeted anti-leukemia drugs azacitidine and decitabine monitored using surface-enhanced Raman scattering (SERS) spectroscopy, Mediterranean Journal of Chemistry 6(4) (2017) 125.

[25] A.C. Lima, P. Sher, J.F. Mano, Production methodologies of polymeric and hydrogel particles for drug delivery applications, Expert Opinion on Drug Delivery 9(2) (2012) 231-248.

[26] J. Venkatesan, S. Anil, S.-K. Kim, M. Shim, Seaweed Polysaccharide-Based Nanoparticles: Preparation and Applications for Drug Delivery, Polymers 8(2) (2016) 30.

[27] E.J. Lee, K.-H. Lim, Formation of chitosan-fucoidan nanoparticles and their electrostatic interactions: Quantitative analysis, Journal of Bioscience and Bioengineering 121(1) (2016) 73-83.

[28] S.-K. Kim, Chitin and Derivatives: Advances in Drug Discovery and Developments, CRC Press 2013.

[29] J.V. Staros, R.W. Wright, D.M. Swingle, Enhancement by N-hydroxysulfosuccinimide of water-soluble carbodiimide-mediated coupling reactions, Analytical Biochemistry 156(1) (1986) 220-222.

[30] A.D.A. Wahed, Water, Homeostasis, Electrolytes, and Acid–Base Balance, Clinical Chemistry, Immunology and Laboratory Quality Control 2014, pp. 67-84.

[31] J. Jiang, G. Oberdörster, P. Biswas, Characterization of size, surface charge, and agglomeration state of nanoparticle dispersions for toxicological studies, Journal of Nanoparticle Research 11(1) (2009) 77-89.

[32] V. Filipe, A. Hawe, W. Jiskoot, Critical evaluation of Nanoparticle Tracking Analysis (NTA) by NanoSight for the measurement of nanoparticles and protein aggregates, Pharm Res 27(5) (2010) 796-810.

[33] K. Derakhshandeh, S. Fathi, Role of chitosan nanoparticles in the oral absorption of Gemcitabine, Int J Pharmaceut 437(1) (2012) 172-177.

[34] P.-A. Hwang, X.-Z. Lin, K.-L. Kuo, F.-Y. Hsu, Fabrication and Cytotoxicity of Fucoidan-Cisplatin Nanoparticles for Macrophage and Tumor Cells, Materials 10(3) (2017) 291.

[35] R. Kimura, T. Rokkaku, S. Takeda, M. Senba, N. Mori, Cytotoxic Effects of Fucoidan Nanoparticles against Osteosarcoma, Marine Drugs 11(11) (2013) 4267-4278.

[36] Y.H. Lin, K.Y. Lu, C.L. Tseng, J.Y. Wu, C.H. Chen, F.L. Mi, Development of genipin-crosslinked fucoidan/chitosan-N-arginine nanogels for preventing Helicobacter infection, Nanomedicine (Lond) 12(12) (2017) 1491-1510.

[37] M. Parsian, G. Unsoy, P. Mutlu, S. Yalcin, A. Tezcaner, U. Gunduz, Loading of Gemcitabine on chitosan magnetic nanoparticles increases the anti-cancer efficacy of the drug, European Journal of Pharmacology 784(Supplement C) (2016) 121-128.

[38] R. Zhang, Y. Ru, Y. Gao, J. Li, S. Mao, Layer-by-layer nanoparticles co-loading gemcitabine and platinum (IV) prodrugs for synergistic combination therapy of lung cancer, Drug Des Devel Ther 11 (2017) 2631-2642.

[39] S. Agrawal, H. Ahmad, M. Dwivedi, M. Shukla, A. Arya, K. Sharma, J. Lal, A.K. Dwivedi, PEGylated chitosan nanoparticles potentiate repurposing of ormeloxifene in breast cancer therapy, Nanomedicine (Lond) 11(16) (2016) 2147-69.

[40] V. Maney, M. Singh, An in vitro assessment of novel chitosan/bimetallic PtAu nanocomposites as delivery vehicles for doxorubicin, Nanomedicine (Lond) 12(21) (2017) 2625-2640.

[41] J.Y. Wang, Y. Wang, X. Meng, Chitosan Nanolayered Cisplatin-Loaded Lipid Nanoparticles for Enhanced Anticancer Efficacy in Cervical Cancer, Nanoscale Res Lett 11(1) (2016) 524.

[42] A. Abruzzo, G. Zuccheri, F. Belluti, S. Provenzano, L. Verardi, F. Bigucci, T. Cerchiara, B. Luppi, N. Calonghi, Chitosan nanoparticles for lipophilic anticancer drug delivery: Development, characterization and in vitro studies on HT29 cancer cells, Colloids Surf B Biointerfaces 145 (2016) 362-372.

[43] V.M. Kulkarni, D. Bodas, D. Dhoble, V. Ghormade, K. Paknikar, Radio-frequency triggered heating and drug release using doxorubicin-loaded LSMO nanoparticles for bimodal treatment of breast cancer, Colloids Surf B Biointerfaces 145 (2016) 878-890.

Chapter VII

Marine-polymeric nanoparticles targeting ErbB-2 impair breast cancer cells growth and metastasis

Chapter VII

Functionalized marine-polymeric nanoparticles targeting ErbB-2 impair breast cancer cells growth and metastasis††

ABSTRACT

Overcoming the side effects of current chemotherapeutic drugs is still a major challenge in cancer therapies. The development of targeted strategies would be of great interest to direct drugs specifically to cancer cells, diminishing the side effects over normal healthy tissues. Since human epidermal growth factor receptor 2 (HER-2 or ErbB-2) is overexpressed in some subtypes of breast cancer, herein the ErbB-2 antibody was used to direct the delivery of a chemotherapeutic drug, gemcitabine (Gem). Specifically, this work reports the development of fucoidan/chitosan nanoparticles (NPs) loaded with Gem (NPs+Gem), and immobilizing ErbB-2 antibody at their surface (NPs+Gem+Ab). The maximum immobilization was set at 10 μg ml^{-1} and resulted in NPs with a size around 160 nm and a polydispersity index of 0.178. The targeting capability of the NPs+Gem+Ab system was confirmed with internalization assays for the SKBR3 (ErbB-2 positive breast cancer cells), but not for the MDA-MB-231 (ErbB-2 negative) cell line. To further validate the efficacy of the targeting, a co-culture system with human endothelial and SKBR3 cells was established mimicking the endothelial barrier *in vitro*. The NPs+Gem+Ab system presented an increased toxicity over breast cancer cells, above 80% at day 1, whereas free Gem and NPs+Gem only presented toxicity around 15% and 20%, respectively. Inversely, free Gem was about 20% more toxic over endothelial cells than the NPs with and without ErbB-2 antibody immobilization. *In vivo* studies demonstrated that the developed targeting system was able to significantly reduce tumor growth and the appearance of lung metastasis in comparison with untreated controls. In summary, the efficacy of the NPs+Gem+Ab system to target cancer cells was established and validated both *in vitro* and *in vivo*, constituing a compelling alternative strategy to current chemotherapeutic approaches.

†† This chapter is based on the following publication:

Oliveira C., Gonçalves C.S., Neves N. M., Reis R. L., Costa B.M., Silva T. H., Martins A. Functionalized *marine-polymeric nanoparticles targeting ErbB-2 impair breast cancer cells growth and metastasis*. (Submitted).

VII-1. INTRODUCTION

Breast cancer is the most common and deadliest malignant disease in women [1]. Like other types of cancer, breast cancer is highly heterogenous and can be divided in different molecular subtypes: triple negative, HER2$^+$, luminal A and luminal B, depending on their immune profile. Luminal A are the most common (around 40%), followed by luminal B (around 20%), being both estrogen receptor positive and the ones with better prognosis. The triple negative breast cancers are the ones with the worst diagnosis, representing 15-20% of the cases. HER2$^+$ breast cancers have a better prognosis than the triple negative, but worst than Luminal A, accounting for 10-15% of all breast cancers [2, 3]. Due to the heterogeneity of breast cancer, complex and multidisciplinary treatment approaches are required. Current treatments are mainly based in the combination of surgery, chemotherapy and radiation. Despite an increase in the survival rates over the last years, more precise treatments that minimize the side effects to current therapes are still required [4, 5].

Nanoparticles (NPs) have attracted increasing interest over the last years, namely has drug delivery systems due to their particularities. Specifically, they can increase macromolecules stability by protecting drug from degradation, increasing drug concentration in cancer cells. NPs tend to accumulate at tumor sites which may be due to a leaky vascularization, enabling and enhancing the permeability and retention effect (passive targeting) [6]. On the other hand, nanoparticles have an high surface area that allows an easy functionalization, which is of great interest when designing targeted approaches (active targeting) [7]. However, drug loss during circulation may occur and only certain types of cells express specific cell surface receptors, which limits its application in the clinic [8].

Different ligands can be used for nanoparticles active targeting purposes, namely antibodies, growth factors and cytokines, which effectiveness will depend on the type of receptors expressed on cancer cells membrane [9]. This ligand–receptor interaction results in increased cellular uptake by receptor-mediated endocytosis and respective internalization of the NPs, being the drug released inside the targeted cells, leading to a more effective action of the drug [10, 11]. Antibodies are one the most common target ligands since they have an high binding affinity to antigens or receptors on cancer cell membrane [12]. The use of active targeting ligands that are over expressed in cancer cells may offer an interesting alternative, trying to overcome some of the limitations, namely the toxic effects over normal tissues. It is the case of human epidermal growth factor receptor 2 (HER-2 or ErbB-2), which is over expressed in around 30% of breast cancers and weakly expressed in normal cells [13].

ErbB-2 antibodies have been approved by the US Food and Drug Administration (FDA) for the treatment of HER2-positive breast cancer [14]. Different studies have shown that the combination of ErbB-2 antibody and chemotherapeutic drugs presented promising biological responses [15-17]. Therefore, the immobilization of a specific antibody that recognizes the HER2 receptor may offer an opportunity to target the NPs to breast cancer cells, reducing the side effects to other tissues.

Marine natural products present interesting features like low toxicity and similarities to the components of human native tissues, which make them attractive material sources for the production of nanoparticles [18]. Particularly, fucoidan and chitosan have been studied and reported has good candidates to develop more effective drug delivery systems, namely for cancer therapies [19-22]. Aiming to develop more effective therapeutics, ErbB-2 antibody has also been immobilized at the surface of chitosan-based nanoparticles to target ErbB-2^{+} breast cancer cells [23, 24]. However, to the best of our knowledge, there is no study reporting the use or immobilization of ErbB-2 antibody within fucoidan-based approaches.

As so, herein ErbB-2 antibody was immobilized at the surface of fucoidan/chitosan nanoparticles loaded with gemcitabine, aiming to enhance the efficacy of a drug delivery system for breast cancer treatment. To assess the efficiency of immobilized antibody, two different human breast cancer cells were used for cellular uptake assays: SKBR3 (ErbB-2 positive) and MDA-MB-231 (ErbB-2 negative) cell lines. After validating the nanoparticles efficiency to target ErbB-2 positive cancer cells, a co-culture system was established with human endothelial cells (EA.hy.926 cell line as a model of normal cells) and SKBR3 cells mimicking physiological conditions *in vitro*. Furthermore, immunosuppressed female mice injected with human cancer cells were used as a model to study the efficacy of the develop targeting system *in vivo*.

VII-2. Materials and Methods

VII-2.1. Materials

Fucoidan from *Fucus vesiculosus* was purchased from Marinova (batch number: DPFVF2015505; molecular weight [MW] by gel permeation chromatography [GPC] 45–75 kDa), whereas chitosan, CH 95/20, was purchased from Heppe Medical Chitosan GmbH (Halle, Germany; batch number: 212-261115-04, MW by GPC 40–150 kDa). 2′-Deoxy-2′,2′-difluorocytidine (Gem – $C_9H_{11}F_2N_3O_4$) was purchased from Carbosynth (Berkshire, UK). 1-[3-(Dimethylamino)propyl]-3-ethylcarbodiimide hydrochloride (EDC),

N-hydroxysuccinimide (NHS) and Fluorescein isothiocyanate–dextran average mol wt 4,000, (FITC:Glucose = 1:250) and phalloidin-Tetramethylrhodamine B isothiocyanate (Phalloidin) were all purchased from Sigma-Aldrich (Misssouri, USA). 4,6-Diamidino-2-phenyindole, dilactate (DAPI) was purchased from Biotium (California, USA). ErbB-2 antibody (ERBB2 Monoclonal Antibody (clone 7H3L20), ABfinity Recombinant) was purchased from Thermo Fisher Scientific (Massachusetts, USA). Alexa Fluor 488 was purchased from Molecular Probes (Oregon, USA). Human umbilical vein endothelial cells (EA.hy.926 cell line) and breast cancer cells (SKBR3 and MDA-MB-231 cell lines) were both purchased from ATCC (Virginia, USA).Centrifugal concentrators Vivaspin 20 300 KD (Sartorius; Stonehouse, UK) were purchased from Fisher Scientific.

VII-2.2. Nanoparticles production and characterization

VII-2.2.1. Production of nanoparticles delivery systems

Nanoparticles were produced by polyelectrolyte complexation as previously described [19]. Briefly, fucoidan was added drop-by-drop, with a precision syringe pump, into chitosan solution (with gemcitabine, 1:3 w/w). EDC/NHS (300 mM+120 mM) was added to increase nanoparticles stability. The nanoparticles were than separated by using an centrifugal concentrator to remove unbound polymers. Lastly, nanoparticles were re-suspended in ultrapure water (UPW).

VII-2.2.2. ErbB-2 antibody immobilization and quantification

ErbB-2 antibody was immobilized at the surface of the developed nanoparticles, based on a previous reported work [25]. A wide range of antibody concentrations (from 0 to 20 μg mL^{-1}) were tested to determine the maximum immobilization capacity of the NPs. The antibody was previously activated with EDC/NHS for 15 minutes (26 mM EDC + 104 mM NHS in 0.1 M MES) and NPs were incubated with different concentrations of antibody for 2h under stirring. The solution was then centrifuged to remove unbound antibody and the NPs re-suspended in UPW. In order to determine the degree of immobilization, an indirect method was used to quantify the fluorescence of unbound secondary antibody solution. Alexa Fluor 488-conjugated (1:100) was incubated for 1h, with the following reading parameters: 495 nm for the adsorption and 519 nm for the emission. Negative controls were also prepared, where all antibody

immobilization steps were performed with the exception of the primary antibody incubation, which was replaced by UPW.

VII-2.2.3. Dynamic light scattering

The NPs' size and polydispersive index (Pdi) were determined by dynamic light scattering (DLS) using a Zetasizer Nano ZS (Malvern Instruments, Malvern, UK). Samples were diluted in UPW and the size analysis lasted 180s and was performed at 25°C, in triplicate for n=3.

VII-2.2.4. Morphological analysis

Morphological analysis of the develop targeting NPs was obtained using Atomic Force Microscopy (AFM) by a MultiMode STM microscope controlled by a NanoScope III from Digital Instruments system, operating in tapping mode at a frequency of 1 Hz. Briefly, a drop of NPs solution was placed in a glass slide and left to dry overnight. The analysis were performed using a MultiMode STM microscope controlled by a NanoScope III from Digital Instruments system, operating in tapping mode at a frequency of 1 Hz.

VII-2.3. Biological assays

VII-2.3.1. Cell culture and expansion

Human endothelial cells (EA.hy926 cell line) were cultured in D-MEM Low Glucose medium supplemented with 10% FBS (Biochrom; Germany) and 1% Pen/Strep (100 U/100 g mL^{-1}; Life Technologies). Human breast cancer cells (SKBR3 and MDA-MB-231) were cultured in D-MEM high glucose medium (Sigma-Aldrich; USA) supplemented with 10% Fetal Bovine Serum (FBS) (Thermo Fisher; USA), Pen/Strep (100 U/100 g mL^{-1}; Life Technologies) and 1% MEM sodium pyruvate solution 100 × 10^{-3} M (Thermo Fisher; USA). The three cell lines were incubated at 37°C in a humidified 5% CO_2 atmosphere. Media were exchanged every 2–3 days until cells reached a 80-90% confluence.

VII-2.3.2. NPs Cellular uptake

FITC was added to chitosan solution at 2mg ml^{-1} to fluorescently label the nanoparticles, produced as described in a previous section. Three different cell types were seeded in tissue culture coverslips at a density of $1.5x10^4$. After cells' adherence, NPs (NPs+FITC) and NPs with the immobilized ErbB-2 antibody (NPs+FITC+Ab) were added to the culture; a negative control with only cells was performed for each cell type. After 24h, the different conditions were rinsed with PBS and the cells were fixed with 10% formalin (Bio-optica, Italy). To evaluate whether and where the NPs have been internalized the cytoskeleton and nucleus of those cells were also fluorescent labeled. For that, phalloidin (1:250 in PBS) was added and left to incubate for 45 min. Another washing step was performed and the same samples were incubated with DAPI (1:1000 in PBS) for 15 min. Cell were washed with PBS and observed in an Inverted Confocal Microscope with Incubation (TCS SP8, Leica) at 20x magnifications.

VII-2.3.3. Co-culture system with endothelial and ErbB-2 positive breast cancer cells

The co-culture system was performed using Nunc Polycarbonate Cell Culture Inserts in Multi-Well Plates (Thermo Fischer, USA). Endothelial cells were seeded and cultured on top as $3x10^4$ cells/insert for 3 days, to allow cells proliferation and the formation of an endothelial monolayer. After that, ErbB-2 positive breast cancer cells (SKBR3 cell line) were cultured, as $1.5x10^4$ cells were seeded and cultured at the bottom of 24 well-plates. The culture medium of each cell type was maintained separatly. In the following day, the developed trageting system (NPs+Gem+Ab) and the controls (NPs+Gem or free Gem) were added over endothelial cells at a previously predefined concentration (50 µl NPs mL^{-1}) [19]. MTS assay and live/dead stainning was performed at days 1, 2 and 3 after co-culture establishment.

VII-2.3.4. MTS assay

The CellTiter 96 AQueous One Solution cell proliferation assay (Promega; WI, USA) was performed at the defined time points. Firstly, the culture medium was removed and the testing samples were rinsed with sterile phosphate-buffered saline (PBS). A mixture of culture medium (without Fetal Bovine Serum and phenol red) and MTS reagent (5:1 ratio) was added to each well and left to incubate for 3h, at 37°C, in a humidified 5% CO_2 atmosphere. Thereafter, the absorbance of the MTS reaction medium from each

sample was read in triplicate at 490 nm in a microplate reader (Synergy HT, Bio-TEK; USA). All experiments were performed three times, independently.

VII-2.3.5. Live/dead staining

Cells were labeled with calcein (AM)/propidium iodide (PI) as live/dead cells, respectively. Briefly, the medium of both cell types was removed and replaced by an Calcein AM (1:500) and PI (1:1000) solution in culture medium. After 10 min of incubation, samples were immediately visualized with Transmitted and Reflected Light Microscope with Apotome 2 (Axio Imager Z1m, Zeiss) at 5x magnification.

VII-2.4. Mammary fat pad mouse model

NSG (NOD.Cg-Prkdc^{scid} Il2rg^{tm1Wjl}/SzJ) immunosupressed female mice (n=12; 6 per group) were injected with 1x10^{6} breast cancer cells (SKBR3 cell line) suspended in PBS and matrigel (Corning, USA; 1:1) into the mammary fat pad (total volume of 50 µL). Mice were maintained under standard laboratory conditions, as previously described [26]. After 5 days post-implantation, the developed targeting system (NPs+Gem+Ab) and a saline solution (control conditions) were admnistered into each animal group, every week (day 5, 12, 19 and 26). First measurement of the tumor size was possible 26 days after breast cancer cells' injection, being measured at day 29 and 32 (end of experiment). Animal body weight and tumor size (calculated by measuring the two largest side and applying the Equation VII-1, being L1 the largest side, and L2 the other one) was measured and recorded once a week.

Equation VII-1 Equation for the tumor volume measurements.

$$V = \frac{3.14 \times L1 \times L1 \times L2}{6}$$

At day 32, animals were sacrificed using CO_2 due to the tumors' size. Tumors were excised, as well as other organs of interest like lungs, liver and kidneys to assess possible metastasis. Afterwards, the tumor and organs were fixed in 4% formaldehyde and subsequently embedded in paraffin for further histological analysis. All animal procedures were conducted in accordance with the guidelines for the care and use of laboratory animals (European Directive 2010/63/EU) and approved by the Direcção Geral de Alimentação e Veterinária (DGAV, reference 017761), the competent national authority for animal protection.

VII-2.5. Histological analysis

Retrieved tumors and organs of each mice specimen were dehydrated in a automatic stainer, embedded in paraffin and sectioned in sections of 4 μm thickness. Briefly, sections were deparaffinized with xylene, rehydrated in ethanol and stained with hematoxylin and eosin. Afterwards, sections were dehydrated and mounted with resinous mounting medium. The histological sections were analyzed under Leica DM750 microscope at 4× magnification.

VII-2.6. Statistical Analysis

Statistical analysis was performed using Graph Pad Prism Software. Considering that the data do not present a normal distribution and homogeneity of variance, the cell biological assays were analyzed using nonparametric test (Kruskal–Wallis test) and a $p < 0.05$ was considered significant. Data are presented as mean ± standard deviation.

VII-3. RESULTS

VII-3.1. Antibody immobilization at the surface of nanoparticles

A defined ErbB-2 antibody was immobilized at the surface of fucoidan/chitosan nanoparticles by a covalent bond mediated by EDC/NHS coupling agent. To ensure that the antibody was immobilized at the surface of the NPs at the maximum capacity of the NPs, a wide range of antibody concentrations was tested (0-20 μg mL^{-1}). An indirect method was used to quantify the immobilization efficiency, based on the measurement of unbound secondary antibody fluorescence, after its incubation with the immobilized primary antibody (**Figure VII-1 A**). As observed in **Figure VII-1 B**, higher amounts of immobilized ErbB-2 antibody correspond to a lower fluorescence signal of the free secondary antibody. At 10 μg mL^{-1} the NPs presented its maximum immobilization capacity and above this concentration the system was saturated. This optimized concentration was further used in all biological assays.

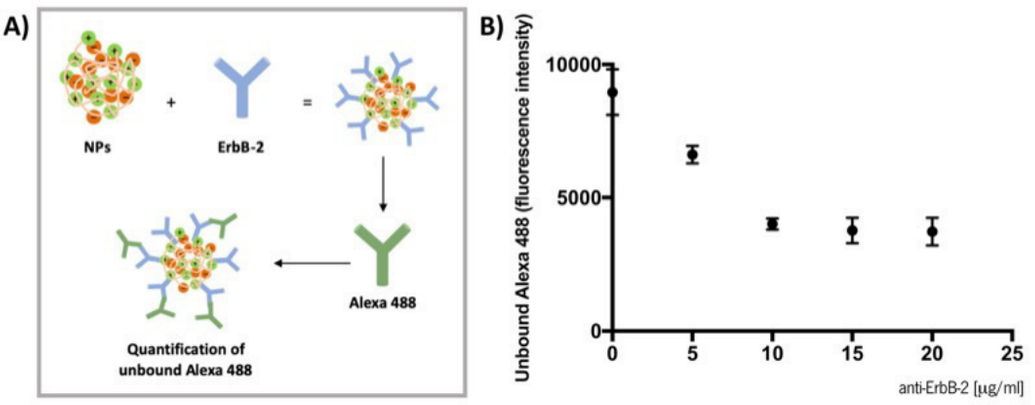

Figure VII-1 Schematic representation of the indirect quantification of immobilized antibody by measuring the fluorescence of unbound secondary antibody Alexa 488 (A) and quantification results obtained by this method (B).

VII-3.2. Nanoparticles characterization

In **Figure VII-2 A**, the size distribution of the developed nanoparticles targeting system (NPs+Gem+AB) as determined by light scattering is represented, showing an unimodal distribution, quantitatively characterized by the size and polydispersity index (Pdi) depicted in the table in Figure **VII-2 B**. The mean size of NPs+Gem+Ab is 159±23 nm, with a Pdi = 0.178±0.027. The targeting system has a positive zeta potential (ZP) of 21.3±2.68 mV. Furthermore, the round morphology of the nanoparticles was confirmed by AFM observation (**Figure VII-2 C**).

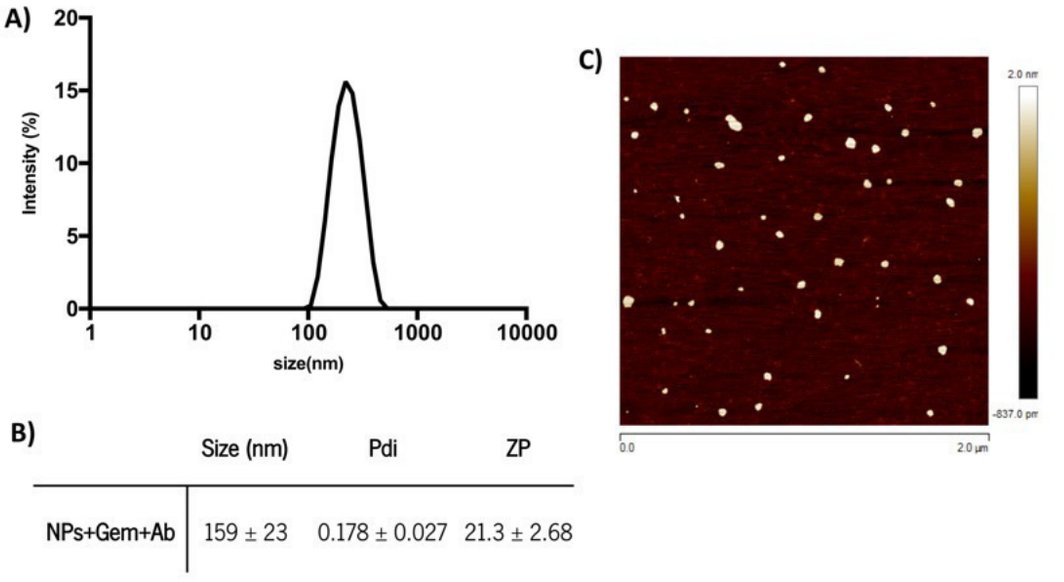

B)

	Size (nm)	Pdi	ZP
NPs+Gem+Ab	159 ± 23	0.178 ± 0.027	21.3 ± 2.68

Figure VII-2 Size distribution (A), size, Pdi and ZP B) and morphology C) of the developed targeting system (NPs+Gem+Ab).

VII-3.3. Cell targetting studies

Figure 3 shows confocal microscopic images of human endothelial (EA.hy.926 cell line) and breast cancer cells (MDA-MB-231 and SKBR3 cell lines) after exposure to the FITC-labeled nanoparticles with (NPs-FITC-Ab) or without immobilized ErbB-2 antibody (NPs-FITC). From the observations, SKBR3 cells were the only ones presenting the nanoparticles immobilizing the ErbB-2 antibody, more efficiently than the nacked nanoparticles (NPs-FITC). These NPs-FITC-Ab were mostly presented around the cells cytoplasm, due to the expression of ErbB-2 receptor at the cell membrane. Inversely, the MDA-MB-231 cells (ErbB-2 negative) did not uptake any type of NPs. Only a slight green fluorescence is observed in the cytoplasm of endothelial cells (**Figure VII-3**).

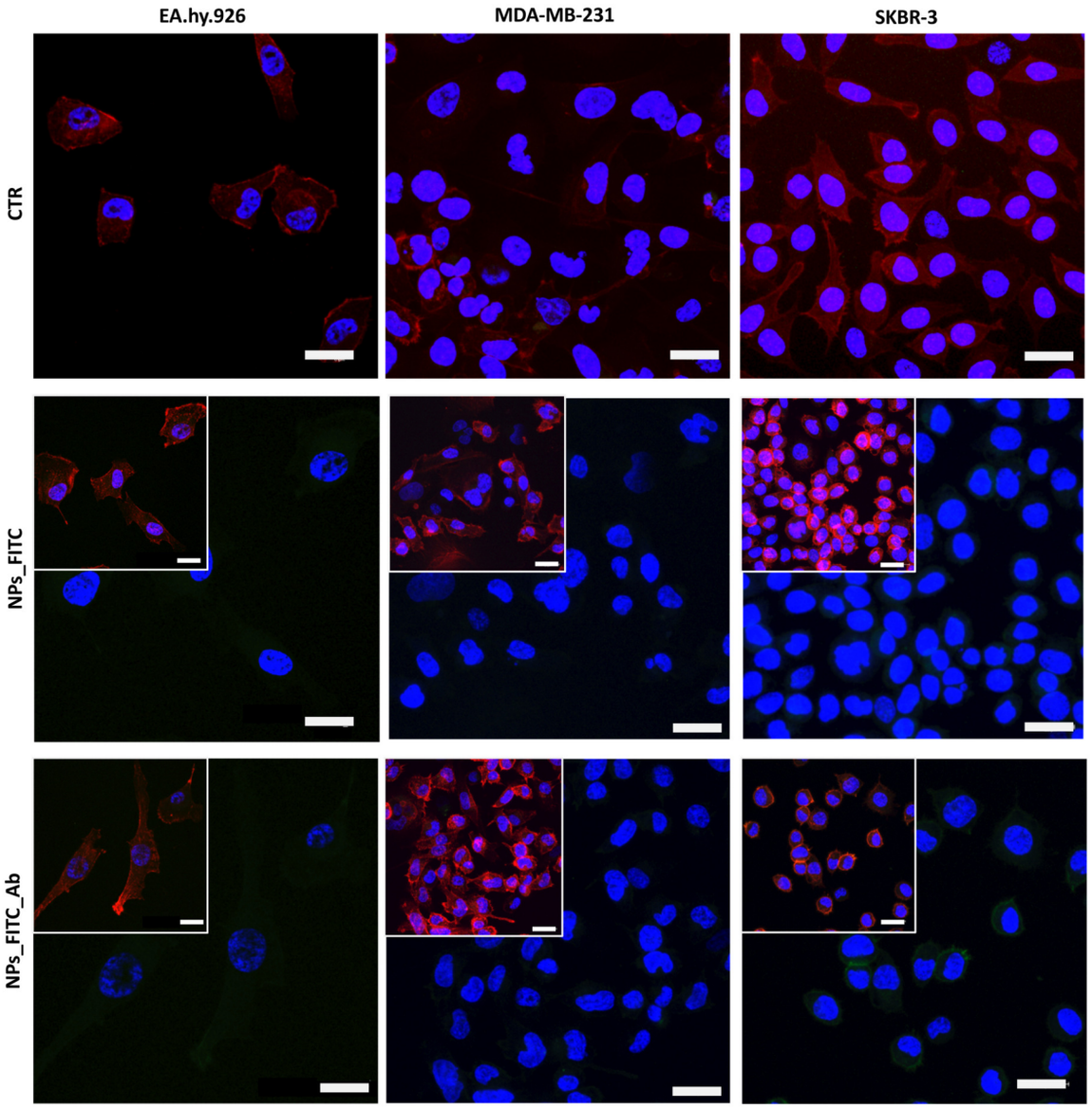

Figure VII-3 Confocal microscopy images of human endothelial (EA.hy926) and breast cancer (MDA-MB-231 and SKBR3) cells. Nanoparticles were labeled with FITC (green), the cells' nuclei with DAPI (blue) and the cytoskeleton with phalloidin (red). Scale bar=25 µm.

VII-3.4. Co-culture system

VII-3.4.1. Endothelial cells – EA.hy926

To validate the *in vitro* efficacy of the ErbB-2 antibody immobilized at the surface of nanoparticles, a co-culture system was established, mimicking the endothelial barrier. At day 1, all testing conditions presented similar values (between 24 and 30%), with th exception of the CTR condition that did not

present toxicity along the tested time points (**Figure VII-4 A**). The free Gem presented increased values of toxicity over endothelial cells when compared to both NPs+Gem and NPs+Gem+Ab, at days 2 and 3. Specifically, Gem is around 28% more cytotoxic than the developed NPs systems at day 2, and around 20% more cytotoxic at day 3. Live/dead images confirmed these quantitative results, since less green signaling is observed for the Gem condition (**Figure VII-4 B**). Inversely, endothelial cells viability remains constant for the NPs systems conditions.

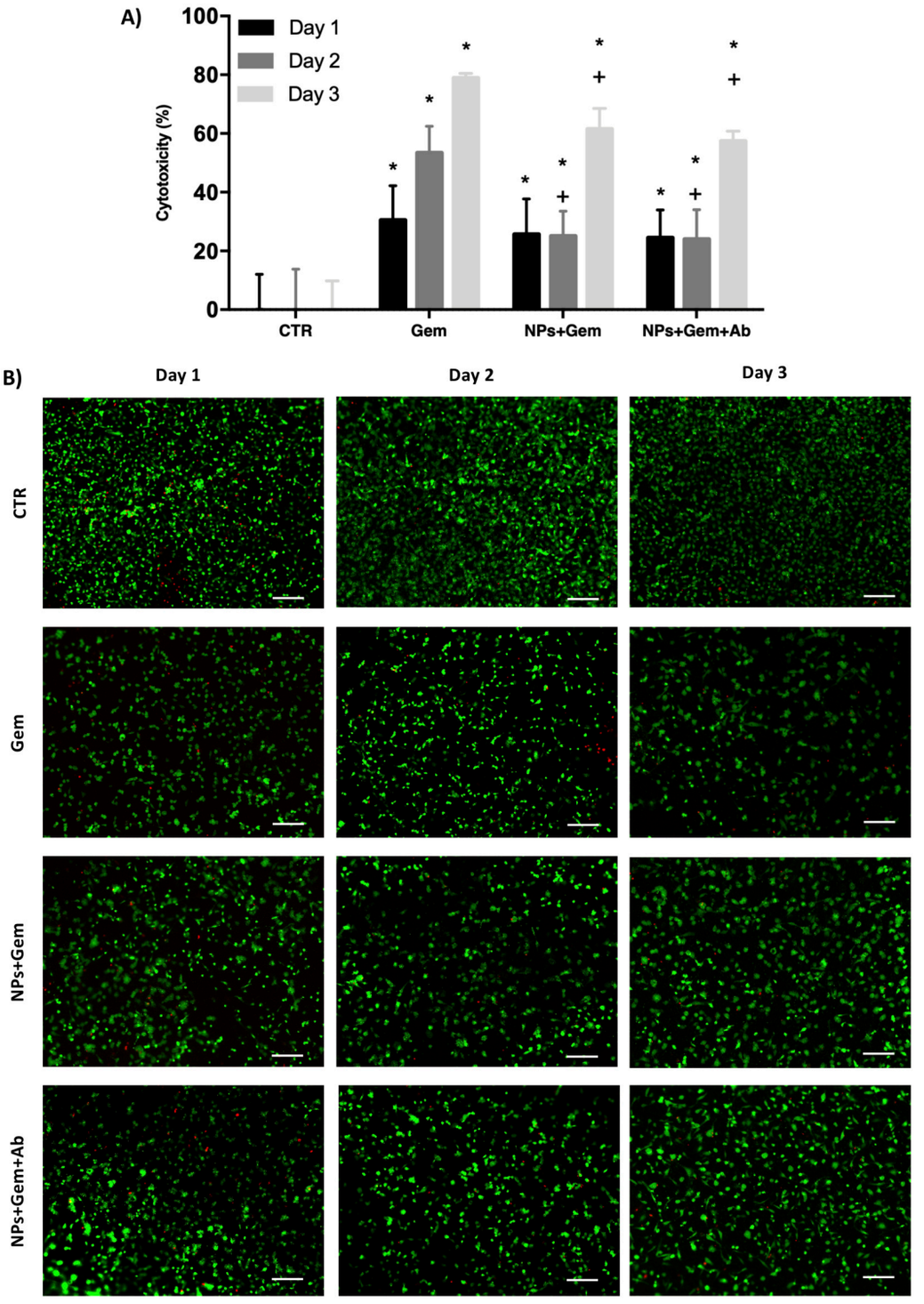

Figure VII-4 Cytotoxicity of the free drug (Gem), drug-loaded and functionalized drug-loaded nanoparticles over human endothelial cells (EA.hy926 cell line) at different time points (days 1, 2 and 3). MTS (A) and Live/Dead assay (B). Data was considered statistically different if $p < 0.05$. * when compared to CTR; + when compared to Gem. Scale bar=200 μm.

VII-3.4.2. Breast cancer cells

Regarding the effect over breast cancer cells (SKBR3:ErbB-2+), the main differences are observed at day 1 (**Figure VII-5 A**). Spcifically both NPs systems present increased toxicity when compared to free Gem (only 12%). However, the immobilization of the ErbB-2 antibody at the surface of the nanoparticles (NPs+Gem+Ab) resulted in an increased toxicity of this system of around 60% when compared to NPs+Gem (24%). For the other time points (day 2 and 3) all the conditions (except the CTR) presented a cytoxicity around 100%. These evidences were further confirmed by the live/dead stainning (**Figure VII-5 B**). At day 1, an increased red fluorescence signalling is observed for the targeting system in contrast to all the other conditions. At the other two time points, a significant the decrease in green signallng is observed for all the other conditions (except the CTR).

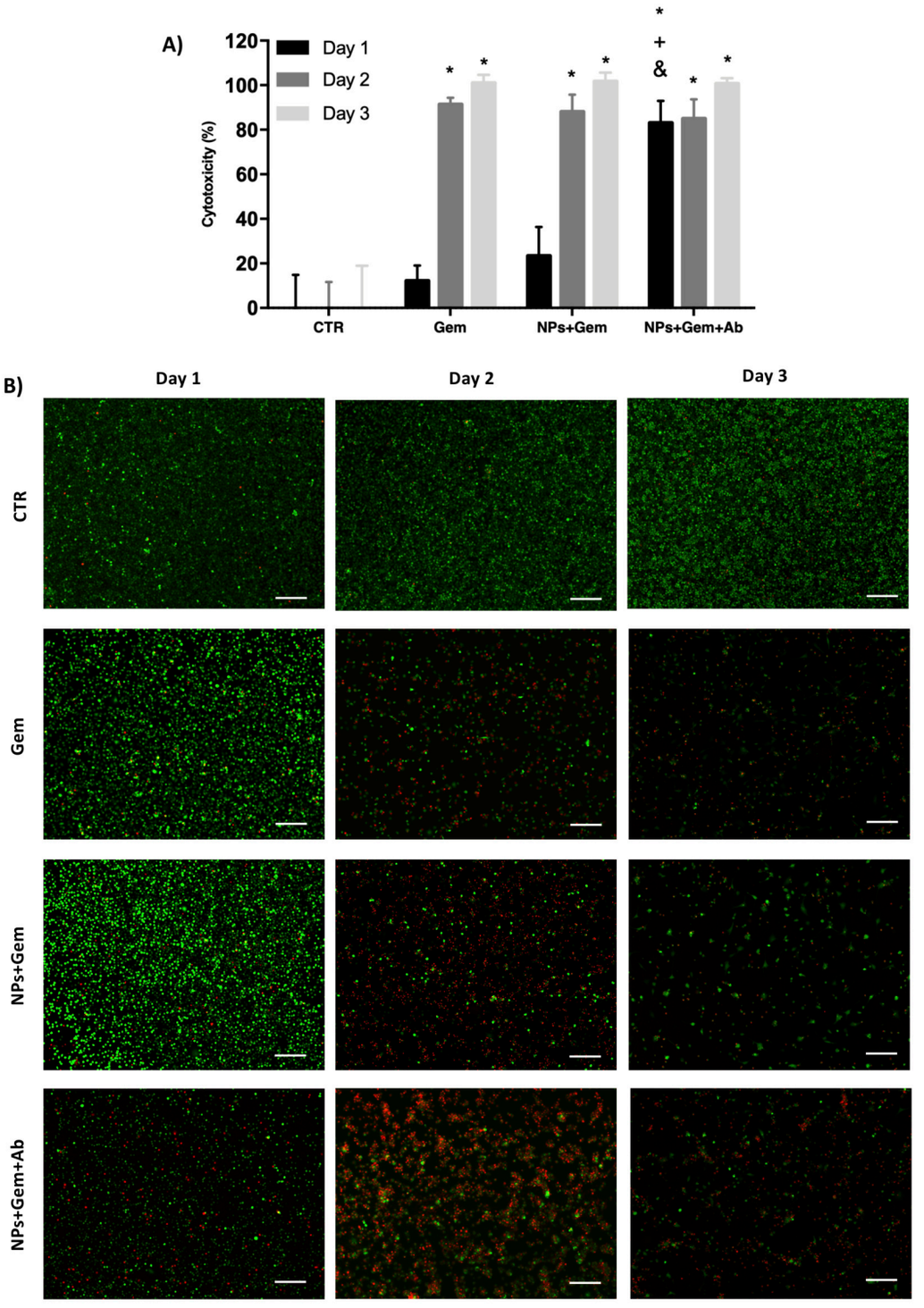

Figure VII-5 Cytotoxicity of the free drug (Gem), drug-loaded and functionalized drug-loaded nanoparticles over human breast cancer cells (SKBR3 cell lines) at different time points (day 1, 2 and 3), as adressed by MTS assay (A) and Live/Dead assay (B). Data was considered statistically different if $p < 0.05$: * when compared to CTR; + when compared to Gem; & when compared to NPs+Gem. Scale bar=200 µm.

VII-3.5. Breast cancer early model

Considering the *in vitro* results of the developed targeting system, its efficacy was also assessed in an immunosuppressed mice injected with breast cancer cells, constituting an early tumor model. Regarding the tumor volume, measurnments were performed at days 26, 29 and 32 after injection of breast cancer cells. Aiming to compare tumor volume progession, ratios between the different time points were calculated (**Figure VII-6 A**). The tumor volume of V_{29d}/V_{26d}, presented similar sizes for both conditions. For the latter time points, significant differences were observed between the CTR and the targeting system (NPs+Gem+Ab) tumor volumes ratio (V_{32d}/V_{29d}). When compared the final tumor volume to the initial one (V_{32d}/V_{26d}) significant differences were also observed. The number of mice that developed (or not) metastasis in the lungs is quantified in **Figure VII-6 B)**. No other organ (liver or kidney) presented abnormal conditions. Metastasis in the lungs were observed in mice treated with NPs+Gem+Ab, whereas in respect to the CTR group, 4 mice developed metastasis and 2 not. This assessment was performed by microscopic analysis of the lungs (**Figure VII-6 C**), where the metastasis are clear and easily identified. Even the one non-metastatic lung of the CTR seems to be more damaged than the non-metastatic lungs from the testing group.

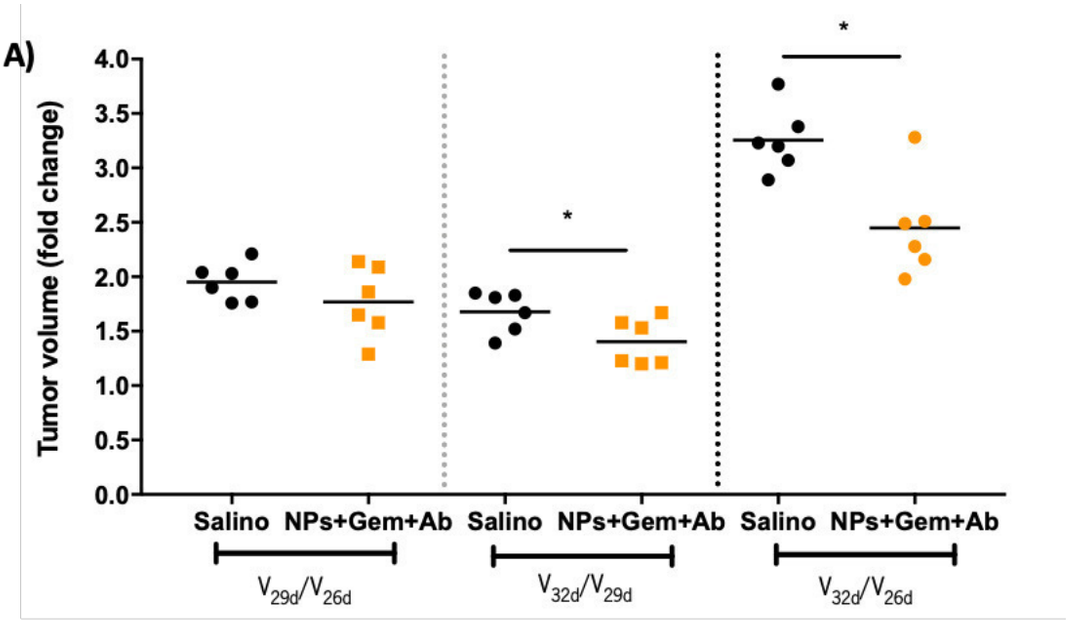

B)

Lungs	Metastatic	Non-metastatic
CTR	4	2
NPs+Gem+Ab	2	4

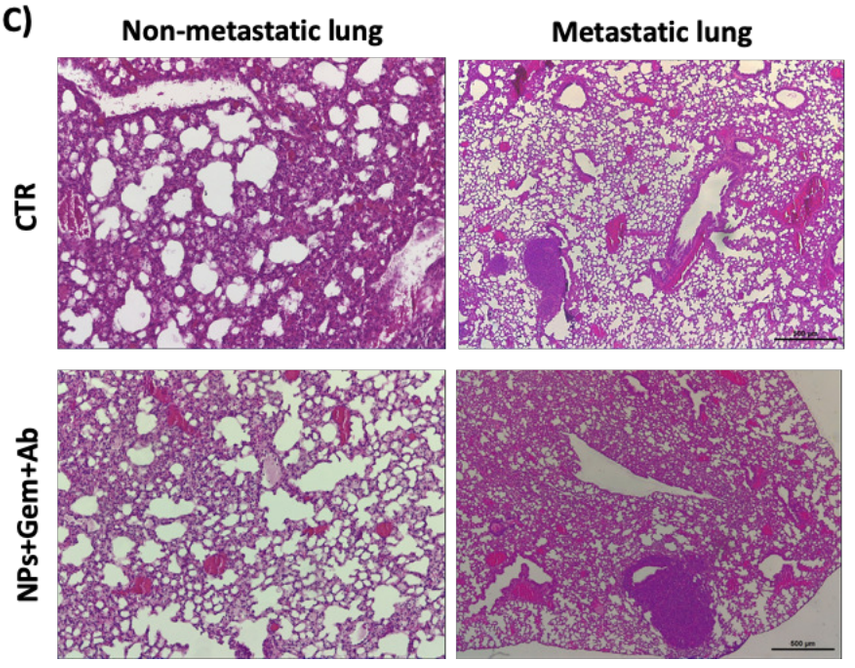

Figure VII-6 *In vivo* assays with NSG (NOD.Cg-Prkdc^{scid} Il2rg^{tm1Wjl}/SzJ) immunosupressed female mice. Tumor volume ratios for the different measurments A) number of metastatic and non-metastatic animals B) and H&E staining of metastatic and non-metastatic lungs at 4x magnification C). Data was considered statistically different if $p < 0.05$: * when compared to CTR.

VII-4. DISCUSSION

The main goal of an effective anti-cancer treatment comprise the delivery of therapeutic agents in a targeted and selective way to the tumor site, aiming to reduce the side effects of the cytotoxic compounds used as therapeutic agents over healthy tissues and organs [26]. This work aim was to develop a drug carrier able to target breast cancer cells by targetting an overexpressed cell membrane marker. The maximum immobilization capacity of the system was assessed by testing different antibody concentrations until it reaches saturation at concentrations above 10 μg ml^{-1}. NPs+Gem+Ab were characterized both in terms of size, Pdi and zeta potential and compared with NPs+Gem [19]. As reported by others [24, 27], a slightly increase in the nanoparticles size is observed when the antibody was immobilized at the NPs surface. Nevertheless, a narrow size distribution was observed, with Pdi values <0.2, indicating that the nanoparticles have an homogeneous size distribution [28]. Regarding the zeta potential of aroud 21 mV, the developed system can be considered as moderately stable (±20<ZP<±30 mV), indicating that chitosan is in the outer layer of the NPs [29].Regarding the zeta potential of aroud 21 mV, the developed system can be considered as moderately stable (±20<ZP<±30 mV) [30]. Futhermore, nanoparticles presented the typical round morphology as seen by AFM. This decrease in the zeta potential in comparision with non-functionalized nanoparticles indicates that the antibody has been successfully immobilized. Futhermore, nanoparticles presented the typical round morphology as seen by AFM.

After establishing the best conditions for the production of the functionalized nanoparticles, cellular uptake studies were performed with different cell lines to validate the efficiency of the antibody. Since the envisaged therapeutic strategy is based in intravenous injection, human endothelial cells (EA.hy926 cell line) were used as a model of healthy cells, representing the first barrier faced by the NPs. Regarding the tumor, two different types of human breast cancer cells were used: the MDA-MB-231 cell line that is ErbB-2 negative and the SKBR3 cell line, which is ErbB-2 positive. As expected, the immobilization of the ErbB-2 antibody lead to an increased cellular uptake by SKBR3 cells, when compared to the other two cells types or in comparison with the naked nanoparticles (without the functionalization with the antibody). It was possible to observe that nanoparticles were present in the cell limits, which would be expected since ErbB-2 receptor is present in the cell membrane [30, 31]. These results demonstrate that the developed ErbB-2 conjugated nanoparticles can efficiently and specifically interact with cancer cells and hopefully deliver the loaded drug at the target site, which may thus reduce the drug side effects as tocxicity over healthy tissues.

Gemcitabine (Gem) is a chemotherapeutic drug often used as a single agent or in combination with other drugs in the treatment of different types of cancers such as lung, ovary, pancreatic and breast [32-34]. Gem acts by inhibiting DNA synthesis and also by blocking the progression of cells through the G1/S-phase. Due to its short half-life, that ranges from 32 to 94 minutes (short infusions) and from 245 to 638 minutes (long infusions) and rapid metabolization, increase doses are required to obtain therapeutic efficacy, increasing the risks of side effects. Futhermore, the administered dose will depend on the type of cancer and the patient profile, varying from 10 mg mL^{-1} to 100 mg mL^{-1} [35]. In this work, the concentration loaded into the nanoparticles was substancially bellow the clinical dosage (around 0.4 mg mL^{-1}, as previously reported) [19], but sufficient to present promising results in 2D monocultures. 2D cultures with cell lines are important assays to study the ability of drugs/compounds to inhibit cancer cells' growth. Nevertheless, this strategy can be improved by implementing co-cultures with different cell types, aiming to mimic the tumor microenvironment that does not only comprise cancer cells but also healthy cells [36, 37]. To confirm and validate the targeting efficiency, a co-culture system composed of human endothelial and ErbB-2 positive breast cancer cells (SKBR3) was established. The idea was to assess if the developed nanoparticles would be able to cross an endothelial barrier and target breast cancer cells. Experimental data demonstrate that NPs+Gem+Ab were able to target breast cancer cells within the first 24h. These NPs presented an increased cytotoxicity of 60% when compared with free Gem and NPs+Gem. This indicates that, as previously described in the cell uptake assays, the antibody immobilized at the surface of the nanoparticles was bonded to the ErbB-2 receptor in the cells, and thus enabling the delivery of the drug at the target site. Indeed, the targeting system (NPs+Gem+Ab) was more effective than free Gem and nanoparticles without the antibody. Regarding endothelial cells, free Gem presented significantly higher toxicity than the NPs+Gem and NPs+Gem+Ab systems. This may be attributed to the fact that the endothelium constitutes the first cellular barrier to the drugs adminestered intraveneously, suffereing the direct effect of the drug. However, in the case of the nanoparticles systems, they are able to protect the drug during the first hours, having diminished effects over the endothelial cells. These observations clearly demonstrate that the NPs+Gem+Ab is an effective strategy to target ErbB-2 positive breast cancer cells, having decreased cytotoxicity over an endothelial barrier, when compared with free Gem. A similar trend was observed in a Gem-loaded nanoparticles system that targeted pancreatic cancer cells in 2D mono-cultures [27]. NPs with immobilized ErbB-2 were able to present increased toxicity when compared with free Gem or non-target NPs, which was also attributed to a greater intracellular delivery by receptor mediated endocytosis. Both NPs presented similar effects over normal kidney cells, presenting a slightly decrease in comparison with the free drug. In a different attempt,

NPs incorporating a different chemotherapeutic drug, doxorubicin (Dox), were able to present increased cytotoxic effects over an ovarian cancer cell line, when comparing with NPs without immobilized antibody, showing similar cytotoxic effects to free Dox [23].

The current *in vitro* model is much more representative of the physiological environment and the developed targetting system proven to be more effective on targetting cancer cells, having fewer cytotoxic effects over endothelial cells. To further demonstrate the effectiveness of the developed targeting delivery, an early disease animal model was implemented. Despite there were no significant differences for the first tumor volume ratio measurnments, significant smaller tumor volume ratios (V_{32d}/V_{29d}) were observed for the NPs targeting system when compared with the control saline group. Furthemore, it is possible to state that the developed targeting system was able to delay tumor growth in comparison with the CTR(V_{32d}/V_{26d}). Since breast cancers often metastasize to the lungs, liver and the kidneys, these organs were retrieved from the animals for histological analysis [39]. Liver and kidneys did not present any alterations for both conditions. However, it was possible to observe that there were more metastatic lungs in the control condition than in mice tretated with the NPs+Gem+Ab system. These results validate the efficacy of the developed targeting system in hampering the tumor size as well as the side effects over other healthy tissues, namely the lungs.

VII-5. Conclusions

In this work, a nanoparticles-based drug delivery system able to target ErbB-2$^+$ breast cancers was optimized and validated. The increased cytotoxic effects over cancer cells, but not over endothelial cells, and the specific binding to ErbB-2 receptor shows promising results when compared with non-targeted NPs or free drug, namely in reducing the cytotoxic effects over endothelial cells. The higher uptake of the functionalized NPs by the ErbB-2$^+$ breast cancer cells and the selectivity observed on the co-culture system validated the targeting efficacy of the drug delivery system *in vitro*. The targeting efficacy was also addressed *in vivo*, with the developed system being also able to hamper tumor growth in an early tumor animal model. Another important observation was the significant reduction of metastasis in the lung when the animals were treated with the targeting system. Taken together, the developed targeting system is a promising therapy for ErbB-2 positive breast cancers that should be further investigated in a translational perspective.

VII-6. AKNOWLEDGMENTS

This work was developed under the scope of the Structured projects for R&D&I NORTE-01-0145-FEDER-000013/21/23 supported by the Northern Portugal Regional Operational Programme Norte 2020, under the Portugal 2020 Partnership Agreement. The authors would like also to thank Norte 2020 for financing the PhD scholarship of C.O. "Norte-08-5369-000037" and the Portuguese Foundation for Science and Technology for the Investigator grant of A.M. (IF/00376/2014). The authors would also like to acknowledge Teresa Oliveira for her insights regarding the histological analysis performed for the *in vivo* studies.

VII-7. REFERENCES:

[1] R.L. Siegel, K.D. Miller, A. Jemal, Cancer statistics, 2019, CA Cancer J Clin 69(1) (2019) 7-34.

[2] S.M. Fragomeni, A. Sciallis, J.S. Jeruss, Molecular Subtypes and Local-Regional Control of Breast Cancer, Surg Oncol Clin N Am 27(1) (2018) 95-120.

[3] C.W.S. Tong, M. Wu, W.C.S. Cho, K.K.W. To, Recent Advances in the Treatment of Breast Cancer, Frontiers in oncology 8 (2018) 227-227.

[4] M.I. Nounou, F. ElAmrawy, N. Ahmed, K. Abdelraouf, S. Goda, H. Syed-Sha-Qhattal, Breast Cancer: Conventional Diagnosis and Treatment Modalities and Recent Patents and Technologies, Breast cancer : basic and clinical research 9(Suppl 2) (2015) 17-34.

[5] C.W.S. Tong, M. Wu, W.C.S. Cho, K.K.W. To, Recent Advances in the Treatment of Breast Cancer, Frontiers in Oncology 8 (2018) 227.

[6] R. Bazak, M. Houri, S.E. Achy, W. Hussein, T. Refaat, Passive targeting of nanoparticles to cancer: A comprehensive review of the literature, Mol Clin Oncol 2(6) (2014) 904-908.

[7] S.A.A. Rizvi, A.M. Saleh, Applications of nanoparticle systems in drug delivery technology, Saudi Pharmaceutical Journal 26(1) (2018) 64-70.

[8] W.H. De Jong, P.J. Borm, Drug delivery and nanoparticles:applications and hazards, Int J Nanomedicine 3(2) (2008) 133-49.

[9] A. Schroeder, D.A. Heller, M.M. Winslow, J.E. Dahlman, G.W. Pratt, R. Langer, T. Jacks, D.G. Anderson, Treating metastatic cancer with nanotechnology, Nat Rev Cancer 12(1) (2011) 39-50.

[10] H. Gao, Z. Yang, S. Zhang, S. Cao, S. Shen, Z. Pang, X. Jiang, Ligand modified nanoparticles increases cell uptake, alters endocytosis and elevates glioma distribution and internalization, Scientific Reports 3 (2013) 2534.

[11] S. Behzadi, V. Serpooshan, W. Tao, M.A. Hamaly, M.Y. Alkawareek, E.C. Dreaden, D. Brown, A.M. Alkilany, O.C. Farokhzad, M. Mahmoudi, Cellular uptake of nanoparticles: journey inside the cell, Chem Soc Rev 46(14) (2017) 4218-4244.

[12] I. Trenevska, D. Li, A.H. Banham, Therapeutic Antibodies against Intracellular Tumor Antigens, Frontiers in Immunology 8 (2017) 1001.

[13] N. Iqbal, N. Iqbal, Human Epidermal Growth Factor Receptor 2 (HER2) in Cancers: Overexpression and Therapeutic Implications, Molecular biology international 2014 (2014) 852748.

[14] Hasmann, Chapter 9 - Targeting HER2 by monoclonal antibodies for cancer therapy, in: R. Ganellin, S. Roberts, R. Jefferis (Eds.), Introduction to Biological and Small Molecule Drug Research and Development, Elsevier, Oxford, 2013, pp. 283-305.

[15] M.D. Pegram, G.E. Konecny, C. O'Callaghan, M. Beryt, R. Pietras, D.J. Slamon, Rational Combinations of Trastuzumab With Chemotherapeutic Drugs Used in the Treatment of Breast Cancer, JNCI: Journal of the National Cancer Institute 96(10) (2004) 739-749.

[16] M. Brandão, N.F. Pondé, F. Poggio, N. Kotecki, M. Salis, M. Lambertini, E. de Azambuja, Combination therapies for the treatment of HER2-positive breast cancer: current and future prospects, Expert Review of Anticancer Therapy 18(7) (2018) 629-649.

[17] E.d.S. Lohman, S.C. Linn, M. Kok, Low-dose doxorubicin combined with trastuzumab in HER2-positive metastatic breast cancer: A single institution experience, Journal of Clinical Oncology 32(15_suppl) (2014) e11598-e11598.

[18] G.M. Cragg, D.J. Newman, Natural products: a continuing source of novel drug leads, Biochimica et biophysica acta 1830(6) (2013) 3670-3695.

[19] C. Oliveira, N.M. Neves, R.L. Reis, A. Martins, T.H. Silva, Gemcitabine delivered by fucoidan/chitosan nanoparticles presents increased toxicity over human breast cancer cells, Nanomedicine 13(16) (2018) 2037-2050.

[20] B. Jang, M.S. Moorthy, P. Manivasagan, L. Xu, K. Song, K.D. Lee, M. Kwak, J. Oh, J.-O. Jin, Fucoidan-coated CuS nanoparticles for chemo-and photothermal therapy against cancer, Oncotarget 9(16) (2018) 12649-12661.

[21] H.P. Nam, T.L. Thao, N.P. Minh, D.L. Thinh, V.V. Toi, H.L.T. Phuong, T.D.T. Thao, A Comparison of Fucoidan Conjugated to Paclitaxel and Curcumin for the Dual Delivery of Cancer Therapeutic Agents, Anti-Cancer Agents in Medicinal Chemistry 18(9) (2018) 1349-1355.

[22] J. Jiang, Y. Liu, C. Wu, Y. Qiu, X. Xu, H. Lv, A. Bai, X. Liu, Development of drug-loaded chitosan hollow nanoparticles for delivery of paclitaxel to human lung cancer A549 cells, Drug Dev Ind Pharm 43(8) (2017) 1304-1313.

[23] P. Yousefpour, F. Atyabi, E. Vasheghani-Farahani, A.A. Movahedi, R. Dinarvand, Targeted delivery of doxorubicin-utilizing chitosan nanoparticles surface-functionalized with anti-Her2 trastuzumab, Int J Nanomedicine 6 (2011) 1977-90.

[24] P. Naruphontjirakul, K. Viravaidya-Pasuwat, Development of anti-HER2-targeted doxorubicin-core-shell chitosan nanoparticles for the treatment of human breast cancer, Int J Nanomedicine 14 (2019) 4105-4121.

[25] A.C. Lima, C. Cunha, A. Carvalho, H. Ferreira, N.M. Neves, Interleukin-6 Neutralization by Antibodies Immobilized at the Surface of Polymeric Nanoparticles as a Therapeutic Strategy for Arthritic Diseases, ACS Applied Materials & Interfaces 10(16) (2018) 13839-13850.

[26] C.S. Gonçalves, J. Vieira de Castro, M. Pojo, E.P. Martins, S. Queirós, E. Chautard, R. Taipa, M.M. Pires, A.A. Pinto, F. Pardal, C. Custódia, C.C. Faria, C. Clara, R.M. Reis, N. Sousa, B.M. Costa, WNT6 is a novel oncogenic prognostic biomarker in human glioblastoma, Theranostics 8(17) (2018) 4805-4823.

[27] R. Bayat Mokhtari, T.S. Homayouni, N. Baluch, E. Morgatskaya, S. Kumar, B. Das, H. Yeger, Combination therapy in combating cancer, Oncotarget 8(23) (2017) 38022-38043.

[28] G. Arya, M. Vandana, S. Acharya, S.K. Sahoo, Enhanced antiproliferative activity of Herceptin (HER2)-conjugated gemcitabine-loaded chitosan nanoparticle in pancreatic cancer therapy, Nanomedicine: Nanotechnology, Biology and Medicine 7(6) (2011) 859-870.

[29] J. Panchal, J. Kotarek, E. Marszal, E.M. Topp, Analyzing Subvisible Particles in Protein Drug Products: a Comparison of Dynamic Light Scattering (DLS) and Resonant Mass Measurement (RMM), The AAPS Journal 16(3) (2014) 440-451.

[30] S. Bhattacharjee, DLS and zeta potential – What they are and what they are not?, Journal of Controlled Release 235 (2016) 337-351.

[31] A.M. Hommelgaard, M. Lerdrup, B. van Deurs, Association with membrane protrusions makes ErbB2 an internalization-resistant receptor, Mol Biol Cell 15(4) (2004) 1557-67.

[32] S. Yang, M.A. Raymond-Stintz, W. Ying, J. Zhang, D.S. Lidke, S.L. Steinberg, L. Williams, J.M. Oliver, B.S. Wilson, Mapping ErbB receptors on breast cancer cell membranes during signal transduction, Journal of cell science 120(16) (2007) 2763.

[33] W. Plunkett, P. Huang, Y.Z. Xu, V. Heinemann, R. Grunewald, V. Gandhi, Gemcitabine: metabolism, mechanisms of action, and self-potentiation, Semin Oncol 22 (1995).

[34] V. Heinemann, Role of gemcitabine in the treatment of advanced and metastatic breast cancer, Oncology 64(3) (2003) 191-206.

[35] H. Hayashi, T. Kurata, K. Nakagawa, Gemcitabine: Efficacy in the Treatment of Advanced Stage Nonsquamous Non-Small Cell Lung Cancer, Clinical Medicine Insights. Oncology 5 (2011) 177-184.

[36] H. Sakamoto, M. Kitano, Y. Suetomi, Y. Takeyama, H. Ohyanagi, T. Nakai, C. Yasuda, M. Kudo, Comparison of standard-dose and low-dose gemcitabine regimens in pancreatic adenocarcinoma patients: a prospective randomized trial, Journal of Gastroenterology 41(1) (2006) 70-76.

[37] C. Arrigoni, S. Bersini, M. Gilardi, M. Moretti, In Vitro Co-Culture Models of Breast Cancer Metastatic Progression towards Bone, International Journal of Molecular Sciences 17(9) (2016) 1405.

[38] C. Roma-Rodrigues, R. Mendes, V.P. Baptista, R.A. Fernandes, Targeting Tumor Microenvironment for Cancer Therapy, International Journal of Molecular Sciences 20(4) (2019) 840.

[39] L. Jin, B. Han, E. Siegel, Y. Cui, A. Giuliano, X. Cui, Breast cancer lung metastasis: Molecular biology and therapeutic implications, Cancer Biology & Therapy 19(10) (2018) 858-868.

SECTION 4

GENERAL CONCLUSIONS

Chapter VIII

General Conclusions and Future Perspectives

Chapter VIII

General Conclusions and Future Perspectives

VIII-1. General conclusions

The use of fucoidan as an antitumor agent has been described over the recent past years. However, there are still some concerns regarding fucoidan's usage in clinical settings, namely due to some contradictory results on its toxicity over cancer cells. Trying to elucidate this aspect, the thesis herein presented aims to understand and explore the antitumor activity of fucoidan by developing more effective and consistent fucoidan-based approaches. Particularly, studies on structure-activity relationship, along with the assessment of fucoidan cytotoxic effects over different cell types (either cancer or normal cells), may help to overcome those limitations. In this sense, besides presenting the toxicity over human breast cancer or melanoma cells (depending on the chapter), there was always the concern of evaluating the fucoidan or fucoidan-based systems effects over normal cells (which were selected depending on the work purpose). This was found to be of great importance, enabling more accurate conclusions regarding fucoidan antitumor activity.

As so, in Chapter III, the chemical and biological characterization of different commercial fucoidan extracts revealed interesting results and conclusions. First of all, it was possible to conclude that not all fucoidan extracts present the same biological outcomes, specifically regarding the antitumor activity. Three distinct behaviors were observed, as previously reported, showing the importance of testing the cytotoxicity of the extracts over not only cancer cell, but also normal cells. Having this into consideration, more accurate conclusions regarding fucoidan antitumor capability were performed, being possible to define a specific concentration where fucoidan presented toxicity over breast cancer cells without affecting normal fibroblast and endothelial cells. Most of the works reported in the literature refer to the molecular weight and sulfation degree as the main properties affecting the antitumor activity of fucoidan. However, in Chapter III, these same conclusions were not achieved and, therefore, more studies were performed on structural characterization of fucoidan extracts to shed more light on the structure-activity relationship. From the desulfation and methylation analysis was possible to ensure that the key players influencing the antitumor activity of these fucoidan extracts are related with the sulfate position and the branching degree.

This study allows to have a better understanding of fucoidan intrinsic properties and to assess the different biological performances of fucoidan. Therefore, the following works were planned having in mind the distinct behavior of fucoidan, with the final aim of developing more effective fucoidan-based antitumor strategies. In the studies reported in Chapters IV and V, a fucoidan extract with selective activity (toxicity to cancer cells without affecting normal cells, at a defined concentration) was used, whereas other fucoidan extract without intrinsic antitumor activity was used to develop more effective drug delivery and targeting systems (reported in Chapter VI and VII).

In Chapter IV, and trying to elucidate fucoidan's mechanism of action, the angiogenic potential of a selective fucoidan was evaluated in relation to its antitumor behavior. This fucoidan, at a pre-determined concentration, was able to impair the formation of or to disrupt a pre-formed tubular-like endothelial network, *in vitro*. In addition, the same conclusions were obtained in *in vivo* studies, by performing the CAM assay. This assay was also performed with a tumor onplanted into the CAM, which revealed that this fucoidan was able to significantly reduce the tumor size in a relatively short period of time. These *in vitro* and *in vivo* results corroborate the anti-angiogenic potential of the selective fucoidan, which is of great interest for the development of antitumor therapies. In a different attempt (Chapter V), this fucoidan was proposed to treat melanoma, either as a single bioactive agent or immobilized at the surface of an electrospun nanofibrous mesh. To the best of our knowledge this was the first time that fucoidan has been immobilized in a biomaterial substrate aiming the development of antitumor therapies. These two approaches revealed again the selective behavior of this fucoidan, being able to affect the viability of melanoma cells, presenting diminished effects over normal human skin cells (dermal fibroblasts and keratinocytes). This study presented a promising and valuable dual-therapy strategy that can help fight melanoma, the most aggressive skin cancer.

Regarding the last two chapters of this thesis, fucoidan-based drug delivery and targeting systems were developed aiming to reduce the side effects of current chemotherapeutic drugs. In this sense, a fucoidan extract without intrinsic antitumor activity was complexed with chitosan, forming a marine-based NPs system (Chapter VI). These NPs were optimized in terms of size and Pdi, as well as for the encapsulation efficiency of the drug. This system showed increased cytotoxic effects over human breast cancer cells (around 25%) when compared to endothelial cells. The NPs also presented increased toxicity over cancer cells when compared to the free drug, whereas similar cytotoxicity was observed for endothelial cells. This was an important aspect since the encapsulation of the drug allows achieving increased antitumor effect without increased toxicity over healthy cells. In an attempt to diminish the

effects over healthy tissues, a targeting approach was developed and optimized (Chapter VII). For that, a specific antibody against ErbB-2 was immobilized at the surface of the previously described NPs. This targeting system was able to effectively recognize ErbB-2 positive breast cancer cells (SKBR3 cell line), showing an increased cellular uptake when compared with endothelial cells or ErbB-2 negative breast cancer cells. A co-culture system was setup to validate the targeting efficiency of NPs, by mimicking the endothelial barrier. Just in 24h, the NPs with the immobilized antibody were able to cross the endothelial barrier, presenting increased toxicity over human breast cancer cells when compared with the NPs without the antibody or the free drug. Furthermore, the effect of the targeting system over the endothelial cells were diminished when compared with the free drug. An *in vivo* assay showed a retardment in the tumor development along with less metastatic lungs in mice, when compared with the control condition. These results were able to validate the targeting efficiency of the NPs system, diminishing the side effects of a chemotherapeutic.

Altogether, the work developed in this thesis resulted in new knowledge regarding fucoidan intrinsic properties, which is of utmost importance for the development of more effective therapies. On the other hand, the optimized and developed fucoidan-based systems represent promising antitumor therapies, with diminished side-effects. Therefore, a step forward on the fucoidan usage as an antitumor therapy was made, either as a single bioactive agent or as more effective fucoidan-based systems.

VIII-2. Future Perspectives

Despite the promising results herein presented, there is always room for improvement and the need to validate these strategies with more complex systems that better mimic the tumor microenvironment. In this sense, in this sub-section, a general future perspective on fucoidan usage as antitumor compound will be given, along with more detailed future perspectives for each of the works developed.

Firstly, a standardization regarding the biomass used as a raw-material and the extraction methods should be performed trying to obtain fucoidan with similar chemical properties, avoiding the contradictory results of fucoidan's biological activities. Indeed, currently, each fucoidan extract should be taken as an independent one and biological activities cannot be predicted, requiring always confirmation. Secondly, although some mechanisms of action are already described in the literature, there is no consensus regarding this issue. Despite different cells can present different mechanisms of action, a closer look into this aspect should be considered. Last but not the least, another important

aspect that is missing in most studies is that the authors only present the cytotoxic effects over cancer cells, when it is known by the tumor microenvironment that non-cancer cells should also be considered. In this thesis, this aspect was always considered when designing the experimental work.

In the particular case of these studies and thesis, additional work can be performed to increase the relevance of such discoveries. About the two first Chapters of Section 3 (Chapters III and IV), where fucoidan is used as a single antitumor agent, a deep understanding of the mechanism of action should be studied. Indeed, as previously stated, there are studies in the literature regarding fucoidan antitumor mechanism of action. However, these studies are mainly focused on cancer cells. In Chapter III, a fucoidan with a selective behavior was studied. So, it would be interesting to study the differences between the two cell types (cancer and normal cells) to clarify why fucoidan presents toxicity to cancer and not to normal cells. Having this extract in mind, and the fact that it presents inherent antitumor activity, it would be of great interest to compare fucoidan with currently used chemotherapeutic drugs aiming to diminish the severe side effects that such drugs can inflict to the patients.

Regarding chapter V, interesting and promising results were obtained on the use of a fucoidan-based therapies to treat melanoma. Nevertheless, additional studies can be performed to validate the dual-therapy strategy by the development of an *in vitro* 3D model. This model should comprise the different layers of the skin to better mimic what happens *in vivo*.

In what concerns Chapters VI and VII, additional *in vivo* models should be performed. In Chapter VII, an early tumor model was performed, as a first validation step, showing interesting results in what concerns tumor growth retardation and inhibition of metastasis to other organs. The implementation of a late tumor model would be of great interest, to study the effects of the NPs system after tumor appearance, and evaluate its effects over tumor size and metastasis as well.

Standard extraction methods of fucoidan along with a deep understanding of both the mechanisms of action and chemical features will make fucoidan a step closer to the clinic. The development of alternative and more effective approaches to treat cancer may improve the current clinical outcomes experienced by cancer patients and fucoidan might play a role on this, both as a new antitumor agent (to be used alone or exploring synergies with other drugs) and as component of innovative drug delivery devices targeting specifically the tumors.